Investigating exosomes for regenerative medicine: development of purification techniques and novel analytical strategies for assessment of potency.

By

Thomas Edmund Whittaker

Thesis

Submitted to the Department of Materials,

Imperial College London,

In partial fulfilment of the requirements for the degree of

Doctor of Philosophy

in

Materials Science

December 2018

London, United Kingdom

Abstract

No living cell has yet been reported that does not release extracellular vesicles (EVs). The last decade has seen an explosion of research into their properties as biomarkers, drug carriers, effectors of signalling and potential therapeutics. Within the field of regenerative medicine, EVs have recently been implicated in the therapeutic paracrine signalling of human mesenchymal stem cells (hMSCs) after transplantation. They appear to represent a promising cell-free therapy for myocardial infarction, stroke, and other diseases. However, effective purification of EVs without accompanying contamination from other cell-derived factors is challenging. There is debate within the field as to the fitness for purpose of several commonly-used isolation techniques. Cell signalling via EVs is not typically directly compared to signalling via conventional soluble factors, and there are no widely-adopted standards for assessing potency.

Here, an effective EV isolation system was developed and validated to be capable of fully separating EVs from free protein. HMSC-EVs isolated with this system were found to be ineffective stimulants of *in vitro* assays of angiogenesis and wound healing. It was found that hMSC-EVs could only stimulate these assays when purified by a low-stringency technique or when used at very high concentrations. Ultrafiltration experiments similar to those that initially suggested the necessity of EVs in hMSC signalling were found to be prone to false positives. When evaluated in experiments that allowed direct quantitative comparison with non-EV factors produced by the same cells, non-EV factors were repeatedly found to be necessary and sufficient for hMSC paracrine stimulation of *in vitro* angiogenesis and wound healing. A conceptual framework for quantitative evaluation of the contribution of EVs to signalling processes is proposed.

Acknowledgements

Firstly, I would like to thank my supervisor, Prof. Molly Stevens, for welcoming me into her group and giving me this incredible opportunity to work with so many talented and generous people, and for her support and inspiration over the last four years. It has been a long and worthwhile journey and I feel very lucky to have taken it.

To the postdocs who have guided me from confused undergraduate to marginally less confused graduate student; thank you for your guidance, support, time and friendship. Anika, Ulrike, J.P, Gregor and Rona; you all taught me so much.

To the postdocs and fellow students who became my friends, collaborators and commiserators; thanks for the laughs, the deep conversations and the less profound ones, and for being either good or bad influences when either was most necessary. It was a privilege to share good times and bad. There are too many of you to name here. Y'all know who you are.

To Kay and Uncle Keith; you have always been role models for me as a scientist. Thank you both for gently encouraging me into science before I was too old to know any better.

To my parents, who have always been there for me during and before this PhD, and whose love and support never flickered: Mum and Dad, thank you for everything.

To Ri, where do I even start. You have been a constant source of love, strength and comfort. I'm so glad we did this together, and that we can enjoy whatever comes next together too.

Thank you all.

Declaration of originality

I, Thomas Whittaker, declare that all work presented in this thesis is my own unless otherwise stated.

I am grateful to Dr. Ulrike Kauscher for Cryo-TEM imaging, and to Dr. Anika Nagelkerke for performing Western blots and for provision of GFP-transformed NIH-3T3 cells.

Copyright declaration

The copyright of this thesis rests with the author. Unless otherwise indicated, its contents are licensed under a Creative Commons Attribution-Non Commercial 4.0 International Licence (CC BY-NC). Under this licence, you may copy and redistribute the material in any medium or format. You may also create and distribute modified versions of the work. This is on the condition that: you credit the author and do not use it, or any derivative works, for a commercial purpose. When reusing or sharing this work, ensure you make the licence terms clear to others by naming the licence and linking to the licence text. Where a work has been adapted, you should indicate that the work has been changed and describe those changes. Please seek permission from the copyright holder for uses of this work that are not included in this licence or permitted under UK Copyright Law.

Contents

Abstract 2
Acknowledgements 3
Declaration of originality 4
Copyright declaration 5
List of figures 9
List of abbreviations 11
Scope of the thesis 14
1. Introduction to extracellular vesicles 15
1.1. History of extracellular vesicle research 15
1.2. Classes of extracellular vesicles 17
1.2.1. Formation of exosomes 17
1.2.2. Formation of microvesicles 19
1.3. Content of extracellular vesicles 19
1.3.1. Membrane-bound proteins 20
1.3.2. Luminal proteins 20
1.3.3. RNA 20
1.3.4. DNA 21
1.3.5. Lipids 22
1.4. Extracellular vesicle interactions with recipient cells 22
1.5. Clinical potential of extracellular vesicles 23
1.5.1. Extracellular vesicles as diagnostic targets 23
1.5.2. Extracellular vesicles as drug delivery vehicles 23
1.5.3. Extracellular vesicles as biotherapeutics 25
2. Methods for extracellular vesicle isolation 26
2.1. Literature review 26
2.1.1. Sample collection 26
2.1.2. Methods of concentration 29
2.1.3. Purification methods 32
2.1.4. Assessment of EV purity 36
2.1.5. Conclusions and critical requirements for purification 37
2.2. Materials and Methods 38
2.3. Results: Development and validation of purification techniques 49
2.3.1. Centrifugal concentrator evaluation 50
2.3.2. Initial evaluation of size exclusion chromatography 51

2.3.3. Ultrafiltration and SEC: in-depth characterisation of purification and recovery. 53
2.3.4. Electron Microscopy of SEC-purified EVs 56
2.3.5. EV marker expression from SEC-purified EVs 57
2.3.6. EV-depleted FBS 58
2.3.7. Downstream effects of use of EV-depleted FBS 61
2.4. Discussion: Development of the purification system 63
2.4.1. Conclusions 65
3. Matrix vesicles and mineralisation 66
3.1. Literature review: matrix vesicle-mediated mineralisation of soft tissues 66
3.1.1. Mechanism of Matrix Vesicles 67
3.1.2. Matrix vesicles and extracellular vesicles 68
3.1.3. Tissue engineering applications of matrix vesicles 69
3.1.4. Summary 69
3.2. Materials and Methods 70
3.3. Results: Matrix vesicles 72
3.3.1. Isolation of matrix vesicles from bovine cartilage 72
3.3.2. Characterisation of matrix vesicle size and morphology 73
3.3.3. Characterisation of particle and protein content of matrix vesicle isolates 74
3.3.4. Optimisation of ALP activity assay 75
3.3.5. ALP activity of matrix vesicle isolates 76
3.3.6. Elution profile of ALP activity 77
3.3.7. Mineralisation assay 78
3.3.8. Characterisation of deposited mineral 79
3.4. Discussion: Matrix vesicles. 81
4. HMSC-EVs and their contribution to paracrine signalling 83
4.1. Literature review: human mesenchymal stem cells and their therapeutic properties. 83
4.1.1. Introduction to hMSCs 83
4.1.2. Factors affecting therapeutic use of hMSCs and other stem cells 83
4.1.3. Isolation and identification of hMSCs 85
4.1.4. Differentiation capacity of hMSCs 87
4.1.5. Experimental hMSC therapies and their potential modes of action 88
4.1.6. Cardiac Ischaemia/reperfusion injury 89
4.1.7. MSC soluble factors in treatment of MI and I/R 91
4.1.8. MSC soluble factors in treatment of kidney injury 92
4.1.9. MSC soluble factors in treatment of brain injury 92
4.1.10. MSC EVs in treatment of MI and I/R 93

4.1.11. MSC-EVs in treatment of kidney injury 94
4.1.12. MSC-EVs in treatment of brain injury 95
4.1.13. Summary 96
4.2. Materials and Methods 97
4.3. Results: hMSC-EVs and their role in paracrine signalling 103
4.3.1. Ultrafiltration of hMSC-CM 103
4.3.2. Ultrafiltration of hMSC-CM: membrane pre-blocking 107
4.3.3. Assessing possible loss of activity during concentration of hMSC-CM 110
4.3.4. Equilibrium Dialysis of hMSC-CM 116
4.3.5. Analytical Size Exclusion Chromatography 121
4.3.6. Biological activity of hMSC-EV; resolving the discrepancy 134
4.3.7. hMSC-EVs purification by polymer precipitation 135
4.3.8. Stimulation of angiogenesis with high quantities of pure hMSC-EV 140
4.3.9. EV-Mediated Effect Ratio (EVMER) 143
4.4. Discussion: hMSC-EVs and their role in paracrine signalling 144
4.4.1. Conceptual framework for hMSC paracrine signalling investigation 144
4.4.2. Assessing necessity: conditioned medium without EVs. 144
4.4.3. Assessing sufficiency: direct comparison of separated EVs and protein 146
4.4.4. Resolving the discrepancy 147
4.4.5. Considering quantity 148
4.4.6. Quantifying relative EV potency with EVMER 149
4.4.7. Limitations and caveats 150
4.4.8. Recommendations for EV research 151
5. Future work and conclusions 153
5.1. Future work 153
5.2. Conclusions 157
6. Appendix 158
7. Bibliography 160

List of figures

Figure 1.1: Contents of extracellular vesicles. 16
Figure 1.2: Formation of extracellular vesicles and their interactions with target cells. 18
Figure 2.1: Pre-isolation processing of cell-conditioned media 28
Figure 2.2: Isolation of EVs by ultracentrifugation. 30
Figure 2.3: Density-dependent separation methods 33
Figure 2.4: Purification of EVs by Size Exclusion Chromatography. 34
Figure 2.5: SEC column and sample applicator. 44
Figure 2.6: Evaluation of recovery and processing time from ultrafiltration concentrators. 50
Figure 2.7: Comparison of elution profiles 52
Figure 2.8: Elution of protein and particles from SEC columns. 54
Figure 2.9: Recovery of particles and particle-associated protein from SEC columns. 55
Figure 2.10: Electron microscopy of SEC-purified EVs. 56
Figure 2.11: Detection of EV marker proteins by Western Blot. 57
Figure 2.12: Characterisation of commercial and “homemade” EV-depleted FBS a 59
Figure 2.13: Characterisation of mock-isolated EV-depleted FBS pellets 60
Figure 2.14: Cryo-TEM of h-Pel and c-Pel samples. 60
Figure 2.15: Tubule formation assay to assess proangiogenic effects of c-Pel and h-Pel. 62
Figure 3.1: Calcification of cartilage in a) growth plate and b) articular cartilage. 67
Figure 3.2: Molecular mechanisms of matrix vesicles. 68
Figure 3.3: Isolation of bovine cartilage matrix EVs 73
Figure 3.4: Size of particles isolated from bovine cartilage. 73
Figure 3.5: Recovery of particles and protein from cartilage. 74
Figure 3.6: Influence of magnesium concentration on PNP conversion by FT-EVs. 75
Figure 3.7: ALP activity in particles isolated from each tissue section. 76
Figure 3.8: Elution profile of ALP from SEC column. 77
Figure 3.9: Mineralisation assay images for FT-derived particles 78
Figure 3.10: Characterisation of material deposited by FT-derived particles. 80
Figure 4.1: Isolation of hMSCs from vascular tissues and subsequent differentiation. 86
Figure 4.2: Soluble and EV-associated factors released by hMSCs implicated in their therapeutic effects. 93
Figure 4.3: Investigation of separation performance of 100 kDa membranes. 104
Figure 4.4: Proangiogenic effect of hMSC-CM and sequentially 100 kDa-filtered hMSC-CM batches. 106

Figure 4.5: Separation by 100 kDa membranes after BSA blocking. 108
Figure 4.6: Tubule formation assay for passivated and non-passivated filtration. 109
Figure 4.7: Loss of EVs and VEGF during concentration. 112
Figure 4.8: Tubule formation assay for concentrated/diluted hMSC-CM. 113
Figure 4.9: Scratch wound assay for concentrated/diluted hMSC-CM. 114
Figure 4.10: Equilibrium dialysis of hMSC-CM. 117
Figure 4.11: Tubule formation assay for equilibrium dialysis experiment. 119
Figure 4.12: Scratch wound assay for equilibrium dialysis experiment. 120
Figure 4.13: Analysis plan for analytical SEC 121
Figure 4.14: NTA and Dot blots on analytical SEC fractions 123
Figure 4.15: Protein quantification of analytical SEC fractions 127
Figure 4.16: Quantification of VEGF in analytical SEC fractions. 128
Figure 4.17: Percentage recovery of particles and VEGF during analytical SEC for Donor 1. 129
Figure 4.18: Tubule formation assay for analytical SEC fractions. 130
Figure 4.19: Scratch wound assay for analytical SEC fractions. 132
Figure 4.20: Isolation of hMSC-EVs by TEI and characterisation. 136
Figure 4.21: Tubule formation assay for TEI-isolated EVs. 138
Figure 4.22: Scratch wound assay for TEI-isolated EVs 139
Figure 4.23: Tubule formation assay with high-purity SEC-isolated EVs. 142
Figure 6.1: Initial sucrose cushion purification. 158
Figure 6.2: Evaluation of methods to circumvent pelleting by ultracentrifugation. 159

List of abbreviations

A/A	Antibiotic/Antimycotic
ADP	Adenosine Diphosphate
ALP	Alkaline Phosphatase
Ang 1/2	Angiopoetin 1/2
ANOVA	Analysis of Variance
ATCC	American Type Culture Collection
ATP	Adenosine Triphosphate
BCA	Bicinchoninic Acid
BDNF	Brain-Derived Neurotrophic Factor
bFGF	Basic Fibroblast Growth Factor
BSA	Bovine Serum Albumin
CCM	Concentrated Conditioned Medium
c-FBS	Commercial EV-depleted FBS
CM	Conditioned Medium
c-Pel	Commercial EV-depleted FBS pellet
DGS	Density Gradient Separation
DMEM	Dulbecco's Modified Essential Medium
DMSO	Di-Methyl Sulfoxide
DNA	Deoxyribonucleic Acid
ECM	Extracellular Matrix
ELISA	Enzyme-Linked Immunosorbent Assay
ESC	Embryonic Stem Cell
ESCRT	Endosomal Sorting Complexes Required for Transport
EV	Extracellular vesicle
EVMER	EV-Mediated Effect Ratio
FAL	Float-a-Lyzer
FAL-I	Float-a-Lyzer (Inner compartment)
FAL-O	Float-a-Lyzer (Outer compartment)
FBS	Foetal Bovine Serum
FGF2	Fibroblast Growth Factor 2
FT (Section 3)	Full Thickness
FT (Section 4)	Flowthrough
GDNF	Glial cell line-Derived Growth Factor
GFP	Green Fluorescent Protein
GFR	Growth Factor-Reduced
GPCR	G-Protein Coupled Receptor
GTP	Guanosine Triphosphate
HA	Hydroxyapatite
HDL	High Density Lipoparticle
h-FBS	"Home-made" EV-depleted FBS
HGF	Hepatocyte Growth Factor

hMSC	Human Mesenchymal Stem Cell
h-Pel	“Home-made” EV-depleted FBS pellet
HRP	Horseradish Peroxidase
HUVEC	Human Umbilical Vein Endothelial Cells
I/R	Ischaemia/Reperfusion
IDL	Intermediate Density Lipoparticle
IGF-1	Insulin-like Growth Factor 1
iPSC	Induced Pluripotent Stem Cell
kDa	Kilo-Daltons
LDL	Low Density Lipoparticle
MAPK	Mitogen Activated Kinase
MDZ	Mid/Deep Zone
Mecp2	Methyl-CpG-binding protein 2
MHCII	Major Histocompatability Complex II
MI	Myocardial Infarction
miRNA	Micro RNA
MOI	Multiplicity of Infection
MPS	Mononuclear Phagocyte System
MPTP	Mitochondrial Permeability Transition Pore
mRNA	Messenger RNA
MVB	Multivesicular Body
MWCO	Molecular Weight Cut-Off
NCC	Nucleation Core Complex
NGF	Nerve Growth Factor
NK	Natural Killer
NSF	N-ethylmaleimide-Sensitive Factor
NT-3	Neurotrophin-3
NTA	Nanoparticle Tracking Analysis
o-CPC	o-Cresolphtalein Complexone
PBS	Phosphate-Buffered Saline
PDGF	Platelet-Derived Growth Factor
PEG	Poly-Ethylene Glycol
Pi	Phosphate
PNP	Para-Nitrophenol
PNPP	Para-Nitrophenol phosphate
PPi	Pyrophosphate
PTEN	Phosphatase and Tensin Homologue
PVDF	Polyvinyldiene Fluoride
RIPA	Radioimmunoprecipitation Assay
RNA	Ribonucleic Acid
SBF	Simulated Body Fluid
sCMOS	Scientific Complementary Metal-Oxide Semiconductor
SD	Standard Deviation

SDF	Stromal-Derived Factor
SEC	Size Exclusion Chromatography
SEM	Scanning Electron Microscopy
SMZ	Superficial/Mid Zone
SNAP	Soluble NSF Attachment Protein
SNARE	SNAP Receptor
TB4	Thymosin β-4
TBS	Tris-Buffered Saline
TBS-T	Tris-Buffered Saline with Tween
TEI	Total Exosome Isolation (reagent)
TEM	Transmission Electron Microscopy
TGF-β	Transforming Growth Factor β
TNAP	Tissue Non-Specific Alkaline Phosphatase
UF	Ultrafiltration
v/v	Volume per volume
VEGF	Vascular Endothelial Growth Factor
vLDL	Very Low Density Lipoparticle
w/v	Weight per volume
βGP	B-glycerophosphate

Scope of the thesis

This thesis describes the development and validation of an effective purification strategy for EVs. This purification system was used initially to investigate the properties of matrix vesicles extracted from bovine articular cartilage. Subsequently, this technique was used in the investigation of the contribution of EVs to hMSC paracrine signalling. It was found that conventional soluble signalling factors, but not EVs, were necessary and sufficient for stimulation of angiogenesis and wound healing *in vitro.*

Chapter 1 provides a general introductory review of the history, biology and potential applications of extracellular vesicles.

Chapter 2 provides a critical review of the advantages and disadvantages of commonly-used EV purification strategies and covers the development and validation of the purification techniques used throughout the rest of the thesis.

Chapter 3 provides a brief overview of the function and molecular biology of mineral-forming matrix vesicles. Matrix vesicles were extracted from bovine cartilage and their properties characterised.

Chapter 4 provides a review of the properties of hMSCs and the methods by which they have been reported to mediate paracrine signalling, including via EVs and via soluble factors. The contribution of EVs and soluble factors to hMSC paracrine signalling is investigated by several methods in this chapter.

Chapter 5 provides a summary of the significance of the results of the previous chapters and includes suggestions for future work and overall conclusions.

Chapter 6 is the appendix, and includes preliminary data used in early optimisation of the purification strategy.

1. Introduction to extracellular vesicles

This chapter provides an overview of the history of extracellular vesicle research, the molecular biology of extracellular vesicles, and some of the clinical applications for which they are currently being investigated.

1.1. History of extracellular vesicle research

In 1981, while studying plasma membrane ATPases and 5'-nucleotidases in rat glioma and mouse neuroblastoma cells, Trams *et al* noted that the activity of these enzymes was readily detectable in the cell culture supernatant [1]. As much as 70 % of the enzymatic activity was released into the culture medium over 24 hours, without any indication of cell death or apoptosis. It was found that the activity was mostly eliminated by filtration through a 0.22 μm filter, but mostly retained when filtered with a 0.45 μm filter. Centrifugation resulted in a gelatinous pellet with strong enzymatic activity. Finally, electron micrographs demonstrated the presence of both large (500-1000 nm diameter) and small (~40 nm diameter) lipid vesicles in the pellet. It was concluded that healthy cells were releasing enzymatically active lipid vesicles into their environment. Preliminary investigation suggested that most cell types secreted these vesicles to some degree, and the authors speculated on the possibility that these particles might play a role in signalling. Finally, they suggested a name for these new particles – "exosomes".

Shortly afterwards, a seminal study by Harding et al in 1983 [2] demonstrated that the transferrin receptor in sheep reticulocytes was jettisoned from the cell in lipid vesicles as the cells matured into erythrocytes. In contrast to the Trams paper, these vesicles were observed to originate not from the plasma membrane but from internal membrane structures known as MVBs (multivesicular bodies). These form part of the endolysosomal pathway and conventionally go on to fuse with lysosomes [3] in order to degrade and recycle their contents, and so it was hypothesised that the function of these vesicles was as an alternative disposal mechanism, allowing the maturing cell to dispose of unnecessary protein in bulk. It was only over a decade later, in 1996, that Raposo et al demonstrated strong evidence for a functional role of extracellular vesicles in signalling [4]. It was found that B cell-derived exosomes were enriched for antigen-loaded MHCII (Major Histocompatibility Complex II) and were competent to activate T cell lymphocytes. Since then, extracellular vesicles have been shown to have important roles in coagulation [5], innate [6] and adaptive [4] immunity, morphogenesis [7], the function of spermatozoa [8] and in the progression and metastasis of tumours [9]. Most excitingly from a regenerative medicine perspective, they have been shown to be major mediators of beneficial paracrine effects in experimental stem cell transplantation therapies [10]. The production of

extracellular vesicles seems to be common to all mammalian cells in culture [11] and they have even been isolated from lower metazoa such as helminth worms [12], parasitic protozoa [13], bacteria [14] and plants [15]. Although it is not fully understood how much the underlying mechanisms of formation or functions of EVs between taxa have in common, extracellular vesicles are widespread as a biological structure. EVs have been found to contain a wide range of biological macromolecules including DNA, mRNA, miRNA, soluble and membrane-bound proteins (Figure 1.1) as well as small molecule metabolites. Although the biological cargo of an extracellular vesicle is often reflective of the cell of origin, they are normally enriched for a subset of proteins, nucleic acids and lipids, and depleted of others, compared to their parent cell type [11].

In fact, reference to EVs can be traced back to as early as 1946 [16], as platelet-derived particles that enhance coagulation. Similarly, extracellular vesicles critical in initiating bone mineralisation were described in 1969 [17] by Anderson et al, but were known as “Matrix Vesicles”. It is only recently, with the explosion of research in this field in the last decade, that these phenomena have been conceptually unified, and evidence gathered that they are of common or comparable biological origin [11].

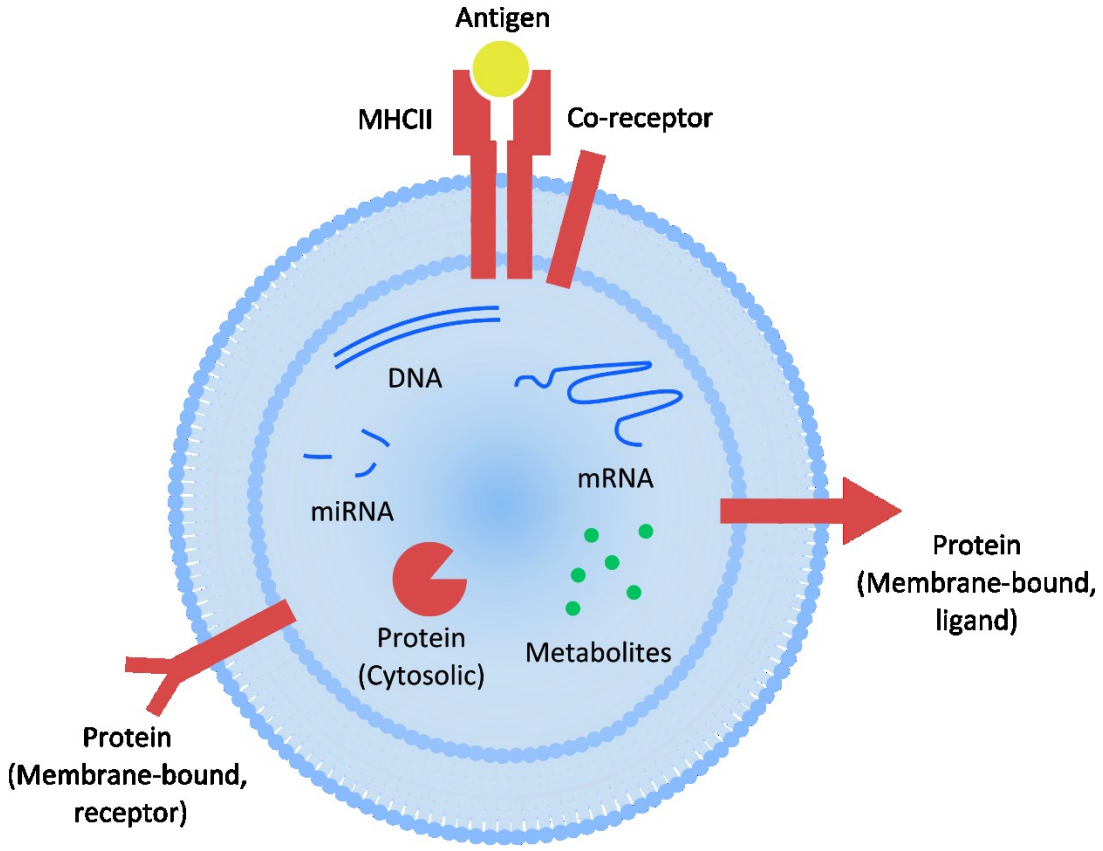


Figure 1.1: Contents of extracellular vesicles. Extracellular vesicles have been shown to present antigens, interact with cells via surface receptors and ligands, and transfer functional protein and RNA to recipient cells.

1.2. Classes of extracellular vesicles

Most cell types generate three major classes of extracellular vesicles, defined by their biological origin within the cell: apoptotic bodies, shedding microvesicles and exosomes (Figure 1.2). Apoptotic bodies are large membranous particles (500 nm diameter and above) that are generated by membrane blebbing during apoptosis [18]. The two major classes of extracellular vesicle typically produced by non-apoptotic cells are exosomes and microvesicles. They have distinct biological origins and some consequent differences in size distribution and expression of marker proteins. However, they have also overlap considerably in these areas and therefore current methods for isolating and purifying extracellular vesicles cannot specifically separate one population from the other [18], and so generate a mixture of the two. Additionally, there are several "special cases" in which a particular cell type or a particular pathology leads to the formation of nonconventional extracellular vesicles. One example is the formation of large oncosomes (1000-10,000 nm) from "pinching" of cellular protrusions, apparently generated only by amoeboid cancer cells [19]. The description "extracellular vesicle" is frequently used as a catch-all term when the identity of the isolate is not clear or is known to be mixed. Indeed, multiple studies have confirmed that EV isolates are typically highly heterogeneous and include multiple molecularly distinct subpopulations of EVs [20-22].

1.2.1. Formation of exosomes

Despite the paper in which the term was coined describing exosomes as large plasma membrane-derived vesicles, the term "exosome" has come to mean specifically vesicles formed as described by Harding et al [2]. The vesicles described by Trams et al [1] would now be considered microvesicles (see section 2.1.3). Exosomes are generated by a complex, multistep process (Figure 1.2). Generally, they are between 40-100 nm in diameter. Initially, late endosomal vesicles invaginate, encapsulating cytosol in internal vesicles. The resulting structures are known as multivesicular bodies [23]. There appear to be at least three mechanisms by which this can occur – ESCRT-(Endosomal Sorting Complexes Required for Transport) dependent, ceramide-dependent, and Tetraspanin-dependent [24]. The exact mechanisms are still poorly understood, and it is not clear why different cell types would be dependent on different mechanisms, or whether multiple mechanisms may act simultaneously.

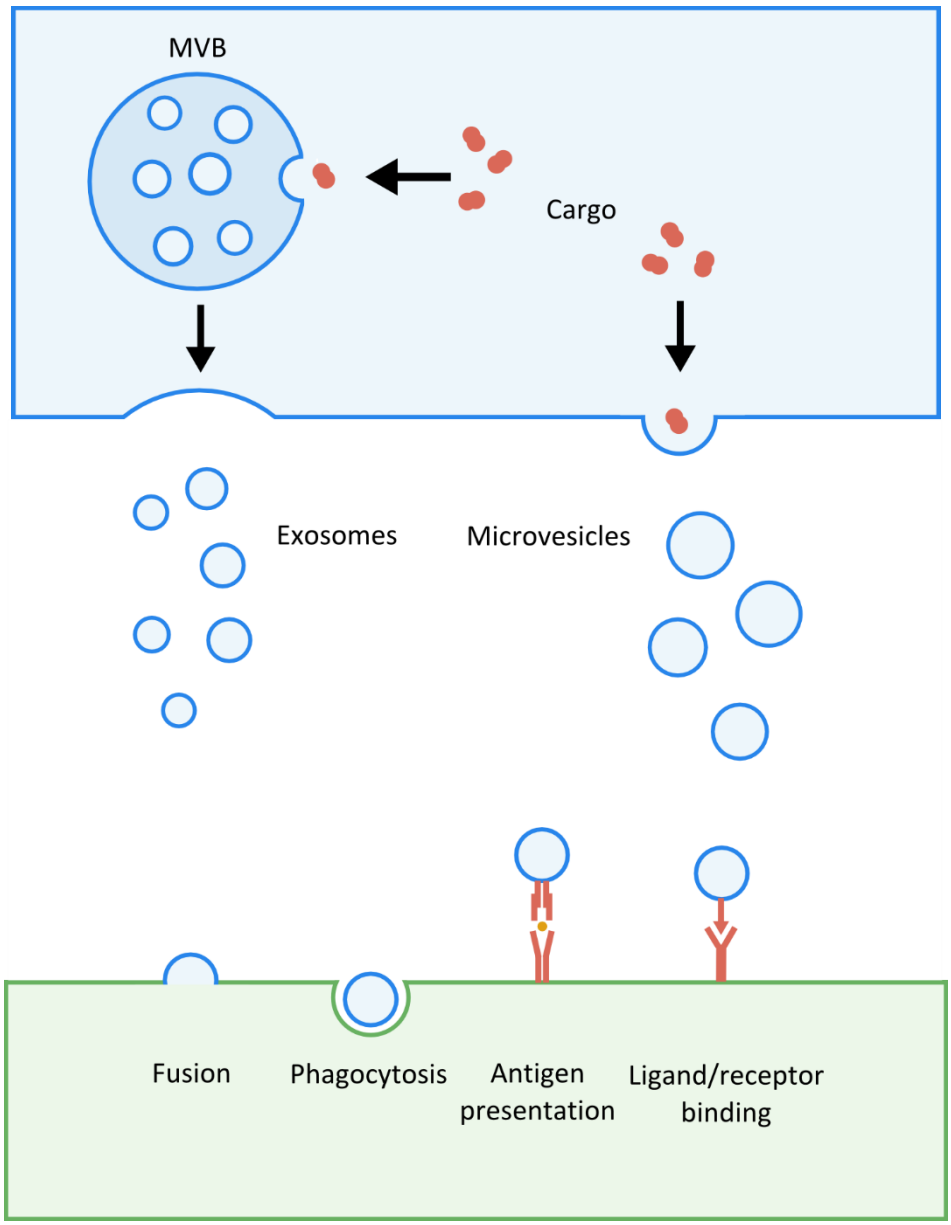


Figure 1.2: *Formation of extracellular vesicles and their interactions with target cells. Exosomes are generated by invagination of late endosomal compartments to form multivesicular bodies, which may then fuse with the plasma membrane. Microvesicles are generated by direct budding from the plasma membrane. Extracellular vesicles may interact with cells via receptor/ligand mediated surface interactions or may be endocytosed by or fuse directly with a cell, transferring their luminal contents.*

It is likely that the mechanism affects the loading of cargo into vesicles. Experiments in which ESCRT genes were silenced led to a reduction in EV secretion and a change in the content of those which remained [24]. Similar results were obtained in studies in which ceramide synthesis was inhibited [25] or tetraspanin expression changed [26]. In general, the mechanisms by which cargo are specifically recognised and incorporated into vesicles are poorly understood, mostly due to a lack of techniques with which to interfere with the processes involved. Similarly, the mechanisms by which MVBs fuse

with the plasma membrane to release exosomes are also poorly understood. It is thought that multivesicular bodies destined for the plasma membrane have a different lipid population to those that will fuse with lysosomes [27]. Fusion is thought to be dependent on SNAP (Soluble NSF(N-ethylmaleimide-sensitive factor) Attachment Protein)/SNARE (SNAP Receptor) complexation [28], in common with vesicle transport mechanisms throughout the intracellular vesicle transport pathway. Both the precise mechanisms and how they are regulated remain incompletely defined.

1.2.2. Formation of microvesicles

In contrast to exosomes, microvesicles are formed by direct budding from the plasma membrane, and are generally between 80-200 nm in diameter or larger (Figure 1.2) [29]. The mechanisms by which cargo are sorted into microvesicles and by which they are released are less well understood than those of exosomes. However, they are known to require much of the molecular machinery common to the rest of the endolysosomal and intracellular vesicular pathways. Namely, release is dependent on the cytoskeleton and associated molecular motors (actin and myosins, and microtubules and kinesins), small Rab-family GTPases (which act as a point of signal integration and "decision-making") and SNARE-family membrane-fusing proteins and their associated medium-range tethers [30].

1.3. Content of extracellular vesicles

As a multifunctional signalling platform, EVs are diverse in content. Proteins, mRNA, miRNA, lipids and even DNA and whole mitochondria have all been shown to be incorporated into and transferred by EVs [11]. Their cargo is thought to be influenced by the cell type, and the stimulus (if any) to which the cell is responding. In general, exosomes and microvesicles are enriched for molecules that are thought to be involved in membrane sorting and EV biogenesis including tetraspanins, TSG101 and Alix. These proteins are generally considered to be reasonable molecular markers for EVs [29]. Different vesicle subpopulations may contain different populations and relative abundances of these proteins.

Aside from proteins that might be considered structural or remaining from biogenesis, there is little consistency in content between vesicles isolated from different sources. The extent to which this heterogeneity reflects genuine physiological diversity is not entirely clear, as proteomic and transcriptomic profiling of extracellular vesicles has been found to be highly dependent on the method of isolation [11, 31] and many -omics studies of vesicular content draw conclusions from a single replicate. In one of the few exceptions to this practice, Lai et al showed that only approximately a third of the total proteins detected in three EV preparations from the same cell line were detected in all three preparations [32]. Efforts have been made to catalogue and standardise EV 'omics studies via a manually curated database (ExoCarta) [33]. The following sections will focus on well-established examples of functional transfer of specific macromolecules.

1.3.1. Membrane-bound proteins

Perhaps the most well-established physiological roles of extracellular vesicles are in immunological signalling, in which they have been shown to carry out a multitude of functions [11]. Raposo et al demonstrated that B lymphocytes release exosomes containing functional, antigen-loaded MHCII molecules [4]. These exosomes were able to stimulate antigen-specific T cell responses when presented to T lymphocytes *in vitro*. Subsequently, Théry et al demonstrated that dendritic cell-derived exosomes were also capable of antigen presentation and could activate T cells *in vitro* and *in vivo* [34]. The likely benefit of this process is a massive amplification in the number of antigen-presenting particles, which is thought to allow a more rapid and effective response. This is thought to be primarily a surface interaction exclusively involving membrane-bound proteins, with uptake or fusion of antigen-presenting EVs not being necessary for the response. Similarly, Natural Killer (NK) cell-derived EVs present functional death receptor ligands and perforins and can induce apoptosis of tumour cells *in vitro* [6]. It is also thought that dendritic cells capture circulating EVs as part of their immune surveillance system for foreign antigens [35, 36].

1.3.2. Luminal proteins

Most of the established roles of EVs in the immune system are essentially as extensions of the cell membrane of a signalling cell and involve EV-cell contact rather than fusion or uptake [11]. Proteins are therefore not necessarily transferred to the recipient cell. A physiological process in which transfer of the luminal protein cargo of EVs is thought to be important is that of spermatocyte maturation. Because spermatozoa have very limited biosynthetic capacity [37] it is considered likely that protein transfer from external sources could be required in order to enact a change in cell identity. After leaving the testes, spermatozoa travel down the epididymis, a long, coiled tract which leads to the vas deferens. The epididymal epithelial cells release EVs that directly fuse to spermatocytes, transferring cytosolic and membrane-bound proteins that are thought to contribute to maturation, including membrane proteins that are critical for binding to the oocyte [38], and cytosolic proteins that allow conversion of glucose into fructose, which spermatozoa rely on heavily as an energy source [39]. Similarly, spermatozoa later come into contact with EVs generated by the prostate (prostasomes), which are thought to transfer proteins directly to spermatozoa in order to increase their motility, prime their acrosomes and potentiate them to fuse with the oocyte [40].

1.3.3. RNA

One of the more surprising and exciting properties of extracellular vesicles is their apparent ability to transfer functional mRNA and miRNA between cells. This was first shown for exosomes in 2007 by Valadi et al [41]. In their landmark study, they isolated exosomes from a series of human and mouse

mast cell lines. They detected both polyadenylated (mRNA) and short RNAs (miRNAs) in their samples and found that transcripts of approximately 1300 genes were present. As the transcripts were insensitive to RNAse treatment, they were concluded to be physically encapsulated inside the exosomes. Importantly, they showed that the transcripts were functional, in that they could be translated *in vitro* into full-length, functional proteins, and therefore were not damaged or truncated. Most importantly, they demonstrated that mouse mast cell-derived exosomes, when administered to human mast cells, led to de novo translation of mouse-specific proteins. Similar work by Ratajczak et al in 2006 [42] had previously suggested that microvesicles could transfer functional mRNA. However, there is relatively little evidence as of yet that this is a major function of extracellular vesicles *in vivo* [11]. *In vitro* studies often use extremely high concentrations of extracellular vesicles, which may be of questionable physiological relevance. Recently, a quantitative study of the abundance of miRNA transcripts and total number of extracellular vesicles in a cancer-derived extracellular vesicle samples concluded that there is less than one miRNA molecule per hundred vesicles [43]. Studies in which direct cell-cell communication via exosomes is observed, rather than in which exosomes are harvested and then applied separately, may be considered more persuasive. As an example of the former study, Mittelbrunn et al demonstrated direct transfer of miRNAs from T cells to antigen-presenting cells at the immunological synapse, dependent on cell-to-cell contact [44]. Recent work has established a putative mechanism by which miRNAs are loaded into EVs, via an RNA trafficking protein, hnRNPA2B1. HnRNPA2B1 has been shown to specifically recognise a tetranucleotide sequence (GGAG), specifically enriched in miRNAs found in EVs [45]. Similarly, a consensus sequence in the 3' untranslated region of mRNAs has been defined which appears to be enriched in mRNAs found in EVs [46].

From a pragmatic point of view, to a certain extent the physiological relevance is unimportant as long as the exosomes in question have therapeutic utility. In addition to intrinsic therapeutic effects that may not necessarily reflect a physiological *in vivo* process, such as the use of MSC-EVs (see section 2.4.1) extracellular vesicles can be modified to act as a carrier for therapeutic RNAs, either by direct loading of previously harvested vesicles [47] or by transfection of the EV-producing cell [48].

1.3.4. DNA

Surprisingly, the presence of DNA in EVs has also been reported [49]. It is questionable as to whether this is involved in functional communication between cells, and to the best of the author's knowledge, no study has yet shown functional transfer of DNA by EVs in a physiological context. Research on the DNA content of EVs is very much within the context of cancer biomarkers, and it has been shown that DNA is shed in cancer-derived EVs non-specifically – indeed, the entire genome is represented [49].

Apoptotic bodies contain DNA and have been shown to be able to transfer oncogenes between cells [50]. Concerningly, it has recently been demonstrated that transfected plasmids can be transferred between cells by EVs [51], which brings into question the methods of many studies in which transfer of a reporter RNA was demonstrated. This may have implications beyond the EV field, as it is likely that many cell biology experiments have been designed with the assumption that plasmids cannot be transferred via soluble factors between mammalian cells.

1.3.5. Lipids

Lipidomics as a field is still very much in infancy, and the full extent of the contribution of bioactive lipids to biological processes is not yet fully understood. The lipid population of an extracellular vesicle is generally enriched for cholesterol, phosphatidylserine, glycosphingolipids and sphingomyelin. These lipids are specifically sorted into the developing vesicles and likely contribute to their formation [52]. It is likely that this complex mixture of lipids contributes to the stability of EV in the extracellular environment – synthetic liposomes containing a varied lipid population have enhanced stability compared to monolipid liposomes [53]. They are also biologically active – sphingomyelin promotes angiogenesis, and this has been shown to contribute to the pro-angiogenic properties of tumour-derived EVs [54]. G-protein coupled receptor (GPCR) activation-triggered lymphocyte chemotaxis and dendritic cell maturation have been proposed to be stimulated by vesicle-mediated transfer of lysophosphatidycholine [23].

1.4. Extracellular vesicle interactions with recipient cells

There is a wealth of evidence that the luminal contents of EVs are delivered to target cells. Quite aside from demonstration of functional transfer of macromolecules, fluorescent dye labelling [55] and luciferase-based [56] approaches have allowed transfer to be visualised in real time by microscopy. As EVs are essentially thought of as physiological liposomes, the most conceptually obvious mechanism by which they could interact with target cells would be membrane fusion. In fact, although this occurs, it appears that EVs are most frequently actively internalised by the cell using cytoskeleton-dependent mechanisms such as endocytosis and phagocytosis (Figure 1.2) [57]. Direct fusion of cell membranes can only occur when they are of similar fluidity. EVs and their parent cells generally have distinct membrane compositions [23] and so it is thought that direct fusion can only occur with certain cell types or at acidic pH values [11]. In terms of active uptake, there is little consensus on the signals that are recognised by the cell, which of the many forms of active uptake is predominantly responsible for EV internalisation, or if EV uptake is constitutive and non-specific or regulated and specific [57]. It is likely that all of these parameters are dependent on the exact identity of the vesicle and recipient cell.

Some EV/cell interactions do not in fact transfer of EV contents to the cell cytosol. Instead, interaction between receptors on the cell and ligands on the EV membrane surface can occur without fusion. Perhaps the most well-established example of this interaction paradigm is the interaction of NK cell-derived EVs with cell surface death receptors [6]. NK-cell derived EVs bear both markers of NK cells and Fas ligand, a well-established inducer of programmed cell death. These EVs were able to crosslink cell surface death receptors and induce apoptosis in a variety of cells, entirely without membrane fusion.

1.5. Clinical potential of extracellular vesicles

The fact that extracellular vesicles tend to have similar membrane and luminal compositions to their parent cells [58] has inspired a range of potential applications of extracellular vesicles to human health. Broadly speaking, they may be divided into three overarching categories:

1. Use of extracellular vesicles as a “liquid biopsy” for diagnostics.
2. Use of extracellular vesicles as a drug delivery vehicle.
3. Use of extracellular vesicles as biotherapeutics.

1.5.1. Extracellular vesicles as diagnostic targets

Extracellular vesicles have been found in all biofluids so far tested, including plasma [59], urine [60], saliva [61] and semen [62]. They are released into the circulation by cells throughout the body. Therefore, tissues in a disease state may produce vesicles with contents reflecting that disease state that could be detected in biofluids. This might reduce the need for tissue biopsies, which in some cases are quite invasive and associated with morbidity [63]. Tissue biopsies may also only take a sample from one or a subset of locations, risking the possibility of misdiagnosis [64, 65] (e.g. by not sampling the invasive edge of a malignant tumour). In contrast, vesicles may be produced by all parts of the tissue and loaded with disease-associated markers. Most current research into exosome diagnostics is focused on the diagnosis of cancer and aim to discriminate between cancerous and healthy tissue by the presence of cancer-associated miRNAs [66-68]. One such diagnostic for ovarian cancer has reached the commercial market [69].

1.5.2. Extracellular vesicles as drug delivery vehicles

Extracellular vesicles are being explored as drug delivery vehicles. Liposomes used for drug delivery are generally comprised of a few lipids, with secondary modifications for passivation or targeting [70]. By contrast, EVs are complex and heterogenous, with a complex lipid, protein and nucleic acid population. It is typically asserted that the advantage of using EVs for drug delivery is their biological membrane. In particular, it is claimed that EVs from certain cell sources are either specifically targeted to certain tissues [71] or immunologically privileged [72]. However, these properties have only been

demonstrated to a limited extent, and only for certain cell types. There is little evidence to suggest that these are general properties of EVs. Typically, studies involving targeted delivery of EVs to tissue use EVs from recombinant cells designed to target a specific pre-designated receptor [73, 74]. Most studies show that the majority of EVs injected systemically are shortly found in the liver, spleen, lung and kidneys [75, 76], including studies where the EVs were engineered for targeting to a specific tissue [73, 74]. EVs appear to be targeted by the mononuclear phagocyte system (MPS) for destruction and clearance. Systemically injected EVs are generally found to be cleared from the circulation within 24 hours and in one case as little as 10 minutes [75], whereas a current clinically approved "stealth" liposome drug has a half-life of approximately 48 hours [77]. Additionally, although it is commonly asserted that human mesenchymal stem cell – derived EVs are immunologically privileged due to shared properties with their parent cell type and *in vitro* immunoregulatory properties [71], it does not appear that it has been experimentally demonstrated that they avoid the MPS response, or that these properties have other relevance to their suitability for systemic drug delivery.

Moreover, use of EVs as drug delivery vehicles has considerable practical challenges compared to the use of liposomes. Manufacturing high quantities of liposomes is relatively inexpensive in terms of both materials and labour, whereas high-quantity EV manufacture is painstaking, time-consuming, low-throughput and orders of magnitude more expensive [78]. Additionally, drug loading is not as straightforward. Liposomes can be formed around cargo drugs, whereas intact EVs must be loaded externally. This involves permeabilisation of the EVs by electroporation, saponification or other processes [79], which necessarily limits the loading efficiency. Overall, it is not clear whether the potential benefits of the use of EVs as drug delivery vehicles will be sufficiently realised to outweigh their practical, clinical and financial disadvantages. However, the field is relatively young and may yet overcome these limitations, and GMP-compliant large-scale exosome manufacturing processes are being developed [80, 81].

1.5.3. Extracellular vesicles as biotherapeutics

As extracellular vesicles are known to be similar to their parent cells in terms of their membrane composition and luminal content, it is possible that they may be able to recapitulate some of the functions of their parent cells. There are two outstanding avenues of research in this area: the use of EVs as vaccines, and the use of EVs to replace stem cells in stem cell therapies.

EVs produced by dendritic cells and other antigen-presenting cells are themselves competent to present antigen processed by their parental cells and can mediate full lymphocyte activation and a productive adaptive immune response [82]. Live cell "vaccines" for cancer therapy are a promising future therapeutic. Some treatments have already been approved – a live dendritic cell vaccine for prostate cancer [83], and genetically modified T-lymphocytes for acute lymphoblastic leukaemia [84]. However, there are problems associated with live cell vaccines, most of which come down to the high cost of extracting, expanding and otherwise processing the cells within appropriate clinical facilities [84]. Additionally, cells must be autologous. Potentially, EV therapeutics may not necessarily need to be autologous, and it may be possible to reduce the cost of manufacture compared to live cells. Several studies have investigated the potential of EVs from antigen-primed cells to stimulate an effective immune response, including several Phase I trials [85-87]. However, so far it has proved challenging to mount a robust immune response using EVs [88]. The major future direction of the field is to investigate ways to increase the immunostimulatory potency of EVs.

Stem cell-derived EVs are a major area of investigation for biotherapeutics and regenerative medicine. This will be discussed in much greater detail in section 4.1, as the use of human mesenchymal stem cell (hMSC)-derived EVs is the main focus of this project. Briefly, EVs from stem cells – particularly from hMSCs – are thought to be a potential replacement for stem cell transplants. Initially, stem cell therapies for injuries involving dead or seriously damaged tissue (such as myocardial infarction, stroke, kidney and liver damage) were proposed on the rationale that stem cells could migrate to and take up residence at the site of injury before differentiating into new, functional tissue. However, it has been found that in general, transplanted stem cells do not engraft in significant numbers, nor do they significantly differentiate into appropriate tissue. Despite this, many studies report a therapeutic effect [89]. It is thought that this effect is mediated by paracrine signalling from the stem cells to the injured tissue. Several studies have implicated extracellular vesicles as the major paracrine factor in this process [90]. The evidence from this study for EV-mediated signalling in the paracrine effect will be explored in section 4.3.

2. Methods for extracellular vesicle isolation

2.1. Literature review

The isolation of EVs represents a considerable challenge. When starting from cell culture media or biofluids, EVs are often present in relatively low quantities, yet potential contaminants (typically soluble protein in cell culture media, but also larger protein and lipoprotein complexes in biofluids and plasma) are present in relatively high quantities. These potential contaminants may potentially themselves be bioactive and able to influence downstream analysis of biological activity, leading to false or exaggerated identification of EVs as signalling molecules. There is an increasing concern in the field that some commonly used isolation techniques are prone to contamination or excessive loss of EVs [91].

The essential challenge for any isolation technique is to recover as many EVs as possible while removing as many contaminating factors as possible. Fundamentally, to separate EVs from other factors one must exploit a characteristic of EVs not widely shared by potential contaminants. The characteristics most frequently used are size, density, and specific epitopes. Typically, there are two stages to an EV isolation protocol: concentration and purification. Typically, EVs are initially concentrated from their relatively dilute state in the media or biofluid, before a secondary process to remove contaminants. Some biofluids such as plasma have high initial concentrations and a concentration stage is not necessary. The purified EVs may then be concentrated again if necessary. Some protocols are essentially concentration-only, with little consideration given to secondary purification beyond removal of media/biofluid supernatant. Commonly used protocols will be discussed here, considering their mechanism of action, primary use (i.e. concentration or purification), and their limitations and pitfalls. It is also important to consider the source of the EV sample and the potential contaminants that can be expected from it.

2.1.1. Sample collection

EVs have been isolated from a wide variety of biofluids, including plasma [92], sweat [93], milk [94], semen [62], urine [60] and saliva [95]. It is even possible to isolate tissue-derived EVs by enzymatic dissociation of solid tissues [96]. Some biofluids require treatment prior to EV isolation: for example, blood must be collected in a blood tube containing an anticoagulant and undergoes additional centrifugation to remove platelet fragments [97]. However, most studies on EVs involve isolation from cells grown in culture. Typically, prior to collection cells are grown in standard tissue culture flasks to near-confluency in their standard growth media. Cell culture media typically contain Foetal Bovine Serum (FBS), a blood product with a very high concentration of bovine EVs [98]. It is therefore

necessary to omit FBS from the cell culture medium for the duration of EV collection to avoid contamination. Many cell types readily tolerate short periods without FBS. However, others will die in sufficient quantities to risk substantial contamination with apoptotic bodies and other cellular debris. For these cell types, researchers may choose to reduce the collection time or utilise chemically defined media that can partially or wholly compensate for the lack of FBS-derived growth factors. However, the most common solution is to use EV-depleted FBS.

2.1.1.1. EV-depleted FBS

EV-depleted FBS may either be purchased commercially or prepared by the researcher. Typically, EV-depleted FBS is prepared by ultracentrifugation of FBS at over 100,000 g. The supernatant is retained and the pellet, containing EVs and other particulate material, is discarded. FBS may be diluted prior to ultracentrifugation to reduce viscosity, and the literature differs on the appropriate timescale of ultracentrifugation (between 3 and 24 hours is common). It was recently demonstrated that > 18 hours ultracentrifugation is necessary for substantial bovine EV depletion [98]. The methods used to prepare commercial EV-depleted FBS are proprietary but are likely to be broadly similar with the possible addition of a Poly-Ethylene Glycol (PEG) to further assist in pull-down of EVs (US patent no. US9005888B2). However, no technique is considered to be able to completely remove EVs – in all cases, remaining EVs are still present and may still co-isolate with EVs produced by cells. It has been found that the use of EV-depleted FBS leads to a slower cell growth rate and alters the expression profile of skeletal myoblasts in culture [99]. This may be due to depletion of EVs themselves, or off-target depletion of soluble proteins.

Due to their high initial concentration in FBS, even if over 95 % of EVs are removed the remaining minority may be a substantial population compared to the EVs produced by cells, and there is therefore still a substantial risk of contamination. Recent work has demonstrated that bovine RNA transcripts are frequently found in publicly available human EV RNA databases, and that many RNAs thought to be enriched in EV populations are in fact misidentified bovine RNAs present at high concentrations in FBS – notably miR-122, miR-451a and miR-1246 [100]. The same study also found that extended ultracentrifugation of FBS did not remove the majority of vesicles. The risks of contamination from EV-depleted FBS could be mitigated by use of a negative control in which the same experimental purification and analysis procedures are performed on the media before and after cell conditioning – however, this experimental approach is not frequently used.

2.1.1.2. Post-collection and processing

After collection of media from cells, it is important to remove all detached cells and any large cellular debris. This is typically achieved by a combination of centrifugation and filtration (Figure 2.1). Commonly, freshly isolated media might be centrifuged at 500 g for five minutes to pellet cells, before centrifugation at 5000 g for 15 minutes to pellet debris. The media may then be passed through a 0.22 µm or 0.45 µm filter to remove any leftover large material. The centrifugation and filtration steps may be performed alone. Filtration may be performed without centrifugation when it is necessary to process large volumes (i.e. several litres). With centrifugation alone, it is potentially possible that some debris might not be removed. With filtration alone, it is possible that under pressure cells and larger debris will be damaged and forced through the pores of the filter. However, to the best of the author's knowledge this has not been observed. After processing, conditioned media is typically stored at -80 °C until use.

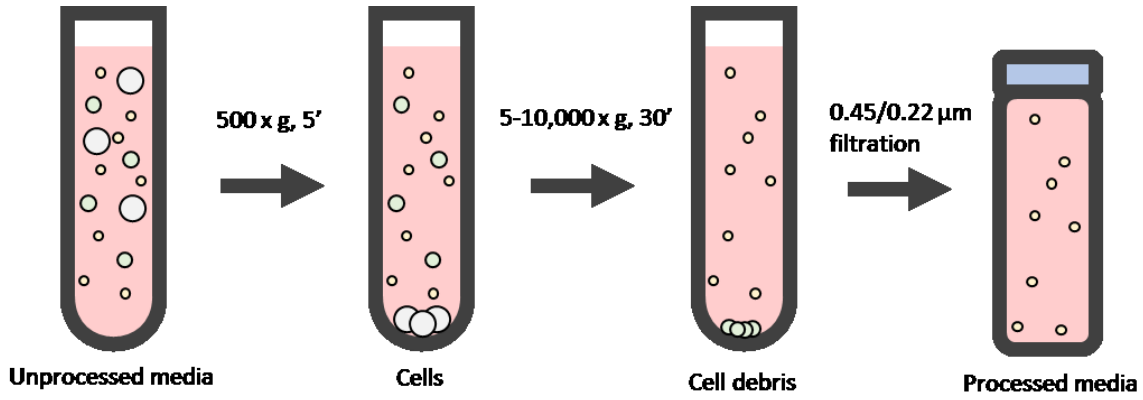


Figure 2.1: Pre-isolation processing of cell-conditioned media. As described in text, cells and debris are pelleted before filtration through a 0.45/0.22 µm membrane.

2.1.2. Methods of concentration

EVs are typically present at relatively low concentrations in conditioned media, and it is necessary to increase their concentration before using them. The techniques discussed here are used to this effect. Many of these techniques may be used with or without further purification or repeated once to "wash" the EV concentrate.

2.1.2.1. Ultracentrifugation

Ultracentrifugation was the first technique used to isolate EVs, and according to a survey conducted in 2016 is still the most commonly used technique in the field [101], with 81 % of respondents using it in some capacity within their workflow. There are a number of reasons for the enduring popularity of this technique. Firstly, it is inexpensive. Although ultracentrifuges have a high up-front cost, they are commonly already available within a research department. Depending on their material and form factor, ultracentrifuge tubes are either disposable and inexpensive or expensive but reusable. Secondly, it is well-suited to processing large volumes of media with minimal hands-on time. Researchers using cell culture media as a starting material may process over 100 ml of medium per isolation [101]. An ultracentrifuge fitted with a Beckman-Coulter Ti-45 rotor can accept up to 350 ml of sample at a time. Thirdly, it is well-established and accepted within the field, with multiple established protocols and troubleshooting resources available.

A typical ultracentrifugation protocol involves pre-processing steps as described in section 2.1.1.2, before centrifugation at approximately 100,000 g for between 1-3 hours [102], sometimes repeated as a washing step (Figure 2.2). However, a wide variety of different rotors and centrifuge tube volumes are in use, yet few studies adjust for the k-factor of their rotor or consider how the volume of media will affect the time or force required for EV sedimentation. The implications of this source of variation have been investigated [103] and it is thought that this may contribute to inconsistency in recovery efficiency as described in the literature. Prior to this stage, a lower-speed spin at approximately 20,000 g is sometimes used [102]. This is intended to isolate only the larger microvesicles, leaving exosomes in solution. However, it is now well-known that the sizes of exosomes and microvesicles overlap substantially and they thus cannot be fully separated by this method. Additionally, while larger particles may travel faster under centrifugation, smaller particles near the bottom of the tube will still travel far enough to be incorporated into the pellet [104]. The viscosity of the fluid is also known to affect sedimentation speed [105], and is likely to vary between biofluids and cell culture media, yet is not widely taken into account or reported.

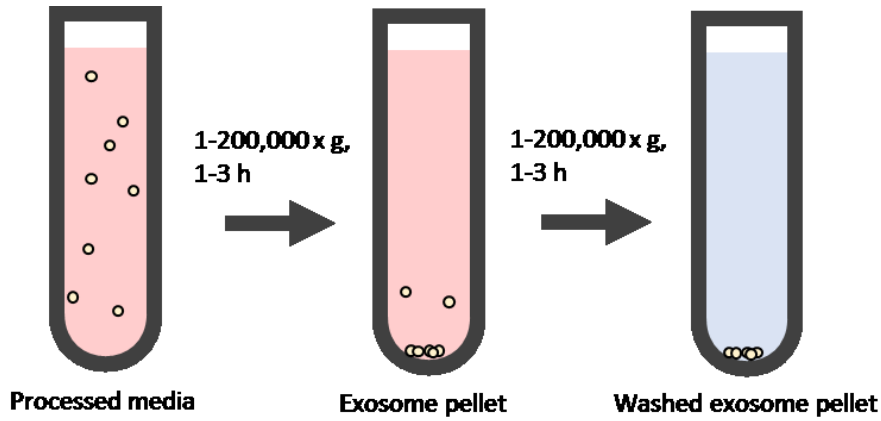


Figure 2.2: Isolation of EVs by ultracentrifugation.

The efficiency of this technique and the purity of the resulting sample are a source of some debate. Recovery efficiency can be estimated by a number of techniques including particle concentration, RNA concentration, or the concentration of EV biomarkers. Between different biofluids and cell culture media, the reported recovery efficiency varies from less than 1 % to over 30 % [105, 106]. Moreover, this technique is prone to contamination from non-vesicular proteins. This may occur by co-sedimentation of high molecular weight protein complexes or lower molecular weight proteins initially present towards the bottom of the tube, or by carry-over of supernatant when resuspending the pellet. Co-sedimentation of large complexes is a particular issue for blood plasma samples, as lipoprotein particles are similar in size to EVs and highly abundant [107]. In general, ultracentrifugation has been found to be ineffective in removing non-EV proteins [108], even if an additional washing step is included. Many studies combine ultracentrifugation with additional downstream purification methods for this reason [101]. There is also some indication that ultracentrifugation can damage EVs and cause aggregation [109].

2.1.2.2. Ultrafiltration

Ultrafiltration (UF) may be used to concentrate the initial EV-containing media or biofluid, prior to additional purification steps. By this method, the initial sample is forced against a membrane containing nano-scale pores that allow the passage of water and smaller biomolecules, but not extracellular vesicles. Typically, a pore size of 100 kDa (~ 7 nm) is used. The required force may be applied either by pressurisation or centrifugation of the ultrafiltration chamber. Current opinion in the field holds that this process is less damaging to extracellular vesicles than ultracentrifugation [109], as the extracellular vesicles are never taken out of solution and there is little evidence of aggregation. By contrast, aggregation is a known consequence of ultracentrifugation [109]. However, extracellular vesicles are lost during this process. It is thought that this at least partially due to adherence to the membrane itself. A recent study has suggested that this can vary with membrane material and pore

size, and that 10 kDa regenerated cellulose membranes recover considerably more than other available concentrators [110]. Use of centrifugal concentrators with low membrane surface areas was found to maximise recovery, compared to pressure-driven, high surface area devices [111]. The same study also found that ultrafiltration recovered approximately twice as many particles from the original sample as ultracentrifugation. Other studies have confirmed that ultrafiltration has a good recovery efficiency and does not damage EVs [109, 112, 113].

Ultrafiltration does not reduce the concentration of non-EV material in the final concentrate. This could in theory be achieved by repeated washing and re-concentration, but in practice this is not done. Unlike ultracentrifugation, ultrafiltration is typically only used as an initial concentration step before downstream processing to remove contaminants, typically by size exclusion chromatography (2.1.3.2).

2.1.2.3. Polymer Precipitation

Recently, several proprietary products have arrived on the commercial market which propose to offer fast and straightforward isolation of EVs from biofluids or conditioned medium. Exoquick (SBI), Total Exosome Isolation Reagent (Invitrogen), and miRCURY (Qiagen) isolation kits contain long, volume-excluding polymers, the exact identities of which are not disclosed - however, a patent filed for Total Exosome Isolation Reagent makes reference to poly-ethylene glycols (PEG), poly-vinyls and dextrans (Patent: US20130273544A1). By binding water molecules that would otherwise form hydration shells, they cause extracellular vesicles (and, potentially, other molecules) to precipitate out of solution. They can then be pelleted by a relatively low-speed centrifugation (10,000 g). Similar principles have long been used to purify virions using long PEG molecules [114], and indeed PEG has also been used to isolate extracellular vesicles without use of commercial kits by similar methods [115, 116]. These kits are popular due to their ease of use and short hands-on time, as well as their integration within product lines that simplify exosomal protein and RNA analysis.

However, despite their advantages in terms of ease of use, the suitability of these products is increasingly under question due to mounting evidence that they are prone to co-isolation of non-vesicular material. In a study by Van Deun et al [117], they were demonstrated to co-isolate non-EV particles, RNA, and soluble protein. Samples isolated by Exoquick or TEI were found to contain approximately 3 and 10 times more protein respectively per 10^8 particles than samples purified by a high stringency method; Optiprep density gradient separation (DGS) (section 1.3.1.). Exoquick and TEI were also found to isolate over 50 times more RNA per particle than DGS. This indicates contamination with non-EV material. Non-EV proteins including albumin and apolipoprotein E were detected, as were RNA-containing Argonaute complexes. It is worth noting that the study also tested an ultracentrifugation-only technique as described in section 1.2.1., and also noted the presence of the

same contaminants in the final sample. Other studies have also noted that these techniques are prone to co-isolation of contaminants, appear to affect the structure of the vesicles, and that the contaminants may impact viability when cells are treated with isolated EVs [118]. There is also potential for carry-over of the polymers themselves.

2.1.2.4. Affinity Capture

Extracellular vesicles characteristically contain membrane-associated Tetraspanin proteins, as a consequence of their biogenesis [119]. Of these, CD63, CD81 and CD9 are frequently used as markers for EVs. Since these proteins are present as a direct result of EV biogenesis, they are assumed to be almost always present on individual EVs, and so are considered a suitable target for immunoaffinity capture. Magnetic beads or columns containing resin conjugated to antibodies against CD63 or other EV markers may be used to capture EVs from solution [120].

In general, this technique is not in wide use as a primary EV isolation method due to the high cost of antibodies and difficulty in processing large volumes. Other, arguably less specific affinity capture techniques have been developed which are inexpensive. EVs have been found to bind Heparin, and this interaction has been used to isolate intact and functional EVs at a low cost [121]. However, the purity of the resulting sample has not been extensively evaluated. It is also possible that due to the heterogeneity of extracellular vesicle populations [22], purifying by a single epitope will bias the resulting isolated population by favouring EVs that have high expression of that epitope. Affinity-based capture systems have the advantage of suitability for low volumes and in some cases are suitable to capture EVs directly from complex biofluids with little additional processing. They are therefore being explored for integration into microfluidic point of care devices for diagnostics [122]. Affinity capture may also be used as a “clean-up” technique to allow the washing away of contaminants after previous isolation and/or concentration by other methods.

2.1.3. Purification methods

Concentration methods allow EVs to be collected from initially dilute biofluids and cell culture medium. Some methods, such as ultracentrifugation, may be used alone or with a single wash. However, as previously discussed, these methods are prone to co-isolation of non-EV material and so further purification is often considered desirable. Besides the possibility of affinity capture as a purification method, as discussed in section 1.2.4, purification is typically achieved by density or size-dependent separation of EVs.

2.1.3.1. Density-dependent centrifugation methods

Density-dependent methods of EV purification are long-standing in the field and are considered by many to be the "gold standard", having been introduced in Raposo's original 1996 study [4] which first attributed a biological role to exosomes. EVs typically have a density between 1.08 and 1.22 g/ml [4], whereas proteins have an approximate density of 1.35 g/ml [123] and nucleic acids a density of 1.71 g/ml [124]. This difference can be exploited to separate EVs from contaminants, either by allowing the sample to fully equilibrate within a density gradient (isopycnic separation) or by the different rates at which components of the sample pass through a dense solution under centrifugation (rate zonal centrifugation) (Figure 2.3).

In isopycnic ultracentrifugation, a density gradient is constructed that spans a wide density range. Sucrose gradients are commonly used [4], however high-concentration sucrose solutions may represent an osmotic stress for vesicles. To avoid this, isosmotic solutions of different densities can be prepared with Iodixanol [111]. Continuous linear gradients may be prepared by use of a gradient mixer, or discontinuous gradients may be prepared by gently layering media of decreasing densities within the ultracentrifuge tube. Discontinuous gradients are often advantageous for preparative techniques, as the densities of the layers can be chosen such that the entire EV population is captured at the interface between two layers. With this approach, EVs should move to the region of identical density (the isopycnic zone) within the gradient and should not pellet out of solution. The sample may initially be layered at the bottom or top of the tube or dispersed throughout the initial medium. However, the time required for the solution to reach equilibrium may be prohibitive. The original protocol suggests a 15-hour centrifugation [4], but subsequent studies have suggested that several days may be necessary for certain vesicle types [21, 125].

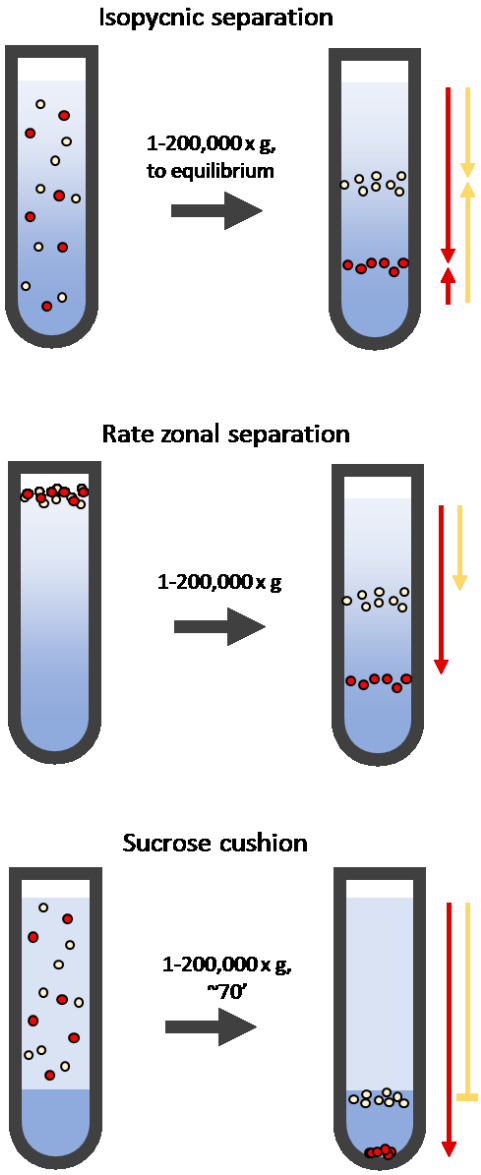


Figure 2.3: Density-dependent separation methods

By contrast, rate-zonal centrifugation does not rely on equilibration of the sample. Samples are added to the top of a pre-formed gradient and centrifuged for a shorter length of time, in order to separate by the rate at which components of the sample travel through the density gradient. This does not separate strictly by density, as particles of identical density but different sizes will sediment at different rates. The separation process is dynamic and time-dependent, and it is possible for the entire sample to pellet at the bottom of the tube if the run time is too long. It is also possible for the process to be run in reverse, with sample initially at the bottom of the tube, and the density gradient chosen such that EVs rise and contaminants stay at the bottom. A commonly used variant of this process is the sucrose cushion [126]. In this process, the EV-containing media is underlaid with a relatively low volume of high-density sucrose (typically 30 % w/v in D_2O), which serves to capture EVs but allows higher-density contaminants to pass through to the bottom of the tube. The cushion can then be retrieved and washed to remove the sucrose and D_2O and recover EVs.

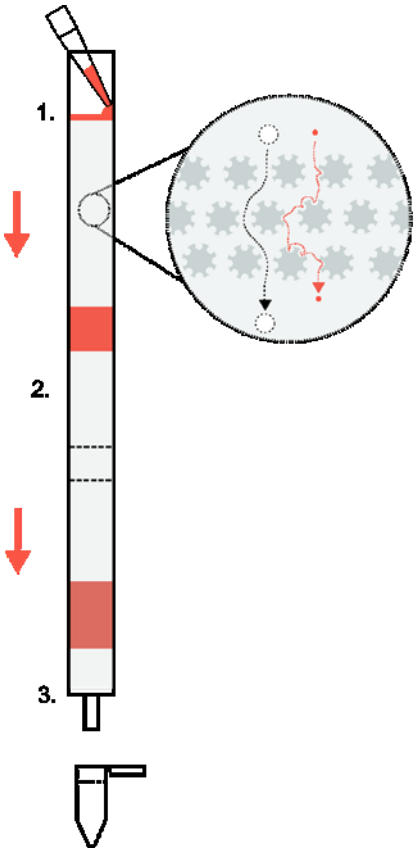


Figure 2.4: Purification of EVs by Size Exclusion Chromatography.

Impure sample is loaded (1), separated as it travels down the column (2), and pure EVs are collected (3).

In general, density-based methods are widely considered to be effective at removing contaminants [111, 117, 127]. However, they are time-consuming, technically challenging, necessitate additional washing steps and are associated with a reduced EV recovery. These drawbacks often necessitate isolation of EVs in large batches, complicating work in which multiple samples must be processed in parallel and making high-throughput studies difficult.

2.1.3.2. Size exclusion chromatography

The other purification method in most common use is size exclusion chromatography (SEC). In this method, EVs are concentrated to a low volume before loading onto a column containing a gel media comprising semi-porous sub-millimetre diameter hydrogel beads (Figure 2.4). As the sample travels down the column, it encounters pores and divots in the beads of various sizes. Molecules and particles that encounter an area large enough for them to enter may move into it. By contrast, larger particles will not enter the same pores. Therefore, the larger particles "see" a smaller volume within the column than smaller particles. Smaller particles hence tend to take a more convoluted and therefore longer path down the column, delaying their elution relative to the larger particles. The largest particles will

be completely excluded from the pores and elute first, followed by intermediate and then the smallest particles [128].

Given that ultracentrifugation and ultrafiltration are both size-based methods of concentration, and that neither is sufficient to isolate a pure EV population, it may appear counterintuitive to use another size-based method to purify EVs subsequently to these methods. However, in practice SEC has been shown to be capable of excellent separation of EVs and smaller non-EV material from cell culture supernatants. SEC is most typically paired with UF to concentrate EVs before loading – by this combination of methods, EVs are never removed from solution and do not experience high g-forces. EVs isolated in this manner have been shown to be highly pure [129, 130], physically intact, and to have improved functionality [118, 131] and different biodistribution properties [132] compared to vesicles isolated by ultracentrifugation or precipitating agents. SEC for EV isolation is a relatively recent development within the field, but due to its efficacy and relative ease of use, it is rapidly becoming widely adopted.

SEC has been used for isolation of EVs from cell culture media and numerous biofluids, including plasma. A potential concern for the isolation of EVs from plasma by this method is the possibility of contamination by lipoprotein particles. Lipoprotein particles are similar in structure to extracellular vesicles in that they have a phospholipid membrane and surface-associated protein (apolipoproteins), but differ in that their lumen is composed of hydrophobic core of triglycerides and cholesterol [133], rather than a cytoplasm-like aqueous space. There are many subtypes, ranging in size from 5-12 nm in diameter (high-density lipoproteins, HDL) to up to 1200 nm (chylomicrons). In particular, intermediate, low and very low-density lipoprotein particles substantially overlap in size with extracellular vesicles. They may therefore co-isolate with EVs if SEC is the major method used for isolation. Their reported densities are lower than that of EVs (0.93 – 1.06 g/ml) due to their lipid cores and so density-based separation methods may be more appropriate. However, the density of HDL overlaps with that of EVs and they have been reported to co-isolate in density-dependent methods [134]. Despite the potential for lipoparticle contamination, use of SEC to isolate EVs from plasma has been reported [129]. In this study, separation from smaller HDLs was demonstrated, but the presence of larger intermediate, low and very low density lipoparticles (IDLs, LDLs and vLDLs) was not assessed. Unpublished data from the author's group suggests significant co-isolation of these particles from plasma.

2.1.4. Assessment of EV purity

Assessment of EV yield and purity is of critical importance for any study. However, the best practice for quantifying and reporting these characteristics is not immediately clear. This is partly because although there are a number of ways to quantify EVs, there are limitations to their reproducibility or their specificity to EVs. EVs are frequently quantified by particle counting technologies such as Nanosight (Malvern), or tunable resistive pulse sensing technologies such as qNano (iZON). These technologies provide the concentration of particles in solution, but those particles may not exclusively be EVs; lipoprotein complexes, protein aggregates and other debris will also be counted. It has been noted in the author's group that Nanosight quantification is not always fully consistent between identical instruments in different labs. Frequently, studies report protein concentration as the primary metric of EV yield, sometimes without further quantification. Unfortunately, this can be inflated by non-EV protein contaminants. The presence of EVs is typically confirmed by detection of EV markers such as CD63, CD9, CD81 or Alix – however this is not quantitative in absolute terms.

Webber and Clayton [108] propose integration of quantification methods to generate a simple metric to assess purity. A ratio of particle concentration to protein concentration provides a "litmus test" for sample impurity. Assessing different isolation techniques, they concluded that for a single source of EVs, more stringent purification resulted in samples with more particles per µg of protein. Therefore, less stringent methods do not remove all contaminants. As a rule of thumb, they propose that samples with 3×10^{10} particles/µg or greater should be considered highly pure, samples with between 2×10^{9} and 2×10^{10} particles/µg should be considered to be intermediate to low purity, and samples with less than 1.5×10^{9} particles/µg should be considered impure. This may vary between cell lines and be subject to instrumental variation but provides a useful reference point. Other methods to assess purity include confirming the absence of non-EV proteins, and confirming that vesicles are not contaminated with debris from disrupted cells – typically by checking for the absence of calnexin, an endoplasmic reticulum protein [135]. Electron microscopy can also give a non-quantitative overview of the sample, by revealing contamination with larger vesicles or protein aggregates.

2.1.5. Conclusions and critical requirements for purification

The isolation of extracellular vesicles is more challenging than it might appear. Many techniques are prone to co-isolation of contaminants, biasing of samples or loss of material. It is often most appropriate to combine multiple techniques to overcome these limitations. However, EVs are not always present in large quantities in the initial sample and long, multi-step purification can lead to losses that limit material availability for experiments. These problems are compounded if it is necessary to process multiple samples in parallel. The limitations of these techniques are by now quite well-established. There is a broad consensus in the field that density gradient centrifugation and size exclusion chromatography are the most preferable techniques in terms of removing non-EV factors. Despite this, many studies still utilise preparative techniques that could be expected to impact their results. Efforts to standardise the requirements for isolation procedures are ongoing [104]. For this study, it was considered critical to identify a robust isolation and purification workflow that could reproducibly remove contaminants and retrieve sufficient EVs for downstream analysis.

2.2. Materials and Methods

Nanoparticle Tracking Analysis (NTA)

Nanoparticles (i.e. EVs) in solution were quantified using a Nanosight NS300 with a 532 nm laser module and sCMOS (Scientific Complementary Metal-Oxide Semiconductor) camera module for the majority of experiments (Malvern Instruments, Salisbury, UK). Particles were diluted in particle-free water from a Select Fusion Milli-Q water purifier (Suez Water UK, Thame, U.K.) to a concentration within the range of 10^8-10^9 particles/mL before measurement. Using NTA V3.0 software, three 60-second videos were recorded and analysed per sample, with software parameters Camera Level 15, Detection Threshold 5 used. The Finite Track Length smoothing algorithm was disabled, as it was found to generate artefactual size peaks from noise. Data was instead analysed in the raw format, without smoothing. Some early work was performed with a Nanosight LM10 with a 642 nm laser module and sCMOS camera and analysed using NTA V2.3 software, with Camera Level 15, Detection Threshold 10 (Malvern Instruments). This data is marked in the appropriate figure legends and not directly compared to data obtained with the NS300.

Transmission Electron Microscopy (TEM)

Holey Carbon 200 mesh EM Grids were glow-discharged (15 sec O_2/H_2 1:1) with a Solarus plasma cleaner (Gatan, Pleasanton, CA, U.S.). Samples were then prepared using an automatic plunge freezer (Leica EM GP). To prepare the samples, 4 µL was pipetted onto a grid in an environmental chamber (relative humidity: 90 %, temperature 20 °C). Excess sample was blotted off and the obtained film was by plunging into liquid ethane. Samples were stored under liquid nitrogen and were transferred under liquid nitrogen into a Gatan model 914 cryo transfer holder. Samples were imaged at -170°C in a JEOL 2100 Plus Transmission Electron Microscope (JEOL, Tokyo, Japan), using an Orius SC 100 camera at 30k magnification (Gatan).

Scanning Electron Microscopy (SEM)

Samples for SEM imaging were prepared by washing EV samples 5 times in an Amicon Ultra-15 centrifugal concentrator with 10 mL 18.2 MΩ water, concentrating to 200 µL, and then allowing 1 µL to dry directly on the stage. The stage was sputter-coated with gold to a depth of 10 nm and imaged on a JEOL JSM-6010LA.

Cell Culture

Unless otherwise stated, cells were grown in Corning Cell Culture Flasks (Corning, NY, U.S.) in a humidified incubator at 37 °C, 5 % CO_2. Cells were split by aspirating media, washing once with sterile PBS (Phosphate-Buffered Saline) (Gibco), and incubating with 0.05 % w/v Trypsin (Thermo Fisher

Scientific, Waltham, MA, U.S.) for 3 minutes (5 minutes for hMSCs) before addition of an equal volume of media. Cells were then spun down at 400 g, for 4 minutes before aspirating the supernatant and resuspending the pellet in fresh media. Exceptions and specific media for each cell type are detailed below.

Cell counting

Cells were counted using a Countess II FL automated cell counter (Thermo Fisher). 10 µL of cell suspension was mixed with 10 µL of 0.4 % w/v Trypan blue (Thermo Fisher), and 10 µL added to each chamber in the counting slide. An average of the concentration of live (dye-excluding) cells between the two chambers was taken.

Frozen stocks

For all cell types, stocks were prepared by resuspending a cell pellet in the appropriate full media, supplemented with 10 % v/v DMSO (Di-Methyl Sulfoxide) before transfer to cryovials (Corning) Cryovials were frozen in a Mr Frosty (Nalgene, Rochester, N.Y., U.S.) before transfer to either liquid Nitrogen (vapor phase) storage or a cryofreezer set at -140 °C. Frozen stocks were recovered by rapid defrosting in a 37 °C water bath, followed by 10x dilution in appropriate full media, spinning down cells at 400 g, for 4 minutes before resuspending the pellet and culturing as normal. Unless otherwise stated, media was then changed 24 hours after thaw.

NIH/3T3

NIH/3T3 cells were obtained from ATCC (American Type Culture Collection, Manassas, Virginia, U.S.) via LGC (Teddington, U.K.). NIH/3T3 cells were grown in DMEM (Dulbecco's Modified Essential Medium) (Gibco, subsidiary of Thermo Fisher Scientific) (4.5 g/mL glucose) supplemented with 10 % v/v FBS (Foetal Bovine Serum) and 1x A/A (Antibiotic/Antimycotic) (Gibco), in Corning cell culture flasks. Cells were split from near-confluence 1:20 every 5-6 days, with a media change every 3 days. After transformation to express GFP (Green Fluorescent Protein), stocks were made at passage 9. Cells were not used past passage 15.

HUVEC

HUVEC (Human Umbilical Vein Endothelial Cells) were obtained pooled from several donors from Gibco (C0155C). HUVECs were grown in M200 media (Gibco) + 1x A/A + low-serum growth supplement, with splitting every 5-6 days and a media change every three days. Cell stocks were frozen at 500,000 cells/vial (1 mL/vial) at passage 2 for experiments. Prior to tubule formation experiments, frozen stocks were thawed in M200 media as above before being cultured for 6 days before use.

MDA-MB-231

MDA MB 231 cells were obtained from ATCC via LGC. MDA MB 231 cells were grown in DMEM (4.5 g/mL glucose), supplemented with 10 % v/v FBS and 1x A/A. MDA MB 231 cells were expanded to multi-layered flasks (Falcon) for conditioned media production.

A549

A549 cells were grown in DMEM (4.5 g/mL glucose), supplemented with 10 % v/v FBS and 1x A/A.

Collection of conditioned media (CM)

MDA MB 231 cells were passaged sequentially, splitting 10-fold into multi-layered flasks for CM collection and an additional T225 flask, from which media was not collected and the subsequent passage was taken. Cultures were not re-used after starvation and were destroyed by addition of Virkon (Thermo Fisher) prior to disposal. Near-confluent cells were washed once with sterile PBS before addition of 35 mL per flask or 20 mL per layer of DMEM, supplemented with 1x A/A, without FBS. A549 cells were incubated for 72 hours, MDA MB 231 cells for 48 hours, and hMSCs for 40 hours.

Media pre-processing

After incubation, media was collected and processed to remove detached cells and other debris. MDA MB 231-CM was centrifuged at 500 g for 5 minutes, then 5000 g for 15 minutes, retrieving the supernatant each time, before passage through a 0.45 µm syringe filter (Sartorius), replacing the filter for every 50 mL of media.

Concentration of conditioned media by Ultrafiltration

Filtered conditioned media was concentrated by passage through Amicon Ultra-15 Centrifugal Filters (Merck, Darmstadt, Germany). For standard EV isolation, 100 kDa MWCO (Molecular Weight Cut-Off) filters were used. For experiments that required retention of all soluble proteins as well as EVs, 3 kDa filters were used. Both were centrifuged at 5000 g, at 4 °C. A series of increasing centrifugation times was used, starting at 5 minutes. Media in the concentrators was topped up between centrifugations to a volume of 12 mL. No more than 120 mL of media was processed per concentrator. Start and end volumes for different experiments are shown in Table 2.1.

Table 2.1: Conditioned media concentration volumes

Experiment	Start volume	End volume	MWCO
MDA MB 231 EV isolation	250 mL	0.5 mL	100 kDa
Large-scale hMSC EV isolation	1.4 L	1.5 mL	100 kDa
Equilibrium Dialysis	50 mL	5 mL	3 kDa
Concentration/Dilution	100 mL	20 mL, 4 mL	3 kDa
Isolation with Total Exosome Isolation Reagent	100 mL	1 mL	3 kDa
Analytical SEC	100 mL	0.5 mL	3 kDa

FBS EV depletion

FBS was EV-depleted by ultracentrifugation for 18 h, 100,000 g at 4 °C in 70 mL polycarbonate bottles (Beckman Coulter 355622) in a Type 45 ti rotor (339160) in an Optima XE Ultracentrifuge (A94471), as in Shelke et al [98]. Upon sample retrieval, FBS was gently removed with a stripette, leaving the last 10 mL of FBS unremoved, to avoid disrupting the pellet and contaminating the depleted FBS. EV-depleted FBS was then aliquoted and stored at -20 °C until use.

EV Isolation by Ultracentrifugation

Pre-cleared media was transferred to 30 mL polyallomer tubes (Beckman Coulter 358126) in a SW 32 ti rotor (Beckman Coulter 369694), or 70 mL polycarbonate bottles (355622) in a Type 45 ti rotor (339160), ensuring that they were balanced. Conditioned media was centrifuged at 120,000 g for 3 hours at 4 °C. The supernatant was aspirated from the presumed position of the invisible pellet before resuspension in 500 µL of PBS. The resuspended EVs were stored at -80 °C.

EV isolation by 100 nm filter capture

EVs were captured on 100 nm membrane filters (Durapore PVDF membrane filter, VVLP01300, Millipore) using a 20 mL syringe attached to a filter holder. The syringe was used to force conditioned medium or EVs resuspended in PBS through the filter. The filter was then removed from the holder and placed in an Eppendorf tube with 250 µL of PBS before vortexing (5 x 20 seconds) to resuspend the EVs.

Mock EV Isolation from Media containing EV-depleted FBS

EV-depleted FBS was diluted 1:10 in DMEM (Gibco) before ultracentrifugation for 3 hours at 4 °C at 100,000 g. Of the 60 mL volume, 59.5 mL was aspirated leaving 500 µL on top of the expected location

of the pellet. This was performed with the centrifuge tube on a scale, such that this volume was determined gravimetrically. This was washed with 59.5 mL PBS and ultracentrifuged again before aspirating supernatant as before. The final sample volume in PBS was 500 µL. For protein concentration measurements, FBS was diluted into PBS instead as DMEM contains phenol red and amino acids which interfere with quantification.

Sucrose cushion centrifugation

A solution of 0.2 M Tris and 30 % Sucrose (w/v) was prepared in D_2O (deuterated water) by stirring overnight at room temperature. The solution was filtered through a 100 nm filter before use. 20 mL of conditioned media was placed in a 30 mL polypropylene open-topped conical centrifuge tube (Beckman Coulter 358126). The plungers were removed from 5 mL syringes, which were then fitted with long 18G needles, and rested on the rim of the centrifuge tubes such that the tip of the needle rested in the base of the sample-filled centrifuge tube. 4 mL of Tris/Sucrose solution was added to each syringe via the open tops. Air was expelled from the needle by gently applying pressure to the open top of the syringe with a thumb, and the sucrose solution was allowed to flow to the bottom of the centrifuge tube under gravity over several minutes. Syringe and needles were removed with great care, so as not to disturb the interface. Tubes were loaded into an SW32 rotor, again with great care, and centrifuged for 90 minutes at 100,000 g, 4 °C. Acceleration and deceleration settings were as gentle as possible without coasting (settings 9 & 9 on a Beckman Optima XE). Tubes were carefully removed, and visually inspected to evaluate mixing at the interface. A syringe fitted with a long 18G needle was used to recover the sucrose cushion via the open top of the tube. The tip of the needle was rested on the side of the tube, just above the bottom of the tube, in order to avoid disturbing any impurities that had settled at the bottom. Approximately 3.5 mL was recovered, or as much as it was possible to recover without also recovering from the media/PBS layer. EVs were then resuspended in PBS and pelleted by ultracentrifugation.

Size Exclusion Chromatography

Column Packing

Approximately 60 mL Sepharose CL-2B slurry (Sigma-Aldrich) was transferred to a wide, shallow container and the gel beads allowed to settle. The solvent was aspirated off and the beads resuspended in approximately 120 mL particle-free 18.2 MΩ water. This was repeated, before resuspending the slurry and pouring into a 1 x 30 cm Econo-Column (Bio-Rad) with a 50 mL syringe barrel attached as a reservoir. The slurry was briefly allowed to sit to allow any large bubbles to be

removed by tapping. The bottom tap was then opened, allowing the column to pack under gravity at ambient pressure. The column was allowed to pack to a final depth of 28 cm.

Column washing and storage

After packing or sample processing, the column was washed with two column volumes of sterile tissue culture PBS (under gravity) before flushing with two column volumes of 20 % v/v ethanol for long-term storage. Prior to use, the 20 % ethanol was placed in a sonication bath for 30 minutes and then left at room temperature for 24 hours with the cap ajar to allow total degassing. Failure to perform this step lead to bubble formation within the column. At least 1 cm of Ethanol was left on top of the column bed during storage.

If cracks or bubbles formed within the column bed, the slurry was ejected from the column by application of a 50 mL syringe of particle-free PBS to the lower Luer port. The slurry was then resuspended and repacked as described.

Sample separation on SEC column

Before use, 60 mL of freshly opened sterile tissue culture PBS (Gibco) was allowed to pass through under gravity to wash away the 20 % ethanol in which the columns were stored. Samples were concentrated to 500 µL by ultrafiltration before loading. Sample were either loaded manually, or in the case of hMSC-CM samples, with the aid of a sample applicator (Bio-Rad), to minimise bed disruption and ensure even sample entry. To manually load the column, the column outlet valve was opened until no fluid remained above the column bed, and then immediately closed. Sample was applied to the bed surface very slowly and evenly, with a 200 µL pipette. The outlet valve was opened to allow sample to enter the column bed. Once sample had fully entered, the column head space was gently filled with PBS using a Pasteur pipette, the reservoir connected, and fraction collection began.

When loading with the sample applicator, the apparatus shown in Figure 2.5 was used to allow switching between applying sample and PBS without introducing air bubbles to the system. The system was assembled, and lines thoroughly washed with particle-free PBS before closure of all taps and valves prior to addition of sample. A 3 mL syringe barrel was attached to the loading port. The reservoir tap and switching valve were opened to connect the reservoir and loading barrel, while leaving the applicator disconnected. Approximately 3 mL of PBS was allowed to flow from reservoir to loading barrel. The reservoir tap was closed, the column tap opened, and the switching valve rotated to connect the loading port and applicator outlet. The column tap was then opened, and PBS allowed to pass from the loading barrel to the column outlet. When the level of the PBS in the loading barrel just reached the tip of the loading barrel, the column tap was closed. 500 µL of sample was then

carefully loaded into the syringe barrel, just on top of the PBS in the port. This ensured that no air bubbles entered the column line, whilst not allowing substantial mixing of sample and PBS. The column tap was reopened, and sample allowed to flow onto the column via the applicator outlet. When the level of sample just reached the blue control body of the switching valve, the column tap was closed. The switching valve was moved to reconnect the reservoir and applicator outlet, disconnecting the loading port. The reservoir and column taps were then reopened, and fraction collection began.

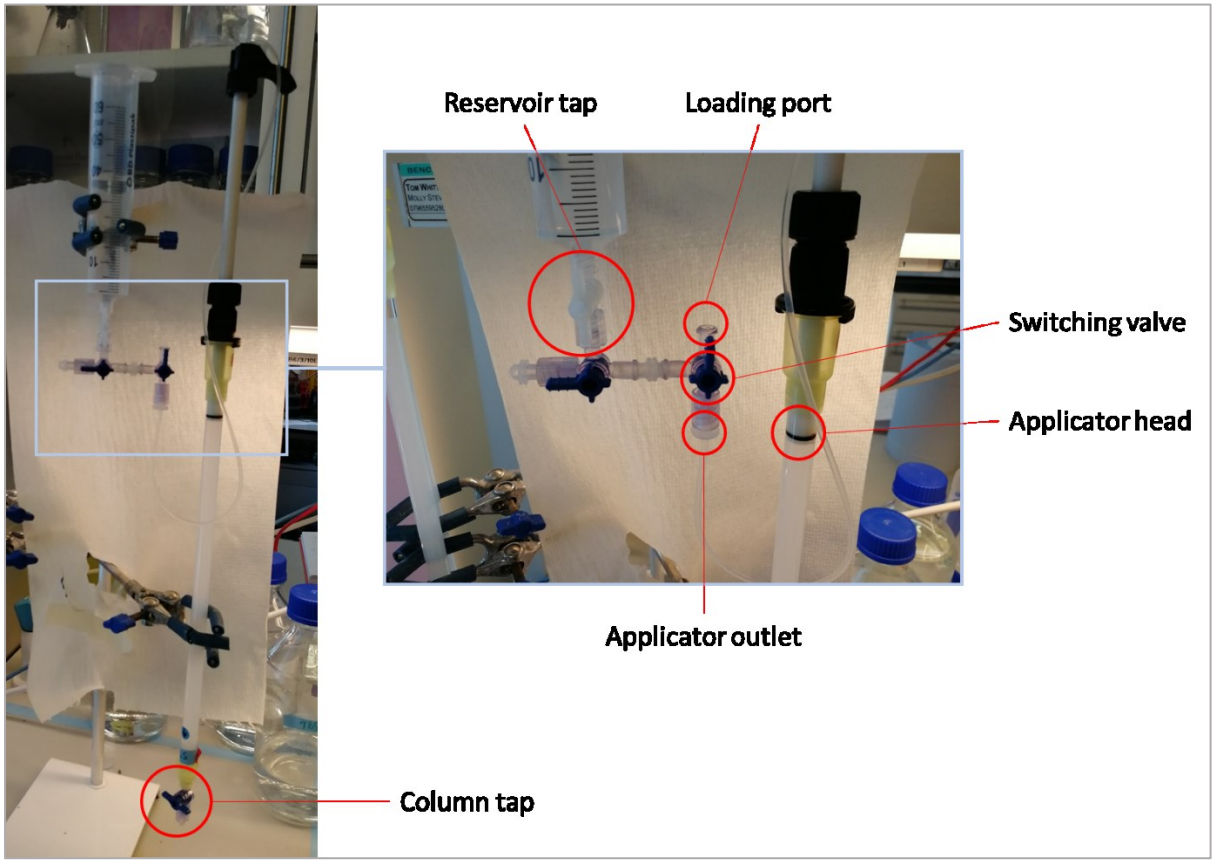


Figure 2.5: SEC column and sample applicator. See text for details of use.

With or without the applicator, unless otherwise stated 30 x 1 mL fractions were collected. Fractions were either aliquoted and stored at -80 °C or used immediately.

Concentration of purified EV samples

EV-containing fractions collected from SEC columns were pooled and concentrated using Amicon Ultra-4 100 kDa centrifugal concentrators, centrifuging at 1000 g in three-minute increments.

Western Blotting

Cell lysis

Media was aspirated from adherent cells before washing once with PBS. 200 µL of RIPA (Radioimmunoprecipitation Assay) buffer with phosphatase and protease inhibitors (Sigma) was added and the cells scraped and resuspended with a pipette. The resuspended cells were sonicated on ice for 20 seconds at 20 % amplitude with a Vibra-Cell 750 sonicator (Sonics & Materials Inc, Newtown, CT, U.S.), before incubation for 1 hour on a roller at 4 °C. The sample was then centrifuged at 16,000 g before retrieving the supernatant for further analysis.

EV lysis

EV lysis was performed as for cell lysis, except that EVs isolated as described by UF/SEC were concentrated with a 100 kDa Amicon centrifugal filter (as previously described) to a final volume of 100 µL prior to addition of 100 µL of RIPA buffer with phosphatase and protease inhibitors. Subsequent steps were identical to those performed for cell lysis.

Sample preparation and setup

Protein samples were mixed with 4x loading buffer (Bio-Rad 161-0791) and 20x reducing agent (Bio-Rad 161-0792) at a ratio of 14:5:1 by volume. Prior to mixing, the protein concentration of the sample was adjusted by dilution for a concentration (after mixing with loading buffer and reducing agent) of 1 mg/mL (unless otherwise stated in the main text). Samples were heated to 100 °C for 3 minutes and then allowed to cool, before briefly vortexing and centrifuging.

Electrophoresis

Precast 12 % w/v Bis-Tris gels (Bio-Rad 345-0118 [18 wells] and 345-0119 [26 wells]) were removed from their packaging and rinsed in water. The electrode-protecting strip was removed before placing in a gel tank and filling with approx. 500 mL of running buffer (20x MOPS buffer, Bio-Rad 161-0788). The comb was removed, and the wells rinsed with a Pasteur pipette. For an 18-slot gel (Bio-Rad 345-0118), 30 µL of sample (at 1 mg/mL) was added per well. For 26-slot gels (Bio-Rad 345-0119), 15 µL was added. For protein marker ladders, half those volumes were added (Precision Plus Protein Standards Dual Colour, Bio-Rad 161-0374). Empty slots were filled with loading buffer. The electrophoresis tray was placed in an icebox. Gels were run at a constant current of 40 mA for one gel, or 80 mA for two gels, for approximately 2½ hours.

Transfer

1.5 L of Tris/Glycine transfer buffer (Bio-Rad 1610734) was prepared. A PVDF (Polyvinyldiene Fluoride) membrane (0.45 µm pore size, 1620-117) was soaked in methanol for 5 minutes before rinsing 3 times with 18.2 MΩ water. Sponges and filter paper were soaked in transfer buffer before assembling the transfer sandwich as follows: Sponge, 2x filter paper, gel, membrane, 2x filter paper, sponge. The gel was extracted from the cassette by cracking open the electrophoresis tray and laying wet filter paper on top of the gel, before gently peeling away the filter paper and gel from the plastic. The transfer was run at a constant voltage of 100 V for 30 minutes, on ice.

Blocking

The membrane was cut for orientation, marked with pencil for identification and then incubated in a solution of 5 % w/v skim milk powder in Tris-buffered Saline (TBS) supplemented with 0.1 % v/v Tween 20 (Merck) (TBS-T) for 1 hour at room temperature.

Primary incubation

Membranes were washed three times, 10 minutes each in TBS-T, before incubation overnight at 4 °C with primary antibody diluted in 5 % w/v BSA (Bovine Serum Albumin)/TBS-T. For CD63, CD81 and CD9 antibodies, a dilution of 1:1000 was used (see Table 2.2).

Secondary incubation and imaging

Membranes were washed three times, 10 minutes each in TBS-T, before incubation with secondary antibody diluted 1:10000 in 5 % w/v BSA/TBS-T for 1 hour, at ambient temperature, protected from light. The secondary antibody used was goat anti-mouse 800 CW (LI-COR 926-32210). Membranes were then washed three times again and imaged using a LI-COR Odyssey imager.

Table 2.2 – Anti-exosome marker antibodies

Antibody	**Dilution factor**	**Species**	**Manufacturer**	**Product code**
Anti-CD63	1000	Mouse	Thermo Fisher	10628D
Anti-CD81	1000	Mouse	Thermo Fisher	10630D
Anti-CD9	1000	Mouse	Thermo Fisher	10626D
Anti-Calnexin	1000	Rabbit	Cell Signalling Technologies	C5C9

Micro-BCA assay

The Micro-BCA (Bicinchoninic Acid) assay was used according to manufacturer instructions to measure protein concentrations. Working reagent was made by mixing components A, B and C in a 25:24:1 ratio and used immediately. Samples and BSA standards were incubated for 2 hours at 37 °C with working reagent in clear-bottom 96-well plates (150 µL of sample + 150 µL working reagent / well). Plates were sealed with a film (Thermo-Fisher AB-1170) to prevent evaporation. Absorbance at 562 nm was then read using a Spectramax M5 platereader (Molecular Devices), and concentrations determined using a linear regression fitted to the standards.

Tubule formation assay

Preparation

5-6 days before beginning the assay, 500,000 p2 HUVECs (Gibco C0155C) were thawed from cryo-stocks and seeded in a T225 flask in 35 mL of M200 (Gibco M200500) media.

6 hours before use, HUVECs were transferred to basal M200 media for pre-assay starvation, to reduce the background level of tubule formation.

1 hour before use, growth factor-reduced (GFR) Geltrex (Gibco A1413202) was mixed with ice-cold PBS at a ratio of 6 volumes Geltrex to 1 volume PBS. 10 µL of diluted Geltrex was added to each well of an ibidi 96-well angiogenesis plate (ibidi, Martinsried, Germany, 89646), on ice. The plate was spun in a plate centrifuge at 50 g for 1 minute at 4 °C to ensure a flat gel surface. The plate was then transferred to a cell culture incubator (37 °C, 5 % CO_2) to gel.

Assay

After the 6 hour starvation, HUVECs were treated with Trypsin and resuspended in basal M200. The cell concentration was measured using a Countess II FL automated cell counter (Thermo Fisher) and adjusted to 1 x 10^6 viable cells/mL. Samples were then prepared as shown in Table 4. The buffer used in the controls matched the buffer of the experimental samples (DMEM or PBS). 12 technical replicates were typically used, at a volume of 50 µL per well. Samples were added to the wells gently, down the side of the well. The assay was then incubated at 37 °C, 5 % CO_2 for 16 hours.

Table 2.3- Sample preparation for tubule formation assays

For 12 replicates	**M200 (basal)**	**M200+ 10x**	**Sample/ buffer**	**Cells at 1 x 10^6 /mL**
Positive Ctrl	120 µL	60 µL	300 µL (buffer)	120 µL
Negative Ctrl	180 µL	0 µL	300 µL (buffer)	120 µL
Samples	180 µL	0 µL	300 µL (sample)	120 µL

Imaging and Analysis

After 16 h, 20 mL of 2 µM Calcein-AM (Invitrogen C3099) in basal M200 media was gently added to the top compartment of the plate. The plate was incubated for 20 minutes, at 37 °C, 5 % CO_2, protected from light. The plate was then washed once and imaged using an Axio Observer live cell imaging microscope with an HXP 120 light source (Carl Zeiss, Oberkochen, Germany) at 37 °C, 5 % CO_2. A 2.5X objective was used and the entirety of each well was imaged.

Images were then processed with FIJI [136]. Images were imported, cropped circularly to remove well edges, and converted to a binary image using a manually set threshold. The threshold was set to highlight all tubule structures without including background. The binary images were then analysed using the "Angiogenesis Analyzer" plugin [137]. Multiple metrics to describe the network structure were available, of which "total tubule length" was used to compare the pro-angiogenic activity of samples.

Statistics

For comparison of the means of two samples, where observations were linked, a two-way paired t-test was used. For comparison of three of more samples, where observations were linked, a one-way within-subjects ANOVA (Analysis of Variance) was used. Post-hoc tests used with ANOVA were either Tukey's test (for comparison of all means) or Dunnett's (for comparison to a single control value). The majority of experiments were designed such that paired/within-subjects tests could be used. Where this was not possible, unpaired t-tests or conventional one-way ANOVA tests were used. Where homoscedasticity was clearly violated, a non-parametric within-subjects Friedman test and post-hoc Dunn's test were used. Calculations were performed using Graphpad Prism 8. Mean +/- Standard Deviation (SD) of replicates is typically presented, but in some cases individual replicates are presented, showing the mean +/- SD of the internal technical replicates for each independent replicate. This is done to better show similarity of trends where differences between samples are similar, but the absolute values tend to differ between experiments.

2.3. Results: Development and validation of purification techniques.

During the initial stages of this project, considerable optimisation and troubleshooting was necessary in order to develop a suitable EV isolation and purification procedure. This was an iterative process in which several techniques and variations to them were investigated, and as such not all experiments were fully repeated. Selected optimisation experiments are shown in the appendix in order to illustrate the decision-making process. These investigations led to the identification of a combination of ultrafiltration and size exclusion as a potential method for high-purity isolation of EVs. Optimisation and validation of this method is described in this chapter. Additionally, EV-depleted FBS was investigated in order to determine whether bovine EVs were sufficiently depleted to avoid downstream contamination.

2.3.1. Centrifugal concentrator evaluation

MDA-MB-231 cells were grown to near confluence before washing once with PBS and incubation in serum-free DMEM with A/A for 48 hours (37 °C, 5 % CO_2). The conditioned medium was then pre-processed by centrifugation at 500 g for 5 minutes to remove cells, then 5000 g for 15 minutes to remove larger debris, before a final filtration through a 0.45 µm syringe filter (as described in section 2.2). Unless otherwise stated, conditioned medium prepared in this way was used for experiments in this chapter.

Exploratory work indicated that concentration of conditioned medium using centrifugal ultrafiltration devices recovered a workable percentage of the input particles. Here, the recovery and processing speed of three pore sizes of 15 mL Amicon centrifugal ultrafiltration tubes were evaluated (Figure 2.6). 20 mL of MDA-MB-231 – conditioned medium was passed through each concentrator, with an initial volume of 12 mL in the upper compartment. The remaining 8 mL was added between subsequent centrifugations, topping up to a volume of 12 mL until no reserve CM remained. Initial centrifugation times were 2 ½ minutes each, 5000 g, 4 °C. As flow rate slowed, 5 and then 10-minute runs were used. The weight of the flowthrough was measured after each run, to quantify gravimetrically the volume of CM that had passed through. The volume of the final concentrate (between 300 and 600 µL) was quantified in the same manner.

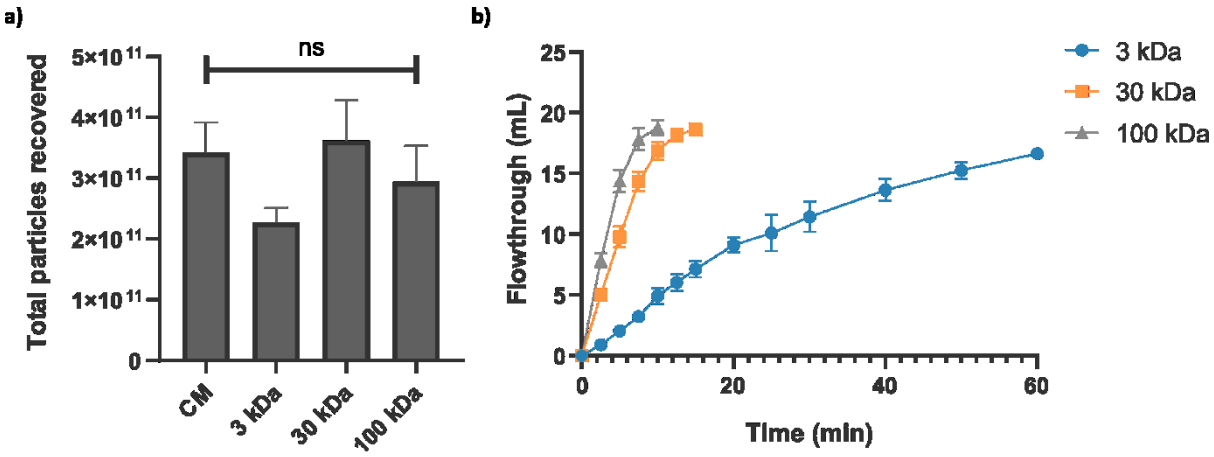


Figure 2.6: Evaluation of recovery and processing time from ultrafiltration concentrators. a) Total particles in input CM and final concentrates from each pore size of concentrator. Mean +/- SD is shown (N = 3, n = 3 x 60 second videos). Differences are not significant (one-way within-subjects ANOVA). b) Cumulative volume of flowthrough from each pore size of concentrator over time. Mean +/- SD is shown (N = 3).

No significant difference was found between the number of particles in the input 20 mL of conditioned medium and the quantity in the final concentrate for any of the three membranes, or between the number of particles recovered from the different pore size membranes (one-way within-subjects ANOVA) (Figure 2.6 a).

Larger pore size membranes allowed substantially more rapid ultrafiltration of the conditioned medium (Figure 2.6 b). The 100 kDa membrane required 10 minutes centrifugation to process the full 20 mL, whereas the 30 kDa membrane required 15, and the 3 kDa membrane required over an hour. As no significant differences in recovery between the different pore sizes were observed, it was decided to move forward with 100 kDa ultrafiltration membranes for routine purification of EVs, except when necessary to use smaller pore sizes to retain non-EV material.

2.3.2. Initial evaluation of size exclusion chromatography

Initial exploratory investigation of density-based methods for purification had been hampered by issues of consistency of separation (see appendix). Other members of the author's research group had previously used size exclusion chromatography (SEC) for separation of small drug molecules from EVs after active loading [138] and so it was considered whether SEC might be appropriate for separation from soluble protein.

Initial testing of a commercially available column (Figure 2.7 a) indicated that particles (as measured by NTA) and protein (as measured by micro-BCA assay) were broadly separated. However, the protein peak slightly overlapped the particle peak. This implied that either it was necessary to collect more frequent, lower volume fractions to increase the resolution, or that a longer column might be necessary. Sepharose CL-2B and Sephacryl S-200 HR were chosen as potential candidate resins for self-packed columns. Sepharose CL-2B appeared to separate particles and protein (Figure 2.7 b), with a small protein peak apparent associated with the particle peak. Sephacryl S-200 HR had a more complex protein elution profile (Figure 2.7 c) with less separation between particle-associated and free protein. Peak protein concentrations differ between the columns shown as different batches of concentrated conditioned medium were separated on them, and optimisation of yield and recovery from conditioned medium was still ongoing. To confirm the suitability of Sepharose CL-2B, 100 µg of BSA was loaded onto a Sepharose CL-2B column. No BSA was detected in the early fractions where particles elute, indicating that free protein was genuinely being separated from particles (Figure 2.7 d). Sepharose CL-2B was therefore selected for more detailed, fully replicated investigation.

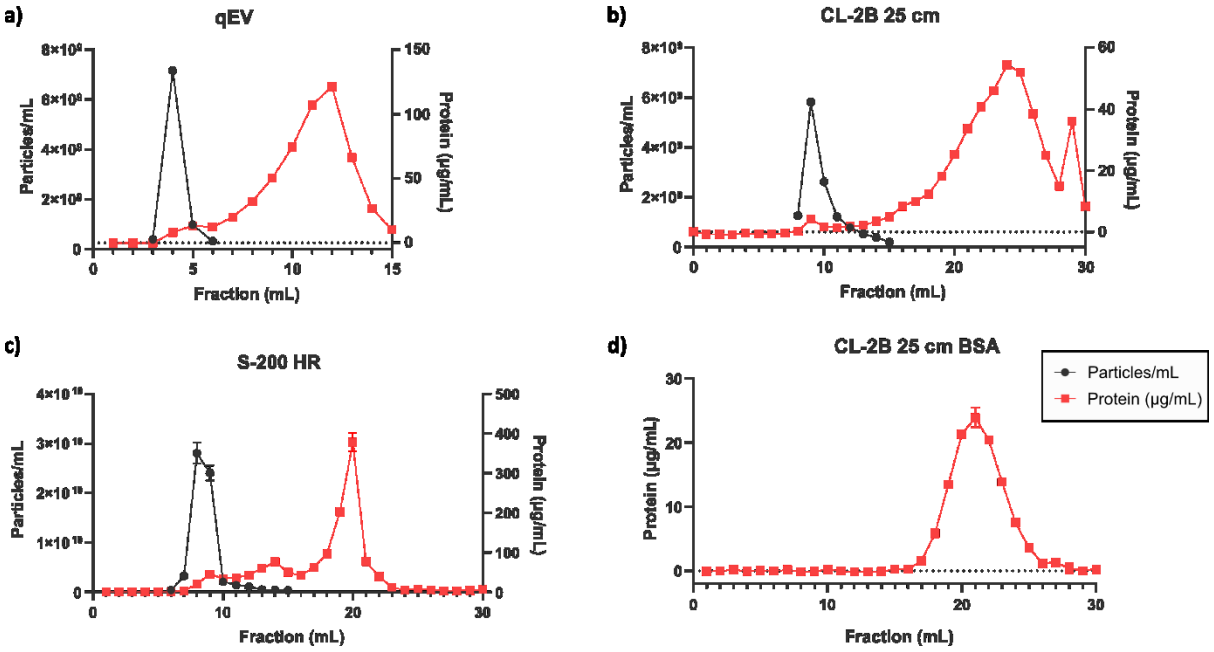


Figure 2.7: Comparison of elution profiles from a) qEV b) CL-2B and c) S-200 HR SEC columns. a) and b) particles were measured with a Nanosight LM10 with a 642 nm laser, and protein quantified by micro-BCA assay (N = 1, n = 1 for both). c) Particles were quantified with a Nanosight NS300 with a 532 nm laser and protein quantified by micro-BCA assay (N = 1, n = 3 for both, mean +/- SD of n shown). d) Elution of BSA from CL-2B column. Protein quantified by micro-BCA assay (N = 1, n = 3 for both, mean +/- SD of n shown).

2.3.3. Ultrafiltration and SEC: in-depth characterisation of purification and recovery.

Initial investigation suggested that a combination of concentration using ultrafiltration and purification by size exclusion chromatography (SEC) could be a viable method for isolating EVs without contamination from free protein. The separation achievable by SEC is dependent on the ratio of the height of loaded sample to the height of the column bed itself. Different column sizes were therefore expected to have differing effectivities in separating EVs and free protein. The separation achieved by three columns was compared; a commercial qEV column, a self-packed 9.5 x 1 cm column, and a self-packed 28 x 1 cm column (Figure 2.8). To determine the separation of EVs and protein, the particle and protein content for each fraction were measured. For some early fractions, 0.5 mL fractions were collected to improve peak resolution – for others, 1 mL was collected. The particle concentration for the input concentrated conditioned medium was also measured. This allowed quantification of recovery from the columns. The input conditioned medium was prepared and concentrated as a single batch, before freezing as aliquots and thawing for each replicate for consistency.

The commercial qEV column achieved a good separation of particles and protein, with particles mostly eluting in fractions 3.5-4.5 and the major protein peak centred at fractions 10-11 (Figure 2.8 a-i). Focusing on the particle peak, a small peak of EV-associated protein can be observed (Figure 2.8 a-ii). It is mostly but arguably not fully distinct from the earliest stages of the major protein peak. By contrast, the self-packed 9.5 cm column does not adequately separate particles and protein (Figure 2.8 b-i). Particles mostly elute in fractions 2.5-3.5, and the major protein peak is centred on fractions 7.5-8.5. Looking in greater detail at the protein associated with the EV peak, although there is clearly a peak of EV-associated protein, it is not adequately separated from free protein and appears as a shoulder of the major protein peak itself (Figure 2.8 b-ii). The strongest performance appears to be from the self-packed 28 cm column (Figure 2.8 c). The particle peak is centred on fractions 8.0-9.5, and the majority of protein elutes in a peak centred at fractions 21-23. As before, there is a clear peak of particle-associated protein (Figure 2.8 c-ii). Unlike the other two columns, there is a substantial gap between the elution of particles and particle-associated protein and the start of the major protein peak, at around fraction 14.5.

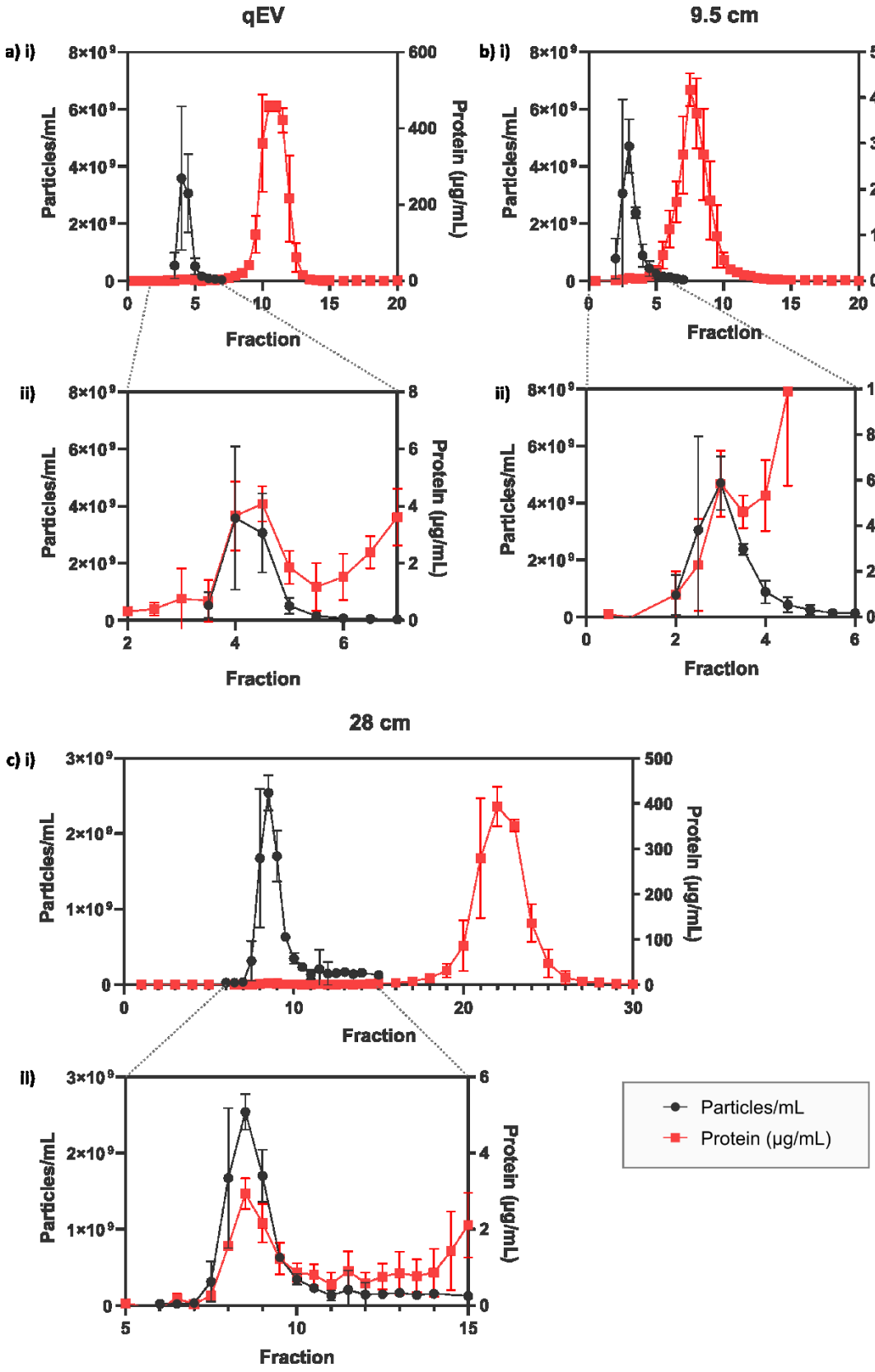


Figure 2.8: Elution of protein and particles from SEC columns. Traces for qEV (a), 9.5 cm (b) and 28 cm (c) Mean +/- SD is shown for both particles and protein (N = 3, n = 3 each). Zoomed-in sections for each graph are used to show the particle-associated protein peaks. These NTA measurements were captured with a 642 nm laser Nanosight LM10 and quantified using v2.3 NTA software, with detection threshold 10.

Assessing the recovery of particles from media, no significant difference was found between the number of particles recovered from any column or the number of particles loaded onto each column (one-way ANOVA) (Figure 2.9 a). There was no difference found between the quantity of particle-associated protein recovered from the qEV and 28 cm columns, but the quantity of protein recovered from the 9.5 cm column was significantly greater than both (one-way ANOVA and Tukey post-hoc) (Figure 2.9 b). This appeared to be due to contamination with free protein. The columns themselves are shown in Figure 2.9 c.

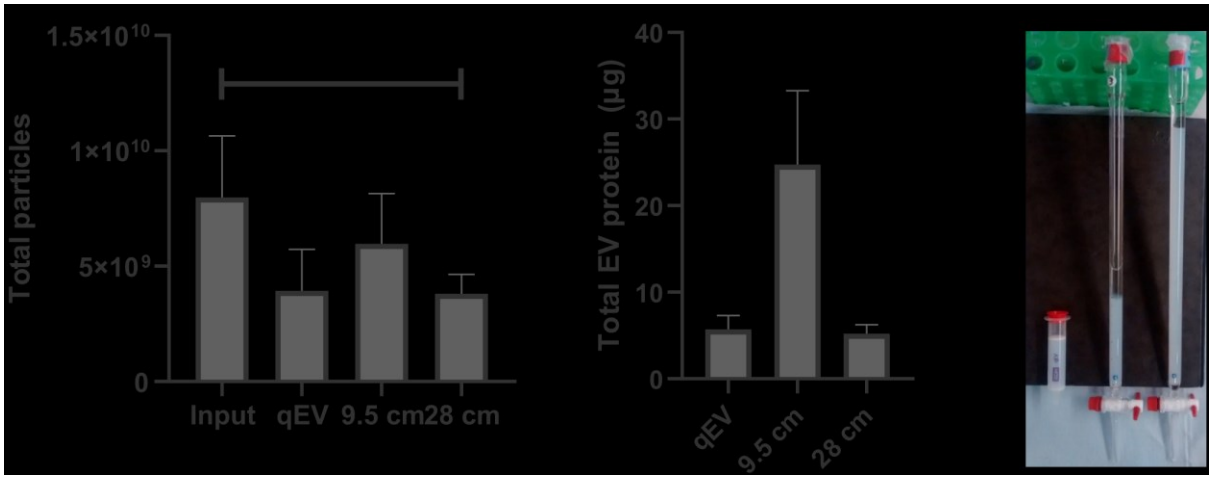


Figure 2.9: Recovery of particles and particle-associated protein from SEC columns. a) Number of particles added to and recovered from columns (N = 7 for input, N = 3 for others, n = 3 x 60 second videos). These NTA measurements were captured with a 642 nm laser Nanosight LM10 and quantified using v2.3 NTA software, with detection threshold 10. Number recovered is the sum of all particles eluting from the column in the peak fractions. No significant difference was found between groups (one-way ANOVA). b) Total quantity of protein recovered associated with the particle peak fractions for each column (N = 3, n = 3). Groups are significantly different if they do not share a letter (One-way ANOVA and Tukey HSD post-hoc test). c) Image of the three columns; from left to right, qEV, 9.5 cm, and 28 cm columns.

2.3.4. Electron Microscopy of SEC-purified EVs

The morphology of MDA-MB-231 EVs eluting from the column was assessed by SEM (Scanning Electron Microscopy) and Cryo-TEM (Cryogenic Transmission Electron Microscopy) (Figure 2.10). Cryo-TEM sample preparation and imaging was performed by Dr. Ulrike Kauscher. SEM images revealed a relatively monodisperse population of particles of approximately 100 nm diameter (Figure 2.10 a). However, the microscope used was relatively low-resolution and so only limited detail could be captured. Cryo-TEM imaging allowed excellent resolution and clarity (Figure 2.10 b). Vesicles between 100-200 nm could be seen.

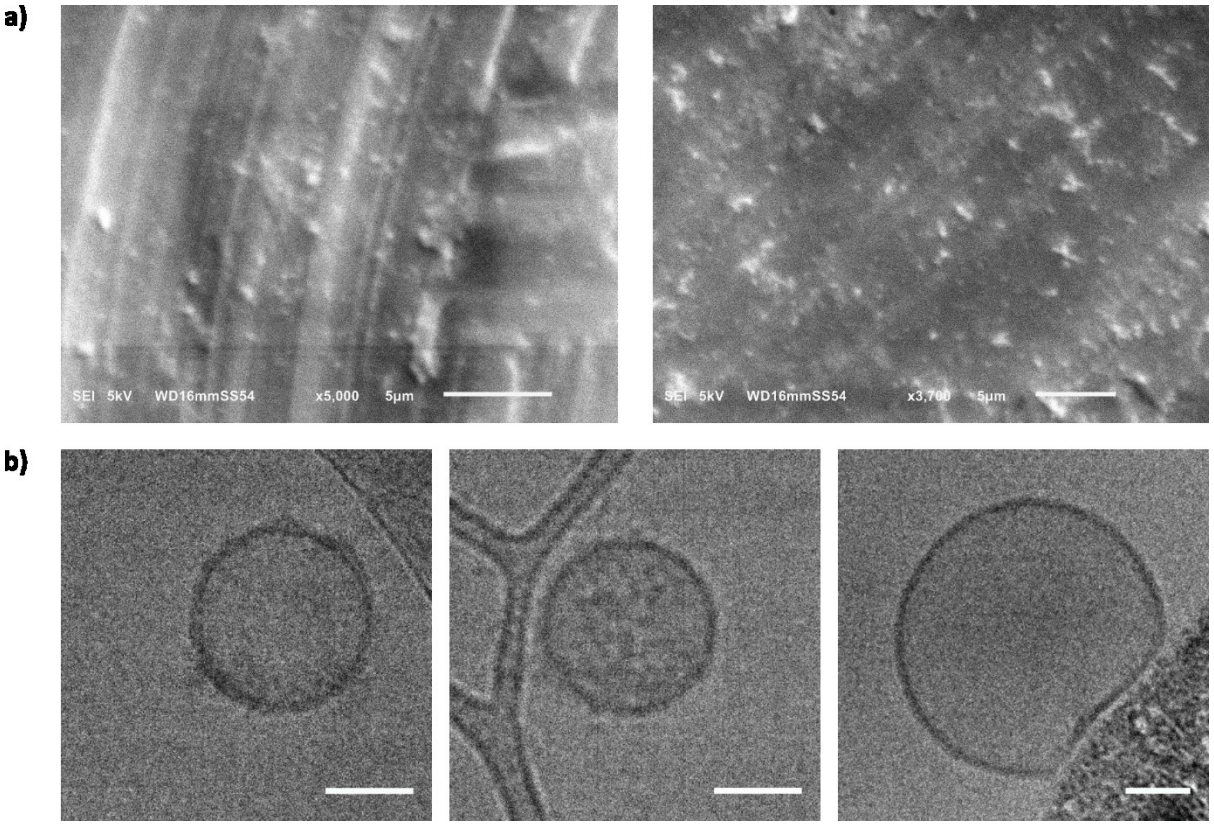


Figure 2.10: Electron microscopy of SEC-purified EVs. Samples were prepared as described in materials and methods. a) SEM images of EVs. Scale bar = 5 µm. b) Cryo-TEM images of EVs. Scale bar = 50 nm. TEM was performed by Dr. Ulrike Kauscher.

2.3.5. EV marker expression from SEC-purified EVs

So far, particles had been observed to elute from the SEC column in early fractions, co-associated with a small quantity of protein. EM of these particle-containing fractions revealed liposome-like particles. It was considered important to validate these liposome-like particles as extracellular vesicles by confirming the presence of EV marker proteins. Peak EV-containing fractions were pooled and prepared for Western blotting as described in materials and methods. Cell lysates were also prepared and ran in parallel. EVs and cell lysates from the previously used MDA-MB-231 cells were used, as were EVs and cell lysates from the A549 alveolar epithelial carcinoma cell line, prepared in the same manner. Membranes were probed for CD63, CD9, CD81 and Calnexin. Calnexin is an endoplasmic reticulum-associated protein expected to be present in cell lysates but not purified EVs.

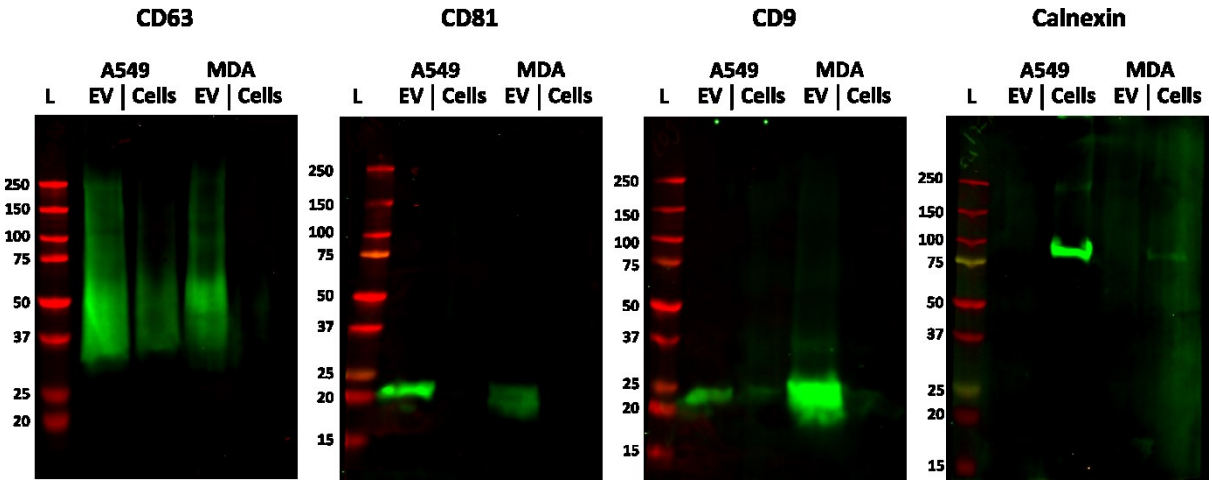


Figure 2.11: Detection of EV marker proteins by Western Blot. Antibodies against EV marker proteins (CD63, CD81, CD9) and Calnexin (an ER-associated protein and potential contaminant) were used. Numbers denote molecular weights of ladder bands in kDa. N = 1. This data kindly provided by Dr. A. Nagelkerke.

CD63 was detected as a broad band with peak brightness between approximately 30-60 kDa (Figure 2.11). CD63 was detected most strongly in the EV samples for both cell lines, although some was also detected in the A549 cell lysate. The predicted molecular weight of CD63 is 25 kDa; however, it is known to be multiply glycosylated and has been detected at a range of molecular weights between 30 and 65 kDa [139]. Multiple antibodies were tested, and all were found to detect the same wide band (data not shown). CD81 and CD9 were detected at their predicted molecular weights of 22 and 24 kDa respectively in EV samples from both cell lines, but not in cell lysates. Calnexin was detected in cell lysates only, most strongly in A549 lysate but also faintly in MDA-MB-231 lysate, indicating no contamination from cellular components in the EV sample. These Western blots were kindly performed by Dr. Anika Nagelkerke and are included in this thesis to demonstrate that the purified

EVs expressed the correct markers and that the antibodies themselves (also used later in the thesis) were initially validated.

2.3.6. EV-depleted FBS

As discussed in section 2.1.1.1, FBS contains very high concentrations of bovine EVs. If cells were cultured in FBS-containing medium, any attempt to isolate cell-derived EVs from that medium would lead to massive contamination from FBS-derived EVs. Typically, researchers choose either to culture cells in basal medium or to use FBS depleted of EVs. So far, EVs had been isolated from basal DMEM conditioned by MDA-MB-231 cells over 48 hours. The viability of the MDA-MB-231 cells did not appear to be significantly compromised by this starvation period. However, later work was intended to involve isolation of EVs from non-cancer cells, which it was thought might be more sensitive to the absence of exogenous growth factors. The possibility of using some form of enriched medium was therefore considered. As the purity of EV samples was a primary concern, the efficacy of a commonly-used FBS EV depletion protocol (ultracentrifugation for 18 hours, at 100,000 g, 4 °C) was investigated, as were the characteristics of commercially available EV-depleted FBS (Figure 2.12). It was found that both commercial (c-FBS) and "homemade" (h-FBS) EV-depleted FBS had a significantly reduced particle concentration compared to unprocessed FBS, with c-FBS significantly less than h-FBS (one-way ANOVA, Tukey HSD) (Figure 2.12 a). However, even the c-FBS sample still contained significant concentrations of particles – approximately 2.6 +/- 0.4 x 10^{10}/mL. Even though this was a nearly 50-fold reduction, once diluted 10-fold into growth media it would still be on the order of 10^9 particles/mL, sufficient to cause substantial contamination. The average modal size of the particles was found to be lower in c-FBS and h-FBS than FBS (Figure 2.12 b), possibly due to preferential sedimentation of larger particles during ultracentrifugation. Finally, it was found that c-FBS had an overall lower protein concentration than FBS, although h-FBS was not found to have a lower concentration than FBS (Figure 2.12 c). This decrease in concentration was likely due to co-sedimentation of other proteins during the depletion process and may underlie the lower growth rates reported for EV-depleted FBS.

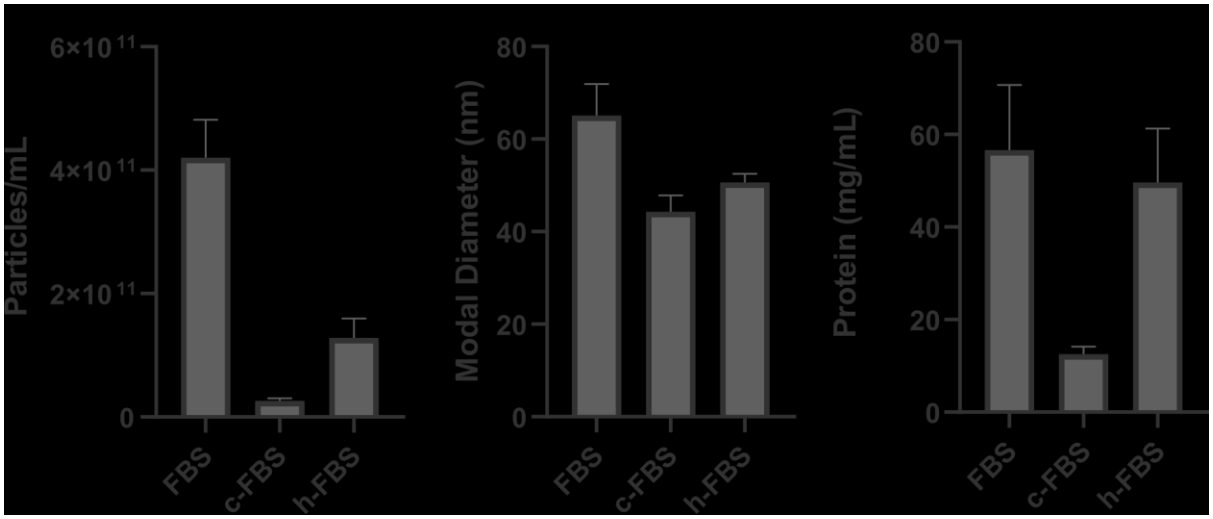


Figure 2.12: Characterisation of commercial and "homemade" EV-depleted FBS a.) Nanosight particle concentration quantification. b) Modal diameters measured by Nanosight. c) Protein concentrations measured by micro-BCA assay. N = 3, n = 3. Mean +/- SD shown. Samples not sharing a letter are significantly different ($p < 0.05$, one-way ANOVA and Tukey HSD post-hoc test).

At this point the decision had been made that both c-FBS and h-FBS were likely to result in unacceptable levels of contamination and that they would not be suitable for use. However, due to their widespread use in the literature without similar validation, it was considered worthwhile to investigate the potential downstream impact of using them as media supplements, especially when paired with an isolation method suspected to result in low purity EV samples.

Mock EV isolations were performed using media supplemented with 10 % v/v c-FBS or h-FBS. These mock isolations used a standard serial ultracentrifugation protocol involving two sequential 3-hour ultracentrifugations at 100,000 g, with a PBS wash step. The resulting invisible "pellet" was evaluated (Figure 2.13). It was found that the mock-isolated pellets contained on the order of 10^{10} particles/mL for both c-FBS and h-FBS supplemented media (Figure 2.13 a) (c-Pel and h-Pel respectively). The diameter of the c-Pel particles was significantly less than that of the h-Pel particles, despite no significant difference in size between particles in h-FBS and c-FBS themselves (Figure 2.13 b). Protein was detected in the pellets of both samples (Figure 2.13 c).

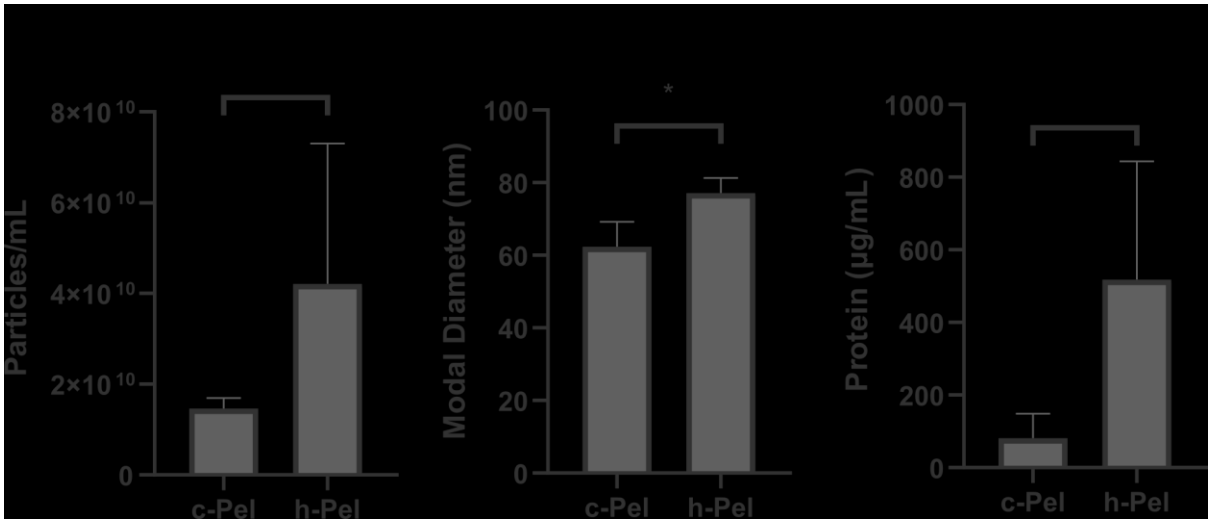


*Figure 2.13: Characterisation of mock-isolated EV-depleted FBS pellets. a) Nanosight particle concentration quantification. b) Modal diameters measured by Nanosight. c) Protein concentrations measured by micro-BCA assay. N = 3, n = 3. Mean +/- SD shown. *: p < 0.05 (Student's T-test).*

Cryo-TEM of the c-Pel and h-Pel samples revealed liposome-like particles of approximately the expected diameter (Figure 2.14), indicating that at least some of the particles were indeed EVs.

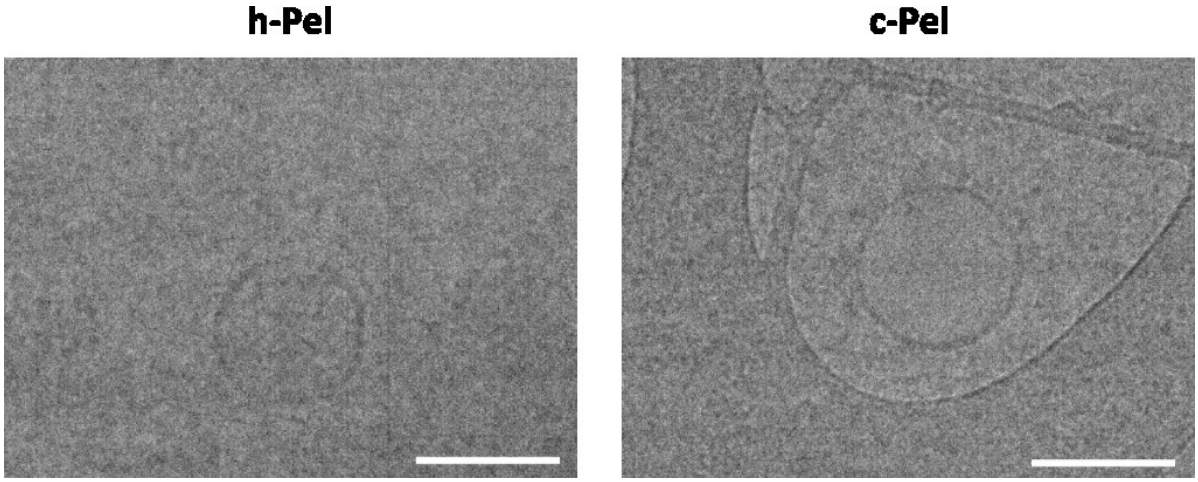


Figure 2.14: Cryo-TEM of h-Pel and c-Pel samples. Scale bar = 100 nm. TEM was performed by Dr. Ulrike Kauscher.

2.3.7. Downstream effects of use of EV-depleted FBS

Due to the presence of detectable protein and particles in the mock-isolated samples, it was anticipated that it might be possible that these contaminants had some ability to affect the behaviour of cells. The ability of these samples to stimulate angiogenesis in an *in vitro* tubule formation assay was assessed (Figure 2.15). In this assay, Human Umbilical Vein Endothelial Cells (HUVECs) were seeded onto a hydrogel made from basement membrane protein extract (GFR-Geltrex). The endogenous growth factors from the basement membrane were removed during production. With appropriate stimulation, HUVECs migrate across the hydrogel surface, come together and form a network of tubule-like structures resembling capillaries. Without stimulation from growth factors, the HUVECs remain mostly viable but do not undergo morphogenesis. The extent to which this morphogenesis has been stimulated can be quantified by image analysis of the tubule network structure. The total length of all the tubes in the network was chosen as the metric for network development. This assay was developed to a 96-well format, allowing simultaneous same-plate analysis of several samples with up to twelve technical replicates (see materials and methods). Fully supplemented endothelial cell growth medium was used as a positive control, and basal medium as a negative control.

It was found that both c-Pel and h-Pel resulted in a significant increase in the formation of capillary-like tubules in this assay (Figure 2.15 a,b). It was not investigated whether this effect was due to FBS-derived particles or free protein. It therefore appears that the combination of EV-depleted FBS and a commonly used isolation technique can lead to contamination with material that is active in biological signalling. This is particularly concerning as the majority of studies using EV-depleted FBS or other enriched media do not include a negative control in which the media is not conditioned, and so are likely unaware of the contribution of FBS-related contaminants to the reported biological effects of their EVs.

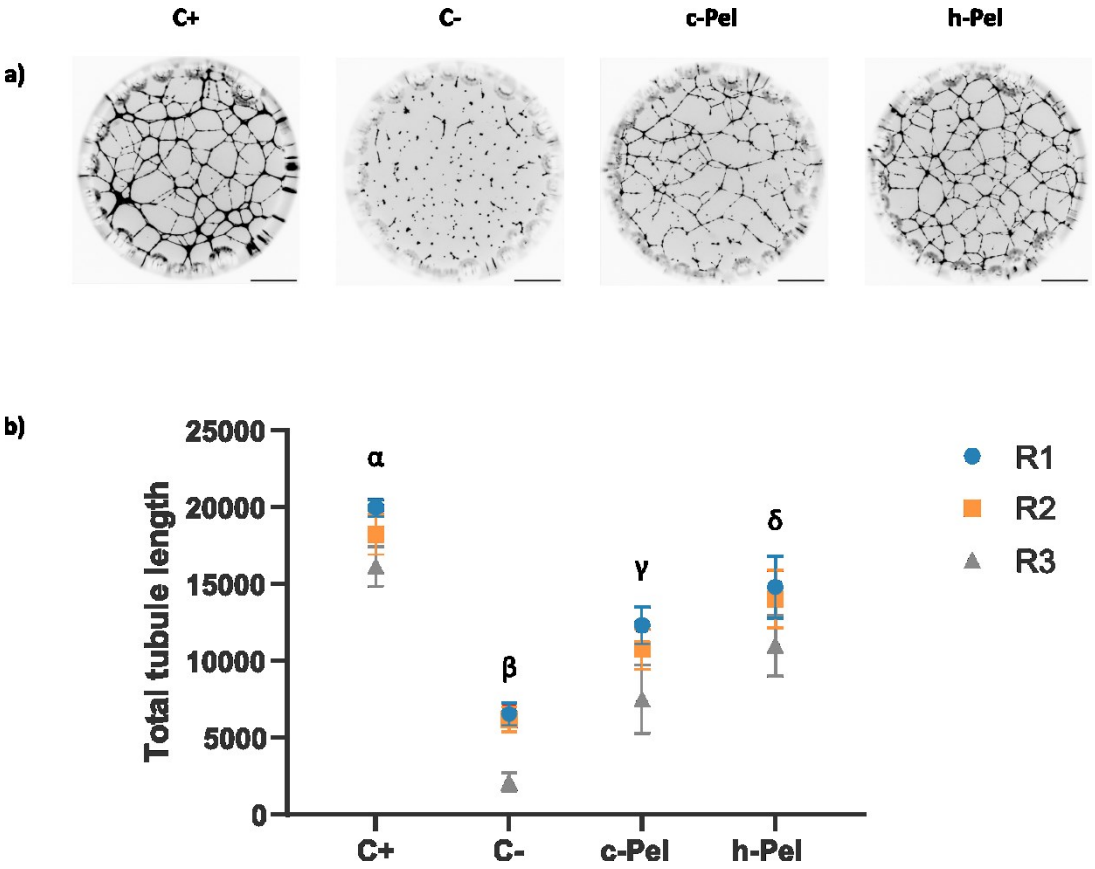


Figure 2.15: Tubule formation assay to assess proangiogenic effects of c-Pel and h-Pel. a) Representative images of each condition. Images inverted for clarity. Scale bar = 1 mm. b) Quantification of total tubule length for each condition. Individual replicates are shown (N = 3, n = 12). Samples not sharing a letter are significantly different ($p < 0.05$, one-way within-subjects ANOVA and Tukey HSD post-hoc test).

2.4. Discussion: Development of the purification system

In this study, the purity of isolated EVs was considered to be critically important. If non-EV contaminants were present in the EV isolate, it would not be possible to separate their signalling properties from those of the EVs. An EV purification system was developed based on ultrafiltration and size exclusion. Initial investigation of Amicon ultrafiltration membranes found that there was no significant difference between the total number of particles in the input conditioned medium and the total number of particles recovered from the resulting concentrate from 3, 30 and 100 kDa membranes. This suggested an excellent recovery and they were considered promising for routine concentration. The time taken to concentrate medium increased with smaller pore sizes, and so the largest (100 kDa) pore size was taken forward for subsequent routine purification. From here on, smaller pore sizes were used when necessary to recover soluble protein as well as EVs from the conditioned medium.

Size exclusion chromatography resins were investigated to see whether they might be suitable for separation of EVs and soluble protein from the ultrafiltration concentrate. Of those tested, Sepharose CL-2B appeared most promising. Separation was assessed by measuring the particle and protein concentrations of the fractions eluting from the column. A column which allowed complete separation of EVs and soluble protein was desired. The length of the column was found to influence the efficacy of separation, with a 28 x 1 cm column being most effective. This is not unexpected, as the resolution of SEC columns is limited by the ratio of the on-column height of the sample to the total height of the column. There were some potential contaminants that might still have co-isolated with EVs with this system. Any material with a similar size to EVs may have contaminated the final isolate. This would have been a concern when isolating EVs from plasma due to the presence of lipoparticles (see section 2.1.3.2). However no similarly sized contaminants were anticipated from cell culture medium.

The recovery of EVs from the column was also assessed. Again, no significant difference was found between the particles added to the column and the number recovered. This may be due to a lack of statistical power. The mean number of particles recovered from the 28 cm column is approximately half that of the mean number of particles added. It worth noting that the number of particles measured to be in the concentrated conditioned medium prior to column separation is substantially less than the concentration measured in the concentrated conditioned medium during Amicon ultrafiltration membrane validation. This is likely because column evaluations were performed using an earlier model of Nanosight (LM10 rather than NS300), with a less powerful laser. Particle concentrations are therefore not comparable between these experiments.

Some EV loss occurs during concentration and column separation, although from this initial validation data this loss appeared minimal. In later work in this thesis losses appeared to be higher. Loss may have been due to adsorption onto the ultrafiltration membrane or column resin. There may also have been some EV destruction during ultrafiltration. The increased loss in later sections may have been due to differences in the initial concentration and composition of the conditioned medium. If the initial concentration is lower, loss of the same quantity of EVs would result in a higher overall percentage loss.

The EVs isolated by this method were characterised. EVs were found to express the EV markers CD63, CD81 and CD9 as expected. Calnexin was not present in the EV isolate. This indicated that there was no contamination from the endoplasmic reticulum, which might have been expected if cells were not viable during starvation. Vesicle – like structures were observed with electron microscopy. EVs therefore appeared to be intact and isolated effectively, without contamination from soluble protein. At the time of development, ultrafiltration and size exclusion had not been widely used for EV purification. However, similar purification procedures are now widely used within the field (see section 2.1.3.2) and have also been validated elsewhere as able to reproducibly isolate intact and functional EVs.

EV-depleted FBS is commonly used as a media supplement in order to maintain cell viability while collecting EVs in cell culture. In many studies preparation of EV-depleted FBS is considered a trivial step involving a single ultracentrifugation, and validation of the success of depletion is rarely fully reported. As the purity of the final EV isolate was considered to be of paramount importance, it was considered necessary to assess the potential downstream consequences of isolating EVs in media containing EV-depleted FBS. It was found that both commercially available and researcher-prepared EV-depleted FBS contained prohibitive concentrations of particles that would have made up a substantial proportion of total particles isolated from the cell-conditioned medium. Additionally, it was found that ultracentrifugation with a wash step was insufficient to remove EV-depleted FBS-derived material from the final isolate. This material included detectable particles and protein and was able to stimulate an *in vitro* assay of angiogenesis.

These results indicated that EV-depleted FBS should not be assumed to be an appropriate media supplement. Assessment of its EV content prior to use should be performed. If use of EV-depleted FBS is unavoidable, a control should be included across all experiments in which a “mock” isolation is performed with supplemented media that has not been conditioned by cells. The pro-angiogenic effect of the final contaminated isolate may have been due to FBS-derived soluble proteins rather than bovine EVs. In the case of later experiments in this study, any addition of growth factors to the

medium would have been inappropriate, as the contribution of cell-derived and exogenous signalling molecules could not have been separated.

2.4.1. Conclusions

A purification strategy based on ultrafiltration and size exclusion was developed and validated. This technique was found to allow an essentially complete separation of EVs from detectable soluble protein, while recovering a workable percentage of the input particles. EVs isolated by this method expressed EV markers and had a liposome-like morphology as imaged by electron microscopy. EV-depleted FBS either prepared in-house or from commercial sources was found to contain particles. When used in combination with an ultracentrifugation-based isolation approach, contamination in the final isolate was observed and found to be capable of stimulating *in vitro* angiogenesis.

3. Matrix vesicles and mineralisation

3.1. Literature review: matrix vesicle-mediated mineralisation of soft tissues

Mineralisation of soft tissue is a critical part of the formation of new bone during growth and development [140]. In long bones, elongation happens progressively at structures towards the ends of the bone known as epiphyseal growth plates (Figure 3.1 a). At the most distal point of the growth plate, a population of stem cells and immature chondrocytes lies in the "resting zone". Below it, in the "proliferative zone", more mature chondrocytes proliferate and secrete extracellular matrix proteins to form cartilage. Below that is the "hypertrophic zone" in which chondrocytes increase in size and secrete signalling factors to encourage ingrowth of blood vessels, attract chondroclasts to digest the cartilaginous matrix, and encourage nearby perichondral cells to differentiate into osteoblasts. As the osteoblasts begin to secrete their own matrix proteins, the chondrocytes apoptose, leaving a scaffold within which osteoblasts then form bone. Growth plates gradually shrink and disappear as puberty is concluded.

A similar organisational structure in which mineralised tissue transitions to cartilage is present in articular cartilage (Figure 3.1 b) [141]. The uppermost superficial zone of articular cartilage contacts the synovial fluid of the joint and contains a relatively dense population of chondrocytes along with tightly packed collagen fibres parallel with the joint surface. The mid-zone contains a relatively sparse chondrocyte population and a transitional population of extracellular proteins. The deep zone below that contains chondrocytes aligned as columns and collagen fibres perpendicular to the articular surface. Immediately below that is a layer of mineralised cartilage integrated into underlying subchondral bone. This layer of mineralised cartilage is critical for the mechanical strength of the articular cartilage and for anchoring it to the bone itself.

In both of these structures, the initiation and regulation of mineralisation appears to involve the deposition of matrix vesicles by the mineralising cells. First observed in the tibial epiphyseal plate of mice in 1969 [17], they appeared in electron micrographs as membranous structures closely associated with needle-like structures of mineral. They were found only in the lower hypertrophic and calcifying zones of the epiphysis. Similarly, mineralisation-competent vesicles are only found in the deepest zone of articular cartilage, near the interface with bone [142].

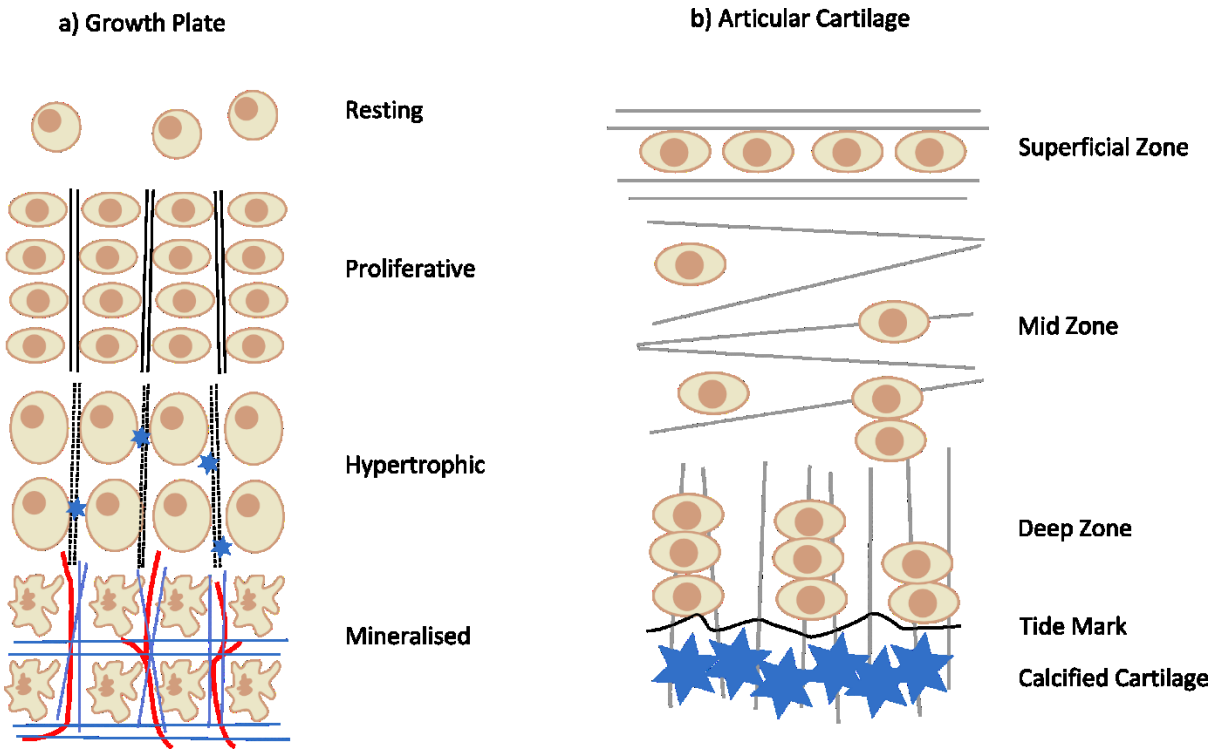


Figure 3.1: Calcification of cartilage in a) growth plate and b) articular cartilage. Matrix vesicles are found in the deeper zones in both, in association with mineralising tissue.

3.1.1. Mechanism of Matrix Vesicles

The initiation of mineralisation by matrix vesicles appears to be a two-step process. Initially, free Ca^{2+} and PO_4^{3-} ions are accumulated within the vesicular lumen and an initial nucleation core of hydroxyapatite is formed (Figure 3.2). The seed crystal then grows and punctures the membrane, growing beyond the original vesicle and into surrounding tissue [143]. Accumulation of Ca^{2+} in the lumen of the vesicle is encouraged by the presence of calcium-binding membrane-associated lipids and proteins, particularly Annexin V, which may also function as a calcium ion channel. PO_4^{3-} flux into the lumen is thought to be enhanced by the presence of PiT1/2 phosphate transporters. Associated with the outer membrane of the vesicle is Tissue Non-Specific Alkaline Phosphatase (TNAP, also known as ALP), which can hydrolyse Adenosine Triphosphate (ATP) into Adenosine Diphosphate (ADP) and Phosphate (Pi) and Pyrophosphate (PPi) into two Pi ions. This creates a high local concentration of around the perimeter of the vesicle, increasing influx of phosphate. Calcium and phosphate are thought to nucleate to form hydroxyapatite on a combination of proteins and acidic phospholipids on the inner membrane surface, known as the Nucleation Core Complex (NCC) [144, 145]. The precise mechanism is not understood, but it has been hypothesised that the acidic head groups of the lipids aid stabilisation of intermediate crystal states between amorphous calcium phosphate and hydroxyapatite, in conjunction with localisation due to the affinity of NCC proteins for calcium ions [146]. Subsequently to nucleation, the crystal grows and ruptures the membrane. This is aided by

the high perivesicular concentration of Pi generated by TNAP, which also reduces the local concentration of PPi, which would otherwise inhibit mineralisation. Mice lacking functional TNAP develop progressive and eventually fatal osteomalacia, yet despite this appear to have normal quantities of mineral within matrix vesicles in bone growth plates [147]. However, the second stage of mineral propagation does not successfully occur.

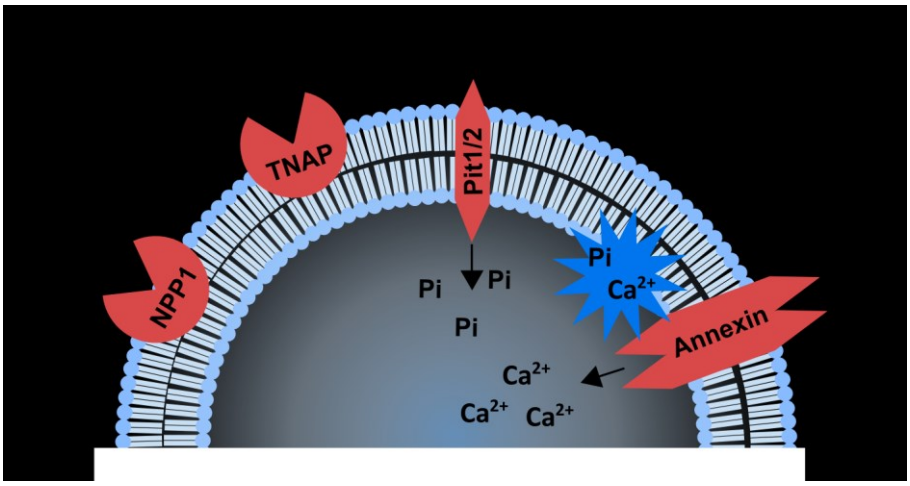


Figure 3.2: Molecular mechanisms of matrix vesicles. As described in the text, outer membrane leaf phosphatases act to generate a high perivesicular concentration of inorganic phosphate, which enters the lumen via phosphate transporters. Calcium ions enter via Annexin and other calcium-binding proteins. Mineral is nucleated at the nucleation core complex (NCC), an incompletely defined site involving lipid headgroups and proteins.

3.1.2. Matrix vesicles and extracellular vesicles

Although matrix vesicles were first described a half-century ago [17], research into their properties and function has occurred essentially in parallel to research on other forms of extracellular vesicles. It is only recently that matrix vesicles have been re-examined in the context of the rapidly growing EV field. It appears that matrix vesicles are indeed a specialised microvesicle. Proteomic analysis of endosomal-exosomes and matrix vesicles demonstrates that they contain many of the same characteristic proteins, such as tetraspanins, ESCRT complex-associated proteins and heatshock proteins [148]. Freeze-fracture studies concluded that matrix vesicles derived from mineralising cells are formed by blebbing at the plasma membrane [149, 150], in common with microvesicles. Specifically, they appear to be formed from microvilli, at least in osteoblast-like cells in culture [151]. However, it may be the case that just as cells typically produce a mixture of exosomes and microvesicles simultaneously, so too do mineralising cells produce multiple vesicle types capable of initiating mineralisation. Both 100-550 nm diameter vesicles and large multivesicular bodies containing vesicles of approximately 100 nm diameter (an apparent parallel to the multivesicular

bodies from which exosomes originate) were found in the skeletal bone of zebrafish. Both contained calcium and phosphate, indicating possible involvement in mineralisation [152].

3.1.3. Tissue engineering applications of matrix vesicles

Biomimetic mineralisation of soft polymer constructs is a long-standing goal of the tissue engineering field. Conventionally, mineralisation of polymer scaffolds is induced by incubation in SBF (Simulated Body Fluid), a medium with ion concentrations approximating or higher than that of human plasma [153]. Mineralisation of a polymer scaffold can occur spontaneously in SBF, however this process is slow, uncontrolled, and generates a mineral phase that may not be entirely similar to biological hydroxyapatite in terms of the relative presence of ions or 3D lattice structure [154, 155]. Current strategies to improve or control mineralisation involve modifying the polymer to contain negatively charged groups [156], which can act as sites of nucleation. More biomimetic approaches involve incorporation of bone extracellular matrix (ECM) proteins that are thought to be able to nucleate mineralisation, such as bone sialoprotein [157]. Use of matrix vesicles (or synthetic mimics of matrix vesicles) could allow a more controlled formation of bio-like hydroxyapatite (HA) within engineered tissue constructs, although exactly how they might impact upon the higher-order structure of the mineral phase cannot necessarily be predicted. Additionally, the ability to control the positions within a scaffold where mineralisation can be initiated might be useful in generating scaffolds that contain a mineralisation interface. For example, it is desirable for an articular cartilage scaffold to be able to integrate into the underlying bone, in order to generate a structurally stable scaffold and allow proper distribution of the patient's weight into the bone [158].

3.1.4. Summary

Here, the properties of matrix vesicles derived from articular cartilage were investigated, with the goal of using them to direct mineralisation of a collagen-based tissue engineering scaffold. It was demonstrated that matrix vesicles purified using the UF-SEC system developed in section 2.3 were enzymatically active. *In vitro* mineralisation associated with matrix vesicles was observed, although challenges were evident in establishing consistent mineralisation behaviour. Although the envisioned endpoint of this subproject was not reached, intriguing data concerning the distribution and properties of matrix vesicles was collected, and characterisation of these vesicles is presented briefly in the following section.

3.2. Materials and Methods

Methods specific to this chapter are detailed below. All others are as previously described.

Isolation of Bovine Matrix Vesicles

Dissection

Matrix vesicles were obtained from the metacarpal-phalangeal articular cartilage of ~3-month-old calves within 24 hours of death. Limbs were received severed at the carpal joint. Limbs were thoroughly washed, and excess blood drained before thorough external sanitisation with 70 % ethanol. Dissection was performed in a tissue culture hood, using a weighted rig to keep the limb flexed. The dermis was cut and lifted away as a flap to expose the underlying joint. From the exposed articular cartilage, superficial/mid zone, mid/deep zone, and full thickness cartilage were obtained. Superficial/mid zone cartilage was obtained as thin shavings from the top and sides of the exposed condyles, and then the underlying mid/deep zone cartilage by deeper cuts at the same location, down to the underlying bone. Full thickness cartilage was obtained by the same method, but without initial separation of superficial cartilage. Cartilage shavings were immediately transferred to unsupplemented DMEM. Typically, cartilage was pooled from four joints per isolation.

Tissue digestion and sample collection

Cartilage shavings were transferred into 100 mm Petri Dishes in unsupplemented DMEM and further cut into 2-5 mm diameter fragments. Fragments were washed once before digestion in 0.1 % w/v Pronase (Roche, 10165921001) for 2 hours, at 37 °C, 5 % CO_2 before washing three times with DMEM and incubating for 16 hours with 0.04 % w/v Collagenase (Sigma, C0130) at 37 °C, 5 % CO_2. Samples were disrupted, and digested tissue resuspended by pipetting up and down with sequentially smaller tip-diameter stripettes (25 mL, 10 mL, 5 mL). Samples were digested for a further 4 hours before final disruption and resuspension with a 1000 µL pipette. Solutions were diluted to 30 mL with unsupplemented DMEM and filtered through 100 µm cell strainers (Corning 431752) to capture remaining fragments of bone before centrifugation at 1000 g, for 5 minutes with slow acceleration and deceleration, to pellet cells and additional debris. Supernatants were collected and centrifuged at 4500 g for 15 minutes. Supernatants were collected again and passed through 0.45 µm syringe filters before storage at -80 °C. Matrix vesicles were then isolated from these samples as previously described.

ALP activity assay

ALP assay buffer (0.2 M Tris-HCl, 0.045 M NaCl, 1.25 mM $MgCl_2$, pH 9.3) was mixed at a v/v ratio of 7:3 with 0.02 M 4-nitrophenol phosphate (Merck) in water, to form a working solution. Working

solution was mixed 1:1 with EV samples (in PBS) previously diluted 1:9 in ALP assay buffer. The mixture was then incubated for 1 hour at 37 °C before reading absorbance at 405 nm using a Spectramax M5 platereader.

Mineralisation assay

SEC-purified matrix vesicles were pooled into 1.5 ml Eppendorf tubes and pelleted by centrifugation at 17,000 g, 18 hours, 4 °C. The pellets were resuspended in 100 µL of DMEM + A/A. Resuspended pellets were quantified by Nanosight. Samples were further diluted in DMEM to match particle concentrations across samples. β-glycerophosphate was added to the appropriate samples at this stage (10 mM final concentration). 200 µL of sample was added per well of a 96-well plate. The 96-well plate was sealed with parafilm to prevent evaporation. Samples were imaged daily on an Olympus IX51 upright microscope (Olympus, Tokyo, Japan), with an Olympus TL4 light source and Thorlabs Quantalux sCMOS camera (Thorlabs, Newton, NJ, U.S).

Raman spectroscopy of mineral

Mineral was mechanically scraped from the bottom of the well, resuspended in a small volume of 18.2 MΩ water and deposited on a Fluorite slide. Once dried, the dried spot was analysed with an alpha300R+ Raman microspectroscope (WITec, Ulm, Germany).

Dissolving deposited mineral

Mineral deposited at the bottom of wells was washed 4 times with 18.2 MΩ water and left to dry, before addition of 90 µL 0.1 M HCl to each well. HCl was left on mineral for 10 minutes before pipetting up and down to ensure full collection and mixing and retrieving the dissolved mineral for further analysis.

O-Cresolphtalein complexone assay

A solution of 0.01 % w/v o-Cresolphthalein Complexone (Sigma-Aldrich) was prepared in 0.1 M Sodium Borate. 160 µL of this working solution was added to 40 µL of sample per well of a 96-well plate and absorbance measured immediately on a Spectramax M5 platereader at 570 nm.

Ammonium Molybdate assay

A solution of 0.42 % w/v Ammonium Molybdate (Sigma-Aldrich) was prepared in 1 N H_2SO_4. This was mixed with a solution of 10% w/v Ascorbic acid (Sigma-Aldrich) in water at a ratio of 6:1 Ammonium Molybdate: Ascorbic acid. 150 µL of working solution was added to 50 µL of sample per well of a 96-well plate. The sample was left for 1 hour at 37 °C before reading absorbance at 620 nm with a Spectramax M5 platereader.

3.3. Results: Matrix vesicles

This chapter describes the isolation and characterisation of matrix vesicles from bovine articular cartilage.

3.3.1. Isolation of matrix vesicles from bovine cartilage

Matrix vesicles were anticipated to be present within the hard tissue of articular cartilage itself. This presented a challenge for isolation compared to isolation from biofluids, as the tissue had to be harvested and broken down without damaging the matrix vesicles. In order to accomplish this, a technique more typically used to isolate bovine chondrocytes was adapted for EV isolation (Figure 3.3). Briefly, the lower forelimb was opened to expose the metacarpal-phalangeal articular cartilage, from which shavings were harvested using a scalpel. Superficial shaving of the joint isolated only the topmost, superficial layer of cartilage (Superficial/Mid-Zone, SMZ). Deeper shaving at the same location isolated the lower, Mid/Deep Zone cartilage (MDZ) and some underlying bone. A deep shaving at a single location collected the full thickness (FT) of the cartilage. The tissue was divided in this way as mineralising chondrocytes are typically found in the deep zone but not the superficial zone [141], and so it was anticipated that mineralising matrix vesicles would be present in the deep zone only. The other tissue sections were collected to allow comparison.

These shavings were minced in basal DMEM with a scalpel before sequential enzymatic digestion by Pronase (an aspecific mixture of bacterial proteases) and Collagenase, to break down the extracellular matrix. After a 16-hour incubation (37 °C, 5 % CO_2) the matrix was mostly broken down but was mechanically disrupted further by pipetting up and down with progressively smaller stripettes and pipettes (25, 10, 5, and 1 mL). After another 4 hours, the mixture was mechanically disrupted again before being passed through a 100 µm cell strainer to remove any shards of bone before centrifugation to pellet cells. Instead of harvesting the cells, the supernatant was collected, and subsequently EVs were isolated from it using the same pre-processing, UF and SEC protocols as in section 2.3. EVs were typically collected as a single pooled sample, discarding the first 6.5 mL of eluate and collecting fractions 6.5 – 13.

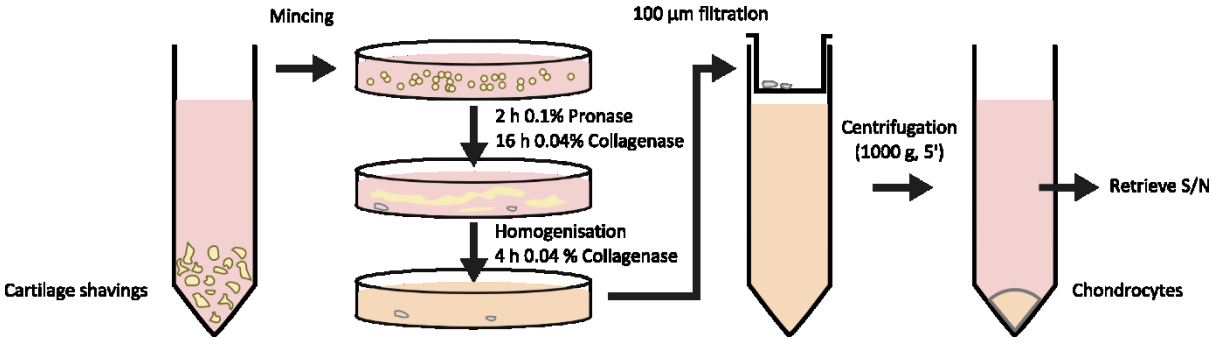


Figure 3.3: Isolation of bovine cartilage matrix EVs. Method is described in greater detail in Materials and Methods.

3.3.2. Characterisation of matrix vesicle size and morphology

Particles were isolated from SMZ, MDZ, and FT cartilage shavings. NTA quantification of particles from each tissue layer found them to have similar size distributions with modal diameters of approximately 80-90 nm (Figure 3.4 a). SEM of particles from FT shavings appears to confirm this observation (Figure 3.4 b). The images show large aggregates of particles, also approximately 80-90 nm in diameter. The aggregation was likely caused by the drying process during SEM sample preparation.

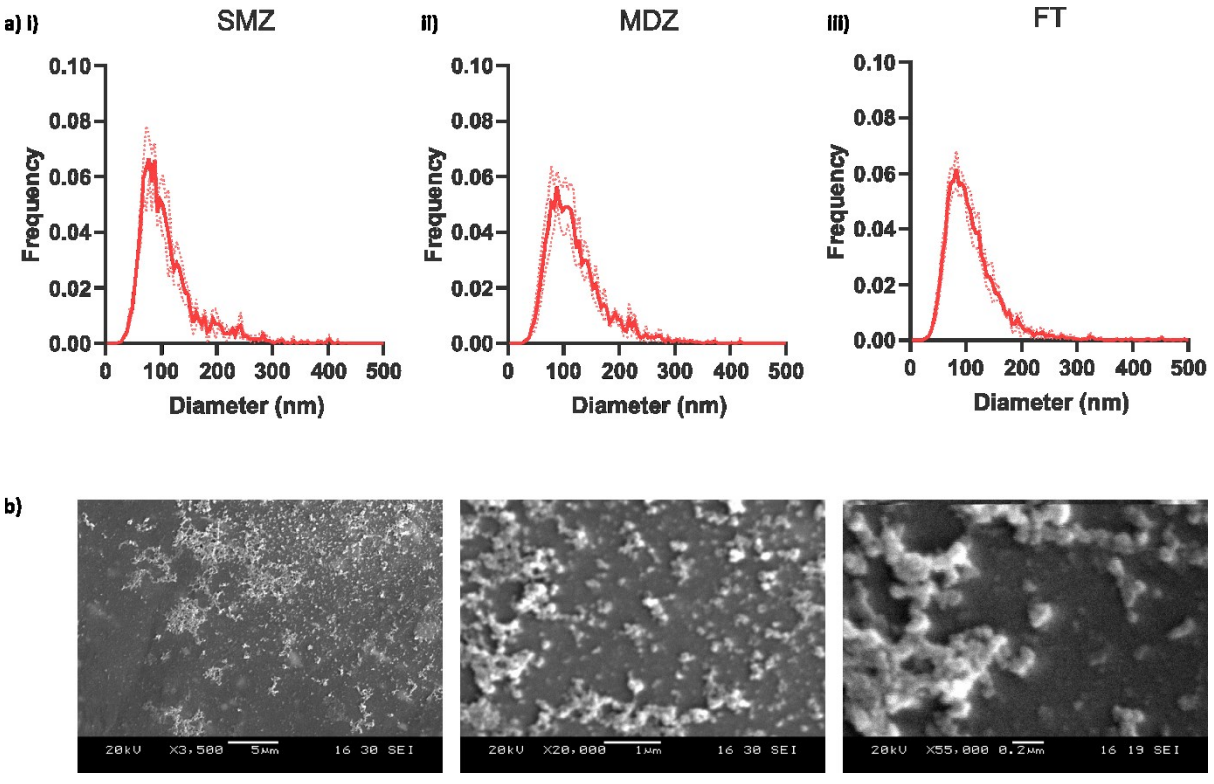


Figure 3.4: Size of particles isolated from bovine cartilage. a) Normalised size distribution of particles from i) SMZ, ii) MDZ, and iii) FT cartilage shavings, as measured by NTA. Mean +/- SD shown (N = 3, n = 3 x 60 second videos). b) SEM images of particles isolated from FT cartilage shavings. Scale bars are shown for each image.

3.3.3. Characterisation of particle and protein content of matrix vesicle isolates

It was found that the quantity of EV protein isolated per gram of tissue shavings (wet weight) was not significantly different between SMZ, MDZ and FT isolations (Figure 3.5 a). Similarly, the number of particles isolated per gram of wet tissue weight after UF/SEC purification did not differ significantly between tissue sections (Figure 3.5 b). The particle to protein ratio was calculated to assess purity (Figure 3.5 c). Ratios were approximately 2.5 – 3.5 x 10^9 particles/µg of protein. By the standards suggested by Webber and Clayton [108], this falls short of the 3 x 10^{10} particles/µg ratio suggested as a benchmark for high purity, but above the threshold of 1.5 x 10^9 particles/µg considered to indicate an impure sample. The quantity of genuinely EV-associated protein is likely to differ between sources and so given that the UF/SEC system had already been validated, this was not considered a cause for concern. There was a statistically significant difference between the particle to protein ratio for SMZ and MDZ isolations, with MDZ having a slightly lower purity; however, given the small size of the difference and the lack of significance in other analyses this was not considered to represent a major biological distinction.

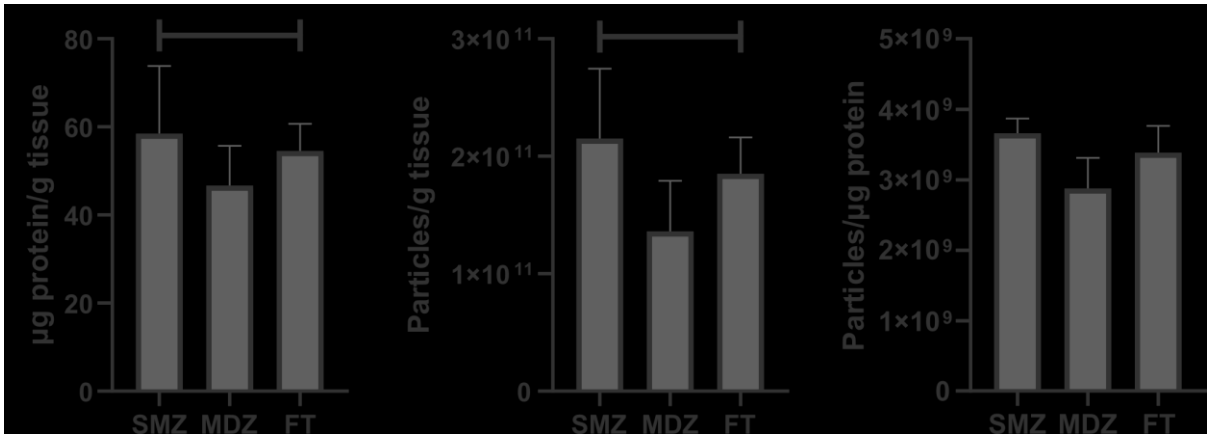


Figure 3.5: Recovery of particles and protein from cartilage. a) Micrograms of particle-associated protein isolated per gram of wet tissue. b) Particles recovered after UF/SEC purification, per gram of wet tissue. c) Particle to protein ratio for UF/SEC purified particles. Protein concentration measured by micro-BCA assay (N = 3, n = 3) and particle concentration by NTA (N = 3, n = 3 x 60 second videos). Differences between groups are significant if they do not share a letter ($p < 0.05$, one-way within-subjects ANOVA and post-hoc Tukey's HSD test).

3.3.4. Optimisation of ALP activity assay

Mineralising matrix vesicles are reported to contain alkaline phosphatases involved in the initiation of mineralisation. The ALP activity of vesicles from each tissue section was investigated using an assay in which colourless para-nitrophenol phosphate (PNPP) is dephosphorylated by ALP, converting it into yellow (λmax = 405 nm) para-nitrophenol (PNP). An assay protocol developed for cell lysates was initially used. Very low ALP activity was initially observed. It was realised that the assay buffer used in the assay developed for cell lysates did not contain magnesium, which is an essential cofactor for ALP [159]. Addition of magnesium to the buffer significantly increased ALP activity (Figure 3.6). Sufficient magnesium may typically carry over in cell lysates for this assay, but the UF/SEC purification may have diluted it away, as vesicles were eluted in PBS without magnesium.

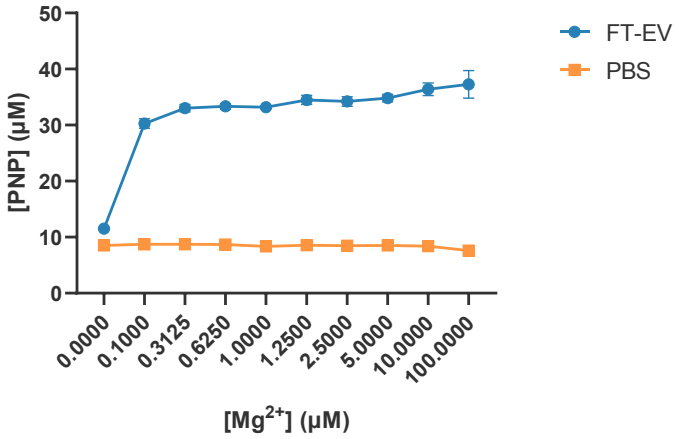


Figure 3.6: Influence of magnesium concentration on PNP conversion by FT-EVs. N = 1, n = 3 (mean +/- SD shown).

3.3.5. ALP activity of matrix vesicle isolates

Using modified assay buffer containing 1.25 mM $MgCl_2$, the ALP activity of particles from each tissue layer was quantified (Figure 3.7). EVs were collected from fractions 6.5-13 from the column and pooled. 10 µL of the pooled EVs was added per well of a 96-well plate. It was found that although MDZ and FT-derived particles had detectable activity across all replicates but SMZ-derived particles did not, no significant difference between groups was detected with a non-parametric within-subjects Friedman and post-hoc Dunn's test (Figure 3.7 a). The pattern of activity was the same when normalised to the number of particles in the assay as measured by NTA (Figure 3.7 b), and when normalised to the quantity of protein added to the assay (Figure 3.7 c). However, when normalised in this way, a difference is found between SMZ and FT activities. The lack of detection of a difference despite SMZ activity being essentially undetectable and MDZ and FT samples being well above the limit of detection for all samples is likely due to the high variation of activity in MDZ and FT samples.

It is interesting to note that the concentration of particles in each tissue layer appeared to be very similar, yet the enzymatic activity of the particles differed between layers. This is consistent with two models – one in which the mineralising vesicles are a small subpopulation in a much larger population of inactive particles, only present in mineralising tissues, or one in which the average mineralising ability of all tissue-associated vesicles is increased deeper in the cartilage.

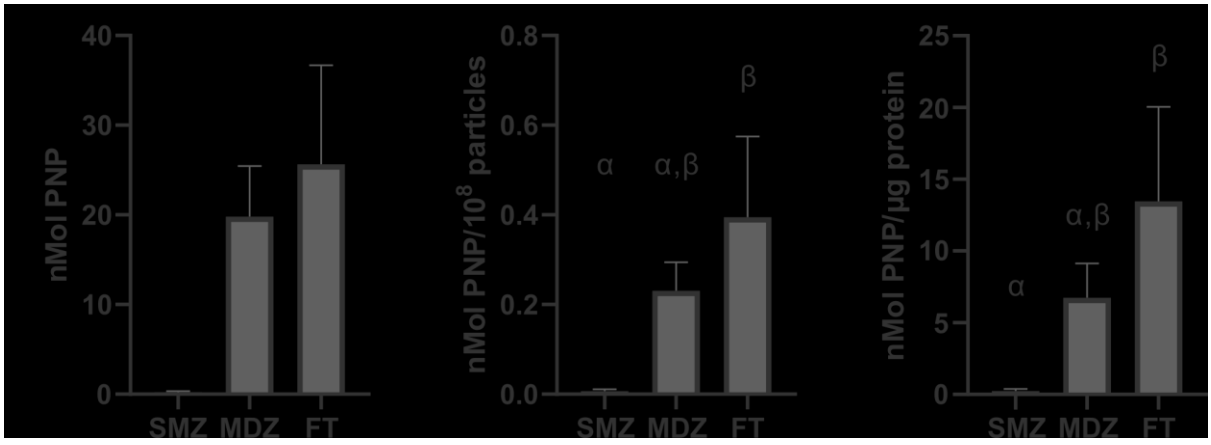


Figure 3.7: ALP activity in particles isolated from each tissue section. a) nMol PNP produced by 10 µL SEC eluate. b) nMol PNP produced normalised to number of SEC eluate particles added per well. c) nMol PNP produced normalised to quantity of SEC eluate protein added per well. (Normalisation data for B and C from Figure 3). Differences between groups are significant if they do not share a letter ($p < 0.05$, within-subjects Friedman non-parametric test and post-hoc Dunn's test). A non-parametric test was used as the assumption of homoscedasticity was clearly violated.

3.3.6. Elution profile of ALP activity

Up to this point, vesicles had been collected from the column as a single volume encompassing the peak fraction, and so it had not been explicitly demonstrated that the ALP activity was associated with the vesicles themselves. An experiment was performed in which sequential 1 mL fractions were collected between fractions 5 and 20, and the ALP activity and protein concentration measured for each fraction (Figure 3.8). An early-eluting protein peak characteristic of the EV peak (as seen previously) was detected for all samples. No activity was detected for SMZ samples (Figure 3.8 a), as before. ALP activity was found to be closely associated with the EV-associated protein peak between fractions 7-10 for both MDZ (Figure 3.8 b) and FT (Figure 3.8 c) samples.

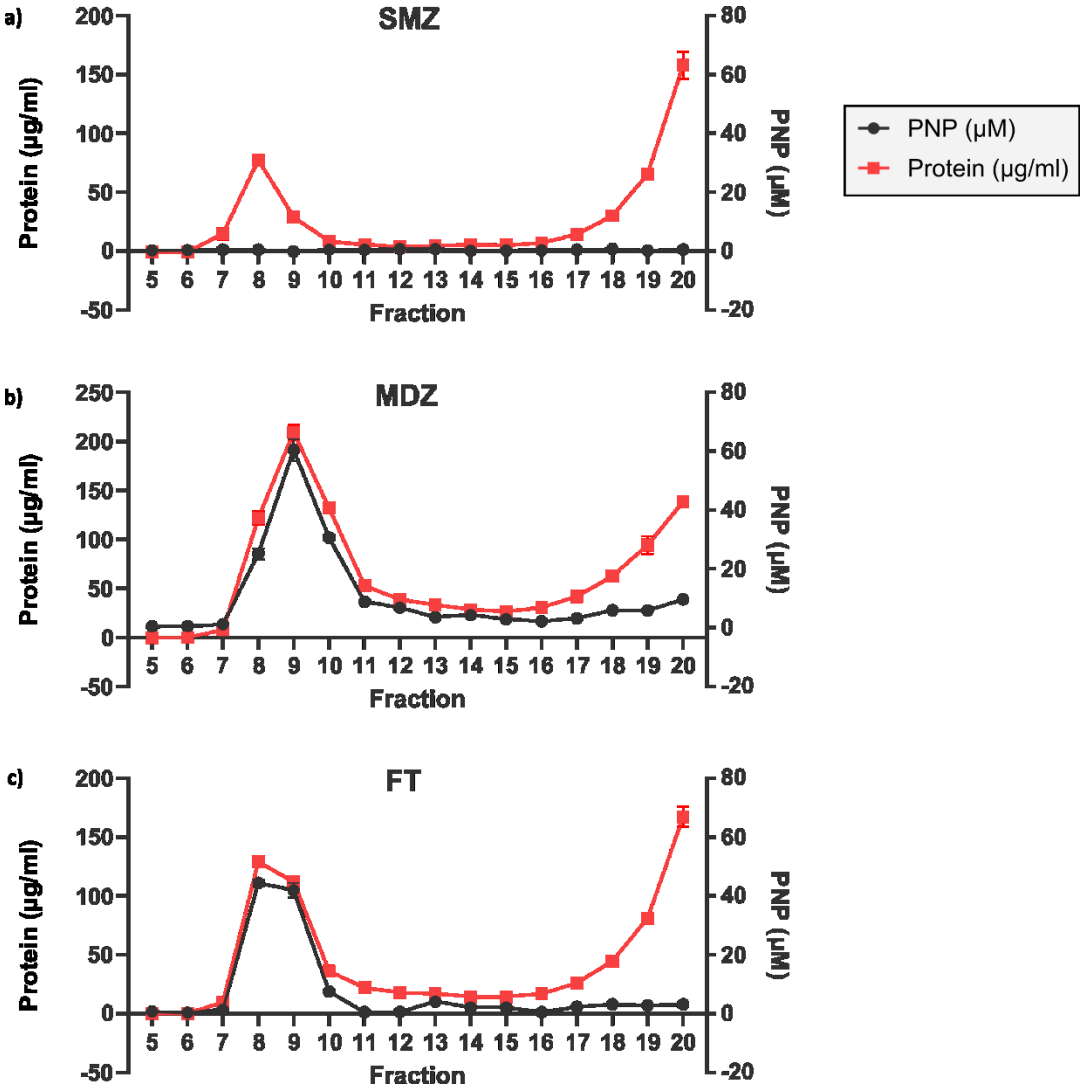


Figure 3.8: Elution profile of ALP from SEC column. Profiles shown for a) SMZ, b) MDZ and c) FT samples. N = 1, n = 3, mean +/- SD of technical replicates shown.

3.3.7. Mineralisation assay

Having established that particles isolated from the mineralising layers of bovine cartilage have enzymatic activity associated with initiation of mineralisation, an assay was designed to measure the ability of these particles to initiate mineralisation. Surprisingly, it was found that an 18-hour centrifugation in a 1.5 mL Eppendorf tube at 17,000 g effectively pelleted these particles. This was unexpected as during initial investigation of purification procedures, it had been found that ultracentrifugation of conditioned medium-derived EVs led to very low recoveries (Section 6). It was hypothesised that this was due to the shorter tube height, the higher initial concentration of particles, and potentially a higher particle density, as matrix vesicles have been reported to contain mineral when isolated [145].

After concentrating SEC-purified particles using this method, 2.5 x 10^{10} particles were added per well of a 96-well plate, in DMEM, with or without 10 mM β-glycerophosphate (βGP). βGP is a substrate for phosphatases, and when hydrolysed releases free phosphate. It therefore provided a source of phosphate for mineralisation only accessible to enzymatically active particles. It was anticipated that MDZ and FT-derived particles would initiate mineralisation more rapidly compared to SMZ-derived particles, dependent on the presence of βGP. In the experiment shown, a grainy texture became apparent on the bottom of the wells in which FT-derived particles were present with βGP (Figure 3.9). This grainy texture was not evident for MDZ or SMZ-derived particles (not shown), or wells without βGP.

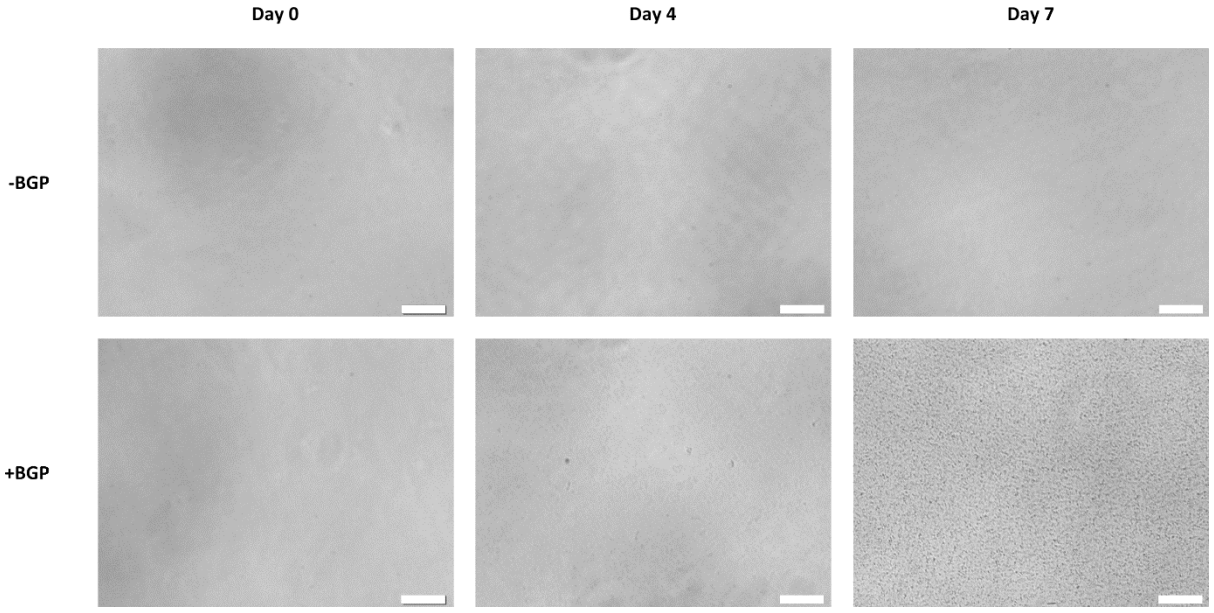


Figure 3.9: Mineralisation assay images for FT-derived particles. Scale bar = 50 µm. One set of images from three internal replicates is shown. SMZ and MDZ images not shown. Images shown in greyscale and contrast-adjusted for clarity.

However, the results of this experiment were not readily reproducible. Deposits would sometimes be apparent within a day or might not be observed within two weeks. Formation of deposits was also sometimes observed in SMZ or MDZ wells, or in the absence of βGP (data not shown). It was therefore hypothesised that the appearance of deposits that were observed in this assay might simply be sporadic, rather than driven by the enzymatic activity of the particles. It was thought that it would be informative to characterise the grainy deposits to confirm whether they were indeed mineral.

3.3.8. Characterisation of deposited mineral

For the experiment shown in Figure 3.9, each well was washed with water before addition of 90 µL 0.1 M HCl to dissolve any mineral. The quantity of calcium and phosphate in each well was measured using o-cresolphtalein complexone (o-CPC) and ammonium molybdate assays respectively (Figure 3.10 a,b). Calcium and phosphate were detected in FT/βGP+ wells only, consistent with images. However, the molar ratio of calcium to phosphate was not consistent with the presence of Hydroxyapatite. Hydroxyapatite is expected to have a molar ratio of 1.67 Ca^{2+}/PO_4 [160]. Synthetic HA was measured to have a molar ratio of 1.42, whereas the material recovered from the mineralisation assay had a molar ratio of 2.58 (Figure 3.10 c). This is more consistent with the formation of tetracalcium phosphate (expected ratio of 2), possibly with additional calcium-containing contaminants. A Raman spectral analysis of deposited material from FT-derived particles was performed. Wells were washed with water and material was scraped up and deposited on fluorite slides. Due to the small quantity of material, the Raman spectrum acquired was quite noisy. However, a clear peak was evident at approximately 960 cm^{-1} (Figure 3.10 d). This is characteristic of calcium phosphate compounds including hydroxyapatite [161]. Additional peaks can be used to more specifically identify the compound; however due to the noise in this acquisition, this was not possible.

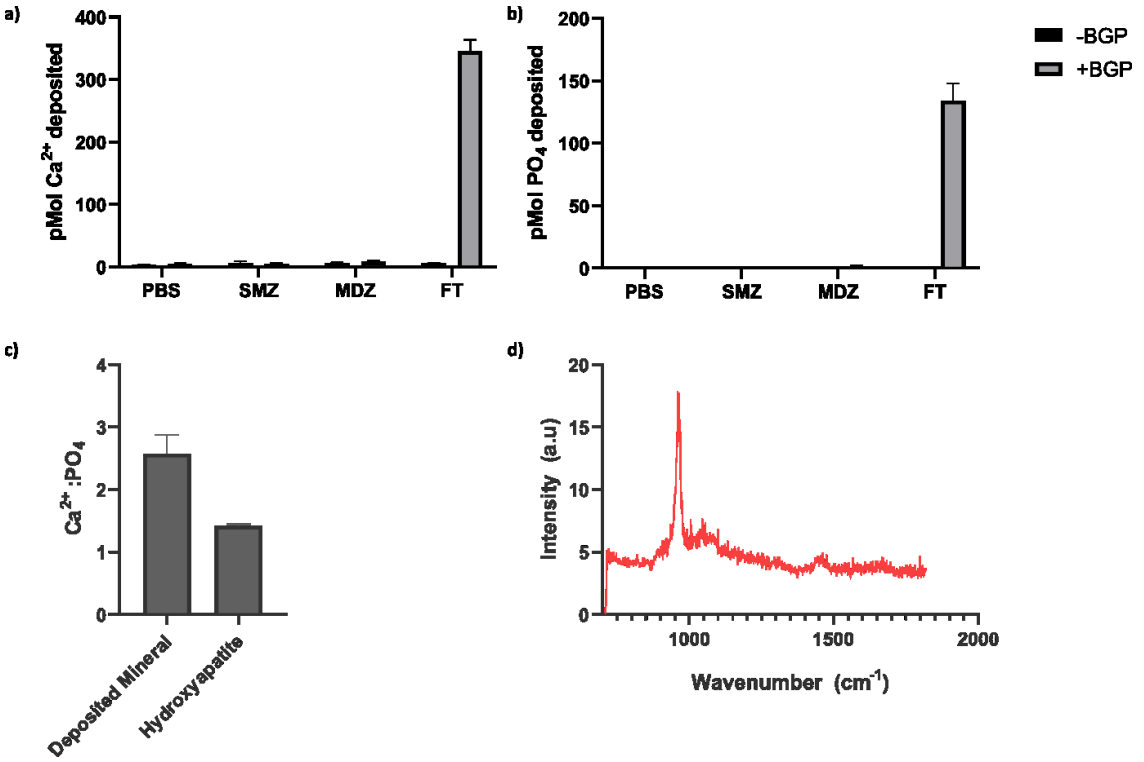


Figure 3.10: Characterisation of material deposited by FT-derived particles. a) pMol Ca^{2+} and b) pMol PO_4 deposited by 2.5 x 10^{10} FT-derived particles in a 96 well plate well (N = 1, n = 3, mean +/- SD of technical replicates shown). c) Ratio of Ca^{2+} to PO_4 for deposited mineral and synthetic HA. Ratio calculated from means (n = 3), SD calculated by sum of squares error propagation. D) Raman spectrum of material deposited by FT-derived particles. Intensity in arbitrary units (a.u).

3.4. Discussion: Matrix vesicles.

Matrix vesicles derived from bovine articular cartilage were isolated using the ultrafiltration/size exclusion purification system in conjunction with a tissue digestion protocol more commonly used to isolate bovine chondrocytes. Intriguingly, although the same number of particles were isolated per gram of tissue from each tissue section, only particles from the mid-deep and full thickness tissue isolations were enzymatically active. The presence of matrix vesicles in the deep section only is expected from the literature (section 3.1). These results suggested that vesicles were present throughout the articular cartilage tissue, but that the identity of the vesicles in each tissue area was different. The matrix vesicles might themselves have only made up a small proportion of the total particles isolated. It was not directly shown that the particles isolated from bovine cartilage were predominantly vesicles, and hence they have been referred to as particles throughout this work, in order to account for the possibility that some of the particles seen were not EVs. The quantity of protein associated with the particles was consistent across tissue sections. The particle to protein ratio of the isolated particles was consistent with isolation of EVs at a good standard of purity. This also further suggests that the particles are mostly EVs. If a majority of the particles were, for example, nano-sized fragments of mineral present as contaminants, this ratio would have likely been higher.

Crucially, the ALP activity co-isolated with the particles appeared to be directly associated with the EV protein peak, confirming that the particles themselves were enzymatically active, rather than the activity being due to contamination with soluble protein. Confirmation that the UF/SEC purification protocol could purify enzymatically active particles was taken as further validation of the suitability of the technique for EV purification.

Despite the reproducible and tissue section-specific enzymatic activity of the particles, they were not found to reproducibly initiate mineralisation. Raman spectral analysis and chemical analysis methods found that some form of calcium phosphate mineral was being deposited during mineralisation assays. However, the identity of the mineral was unclear. The ratio of Calcium to Phosphate of the mineral did not appear to be consistent with the formation of hydroxyapatite.

It is possible that the enzymatic treatment used to dissociate the cartilage tissue also led to damage of the vesicles. In particular, Pronase was used. Pronase is a broad-spectrum cocktail of proteases. The activity of these proteases could have damaged outer membrane-associated proteins involved in phosphate production and ion transport into the vesicle, which could have compromised mineral initiation. Pronase could potentially also damage chondrocytes when this dissociation technique is used to isolate cells alone; however, cells would have been able to resynthesize and replace their outer membrane proteins, whereas EVs would not. Future work might involve re-evaluating the tissue

dissociation protocol. If damage by proteases had been a factor in the lack of observed mineralisation, use of more specific enzymes or collagenase alone might allow that damage to be avoided. The potential for matrix EV (or synthetic mimics) to direct mineralisation in a cartilage tissue engineering scaffold could then be investigated.

4. HMSC-EVs and their contribution to paracrine signalling

4.1. Literature review: human mesenchymal stem cells and their therapeutic properties.

This literature review provides an overview of the isolation, identity and potential therapeutic use of human mesenchymal stem cells (hMSCs). It also provides a discussion of the mechanisms by which they might mediate their therapeutic properties, including by EVs but also by other factors.

4.1.1. Introduction to hMSCs

Mesenchymal stem cells (or mesenchymal/marrow stromal cells) are pluripotent stem cells that can differentiate into various cell types from all three germ layers [162]. Unlike other stem cell populations, they can be obtained autologously and relatively non-invasively. In comparison to induced pluripotent stem cells, no genetic modification or transient expression of exogenous factors is required to initiate or maintain their potency [163]. They are therefore a promising source of cells for adult regenerative therapies. The major challenge in developing their potential as a therapy is to understand how to direct their abilities appropriately. Experimental treatment of various injuries (such as cardiac ischemia, kidney injury and stroke) using hMSCs has been explored, with promising results. These treatments were initially predicated on the basis that hMSCs would engraft at the site of injury and differentiate into new tissue of the appropriate cell type, replacing tissue that was damaged or absent. However, increasing evidence suggests that hMSC engraftment is often infrequent and short-term [164, 165]. Differentiation at the site of injury is not always observed. It is currently thought that a substantial proportion of the reported benefits are due to paracrine signalling from hMSCs to the surrounding tissue. There is little consensus as to the signalling mechanisms used, but some studies have suggested that EVs are a major factor in this process. The experimental portion of this chapter details investigation of the contribution of hMSC-EVs to angiogenesis and wound healing, within the context of hMSC paracrine signalling as a whole.

4.1.2. Factors affecting therapeutic use of hMSCs and other stem cells

Many of the most disabling non-communicable diseases have a simple common factor; an insufficiency in the human body's ability to replace dead or damaged tissue. Myocardial infarction leads to death of cardiac tissue by ischaemia – patients who survive are typically left with reduced cardiac function due to a loss of contractile tissue and the formation of a stiff fibrotic scar [166]. Similarly, the effects of a stroke may last for the rest of the patient's life, due to the apparent inability of the adult brain to generate and integrate new neurons [167]. These and other diseases can be

partially treated with symptom-alleviating drugs to improve patient quality of life, but until recently the damage was considered irreparable.

The discovery of human stem cells, and perhaps more importantly, development of protocols allowing them to be grown, manipulated and differentiated has suggested the possibility of therapies that can overcome this apparently irreversible damage. If cells with the apparent characteristics of specific tissue types can be made in the lab, could they be used to replace damaged tissue in human patients? Embryonic stem cells (ESCs), induced pluripotent stem cells (iPSCs), and mesenchymal stem cells are all potential sources for replacement tissue. ESCs and iPSCs both have the capacity to differentiate into any tissue type, having been demonstrated to be competent for germline transmission in mice [168]. That is, when mixed into the developing blastocyst, the differentiated descendants of the introduced stem cells are not only detectable in tissues throughout the resulting mice but also their eventual progeny, having contributed to forming functional gonad tissue. Although there is some doubt as to whether human ESCs are entirely similar to those derived from mice [169], ESCs and iPSCs could potentially form any replacement tissue if appropriately directed. There are, however, some issues with both of these cell sources. ESCs are ethically controversial, as they are derived from early-stage human embryos that were surplus in *in vitro* fertilisation treatments and would otherwise have been destroyed [170]. They are also necessarily allogenic and therefore likely to elicit an immune response. iPSCs, in contrast, can be derived from the patient themselves and are therefore not ethically controversial or inherently immunologically incompatible. However, it is currently necessary to transform them by exogenous expression of transgenes. Even though integration-free methods for transformation exist [171], the transformation process remains a point of concern. Additionally, development of a patient-specific iPSC line is labour-intensive and costly. It also appears that differentiated iPSCs are not entirely similar to mature differentiated cells; iPSC-derived cardiomyocytes are initially structurally and functionally immature, and research to develop maturation strategies is ongoing [172].

By contrast, hMSCs are readily harvestable from patients and do not require any chemical treatment or genetic transformation. Their main disadvantage is their apparently relatively restricted potency. However, direct therapies with hMSCs have nevertheless been explored for various different diseases, with the fundamental intention that the hMSCs introduced into patients might migrate to the site of damaged tissue, replicate, differentiate, and integrate, replacing tissue that was previously lost.

4.1.3. Isolation and identification of hMSCs

hMSCs were first described in 1970 by Friedenstein and colleagues as fibroblast-like non-haematopoetic stem cells isolated from bone marrow aspirates [173]. When grown in adherent culture, an initially mixed population of cells attaches, but over time a population of fibroblast-like cells comes to dominate. These fibroblast-like cells were found to fulfil two major criteria for the definition of a stem cell: the ability to differentiate into multiple other cell types, and the ability to self-renew; that is, a single cell could give rise to a colony of identical cells with undiminished differentiation ability.

Over subsequent years, there has been substantial research into the properties of hMSCs. Differentiation into tissues from all three germ layers has been described [174], although differentiation into the mesodermal lineage is the most well-established. Other therapeutically promising properties that have been reported include immunomodulation [175] and the ability to home to damaged tissue after peripheral injection [176]. They are typically isolated from solid tissues by mincing the tissue into 1-2 mm diameter pieces before either enzymatic digestion or allowing the hMSCs to migrate out from the tissue in 2D culture (Figure 4.1) [177]. Although bone marrow is still the most commonly used source of hMSCs, they are also commonly isolated from adipose tissue [178] and umbilical cord blood [179], and less commonly from other tissues such as skin [180] and endometrium [181]. A concomitant diversity in characterisation of these cells led to difficulty in cross-laboratory interpretation of results, resulting in unresolved controversies and ambiguities. This diversity of methods led the International Society for Cellular Therapy to suggest a set of minimal criteria required for definition of an hMSC [182]:

- Adherence to plastic under standard cell culture conditions.
- > 95 % cell population expression of CD105, CD73 and CD90, and <2 % expression of CD45, CD34, CD14 or CD11b, CD79α or CD19, and HLA-DR.
- The capacity to differentiate into osteoblasts, adipocytes, and chondrocytes.

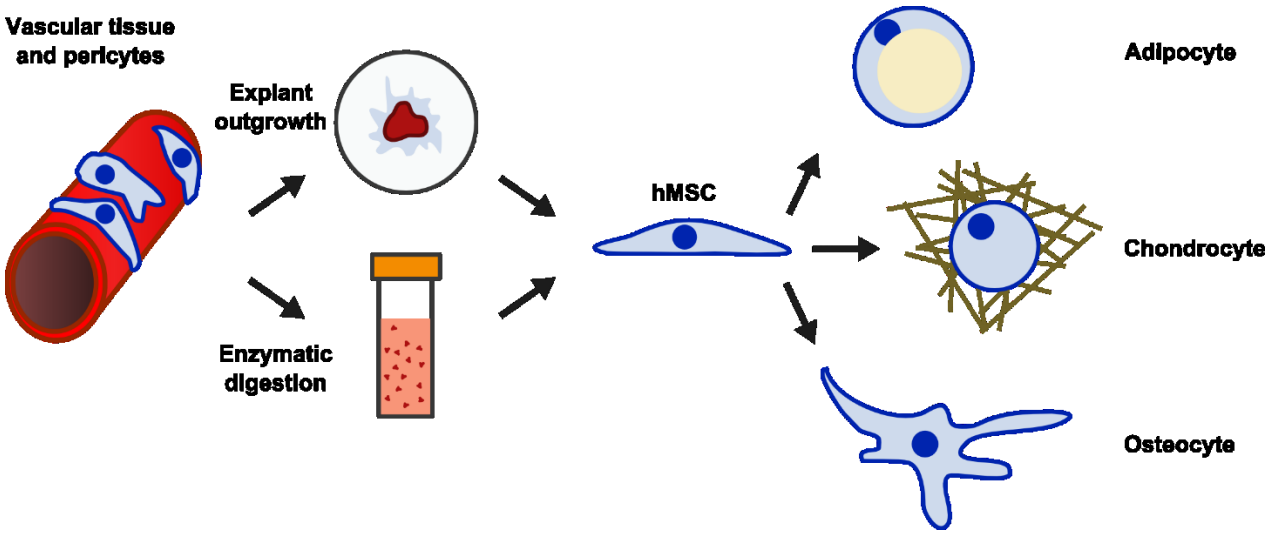


Figure 4.1: Isolation of hMSCs from vascular tissues and subsequent differentiation. HMSCs are thought to be derived from pericytes. After isolation by either explant outgrowth or enzymatic digestion, hMSCs can be differentiated into adipocytes, chondrocytes and osteocytes.

Plastic adherence is critical in separating hMSCs from other cell types, particularly when isolating from bone marrow aspirates. The choice of a combination of markers is necessary due to the apparent lack of a single unique defining marker for hMSCs. CD105, CD73 and CD90 are also expressed on other, non-adherent cells from bone marrow and so the exclusion of leukocyte markers is considered critical. Finally, their "stem-ness" must be confirmed by trilineage differentiation (typically assessed by histological stains). These criteria have been widely adopted. Even with these criteria, substantial variation is observed between donors and tissue sources, and the isolated populations themselves are known to be heterogenous [183]. The relative expression of markers and other genes may vary considerably. Some hMSC populations may be more efficiently differentiated into bone, cartilage or adipose than others or may not be competent for differentiation into some lineages at all [177, 184, 185]. Whilst all hMSC populations will eventually undergo senescence (and differentiation potential is reported to start declining immediately after isolation [186]), some will be competent to undergo a greater number population doublings than others [187]. This may be related to donor age and telomere length, as telomerase is inactive in hMSCs. Stable transgenic expression of telomerase has been investigated as a method of hMSC immortalisation, in order to facilitate the expansion of the initially small cell population to the large cell quantities required for cell therapy, without oncogenic transformation [188]. In general, the variability between different isolated hMSC populations necessitates accurate reporting of the tissue of origin and the age, sex and ethnicity of the donor, and the use of multiple donors within the same study is strongly encouraged.

A contributing factor to the uncertainty over hMSC definition until recently was uncertainty over the identity of their *in vivo* counterpart. The hMSC, or hMSC-like precursor, is thought to be present at a

very low frequency within bone marrow aspirate (1-10 in 10^5 cells) [189]. Combined with the unavailability of specific markers, this complicates prospective isolation. Despite these difficulties, there is now compelling evidence that hMSCs either are or are in some way derived from a population of pericytes – mesenchymal cells associated with the microvasculature. Pericytes are known to be critical for the maintenance of non-leaky blood vessels [190, 191], involved in angiogenesis [192, 193] and wound healing [194], and intriguingly are critical for the maintenance of the haematopoetic stem cell niche within bone marrow [195]. They have been described in multiple different tissues and have heterogenous morphology and marker expression depending on their location [190]. In 2008, Crisan et al [196] developed a combination of immunohistological markers for pericytes by extensive tissue staining, looking specifically for exclusive staining of perivascular cells consistently across several tissue types. Using the identified combination of markers, pericytes were isolated from tissue digestions by fluorescence-activated cell sorting (FACS) and demonstrated to be consistent with the ISCT definition of hMSCs: they were plastic-adherent, expressed characteristic markers, and were capable of trilineage differentiation. In fact, they were also capable of myogenic differentiation. The identification of an *in vivo* counterpart for hMSCs is conceptually important for regenerative medicine, as it allows rationalisation of the mode of action of potential therapies in relation to the *in vivo* involvement of pericytes in wound healing and angiogenesis, although the treatments themselves may not be strictly similar to physiological processes.

4.1.4. Differentiation capacity of hMSCs

The capacity of hMSCs to differentiate into mesodermal tissues – specifically, osteoblasts, chondrocytes and adipocytes – is well established (Figure 4.1). hMSCs may be induced into osteogenic differentiation by manipulation of glucocorticoid signalling with the artificial glucocorticoid dexamethasone, supported by sodium β-glycerophosphate and ascorbic acid [197]. Adipogenic differentiation is induced by treatment with dexamethasone, insulin, indomethacin and 1-methyl-3-isobutylxanthine, and chondrogenic differentiation by an initial centrifugation of the hMSCs to allow them to be cultured in high density as a cell pellet, followed by treatment with transforming growth factor β (TGF-β) in the absence of serum [184].

Differentiation into multiple other tissue types from all three germ lineages has also been reported: cells with characteristics of cardiomyocytes [198], neuronal cells [199], hepatocytes [200] and pancreatic cells [201] have all been obtained from hMSCs. However, there is debate around whether the capacity for differentiation outside of the mesodermal lineage is a typical property of hMSCs: informal communication indicates that hMSCs from most donors do not respond strongly to the differentiation protocols, and the extent to which the cells are differentiated is not entirely certain. If hMSCs are to be used as a source of new cells in regenerative medicine therapies for organ failure,

their potential to differentiate into appropriate cell types will be critical. It may be the case that the apparent *in vitro* differentiation capacity of hMSCs is rather reduced compared to their true capacity when reimplanted *in vivo*, due to potential for complex, dynamic stimulation from the host tissue. However, if it is the case that the majority of donors are not competent for appropriate tissue differentiation, this could be a major barrier to therapy.

4.1.5. Experimental hMSC therapies and their potential modes of action

Some experimental therapies involving hMSCs (and their exosomes) are intended to leverage their immunomodulatory properties to treat autoimmune conditions such as graft versus host disease [202]. However, the existence of an autologous source of multipotent stem cells immediately invites exploration of their potential for use in regenerative medicine, and the majority of experimental therapies have been predicated on the "stemness" of hMSCs. Experimental hMSC therapies have been tested in numerous clinical and pre-clinical trials. As of 17-09-18, clinicaltrials.gov lists 528 registered trials involving hMSCs as either recruiting, active, or completed [203].

Trials for treatment of ischemic kidney injury [204], cardiac fibrosis and ischemia/reperfusion injury [205], and immunological disorders [206] have all been conducted, with encouraging results. These effects were originally attributed to MSCs migrating to sites of injury, engrafting and differentiating into new tissue cells in situ, replacing or supplementing the damaged tissue [207]. However, it has become increasingly clear that this cannot be the main mechanism by which MSC therapies function, and it appears that the observation of transdifferentiation of hMSCs into cardiomyocytes may be due to cell fusion [89]. The beneficial effects occur over too rapid a timescale to be attributable to MSC differentiation [208]. Moreover, extremely low levels of engraftment are seen in models of treatment of kidney [209] and cardiac [89] disease, with the majority of transplanted MSCs becoming trapped in the pulmonary capillaries. It is now well accepted that much of the therapeutic benefit of current MSC therapies must be due to paracrine signalling of hMSCs to the damaged tissue [164, 165] during the apparently brief window in which they are present at the site of injury and viable, although this is not to say that future therapies that can appropriately direct engraftment and differentiation could not be developed.

It should be mentioned that the existence of significant benefit from hMSC therapies is itself not uncontroversial, and there is some dispute as to the magnitude of the effect and its potential clinical relevance. In a meta-analysis of trials of use of autologous hMSCs for ischaemic heart disease in humans, Nowbar et al [210] found that several key papers had numerous mathematical and logical discrepancies within their own data. Moreover, across 49 trials, the reported efficacy of treatment correlated with the number of discrepancies, with the 5 trials with no discrepancies reporting no

significant effect of hMSC treatment on ejection fraction (EF). This meta-analysis is itself controversial. Many researchers are of the opinion that the design of the study and the statistical methods used were essentially unsuitable [211], giving too much weight to the significance of minor errors and not accounting for potential confounding factors. Other meta-analyses have found a statistically significant improvement in ejection fraction [212, 213], although it is not clear whether the level of improvement reported is sufficient for meaningful patient benefit.

Despite this controversy, there is still considerable evidence that hMSC transplantation may be therapeutic in a variety of injury types. If it is the case that signalling from hMSCs to surrounding tissue is responsible for the observed therapeutic effects, could it be possible to develop a cell-free therapy consisting of the signalling molecules being used? In theory, this would have nothing but advantages over a similarly effective cell therapy. If the relevant signalling factors could be identified and synthesised chemically or by microbial expression, there would be no need to harvest or expand patient cells, fewer concerns over immunogenicity and no potential for transformation and tumourigenesis. Production would be far less costly, which would mean wider availability to patients. There is also potential to improve the efficacy of the treatments, taking the factors produced by hMSCs and their concentrations as a starting point. Bulk injection of stem cells into sites of injury is manifestly un-physiological, and therefore it is quite possible that the behaviour of the stem cells or the cocktail of factors they release has not been thoroughly optimised by evolution for treatment of these injuries.

However, the identity of these paracrine factors is still uncertain. This is likely in part due to the aforementioned variability between different hMSC donors. It is also quite possible that different tissues respond to different hMSC-derived signalling factors. Recently, many studies have suggested that EVs are critically important in this paracrine signalling process. EVs isolated from hMSC-conditioned media (CM) have been demonstrated to recapitulate the effects of the CM itself, and in some cases appear to be required for its effect. However, there is also strong evidence that more conventional signalling is involved. Evidence for various mechanisms of the paracrine effect are reviewed below, for three key injuries that are frequently studied in the context of hMSC-CM and hMSC-EV mediated therapy: myocardial infarction, kidney damage, and stroke.

4.1.6. Cardiac Ischaemia/reperfusion injury

Myocardial Infarction (MI) remains one of the leading causes of death and disability in the world [214]. Patients who survive the initial event will frequently suffer a decline in heart function, the severity of which is proportionate to the amount of cardiac tissue that fails to recover and becomes fibrotic. This leads to a loss of quality of life and a decline in health. Consequently, a critical development in the treatment of MI has been the introduction of reperfusion therapy, in which the clot that caused the

blockage of blood to the heart is broken up, either by thrombolytic drugs, percutaneous coronary intervention (in which a surgical device is threaded into the coronary artery and the clot physically disrupted) or, failing that, bypass surgery [215]. It is critically important to restore blood flow as rapidly as possible in order to salvage the maximum possible amount of myocardial tissue and restore a good level of heart function.

Paradoxically, it has become apparent that although it is necessary to reperfuse tissue in order to salvage it, much of the irreparable damage actually occurs when ischaemic tissue is reperfused [216]. This is referred to ischaemia/reperfusion injury (I/R) This process can essentially be understood as a metabolic shock. Ischaemic tissue undergoes a series of metabolic changes, including a shift to non-aerobic, glycolytic ATP production. This has a knock-on impact on the pH of the cell, which affects sodium and calcium ion transport and leads to an inhibition of myofibril contracture. Upon restoration of blood flow, the cell is essentially unprepared to deal with a massive influx of oxidising potential, as the aerobic respiration pathways are inactive. The pH of the cell changes rapidly, the cell becomes overloaded with calcium ions and a burst of highly damaging reactive oxygen species is produced. This leads to inflammation, hyperactivation and destruction of the contractile machinery, and the opening of the mitochondrial permeability transition pore (MPTP) which short-circuits energy production and leads to rapid ATP depletion [217]. Necrotic cell death ensues, and the local vasculature can become damaged, further limiting reperfusion.

Pharmacological interventions at several points in this process have been tested, with some success. For example, the opening of the MPTP can be inhibited with cyclosporin A, and this has shown promise in early stage trials [218]. However, there is currently no treatment in widespread clinical use. As reperfusion injury is thought to contribute to up to 50 % of the infarct size [219], there is clearly scope for investigation of novel therapies.

4.1.7. MSC soluble factors in treatment of MI and I/R

As reviewed in the previous section, MSCs do not appear to engraft significantly in injured myocardium and so signalling from hMSCs is thought to be critical. To the best of the author's knowledge, the first study to explicitly demonstrate the importance of the paracrine effect was published in 2005 by Gnecchi et al [220]. Treatment with hMSC-conditioned medium alone led to a reduction in infarct size and an improved functional recovery within 72 hours. In this study, cell culture medium conditioned by bone marrow-derived Akt-overexpressing MSCs was injected directly into the myocardia of mice, shortly after inducing myocardial infarction. Subsequent work by the same group investigated the process more closely [208]. In this follow-up study, they described an upregulation of vascular endothelial growth factor (VEGF), basic fibroblast growth factor (bFGF), hepatocyte growth factor (HGF) and thymosin beta-4 (TB4) by both AKT-modified and unmodified hMSCs after exposure to hypoxia and speculate that these growth factors – well established as pro-angiogenic and cardioprotective – may be key factors in the signalling process. The protection appeared to occur via prevention of adverse remodelling, rather encouraging the growth of new endogenous cardiomyocytes.

Many subsequent studies have investigated which signalling factors are responsible for this effect. A study by Uemara et al in 2006 also found that hMSC-CM reduced infarct size after MI, via inhibition of cardiomyocyte apoptosis [221]. They noted a significant release of VEGF, bFGF, insulin-like growth factor 1 (IGF-1) and stromal cell-derived factor (SDF) from hMSCs under normoxic conditions and increased release under hypoxia. Takahashi et al also found upregulation of growth factor release and decrease of cardiomyocyte apoptosis, as well as a potential role of stimulation of neoangiogenesis. Many additional subsequent studies found essentially similar results; inhibition of cardiomyocyte apoptosis in the infarcted heart, stimulation of angiogenesis, and substantial secretion of a handful of key growth factors by the hMSCs [222, 223].

Many growth factors have been confirmed to be present in significant quantities in hMSC-CM by multiple studies. These studies mostly did not attempt to recapitulate the therapy with growth factors alone. Other studies, however, have. VEGF, bFGF, HGF, platelet-derived growth factor (PDGF), IGF-1 and Angiopoetin 1/2 (Ang-1/2) (among others) have all been explored for direct therapy, alone and in combinations [224], even before the discovery of hMSC-mediated paracrine signalling [225]. All appear to have some benefit to cardiac remodelling, via either promotion of angiogenesis, inhibition of apoptosis, or promotion of new cardiomyocyte growth.

4.1.8. MSC soluble factors in treatment of kidney injury

In common with MSC treatment of cardiac injury, MSC treatment of kidney injury was initially investigated under the rationale that intravenously administered MSCs would home to the site of injury, engraft and differentiate to replace injured tissue. Initial studies appeared to confirm significant levels of engraftment [204] [226]. However, later studies by other groups demonstrated that although MSC transplantation was indeed beneficial, there was no significant long-term engraftment [227, 228]. The discrepancy is thought to be due to inappropriate reporters used to track the cells – beta-galactosidase and green fluorescent protein were originally used, but ischaemic kidney has high levels of intrinsic beta-galactosidase activity and autofluorescence [209]. Authors of one of the original studies revisited their earlier experiments with a different reporter system and found a much lower (2 % vs 22 %) engraftment rate than they had previously reported [229].

As before, it appears likely that a paracrine effect is responsible for the therapeutic benefit. As before, hMSC were found to secrete a cocktail of potentially renoprotective factors including VEGF, HGF and IGF-1, and hMSCs injected into the kidney prior to ischemia/reperfusion injury were observed to inhibit apoptosis in neighbouring cells [230]. Further suggesting a role for conventional paracrine secretion, hMSCs modified to overexpress VEGF were found to have an enhanced ability to protect against cisplatin-induced acute kidney injury [231].

4.1.9. MSC soluble factors in treatment of brain injury

MSCs have also been explored for the repair of brain tissue after stroke. As with other tissues, it appears that intravenously injected MSCs do not engraft in the brain in significant numbers, nor do they transdifferentiate *in vivo* into neuronal cells. Instead, the release of paracrine factors appears to be of major importance [232]. MSCs secrete neurotrophins such as brain-derived neurotrophic factor (BDNF), and MSCs modified to overexpress BDNF have been shown to be more effective in treatment of a rat model of stroke than unmodified MSCs [233]. A similar study demonstrated that hMSCs produce nerve growth factor (NGF), BDNF, glial cell line-derived neurotrophic factor (GDNF) and neurotrophin-3 (NT-3) when cultured *in vitro*, and that when MSCs were injected into the brains of mice after traumatic brain injury they expressed NGF while within the mouse brain. This led to an increase in detectable NGF within the cerebrospinal fluid, and was concomitant with a decrease in cholinergic cell death [234]. Similarly, MSCs secrete pro-angiogenic factors such as VEGF and Ang-1, which also improve therapeutic performance when overexpressed [235, 236].

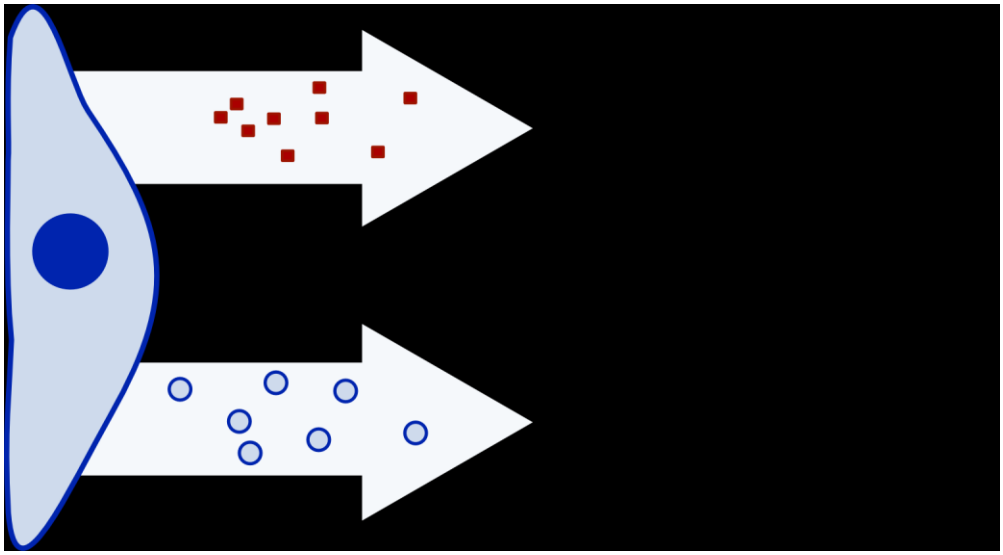


Figure 4.2: Soluble and EV-associated factors released by hMSCs implicated in their therapeutic effects. Classical growth factors are implicated in for conventional signalling, whereas EV-associated factors are typically miRNAs. Arslan et al [237] propose mass transfer of multiple cytoplasmic components (see text).

4.1.10. MSC EVs in treatment of MI and I/R

Shortly after the realisation of the significance of paracrine signalling to hMSC therapy, the first paper to implicate EVs in hMSC paracrine signalling was published by Timmers et al [238] in 2007. They confirmed that hMSC-CM was cardioprotective in a porcine model of myocardial infarction and ischaemia/reperfusion injury. Critically, they also demonstrated that filtration of the conditioned media through a 1000 kDa (~100 nm) filter membrane removed the cardioprotective bioactivity of the media, providing the first indication that EVs were involved in protection. Subsequent studies by Lai et al [239] purified, identified and concentrated EVs from MSC-CM by HPLC and demonstrated that they could recapitulate the therapeutic benefits of MSC-CM alone. Since then, similar results have been reported by other groups [240-243].

In contrast to the effects of soluble factors, there is little agreement on the mechanisms by which MSC-EVs are thought exert their effects. There are many potential points in the I/R injury process where they might act. MSCs are generally considered to possess strong anti-inflammatory properties [244], so they might act to mitigate inflammation. However it is not clear whether the inflammation in ischemia/reperfusion injury is a cause or consequence of cell death, and clinical trials of anti-inflammatory drugs have not met with any success in mitigating injury [217].

Arslan et al [237] proposed that MSC-EVs act by “proteomic complementation”. They found that the proteome of the I/R injured heart was depleted in proteins involved in fatty acid oxidation, the TCA cycle, redox homeostasis and protein stability (glutathione S-transferase and heatshock enzymes) and enriched for proteins involved in apoptosis and the electron transport chain. They argued that this

predicted ATP depletion, oxidative stress and apoptosis, which would be consistent with the classic pathology of I/R injury. Interestingly, they found that MSC-EVs were enriched for enzymes involved in glycolysis and the mitigation of oxidative stress, and that MSC-EVs appeared to rescue the metabolic activity of ischaemic cardiac cells *in vivo*. Contrastingly, many papers present evidence that the main function of the EVs is to deliver therapeutic microRNAs. Yu et al [242] implicate anti-apoptotic miRNAs, particularly miR-19a. This was thought to act by reducing PTEN (phosphatase and tensin homologue) activity, leading to downstream upregulation of Akt and mitogen-activated kinase (MAPK) signalling, inhibiting apoptosis. Feng et al [241] found a critical role for miR-22, again in preventing apoptosis, in this case by targeting methyl CpG binding protein 2 (Mecp2). Despite the lack of consensus on the mechanisms by which they act, MSC-EVs have been repeatedly demonstrated to have some potentially therapeutic activity in *in vivo* models of MI.

4.1.11. MSC-EVs in treatment of kidney injury

MSC-EVs have been shown to be capable for recapitulating the effect of hMSCs in treatment of glycerol-induced kidney injury [245]. RNA transfer appears to be the critical mechanism in this instance – treatment with RNAse abrogates the effect, and the EVs are enriched for mRNAs involved in MSC identity, transcription, proliferation and immunoregulation. The protective effect appears involve induction of proliferation of endogenous tubular epithelial cells and inhibition of apoptosis. Interestingly, the EVs were effective when injected three days after injury, indicating a potentially longer timescale within which intervention might be possible compared to myocardial I/R injury. The same group has also showed a therapeutic effect with models of lethal acute cis-platin – induced injury [246] and ischemia/reperfusion injury [247].

It is, however, worth mentioning that their methods for purification of EVs are not considered best practice. These studies employed a purely ultracentrifugation-based approach, without a subsequent density or size-dependent purification step. This approach is known to co-isolate protein contaminants and extracellular protein/RNA complexes [108] and so these factors may contribute to the observed effects.

4.1.12. MSC-EVs in treatment of brain injury

Despite the established importance of conventional soluble factors, MSC-derived EVs have been also been demonstrated to be an important mechanism of paracrine therapy in a rat model of stroke [248]. Xin et al found that MSC treatment of rats led to enhanced neurite outgrowth, accompanied by an increase in miR-133b in the treated hemisphere. They established that MSCs exposed to ischaemic brain tissue *in vitro* released miR-133b – containing EVs. They also established that MSCs which were deficient for miR-133b production were less therapeutically effective. A follow-up study from the same lab [249] demonstrated that MSC-EVs were therapeutic alone, and that rats which received exosome treatment experienced less brain tissue deterioration and retained greater cognitive ability compared to control rats, as measured by behavioural tests. In these studies, rats were treated 24 hours after the induction of stroke. The extent to which later treatment might still be effective is unknown.

4.1.13. Summary

There is now a consensus that hMSC paracrine signalling is the major mechanism of the apparent benefits of hMSC transplantation. Indeed, the original discoverer of hMSCs has argued that as their multipotency appears not to be primarily important for their *in vivo* function, their name should be changed to remove the words "stem cell", as it leads to unrealistic expectations for cell therapy [250]. Although the potential beneficial effect is modest compared to a hypothetical therapy in which damaged tissue could truly be replaced, it is still considered potentially clinically significant and worth pursuing. However, it is not clear how the paracrine effect is mediated. In the injury types studied, there is evidence both for signalling via EVs and via conventional soluble signalling factors. There is also little agreement as to the mechanisms by which hMSC-EVs exert their effect. By contrast, there appears to be a reasonable consensus on which soluble factors are thought to be important, perhaps due to the existence of a greater body of relevant work.

In a 2017 review [251], Phinney and Pittenger summarised 35 reports of pre-clinical *in vivo* experimental therapies using MSC-EVs. Multiple applications were investigated, including treatment of myocardial infarction, acute and chronic kidney injury, stroke and wound healing. Of the 33 papers using purified EVs rather than conditioned medium, only four used chromatographical methods to purify EVs, and only two used density-dependent methods. All other studies used ultracentrifugation or polymer precipitation, without further purification beyond one wash. Given the well-established risks of ultracentrifugation and polymer precipitation in terms of co-isolation of contaminants (as discussed in section 2.1), it is possible that the role of EVs in these processes may have been overstated, due to co-isolation of other signalling molecules. Additionally, the author is not aware of any studies which directly compare the effect of hMSC-derived EVs and conventional signalling factors.

In this chapter, the relative contributions of EVs and soluble factors to hMSC paracrine signalling were investigated; specifically, enhancement of *in vitro* assays of angiogenesis and wound healing. These assays are widely used to assess the regenerative potential of hMSC-derived EVs [252-257]. Ultrafiltration experiments similar to those used to indicate the role of EVs in hMSC signalling were found to generate false positives, as was a low-purity EV isolation technique. Improved ultrafiltration experiments and high-purity isolation techniques combined with an experimental structure that permitted direct comparison of the contribution of EVs and soluble factors strongly indicated that non-EV factors were necessary and sufficient for hMSC paracrine signalling in these assays, whereas EVs were neither.

4.2. Materials and Methods

Methods specific to this chapter are detailed below. All others are as previously described.

Cell culture

hMSCs

Bone marrow-derived human Mesenchymal Stem Cells were obtained from Lonza (Basel, Switzerland) (PT-2501) (Table 4.1). HMSC identification tests (trilineage differentiation and marker expression) were performed and certified by the manufacturer. hMSCs were grown in DMEM (1 g/mL glucose) + 20 % v/v hMSC-qualified FBS (Gibco) + 1x A/A. HMSC stocks were made at passage 4 for experimental use. See conditioned media production protocols.

Conditioned medium production

Prior to conditioned medium production, hMSCs were expanded from passage 4 to passage 6, splitting from one T175 to eight T225, and then to 72 T225 flasks. Near-confluent cells were washed once with sterile PBS before addition of 35 mL per flask DMEM (1 g/ml glucose) supplemented with 1x A/A, without FBS. Cells were incubated for 40 hours before media was harvested and pre-processed as stated in previous sections.

Table 4.1: Bone marrow-derived Human Mesenchymal Stem Cell Donors

Donor	Lot number	Age	Sex	Race
1	372262	39	M	Black
2	539540	18	F	Black
3	588695	22	M	Hispanic

Conditioned media pre-processing

Due to the large scale of hMSC-CM production, centrifugation was not practical and therefore hMSC-CM was clarified by passage through a 0.45 µm bottle-top filter (Jet Bio-Filtration, Guangzhou, China), replacing the filter for every 500 mL of media. Media was then immediately stored at -80 °C until further processing.

Collection of hMSC-CM Ultrafiltration flowthrough

For large-scale hMSC-CM isolation experiments, 1.4 L of media was processed using 12 centrifugal filters concurrently. Flowthrough from concentrators was pooled in sequential 240 mL fractions (20 mL per fraction per concentrator) and stored at -80 °C.

Ultrafiltration blocking

100 kDa Ultra-15 Amicon filters were washed once with 18.2 MΩ water by adding 12 mL to the upper compartment and centrifuging at 5000 g for 3 minutes. Subsequently, 12 mL of 1 % (w/v) BSA in PBS was added to the top compartment and left undisturbed for 2 ½ hours, to block the membrane. Subsequently, the upper compartment was washed out 4 times with PBS, without centrifugation. The filter was then washed once with PBS by centrifugation and then used immediately to avoid drying out the membrane. 10 mL of conditioned medium or DMEM was added to the top compartment of either blocked or untreated Amicon filters and centrifuged at 5000 g until all medium had passed through (approximately 10 minutes), except that which was retained in the deadstop.

Equilibrium Dialysis

Equilibrium dialysis was performed using 300 kDa Float-a-Lyzer G2 dialysis devices (Spectrum Laboratories, Rancho Dominguez, CA, U.S.). Before use, membranes were rehydrated by incubation in 10 % v/v Ethanol for 15 minutes, before washing twice for 20 minutes in water. The membranes and outer compartments were then blocked to reduce binding of CM protein to the membrane and plastic surfaces. Membranes and outer compartments were incubated with 1 % w/v BSA in PBS for 1 hour, before washing three times in PBS. Membranes were then kept hydrated in PBS and used within 1 hour.

To perform equilibrium dialysis, 1.25 mL of fresh, non-conditioned DMEM + A/A was added to the inner compartment, and 6 mL of 10x concentrated hMSC-CM (CCM) to the outer compartment. CCM was prepared as previously described and stored aliquoted at -80°C until use. The inner and outer compartments were sealed with Parafilm and the assembly placed in a 50 mL Falcon tube, kept in place with an aluminium foil plug. Dialysis was allowed to proceed over 48 hours at 4°C, on a tube rotator operating at 50 R.P.M. Samples were then retrieved from the inner and outer chambers, aliquoted, and either used immediately (for biological assays) or stored at -80°C (for later analysis).

Concentration/Dilution

HMSC-conditioned medium was prepared and pre-processed as previously described. From 100 ml of pre-processed media, 1.5 mL was removed for later analysis. The remaining 98.5 mL was concentrated

to a final volume of 19.7 mL with two 3 kDa Amicon centrifugal concentrators to form the 5x concentrate. 1.5 mL was removed for downstream analysis and the remaining 18.2 mL concentrated again (in the same concentrators) to a final volume of 3.64 mL to form the 25x concentrate. Volumes were verified gravimetrically. Dilutions were prepared from the 25x concentrate by diluting in fresh DMEM.

Isolation of EVs with Total Exosome Isolation Reagent

HMSC-conditioned medium was prepared and pre-processed as previously described. From 100 ml of pre-processed media, 750 µL was removed for later analysis, and the remaining media was concentrated to a final volume of 1 mL using four 3 kDa Amicon centrifugal concentrators. From the concentrated media, 165 µL was removed for later analysis. 417 µL of TEI reagent was added to the remaining 835 µL of concentrated medium in a 1.5 mL Eppendorf tube before vortexing to mix. The TEI/concentrated media mix was incubated for 16 hours at 4 °C before centrifugation (10 minutes, 10,000 g, 4 °C) to pellet precipitated material. Supernatant was thoroughly aspirated and the pellet (visible, off-white, approximately 2 mm diameter) was resuspended in 100 µL particle-free PBS by thorough pipetting.

Dot Blotting

Setup

A 0.45 µm nitrocellulose membrane (Bio-Rad 162-0117) was soaked in Tris-buffered Saline (TBS, Bio-Rad 170-6435) for 10 minutes. The Bio-Dot apparatus (Bio-Rad 170-6545) was assembled around the wetted membrane, taking care to align the sealing gasket and sample template correctly. All wells were filled with 200 µL of TBS and drained under vacuum, taking care not to dry out the membrane. At least 50 µL of sample or TBS was then added to each sample template well. EV and media samples were added to the blot directly without any further processing. Unless otherwise stated, samples to be compared were normalised by volume. The wells were allowed to drain under gravity, without vacuum. The wells were then washed three times with TBS (200 µL/well), draining with vacuum. The Bio-Dot apparatus was then disassembled, and the membrane retrieved.

Membrane blocking, antibody incubation, and imaging

Blocking, primary incubations, washes and secondary incubations were performed as described for Western blots in section 2.2.

Quantification

Dot blots were quantified using Image Studio Lite V5.2 software (LI-COR). For each image, an ellipse was fitted to the brightest dot and then copied over all other dot positions. The intensity of each ellipse relative to the immediately surrounding background intensity was recorded (Relative Intensity or R.I). To normalise data sets, each value was divided by the average intensity value for the data set to generate Normalised Relative Intensity values (N.R.I).

NanoOrange assay

The NanoOrange assay (ThermoFisher N6666) was used according to manufacturer instructions to measure protein concentrations. Working reagent was made by mixing water, 10x assay buffer, and the Nano-orange reagent in a 450:50:1 ratio. Working reagent was protected from light and used immediately. 10 µL of sample or BSA standards was added to each well of a 96-well plate, before adding 240 µL of working reagent. Plates were sealed using film (Thermo-Fisher AB-1170) and protected from light before incubation at 93 °C for 10 minutes. Plates were then allowed to cool for 20 minutes, protected from light, before measuring fluorescence (excitation at 485 nm, emission at 590 nm) using a Spectramax M5 platereader (Molecular Devices), and concentrations determined using a standard curve generated by second-order polynomial regression.

VEGF ELISA (Enzyme-Linked Immunosorbent Assay)

The VEGF Human ELISA kit (ThermoFisher KHG0112) was used according to manufacturer instructions to determine VEGF concentrations. 50 µL of incubation buffer was added to each microtiter well, before adding 100 µL of standards or samples to each well (samples diluted 1:1 in standard diluent buffer). The plate was sealed with a plate cover and incubated at room temperature for 2 hours. Solution was aspirated, and wells washed thoroughly 4 times. 100 µL of Hu VEGF-biotin conjugate solution was added per well, sealed and incubated as before for 1 hour before washing as before. 100 µL Strepatividin-HRP (Horseradish Peroxidase) solution was then added, incubated for 30 minutes and washed as before. 100 µL of stabilised chromogen was then added to all wells and incubated for 30 minutes protected from light, before 100 µL of stop solution was added per well to terminate the reaction. Absorbance at 450 nm was read using a Spectramax M5 platereader (Molecular Devices, San Jose, CA, U.S.). Concentrations were determined using a standard curve generated by second-order polynomial regression.

Lentiviral transformation

Cytolight Green Lentivirus (Incucyte 4481, Sartorius, Göttingen, Germany) was used to label NIH-3T3 cells. Cells were grown to 20 % confluence, and Lentiviral reagent at a multiplicity of infection (MOI)

of 6 with 8 µg/mL polybrene added in fresh media. Media was replaced after 24 hours. At 80 % confluence, cells were placed on 4 µg/mL puromycin, to select for stable transfection.

Scratch wound healing assay

Preparation

Multiwell plates were collagen-coated by addition of either 200 µL (24-well) or 100 µL (48-well) of 50 µg/mL neutralised Collagen I from rat tail (Corning 354236) in 0.02 N Acetic acid to each well. Plates were coated for 2 hours before thoroughly aspirating fluid and allowing to dry uncovered in a cell culture hood for 3 hours. They were then used immediately or sealed with Parafilm and stored at 4 °C for up to two weeks. GFP-transformed NIH-3T3 cells were seeded at 100,000 cells/well (24-well) or 50,000 cells/well (48-well) on collagen-coated multiwell plates. The cells were allowed to form a confluent monolayer over the course of 24 hours before use.

Assay

Sample mixes were prepared for 24-well plate experiments according to Table 4.2. For 48-well plates, all volumes were halved.

Table 4.2 - Sample preparation for scratch wound healing assays

For 24w plate	**DMEM**	**DMEM + 10% FBS**	**Sample**
Positive Ctrl	600 µL	600 µL	0 µL
Negative Ctrl	1200 µL	0 µL	0 µL
Samples	600 µL	0 µL	600 µL

Cell monolayers were scratched using a 200 µL tip attached to a 200 µL pipette. The tip was held perpendicular to the surface of the plate and moved laterally whilst being kept perpendicular. A slow, smooth motion was used. Faster motion leads to a too-wide, ragged-edged scratch, whereas holding the tip at a non-vertical angle leads to a too-narrow scratch. A ruler was used to support the tip and ensure a straight scratch. The tip was changed between wells. Wells were washed once with DMEM, before addition of sample mixes to each well. 400 µL was added per well for 24-well plates, and 200 µL for 48-well plates, for three replicates.

Imaging and Analysis

The plate was imaged for GFP fluorescence every hour for 15 hours using an Axio Observer live cell imaging microscope with an HXP 120 light source (Carl Zeiss) at 37 °C, 5 % CO_2 with a 10X objective. 4 (24-well) or 3 (48-well) defined positions in each well were imaged.

Images were analysed with FIJI, using the “MRI Wound Healing Tool” [258]. The area of the gap in each image was quantified, and the rate of area reduction determined by linear regression for each individual image set. If a gap closed before conclusion of the assay, the regression was calculated using only the timepoints for which an open area was detected. Each image set was manually checked, and those for which optical artefacts or floating cells had compromised the gap detection were excluded from the final calculation of the well’s area reduction rate. Closure rates for each set of valid images within a well were averaged to generate a closure rate for each well. The three wells for each condition formed three technical replicates.

4.3. Results: hMSC-EVs and their role in paracrine signalling

This chapter describes investigation of the roles of EVs and non-EV factors in hMSC paracrine signalling.

4.3.1. Ultrafiltration of hMSC-CM

The initial goal of this study was to reproduce the widely reported ability of hMSC-EVs to stimulate angiogenesis, using SEC-purified hMSC-EVs and the tubule formation assay as described in section 2.3. However, initial experiments did not indicate pro-angiogenic stimulation by SEC-purified hMSC-EVs (data not shown). In order to troubleshoot these experiments and determine the reasons for the apparent lack of activity, it was decided to employ a bottom-up approach to confirm the activity of hMSC-CM alone and the contribution of hMSC-EVs to it. Early work in the literature indicating the involvement of hMSC-EVs in hMSC paracrine signalling demonstrated that passing hMSC-CM through 100-1000 kDa membrane filters decreased the apparent activity of the conditioned media [238, 239], implicating the involvement of large complexes in signalling (i.e. EVs).

It was decided to examine the activity of hMSC-CM after passage through 100 kDa membrane Amicon ultrafiltration concentrators (approximate pore size of 7 nm), typically used for concentrating CM during EV isolation processes. It was hypothesised that the performance of these membranes might be dependent on the quantity of media passed through them. An experiment was carried out in which media passed through the filter would be collected in sequential batches (Figure 4.3). The concentrators were topped up between centrifugations with 10 mL of CM from a total of 100 mL, and the flowthrough collected in five sequential batches of 20 mL each (FT1-5).

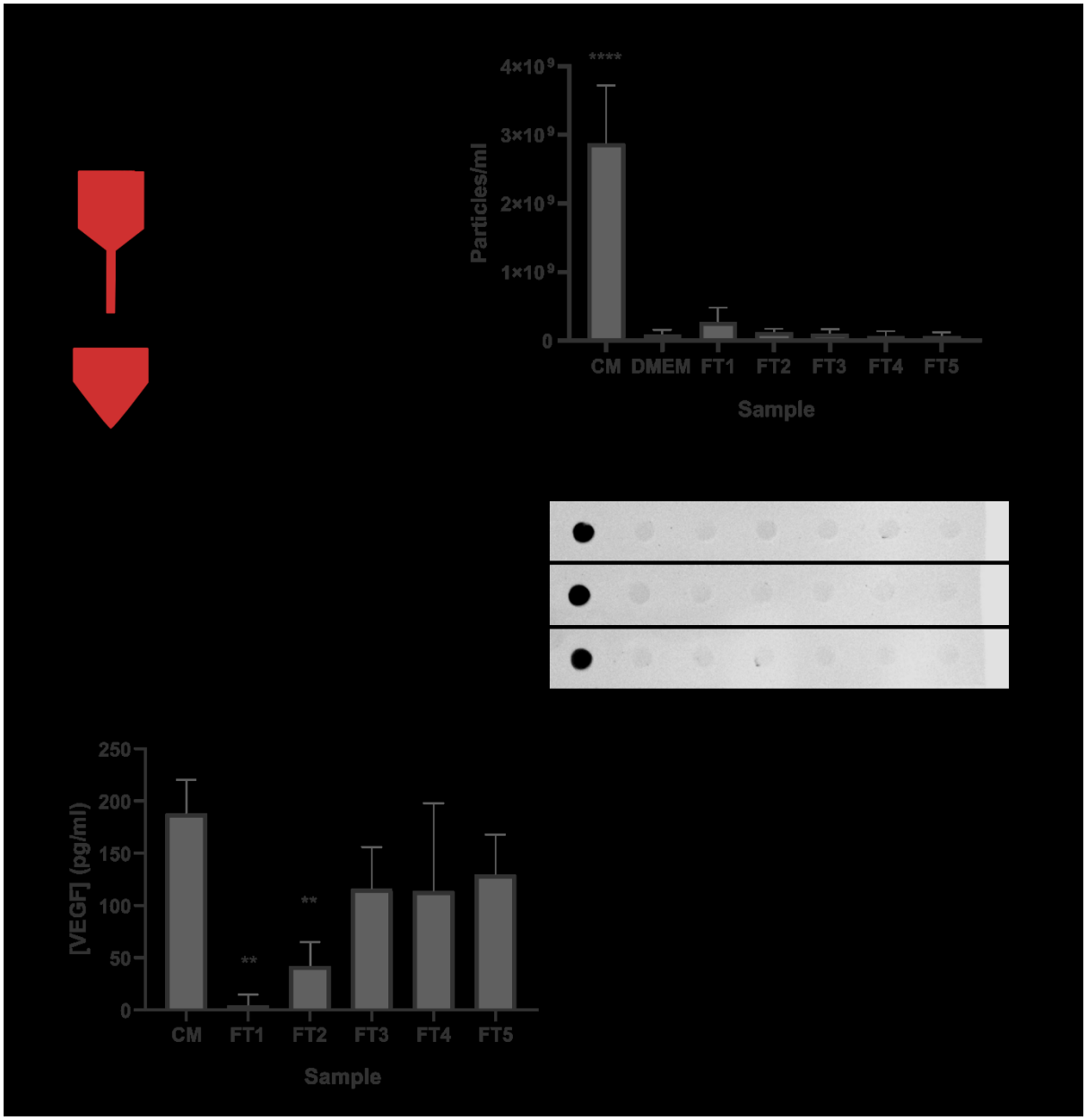


*Figure 4.3: Investigation of separation performance of 100 kDa membranes. a) Experimental setup. Media was passed through a 100 kDa filter and collected in batches, as described in the main text. b) NTA measurements. 3 x 60 second videos were captured for each sample and analysed as described in methods (N = 3, n = 3, mean +/- SD shown). ****: p < 0.0001 (one-way within-subjects ANOVA and post-hoc Dunnett's test vs DMEM). N = 3, n = 3. c) Anti-CD63 dot blots. Independently prepared replicate samples were blotted onto the same membrane and analysed simultaneously (100 µL/well). d) VEGF ELISA. (N = 3, n = 2, mean +/- SD shown) **: p < 0.01 (one-way within-subjects ANOVA and post-hoc Dunnett's test vs CM).*

Investigation of the presence of EVs in CM and FT1-5 confirmed that EVs do not pass through the filter, irrespective of the quantity of CM passed through. NTA (Figure 4.3 b) revealed that only CM contains a significant quantity of particles as compared to unconditioned DMEM, and that the particle concentrations in the flowthrough fractions are not significantly higher than the background. This

result was confirmed by dot blotting against CD63 (Figure 4.3 c). A strong signal for the EV marker was seen for CM, but not for any of the flowthrough fractions.

It was important not just to confirm that the filter was behaving as expected with regards to passage of EVs, but also that it did not have off-target effects on other factors present in conditioned medium. An ELISA was performed against VEGF, a conventional protein signalling factor also implicated in hMSC paracrine signalling. As a 45 kDa homodimer, VEGF is considerably smaller than the filter pore size and so should pass through unimpeded. VEGF is itself unlikely to be the only low-abundance signalling molecule involved in hMSC paracrine signalling (reviewed in section 4.1) and so in these and subsequent experiments is not assumed to be the most important conventional signalling protein but is measured as a general indicator of the abundance of low-abundance signalling proteins as a group.

It was initially hypothesised that the filter pores might become occluded with adsorbed material as more media passed through the filter, restricting flow of VEGF. However, the opposite effect was observed (Figure 4.3 d). In FT1 and FT2, corresponding to the first 40 mL of media passed through the filter, a significant decrease in the concentration of VEGF was found as compared to the input CM. In FT1, VEGF was essentially undetectable, at a mean + SD concentration of 4.4 +/- 10.4 pg/mL, compared to 187.7 +/- 38.2 pg/mL in CM. It was therefore hypothesised that this behaviour was due to a "blocking" effect, analogous to the blocking step of Western blot. If the filter membrane material itself has some affinity to bind proteins in CM, it will initially bind them, removing them from the flowthrough. Once the binding surfaces are occupied by other proteins, subsequent proteins will pass through unimpeded.

The ability of CM and FT1-5 to stimulate angiogenesis was measured (Figure 4.4). CM and FT samples were added undiluted to the previously described tubule formation assay. It was found that while CM was able to stimulate angiogenesis, the level of angiogenesis in the FT1 sample was not different from that of DMEM (the negative control). Subsequent fractions (FT2-5) were significantly more pro-angiogenic than DMEM, with an increasing trend from FT2-5 observed. This pattern was similar to that of the VEGF concentrations in the same samples. The absence of EVs in FT1-5 does not appear to be a significant determinant in the proangiogenic activity of the samples, as later batches achieved a similar level of angiogenesis to that of CM.

This result implies that filtration experiments used to demonstrate the contribution of EVs to signalling may give misleading results. To the best of the author's knowledge, assessment of off-target depletion by filters in this context has not previously been performed. Had only 20 mL of CM been passed through the filter, without off-target assessment, the experiment would have unambiguously indicated a major role for EVs in hMSC-mediated pro-angiogenic stimulation.

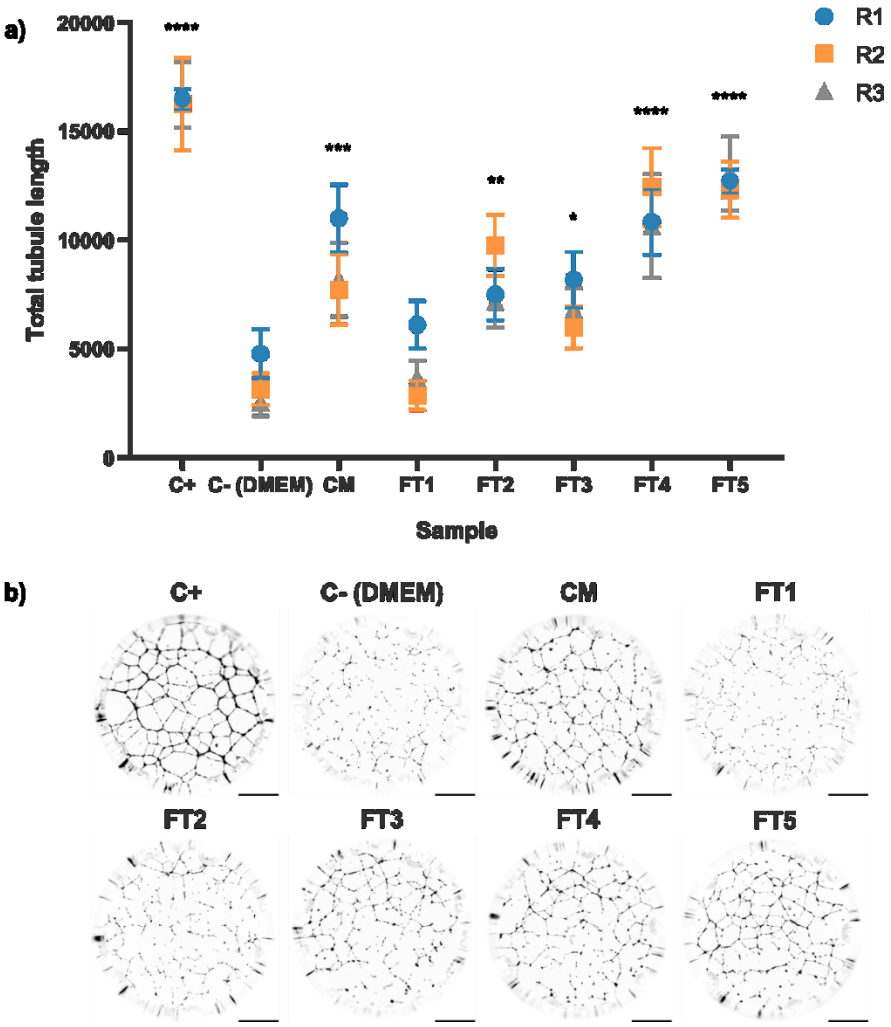


*Figure 4.4: Proangiogenic effect of hMSC-CM and sequentially 100 kDa-filtered hMSC-CM batches. a) Quantification of total tubule length for each sample (N = 3, n = 12, mean +/- SD shown). *: p < 0.05, **: p < 0.01, ***: p < 0.001, ****: p < 0.0001. (one-way within-subjects ANOVA and post-hoc Dunnett's test vs C- [DMEM]). b) Representative whole-well images of tubule structures formed under each condition. Images inverted for clarity. Scale bar = 1 mm.*

4.3.2. Ultrafiltration of hMSC-CM: membrane pre-blocking

In the previous section the off-target depletion of VEGF by the 100 kDa ultrafiltration membranes was attributed to a progressive "blocking" effect. The protein binding capacity of the membrane may actually be quite low in absolute terms but given the relatively low abundance of VEGF in CM (~180 pg/mL), the ability to bind even a few micrograms before saturation could be significant. It was investigated whether the experiment could be modified to remove this off-target depletion by pre-blocking the membrane. If this could be achieved, this would allow the determination of a more accurate picture of the contribution of EVs to hMSC-CM signalling.

In this experiment, a 100 kDa Amicon spin filter was used as before (Figure 4.5). However, prior to use the upper compartment was incubated with 1 % w/v BSA in PBS for 2 ½ hours. The upper compartment was then washed extensively to remove any unbound BSA. In each experiment, 10 mL of hMSC-CM and DMEM were passed separately through both BSA-passivated and untreated filters (Figure 4.5 a). As before, the presence of EVs in samples was assessed by NTA and dot blots against CD63 (Figure 4.5 b,c). As before, NTA (Figure 4.5 b) detected particles in CM only. Particles were not observed above the background rate in other samples, including samples that had been passed through BSA-blocked filters. Dot blots against CD63 (Figure 4.5 c) show a strong signal in CM, but no detectable signal in any other samples. Therefore, the BSA passivation step did not impact the retention of EVs by the filters, nor did it lead to an increase in particle concentration in flowthrough via protein aggregation. However, the BSA passivation step does impact the depletion of VEGF by the filters (Figure 4.5 d). The mean VEGF concentration in CM was measured to be 196 +/- 70.5 pg/mL, whereas that of flowthough through untreated concentrators (CM-FT) was only 15.9 +/- 14.4 pg/mL. However, CM-B-FT (flowthrough from passivated concentrators) was 113 +/- 40.4 pg/mL. Expressed as raw concentrations, CM and CM-B-FT were found to be significantly different to all other samples and not to each other. All other samples were found to not be significantly different to DMEM (Figure 4.5 d-i). However, when expressed as a percentage of the concentration in the input CM to account for variation between samples (Figure 4.5 d-ii), CM-FT was found to recover 8.3 % of the input, and CM-B-FT 57.7 % - both significantly higher than controls.

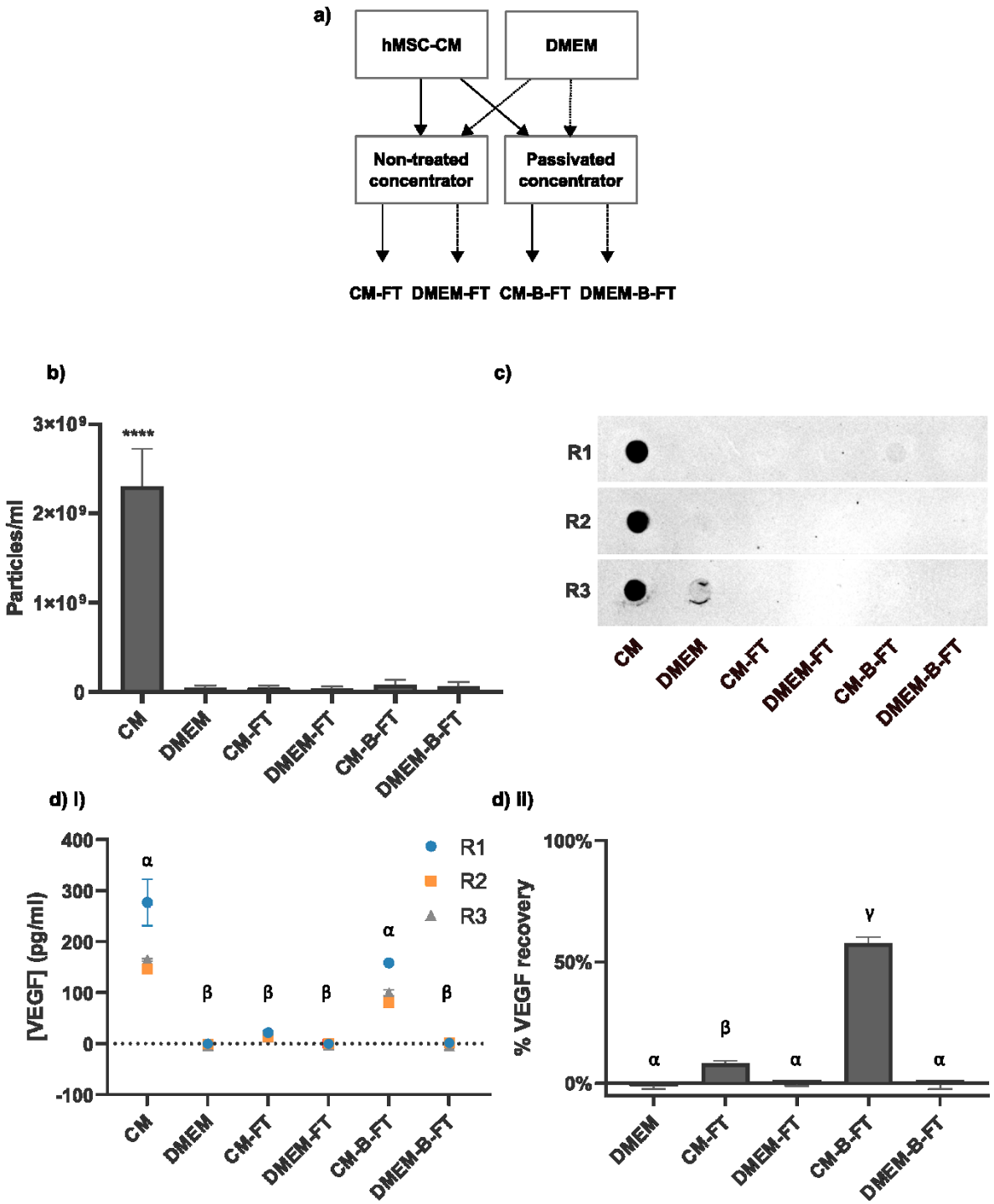


*Figure 4.5: Separation by 100 kDa membranes after BSA blocking. a) Experimental setup. -FT: flowthrough. -B: Blocked. b) NTA measurements. 3 x 60 second videos were captured for each sample and analysed as described in methods. (N = 3, n = 3, mean +/- SD shown) ****: p < 0.0001 (one-way within-subjects ANOVA and post-hoc Dunnett's test vs DMEM). c) Anti-CD63 dot blots. Independently prepared replicate samples (N = 3) were blotted onto the same membrane and analysed simultaneously (100 µL/well). d) i) Absolute concentrations of VEGF in each sample (N = 3, n = 2, mean +/- SD of individual replicates shown). ii) Concentrations of VEGF in each sample expressed as a percentage of the concentration of the input CM. (N = 3, n = 2, mean +/- SD shown). Samples are significantly different unless they share a letter (p < 0.05, one-way within-subjects ANOVA and post-hoc Tukey's HSD test).*

Pre-blocking with BSA appeared to alleviate the depletion of VEGF by the ultrafiltration membranes without interfering with their retention of EVs. It was investigated whether there was still a loss of pro-angiogenic activity in the filtered hMSC-CM (Figure 4.6).

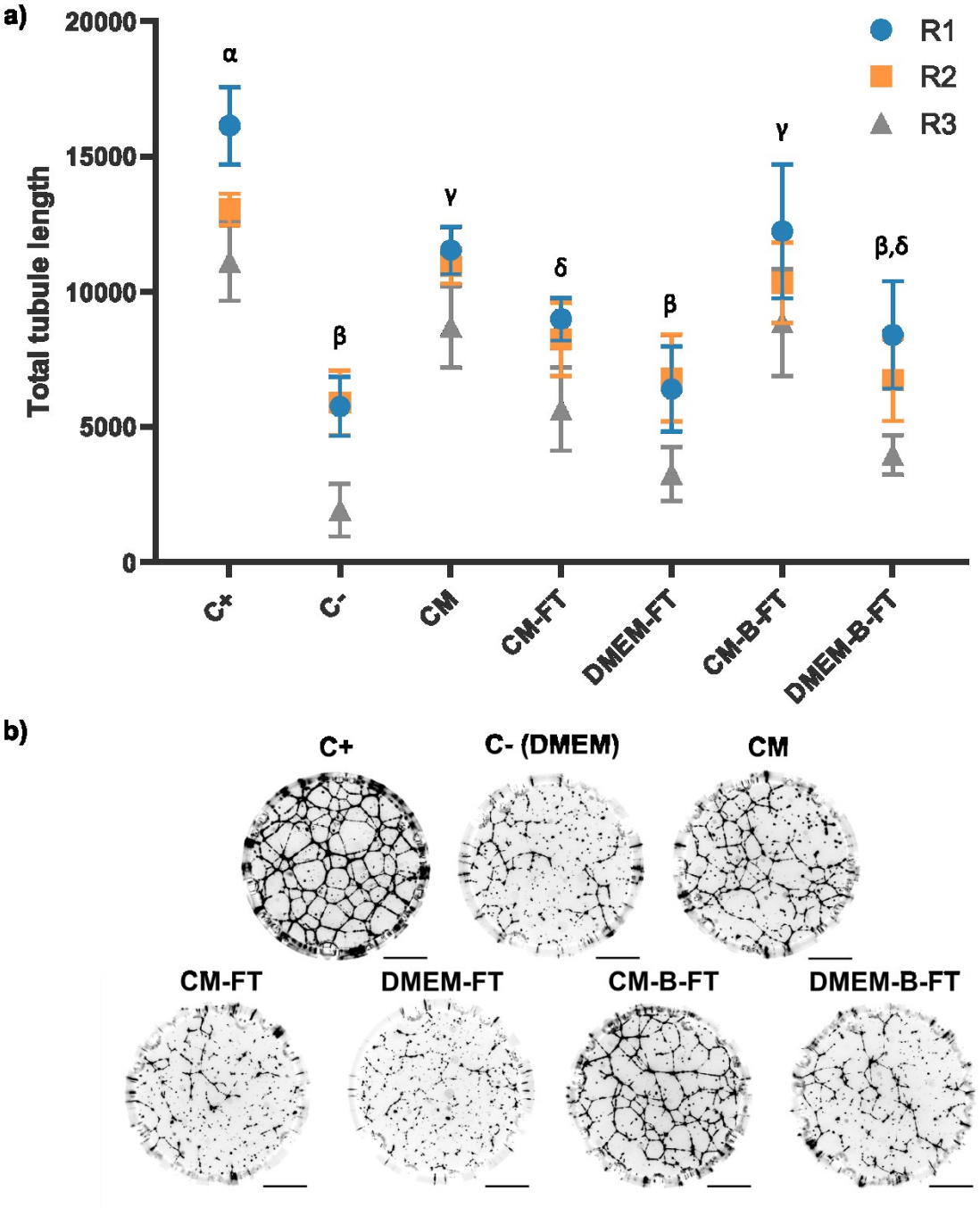


Figure 4.6: Tubule formation assay for passivated and non-passivated filtration. a) Quantification of total tubule length for each sample (N = 3, n = 12, mean +/- SD shown). Samples are significantly different unless they share a letter ($p < 0.05$, one-way within-subjects ANOVA and post-hoc Tukey's HSD test). b) Representative whole-well images of tubule structures formed under each condition. Images inverted for clarity. Scale bar = 1 mm.

The total tubule length formed in CM and CM-B-FT samples was not significantly different (10387.6 +/- 1494.8 and 10470.75 +/- 1697.0 respectively). However, both were significantly higher than CM-FT. DMEM passed through passivated filters was not found to cause significantly different angiogenic activity to DMEM, suggesting that leftover BSA from the passivation itself was unlikely to have contributed to the increased activity in CM-B-FT compared to CM-FT.

In conclusion, pre-blocking ultrafiltration membranes leads to a reduction in their depletion of VEGF (and potentially other low-abundance signalling molecules), without impacting their retention of EVs. When the off-target VEGF depletion of these filters is mitigated, removal of EVs from conditioned media is not found to have any impact on the pro-angiogenic activity of the CM.

4.3.3. Assessing possible loss of activity during concentration of hMSC-CM

For subsequent assays and EV purification by SEC, it was necessary to concentrate hMSC-CM by ultrafiltration. Recovery of both EV and soluble factors was desired, and so 3 kDa pore size membranes were used. It was considered possible that this concentration step might lead to a loss of activity. If concentration led to a loss of activity and was biased towards losing EVs rather than soluble factors, it could have caused misleading results, as the concentrate might have had a majority of biologically active EVs already removed prior to subsequent assays. If, however, there was a loss of activity but loss of EVs and soluble factors was approximately equal, there would be less concern of introduction of bias. Similarly, if no loss of activity was observed, any bias in recovery of EVs or soluble factors would only indicate which of the two was less important to signalling.

Any loss of activity due to use of the concentrators could be revealed by using them to concentrate hMSC-CM by a known factor and then diluting the concentrated hMSC-CM by the same factor. If material was lost during the concentration process, the concentrated-diluted sample should have contained less of it than the initial unprocessed sample. 100 mL of hMSC-CM was used in this experiment. 1 mL was removed for subsequent analysis and the remaining 99 mL concentrated to 19.8 mL (5x concentration). 1 mL was again removed for subsequent analysis and then the remaining 18 mL was concentrated to 3.6 mL (25x concentration). Volumes were verified gravimetrically. Some 25x concentrate was retained for analysis, and the rest diluted back to 5x and 1x concentrations with DMEM (Figure 4.7 a). The samples were then compared.

It was found that concentration led to a significant loss of particles (Figure 4.7 b). As a percentage of the total particles in the 100 mL of CM used in the experiment, approximately 55 % were recovered in the 5x concentrate and 35-40 % in the 25x concentrate and subsequent dilutions. Contrastingly, the absolute concentrations of VEGF in the matched samples were not significantly different (Figure 4.7 c). Although the mean % recovery of VEGF declined to 91 % of the input, there was not found to be any

significant difference between % recoveries in concentrated or diluted samples. Dot blots to assess the abundance of CD63 were performed using 100 μl of each sample (Figure 4.7 d-i) and quantified (Figure 4.7 d-ii). Intensity measurements were normalised to the average of the data set, as described in materials and methods. CD63 intensity was significantly greater for the 5x, 25x, and 5x-d (diluted) samples than for unconcentrated CM or the 1x-d (diluted) CM. There was a decrease in mean intensity between the initial (CM) and final 1x-d sample, however it was not significant. The intensity of the 25x sample might have been expected to be greater than that of the 5x or 5x-d samples, but it was not. This may be due to sample entering the blot at two offset positions instead of one centred position (see Figure 4.7 d-i) for those samples.

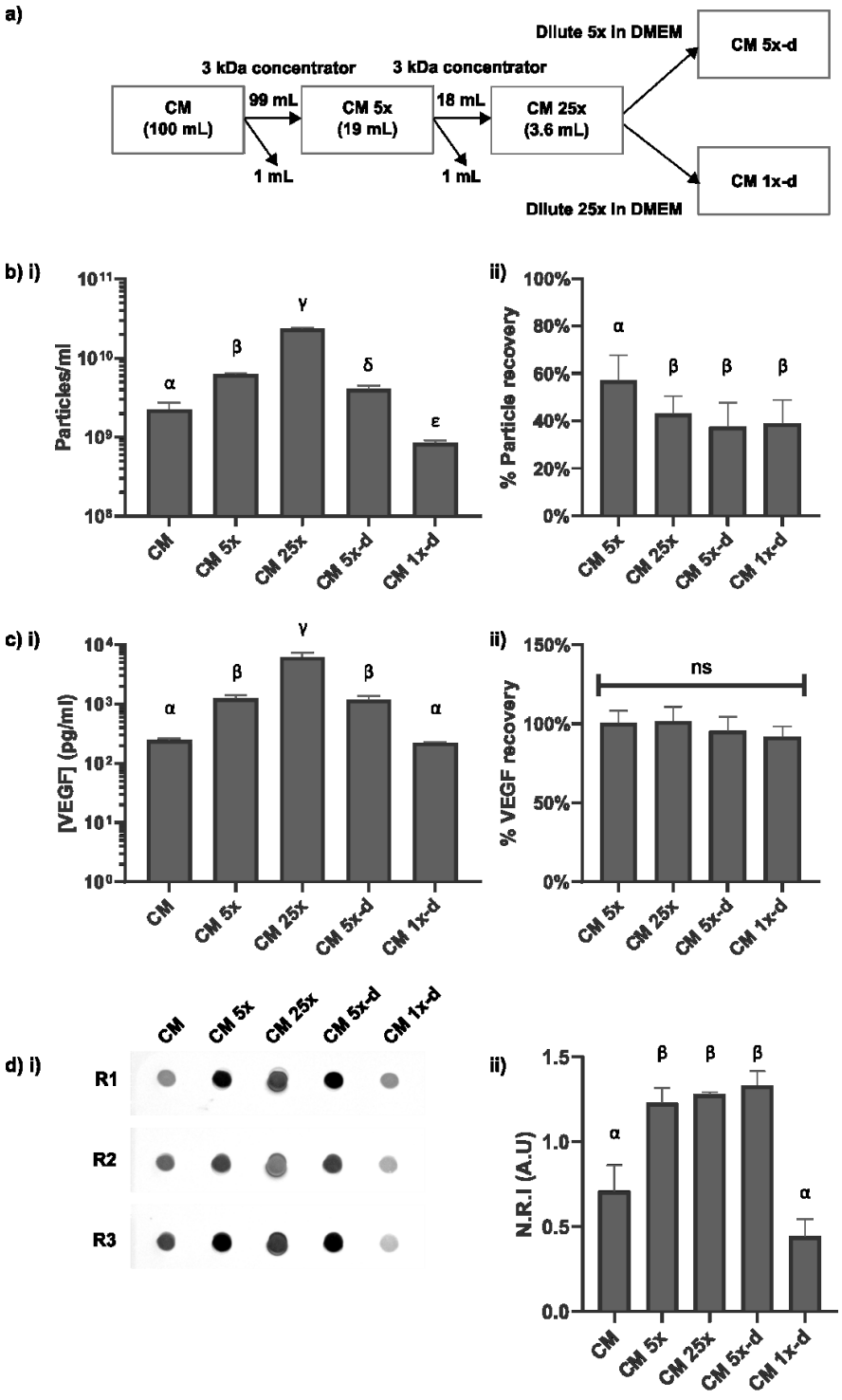


Figure 4.7: Loss of EVs and VEGF during concentration. a) Experimental setup. 5x-d: diluted from 25x to 5x. 1x-d: diluted from 25 x to 1x. Volumes of each sample are shown. b). NTA of samples, expressed as i) absolute concentration values and ii) % recovered from input CM. (N = 3, n = 3, mean +/- SD shown). c) ELISA of VEGF, expressed as i) absolute concentration values and ii) % recovered from input CM. (N = 3, n = 3, mean +/- SD shown). d) i) Anti-CD63 dot blots. Independently prepared replicate samples were blotted onto the same membrane and analysed simultaneously (100 µL/well). Ii) Quantification of dot blots, as described in materials and methods. N.R.I: Normalised Relative Intensity. Mean +/- SD shown (N = 3). Samples are significantly different unless they share a letter ($p < 0.05$, one-way within-subjects ANOVA and post-hoc Tukey's test). Where data is plotted on a logarithmic axis, data was log_{10}-transformed before statistical analysis.

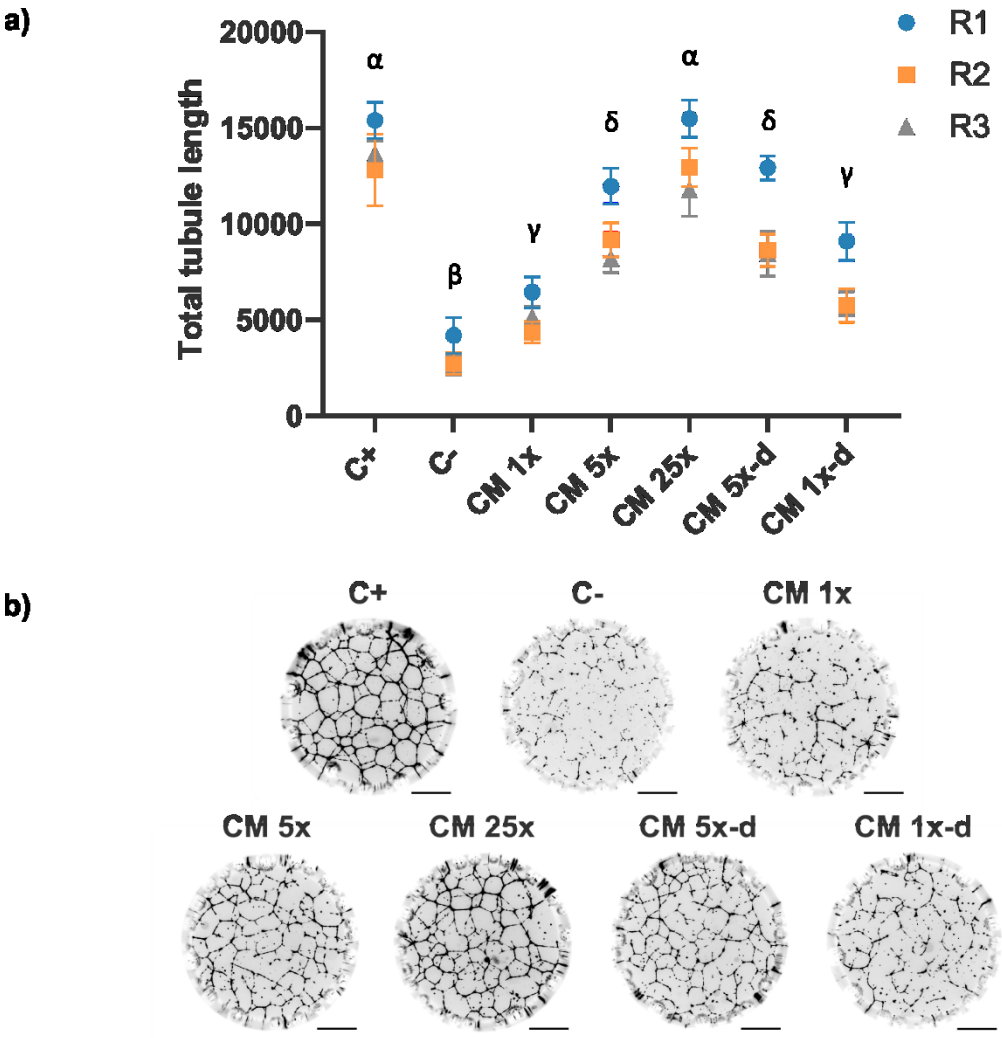


Figure 4.8: Tubule formation assay for concentrated/diluted hMSC-CM. a) Quantification of total tubule length for each sample. (N = 3, n = 12, mean +/- SD shown for individual replicates). Samples are significantly different unless they share a letter ($p < 0.05$, one-way within-subjects ANOVA and post-hoc Tukey's test). b) Representative whole-well images of tubule structures formed under each condition. Images inverted for clarity. Scale bar = 1 mm.

The activity of the concentrated and diluted hMSC-CM samples was assessed by a tubule formation assay as before. As before, hMSC-CM was observed to stimulate angiogenesis (Figure 4.8). Increasingly concentrated CM stimulated a greater degree of tubule formation. Crucially, the pro-angiogenic activities of the diluted samples were not found to be significantly different to their matched, concentrated samples (CM 1x vs 1x-d and CM 5x vs 5x-d). This indicated that the factors responsible for pro-angiogenic stimulation in the sample were not depleted by concentration.

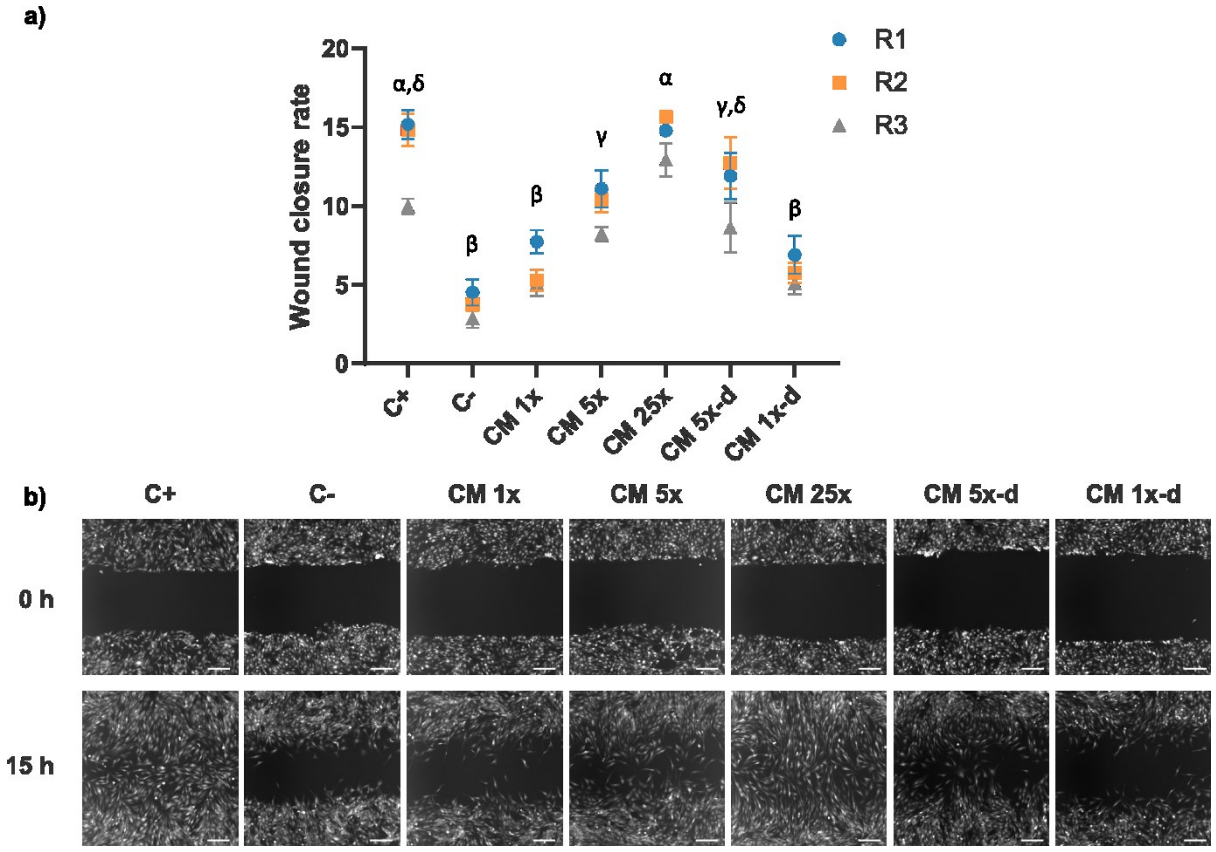


Figure 4.9: Scratch wound assay for concentrated/diluted hMSC-CM. a) Quantification of wound closure rate for each condition. (N = 3, n = 3, mean +/- SD shown for individual replicates). Samples are significantly different unless they share a letter ($p < 0.05$, one-way within-subjects ANOVA and post-hoc Tukey's test). b) Representative images of scratch wounds for each condition are shown for t = 0 h and t = 15 h, the final timepoint of the assay. Scale bar = 100 µm.

It was considered possible that the apparent independence of stimulation of angiogenesis from EV concentration could be specific to this tubule formation assay. To rule out an assay-specific effect, a second *in vitro* assay was introduced that measured the response of a different cell type and assessed a different biological process, whilst still being related to wound healing and regeneration. A scratch wound assay was developed in which GFP-expressing mouse fibroblasts (NIH-3T3 cells) were allowed to grow to confluence on collagen-coated multiwell plates, before mechanically scratching a gap in the monolayer. NIH-3T3 cells had been transformed to express GFP by Dr. A. Nagelkerke, using IncuCyte CytoLight Green Lentivirus (see methods). The wells were washed, and the media was replaced with the samples, diluted 1:1 in fresh DMEM. The closure of the gap was imaged in 3 positions per well over the course of 15 hours, and the rate of closure for each image set quantified.

The scratch wound assay showed a similar pattern of activity to the tubule formation assay (Figure 4.9). Non-concentrated hMSC-CM was not found to cause significantly higher cell migration than the

negative control, while concentrated hMSC-CM caused significant cell migration. Again, the pro-wound-healing activities of the diluted samples were not significantly different to their matched concentrated counterparts (CM 1x vs 1x-d, CM 5x vs 5x-d).

In conclusion, concentrating hMSC-CM did not appear to deplete the as-yet unidentified factors responsible for stimulation of angiogenesis or wound healing. However, it does appear that concentration depleted EVs but not VEGF. This further indicated that EVs were unlikely to be primarily involved in these processes, and that soluble factors may play a greater role.

4.3.4. Equilibrium Dialysis of hMSC-CM

Experiments so far using centrifugal concentrators have indicated that conventional soluble factors are likely to be of greater importance than EVs to hMSC paracrine signalling in *in vitro* assays of angiogenesis and wound healing. However, centrifugal ultrafiltration may have some disadvantages for analytical separation. Firstly, the force exerted on the contents of the media during centrifugation could potentially have been damaging or have led to increased adsorptive losses by forcing EVs or other factors into the membrane itself. Concentration/dilution experiments (section 4.3.3) indicated that this does not impact the critical signalling agents themselves. Secondly, ultrafiltration through a centrifugal concentrator is a non-equilibrium process. The < 100 kDa flowthrough does not necessarily contain the same concentration of < 100 kDa molecules as the input sample, even when the membrane is blocked (see Figure 4.5). It was thought that an experimental system in which conditioned and fresh media could be allowed to fully exchange all components below a certain size cutoff might have allowed generation of EV-containing and EV-free samples that are otherwise equilibrated. Their bioactivity could then be directly compared.

Equilibrium dialysis experiments were set up as in Figure 4.10 a. A dialysis cassette was filled with 1.25 mL of unconditioned medium and placed in 6 mL of hMSC-CM that had previously been concentrated 10x by ultrafiltration against a 3 kDa membrane. The dialysis cassette and external container had previously been blocked with 1 % w/v BSA and washed, as in the previous filter-blocking experiments. A 300 kDa pore size was chosen, as it was expected to prevent the passage of EVs while allowing passage of larger proteins and faster passage of smaller ones than the previously used 100 kDa filter. The cassette was incubated for 48 hours at 4 °C, with rotation, before recovering samples from the outer (FAL-O) and inner (FAL-I) compartments. A separate cassette was run in parallel containing only fresh media as a control.

NTA quantification of samples after incubation (Figure 4.10 b) found that only the input CCM and CCM FAL-O contained detectable quantities of particles. CCM FAL-I did not contain significantly more particles than DMEM, indicating that EVs did not pass through the 300 kDa membrane. The DMEM FAL-O and FAL-I samples were also not significantly different to DMEM, indicating that the incubation process does not itself introduce particles to either compartment.

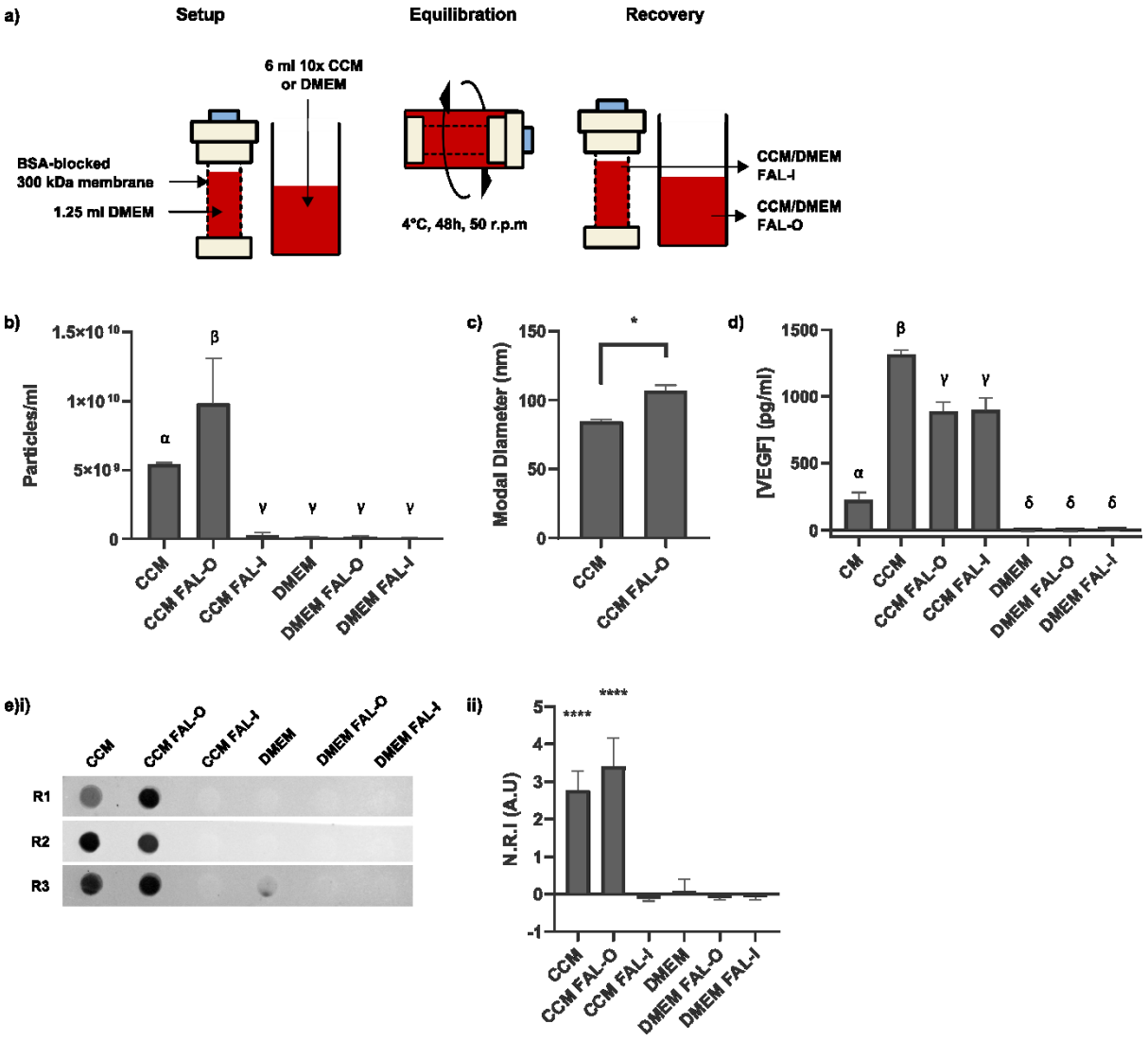


Figure 4.10: Equilibrium dialysis of hMSC-CM. a) Experimental setup. A pre-blocked Spectra-por Float-a-Lyzer was filled with 1.25 mL of DMEM and incubated in 6 mL of 10x concentrated hMSC-CM or DMEM. After incubation, samples were recovered and named as shown. b) NTA quantification of samples. (N = 3, n = 3, mean +/- SD shown). Samples are significantly different unless they share a letter ($p < 0.05$, one-way within-subjects ANOVA and post-hoc Tukey's test). c). Modal diameter of CCM and CCM FAL-O samples (N = 3, n = 3, mean +/- SD shown). (: $p < 0.05$, 2-tailed paired t-test). d) ELISA for VEGF (N = 3, n = 12, mean +/- SD shown). Samples are significantly different unless they share a letter ($p < 0.05$, one-way within-subjects ANOVA and post-hoc Tukey's test). e)i) Anti-CD63 dot blots. Independently prepared replicate samples were blotted onto the same membrane and analysed simultaneously (100 µL/well). Ii) Quantification of dot blots, as described in materials and methods. N.R.I: Normalised Relative Intensity. Mean +/- SD shown (N = 3). Samples are significantly different unless they share a letter ($p < 0.05$, one-way within-subjects ANOVA and post-hoc Tukey's test). ****: $p < 0.0001$ (one-way within-subjects ANOVA and post-hoc Dunnett's test against DMEM).*

Surprisingly, the particle concentration in CCM FAL-O was significantly higher than that of the input CCM. This could have been caused by EVs being damaged and splitting into multiple smaller bodies. Alternatively, NTA is more sensitive to larger particles and so if the EVs had swollen over time this could also have led to a higher measured concentration for the same population of EVs. The diameter of EVs in CCM FAL-O is significantly higher than in CCM (Figure 4.10 c) (106.8 +/- 4.1 vs 84.5 +/- 1.4 nm

respectively), and so the EVs were likely swelling rather than being broken apart. The mechanism and significance of the swelling were unclear. An ELISA against VEGF (Figure 4.10 d) showed that VEGF was fully equilibrated across the outer and inner compartments (888.7 +/- 70.1 pg/mL vs 898.3 +/- 93 pg/mL respectively). However, some VEGF had been lost from the input CCM (1316.9 +/- 30.0 pg/mL). This was partially due to the dilution inherent to the assay, but even accounting for the expected 20 % dilution, some VEGF was unaccounted for. Despite the blocking step, components of the media may have adsorbed to the membrane or other structures of the dialysis cassette.

Dot blots against CD63 (Figure 4.10 e) confirmed the NTA results, demonstrating that CD63 was only detectable in the input CCM and CCM FAL-O, and not in CCM FAL-I or any of the controls. Quantification of dot blots (Figure 4.10 e-ii) showed that only CCM and CCM FAL-O are greater than the negative control (DMEM).

The ability of these samples to stimulate angiogenesis and wound healing was assessed with tubule formation and scratch wound assays as before. CCM was diluted with unconditioned DMEM at a 5:1 v/v ratio prior to addition to the assay to account for the dilution during dialysis. There was no significant difference between the ability of the EV-containing outer compartment and the EV-free inner compartment to stimulate angiogenesis (Figure 4.11). No significant difference was found between either compartment and the input CCM; however, the mean and standard deviation values of the input CCM were somewhat higher than those of CCM FAL-O and FAL-I and so the lack of significant difference found may be due to a deficit of statistical power. The control samples (DMEM FAL-O and FAL-I) were not found to be significantly different to the negative control (C-/DMEM), indicating no interference from any components associated with the pre-blocked dialysis cassettes.

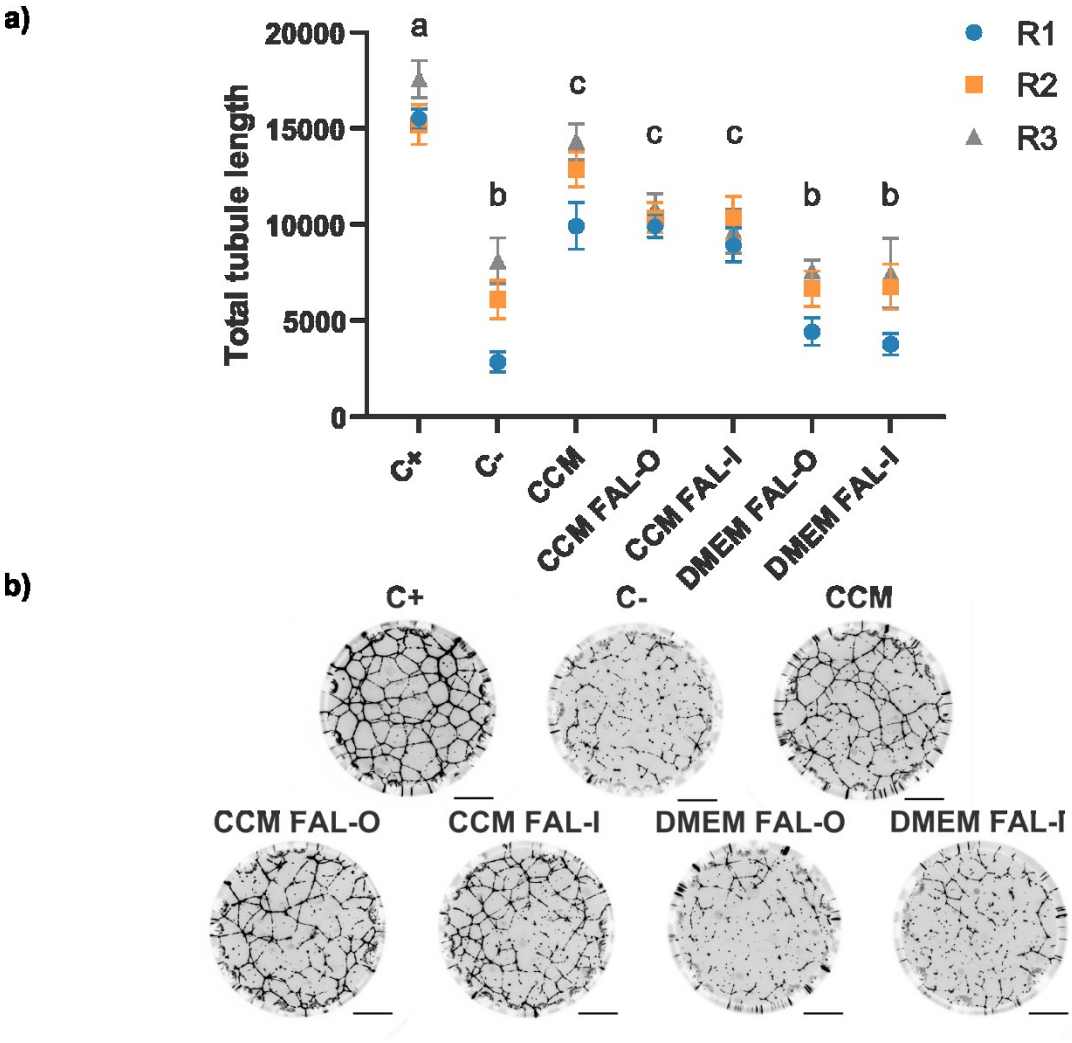


Figure 4.11: Tubule formation assay for equilibrium dialysis experiment. a) Quantification of total tubule length for each sample. (N = 3, n = 12, mean +/- SD shown for individual replicates). Samples are significantly different unless they share a letter ($p < 0.05$, one-way within-subjects ANOVA and post-hoc Tukey's test). b) Representative whole-well images of tubule structures formed under each condition. Images inverted for clarity. Scale bar = 1 mm.

The results indicated that the presence or absence of EVs did not affect pro-angiogenic hMSC signalling in the *in vitro* tubule formation assay. The results of the scratch wound healing assay were more ambiguous (Figure 4.12). There was no apparent stimulation of migration by the DMEM controls, as expected. However, CCM, CCM FAL-O, and CCM FAL-I were not all equivalent. CCM was significantly different to CCM FAL-I, with CCM FAL-O not significantly different to either. The mean values of each were not as similar as they are for the angiogenesis assay, and it is possible again that the lack of statistical significance was a result of insufficient statistical power rather than a genuine lack of difference between samples.

a)

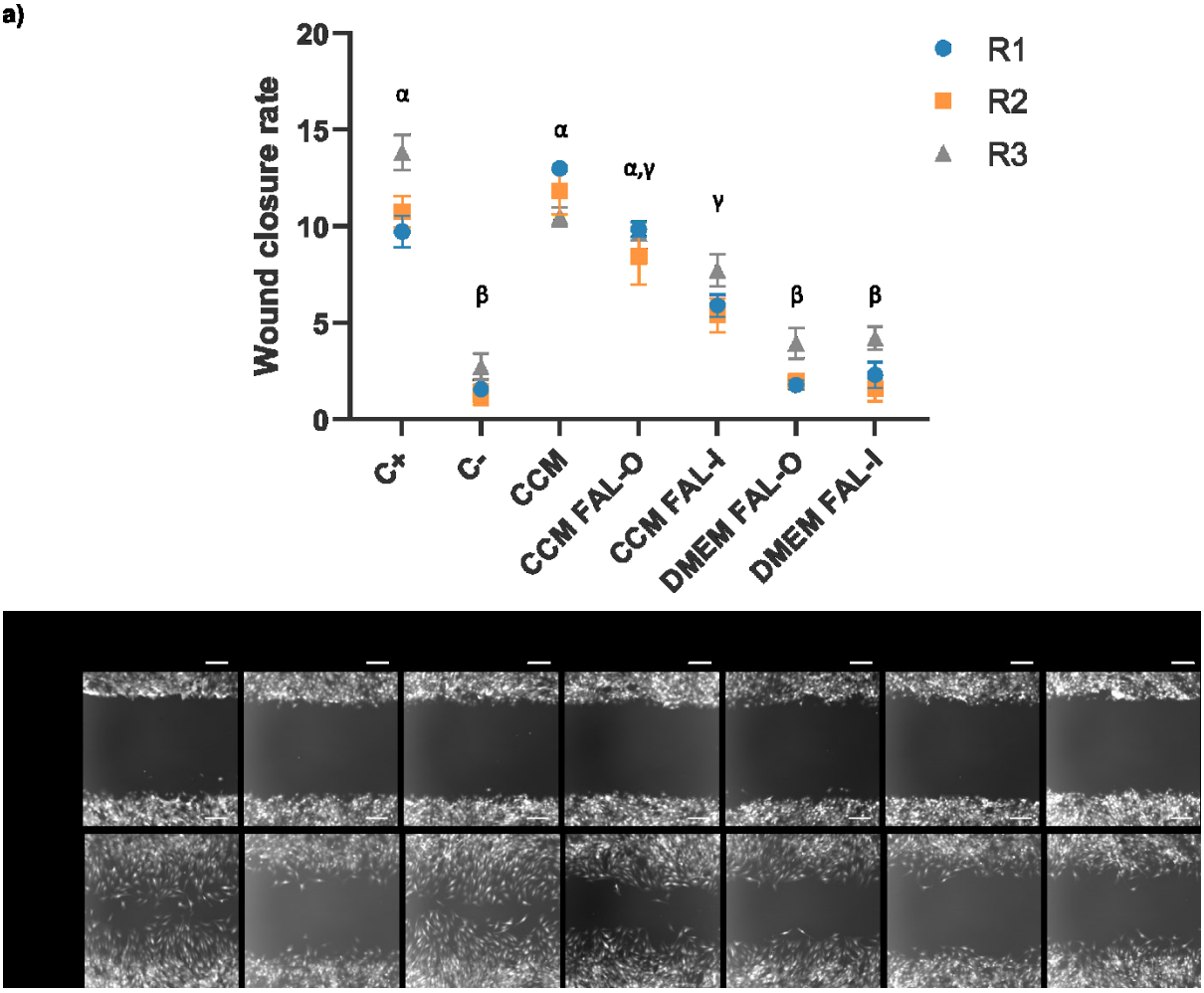


Figure 4.12: Scratch wound assay for equilibrium dialysis experiment. a) Quantification of wound closure rate for each condition. Means of individual replicates (N = 3) and standard deviation of internal replicates (n = 3) are shown. Samples are significantly different unless they share a letter ($p < 0.05$, one-way within-subjects ANOVA and post-hoc Tukey's test). b) Representative images of scratch wounds for each condition are shown for t = 0 h and t = 15 h, the final timepoint of the assay. Scale bar = 100 µm.

Given this caveat, and the substantial decrease in activity between CCM and CCM FAL-I, this result is broadly interpreted to suggest that components involved in stimulating cell migration are less effectively traversing the membrane than those involved in stimulating angiogenesis. This is not inconsistent with a role for EVs; however, it could also simply be due to larger proteins traversing more slowly and therefore incompletely. To investigate differences in diffusion of non-EV proteins across the membrane, it was attempted to assess the soluble protein content of each compartment using SDS-PAGE and silver staining; unfortunately, due to the low quantities of protein available this was not successful.

4.3.5. Analytical Size Exclusion Chromatography

In summary, the experiments thus far utilising ultrafiltration membranes to separate EVs and free protein indicated that EVs are not necessary for hMSC paracrine stimulation of angiogenesis or wound healing. However, they have not explicitly investigated whether EVs in isolation are able to potentiate signalling. It might be possible that both EVs and soluble factors are, entirely independently, able to stimulate angiogenesis and wound healing, and so removing EVs would not necessarily reduce the activity of the sample. This would not be consistent with results so far indicating that the activity of these assays is linked to the concentration of soluble factors and not the concentration of EVs. However, a technique that allowed full separation of EVs and soluble factors would allow explicit comparison of both the necessity and sufficiency of EVs and soluble factors for signalling. Additionally, it was thought that the results of equilibrium dialysis for wound healing were somewhat ambiguous and would benefit from follow-up with a more powerful experiment technique.

It was decided to use the size exclusion chromatography process previously used for EV purification as an analytical technique, to separate EVs and protein from CCM. Previous data indicates a near-total separation between the EV peak and free protein peak (Figure 2.8). Analytical techniques had already been optimised for low-volume, high-sensitivity analysis, and so it was possible to perform extensive characterisation on each of the thirty 1 mL fractions typically collected from the column (Figure 4.13), either individually or as pooled groups of two.

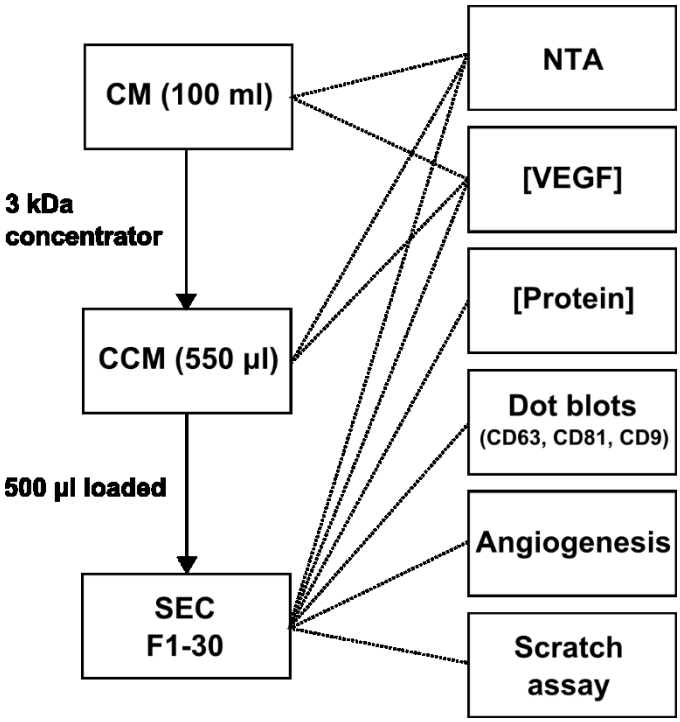


Figure 4.13: Analysis plan for analytical SEC (see text).

It was necessary to rule out the possibility that the lack of contribution from EVs was a peculiarity of the hMSC donor used so far (Donor 1). Therefore, two additional donors (2 and 3) were sourced, and hMSC-CM prepared from them as before. Three replicates were performed per donor, with hMSC-CM prepared separately for each.

HMSC-CM was concentrated from 100 mL to ~550 µL, and 500 µL loaded onto SEC columns as before, with the modification of the use of a sample applicator to ensure even entry of the sample into the column bed. 30 x 1 mL fractions were collected. Fractions were aliquoted upon collection and either used immediately or frozen at -80 °C.

4.3.5.1. Determining elution of EVs

NTA and dot blots against EV markers were performed for each donor (Figure 4.14-1,2,3). Particles were quantified by NTA for fractions 6-25 only. This was because the void volume of the column is approximately 7 mL, and nothing was expected to elute prior to fraction 8. The particle concentration in fraction 6 was used as a background value, to which the particle concentration in other fractions was compared. The majority of particles consistently eluted in fractions 9 and 10, across all replicates and all three donors. However, there was considerable variation between replicates in terms of the concentration of particles detected in the peak fractions, with the lowest peak concentration approximately 5 x 10^9/mL and the highest approximately 2 x 10^{10}/mL. Individual replicates are shown to better demonstrate that the pattern was consistent. Unexpectedly, a smaller secondary peak eluted between fractions 16-18. An increase in mean particle concentration in these fractions was observed across donors but was only significantly greater than baseline for Donor 1.

Dot blots were performed against three commonly used EV markers – CD63 (as before), CD81 and CD9. Images were quantified, and the intensity values normalised as described in Materials and Methods. For all markers, replicates and donors, the highest signal intensity was detected in fractions 9 and 10. This was consistent with the NTA results, which indicate that the majority of EVs eluted in F9-10. However, EV markers are detected in later fractions – at latest, fraction 20. Dot blots may have been more sensitive to smaller EVs than NTA. CD63 signal in particular is of comparable intensity to F9-10 in later fractions. This may be due to different expression of markers on smaller EVs, or different antibody sensitivities. The absolute intensities for CD9 were lower than for CD81 and CD63, and so the data is more variable due to increased influence of noise. These results were interpreted to indicate a majority of EVs eluting in fractions 9-10, with a possibly undercounted secondary population eluting approximately between fractions 15-18. There is no evidence to suggest any EV elution from the column after fraction 20.

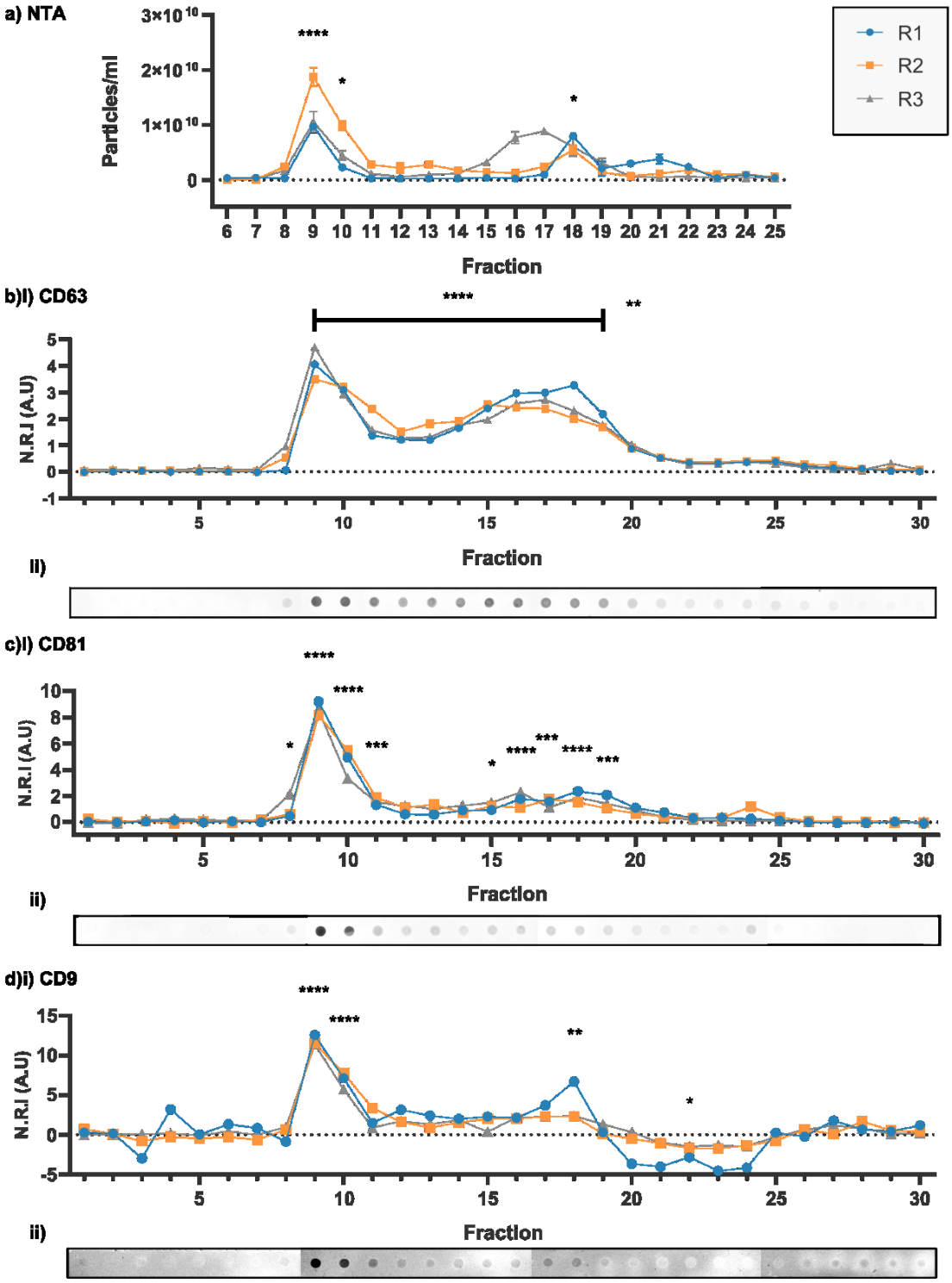


*Figure 4.14: NTA and Dot blots on analytical SEC fractions for Donor 1. a) NTA quantification of sample (N = 3, n = 3, mean +/- SD shown for individual replicates). b-d) Quantification of Dot blots against CD63 (b), CD81 (c) and CD9 (d). Quantifications shown in i). Individual replicates are shown (N = 3). Representative images shown in ii) (25 µL column eluate/well). N.R.I.: Normalised relative intensity (arbitrary units). * : p <0.05, ** : p < 0.01, *** : p < 0.001, **** : p < 0.0001 (one-way within-subjects ANOVA and post-hoc Dunnett's test against a) fraction 6 or b-d) fraction 1). Replicates are matched across a-d.*

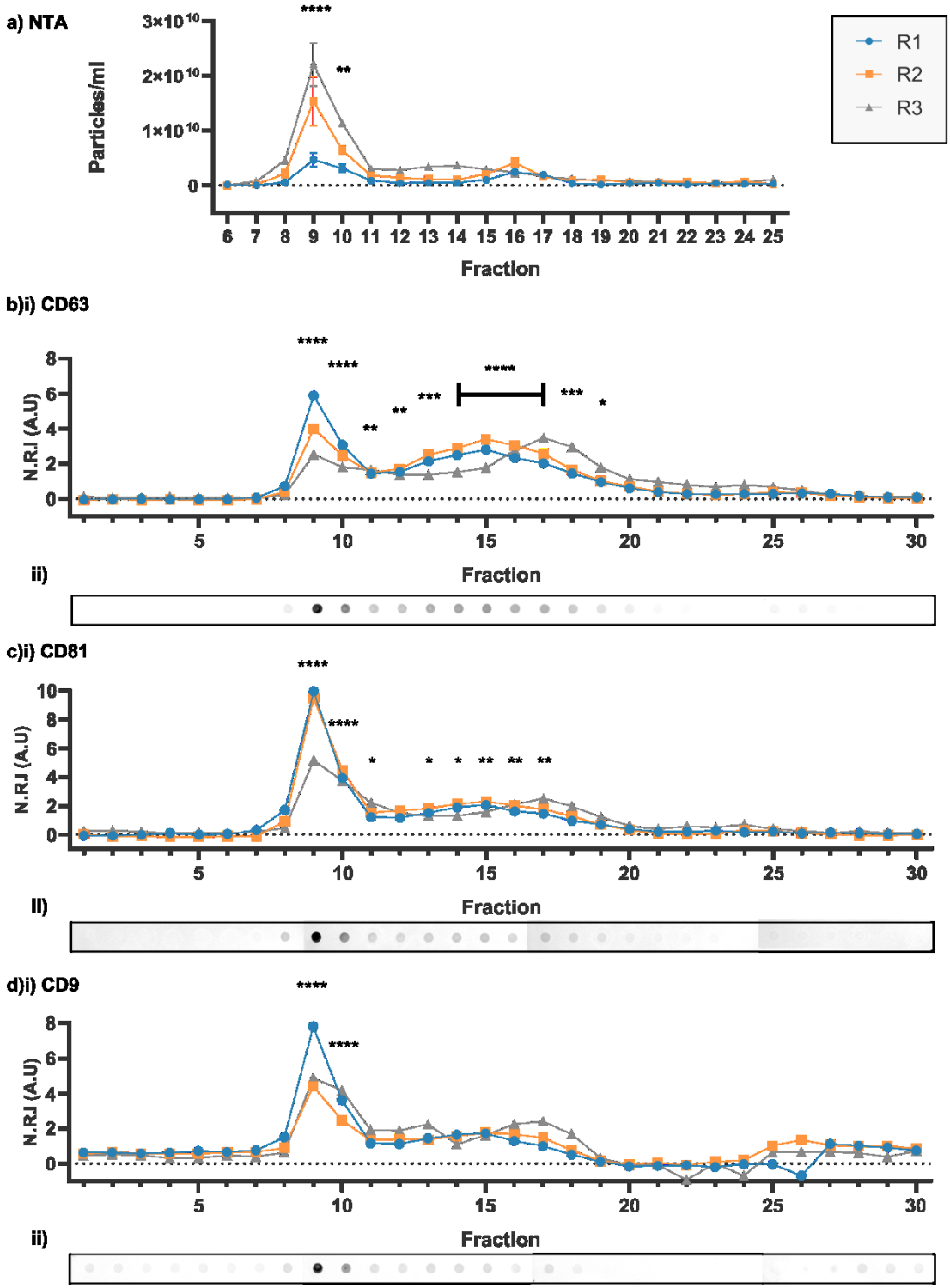


*Figure 4.14-2: NTA and Dot blots on analytical SEC fractions for Donor 2. a) NTA quantification of sample (N = 3, n = 3, mean +/- SD shown for individual replicates). b-d) Quantification of Dot blots against CD63 (b), CD81 (c) and CD9 (d). Quantifications shown in i). Individual replicates are shown (N = 3). Representative images shown in ii) (25 µL column eluate/well). N.R.I.: Normalised relative intensity (arbitrary units). * : p <0.05, ** : p < 0.01, *** : p < 0.001, **** : p < 0.0001 (one-way within-subjects ANOVA and post-hoc Dunnett's test against a) fraction 6 or b-d) fraction 1). Replicates are matched across a-d.*

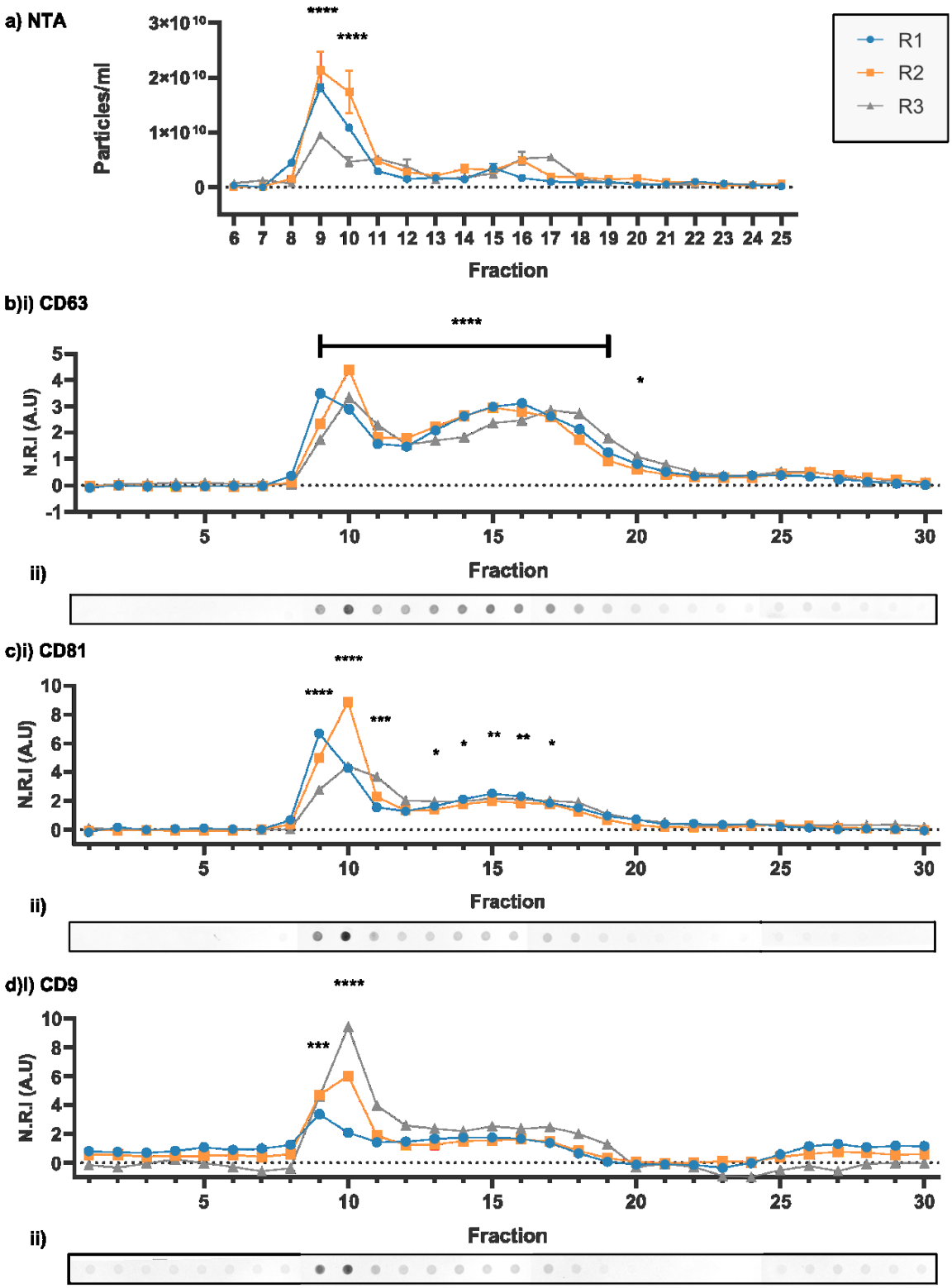


*Figure 4.14-3: NTA and Dot blots on analytical SEC fractions for Donor 3. a) NTA quantification of sample (N = 3, n = 3, mean +/- SD shown for individual replicates). b-d) Quantification of Dot blots against CD63 (b), CD81 (c) and CD9 (d). Quantifications shown in i). Individual replicates are shown (N = 3). Representative images shown in ii) (25 µL column eluate/well). N.R.I.: Normalised relative intensity (arbitrary units). * : p <0.05, ** : p < 0.01, *** : p < 0.001, **** : p < 0.0001 (one-way within-subjects ANOVA and post-hoc Dunnett's test against a) fraction 6 or b-d) fraction 1). Replicates are matched across a-d.*

4.3.5.2. Determining elution of free protein

The protein content of each fraction was quantified using the Nano-Orange fluorescent detection kit (Figure 4.15). Protein was only detected in later fractions for all donors, with the earliest significant increase in protein concentration above baseline (fraction 1) being fraction 17 in Donor 2. Fractions 18-25 are significantly above baseline for all three donors. No free protein was detectable in fractions 9-10, where the main EV peak eluted. There was some overlap with the secondary minor EV peak in fractions 15-18. Notwithstanding the unexpected minor secondary EV peak, this assay confirms an essentially total separation of EVs and soluble protein. The lack of detection of protein in EV fractions is consistent with a high-purity purification; Webber and Clayton [108] propose that a highly pure sample should contain approximately 1 μg protein / 3 x 10^{10} EVs. Given the peak concentrations of between 0.5 and 2 x 10^{10} EV/mL, the expected associated protein would be below the limit of detection of the assay (approximately 1 μg/mL).

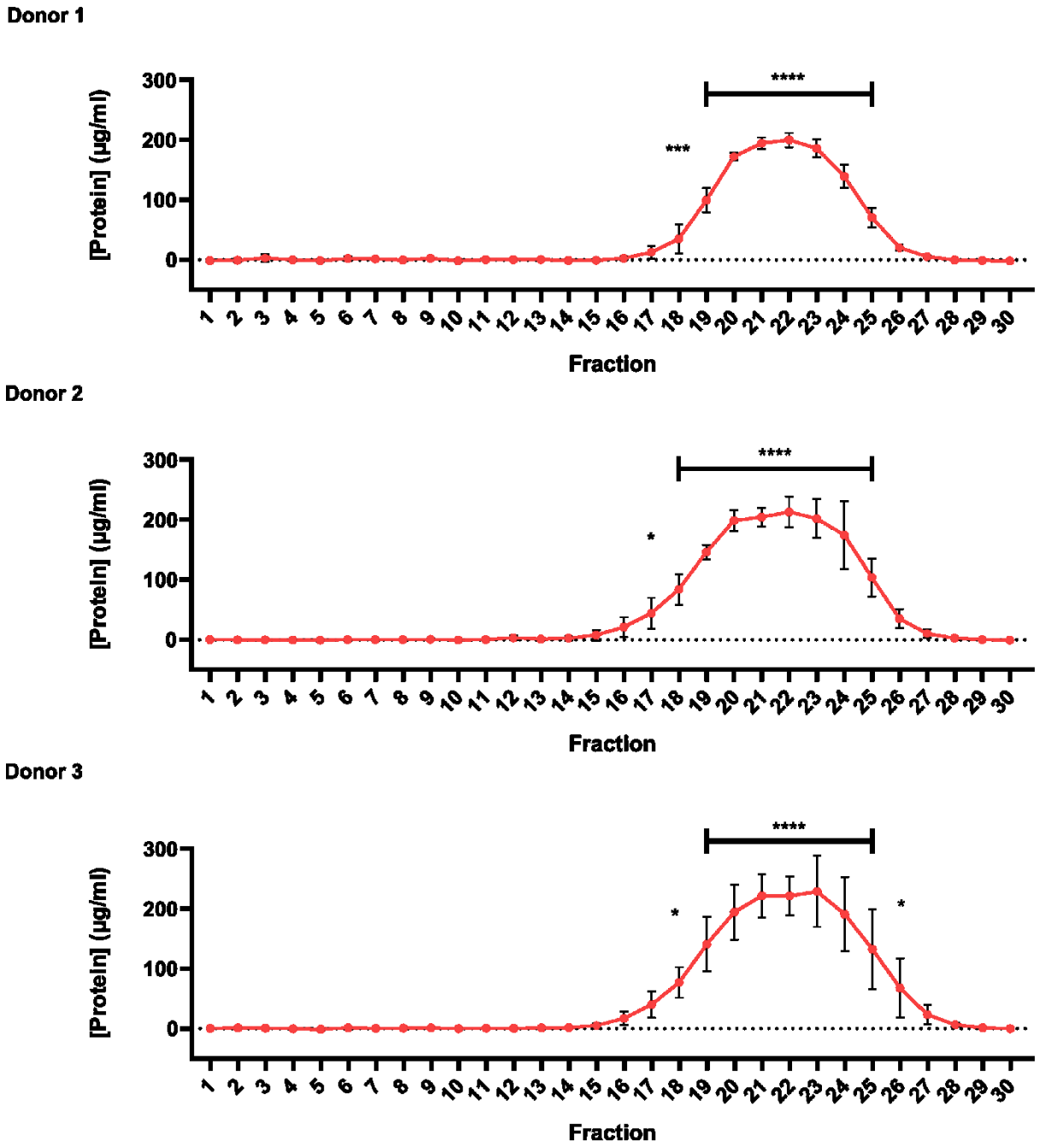


*Figure 4.15: Protein quantification of analytical SEC fractions. Protein concentration was quantified using the Nano-Orange assay (Thermo-fisher). Mean +/- std. dev is shown for each donor (N = 3, n = 3). * : p <0.05, ** : p < 0.01, *** : p < 0.001, **** : p < 0.0001 (one-way within-subjects ANOVA and post-hoc Dunnett's test against fraction 1).*

4.3.5.3. Determining elution of VEGF

Although the Nano-orange assay is a sensitive method of quantifying protein, the reagent will also react with Phenol red and some amino acids, and so the total quantity of protein measured in peak fractions may not be strictly accurate. To confirm the elution of protein in these fractions, and to further characterise the elution of non-EV factors, the elution of VEGF from the column was characterised (Figure 4.16). To conserve resources, adjacent fractions were pooled, void volume fractions (1-6) were not included, and only fractions from Donor 1 were evaluated. The results confirmed those seen with total protein quantification. VEGF was found in fractions 19-26 only, with no detectable VEGF associated with either the major (F9-10) or minor (F15-18) EV peaks.

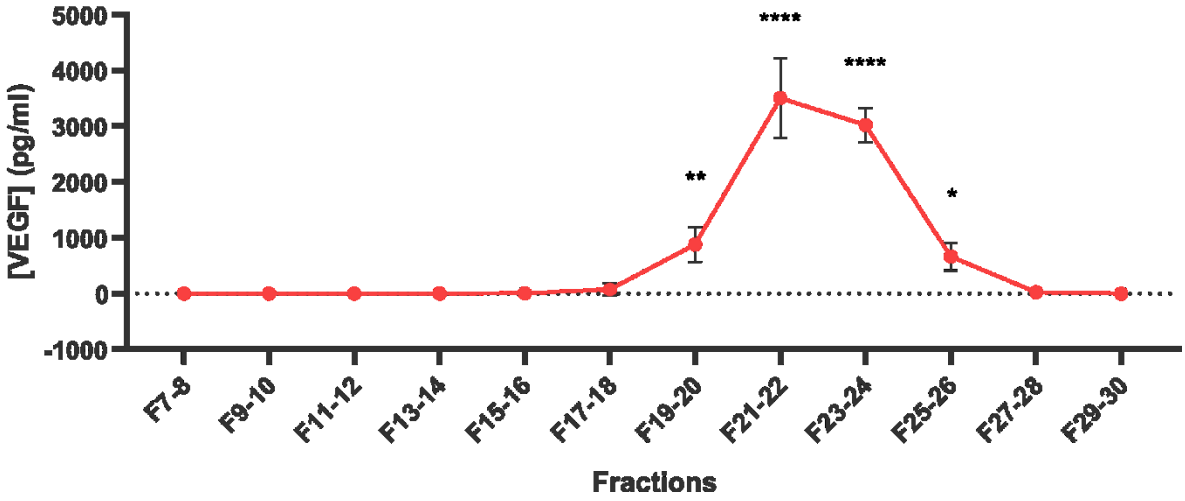


*Figure 4.16: Quantification of VEGF in analytical SEC fractions. (N = 3, n = 2, mean +/- SD shown). * : p <0.05, ** : p < 0.01, *** : p < 0.001, **** : p < 0.0001 (one-way within-subjects ANOVA and post-hoc Dunnett's test against F7-8).*

4.3.5.4. Assessing potential bias in recovery of EVs and soluble factors

A potential concern for this analysis is the possibility that different components of the conditioned medium were preferentially recovered from the column. This could potentially have biased assessment of the relative contribution of EVs and soluble factors to the overall effect. In order to assess this risk, quantifications of the percentage recovery of both VEGF and particles for both the concentration and column stages of processing were carried out. VEGF and particle concentrations were measured as before for CM and CCM. Total particle recovery was calculated as the sum of all particles detected in fractions 6-25. VEGF recovery for Donor 1 was similarly calculated as the sum of VEGF detected across fractions 15-30. VEGF fractions had not been measured for Donors 2 and 3; instead, equal volumes from each of fractions 15-30 were pooled and their combined concentration measured. Total recovery at each stage was calculated using the appropriate volumes. Data for all

three donors was combined for a total of nine replicates. A significant difference was found between the recovery of VEGF and particles from the concentrators (Figure 4.17 a). However, it was already known that concentration does not result in reduction of bioactivity in the assays to be tested, despite unequal loss of media components (Figures 4.7-4.9). Therefore, any bias must have been in favour of the bioactive components. No significant difference was found between the recovery of VEGF and particles for the column separation stage across all fractions (Figure 4.17 b). However, the concentration of the peaks eluting from the column was also relevant. Ideally, the peak concentration of both particles and VEGF should have represented a similar percentage recovery from the input sample. Only samples for Donor 1 could be compared, as VEGF was only measured in individual fractions for Donor 1. As biological assays were planned to be carried out with pooled paired fractions, the particle concentrations in fractions 9-10 were averaged to generate a peak particle concentration. VEGF was already measured as pooled pairs, and the peak values taken from fractions 23-24 (R1, R2) and 21-22 (R3). Comparing peak fractions, no significant difference was detected in recovery (Figure 4.17 c), despite an approximately 2-fold mean difference. Even assuming that the lack of detection of significant difference was due to lack of statistical power rather than a genuine equivalence between recoveries, the data suggested that at the bias between peak values did not exceed a factor of two in favour of VEGF.

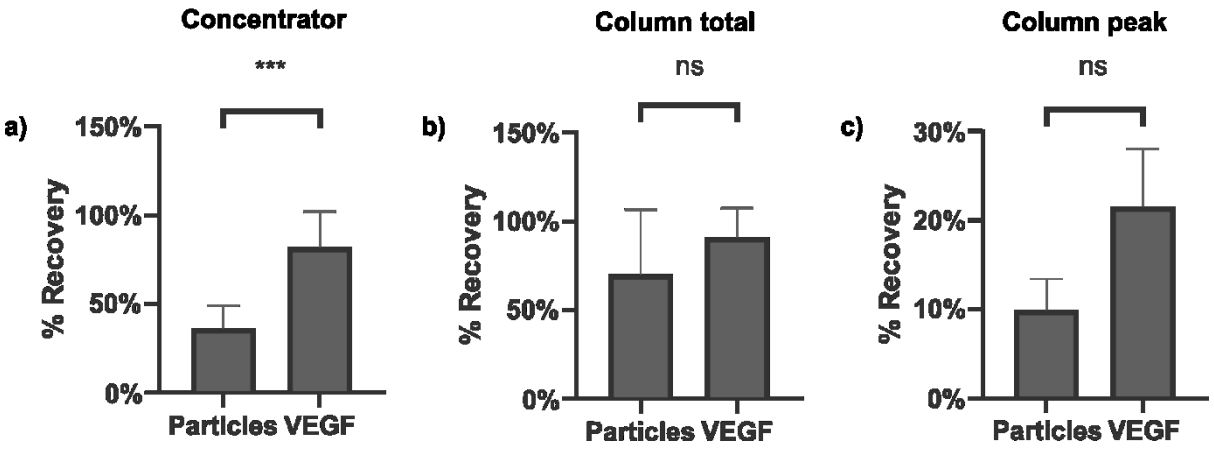


*Figure 4.17: Percentage recovery of particles and VEGF during analytical SEC for Donor 1. a) from concentration step, b) total recovery from column compared to concentrated media, c) peak concentration values compared to concentrated media. * : p <0.05, ** : p < 0.01, *** : p < 0.001, **** : p < 0.0001 (two-tailed paired t-test, N = 9 for a & b, N = 3 for c), mean +/- SD shown.*

4.3.5.5. Pro-angiogenic activity of analytical SEC fractions

Figures 4.14-4.17 describe validation and characterisation of the ability of the size exclusion columns to separate EVs and soluble factors. EVs have been shown to elute from the column predominantly in a peak at fractions 9-10, with a secondary minor peak in fractions 15-18 (Figure 4.14). The major peak was entirely separated from all detectable soluble protein, as assessed by total protein quantification and VEGF detection by ELISA (Figure 4.15, Figure 4.16). There was some overlap between the minor peak and the edge of the total protein peak, but not the elution of VEGF. Any potential bias introduced by the concentration of CM or column separation is likely to be relatively minor (Figure 4.17). Paired fractions (excluding fractions 1 and 2) were assessed for their ability to stimulate angiogenesis, as before (Figure 4.18).

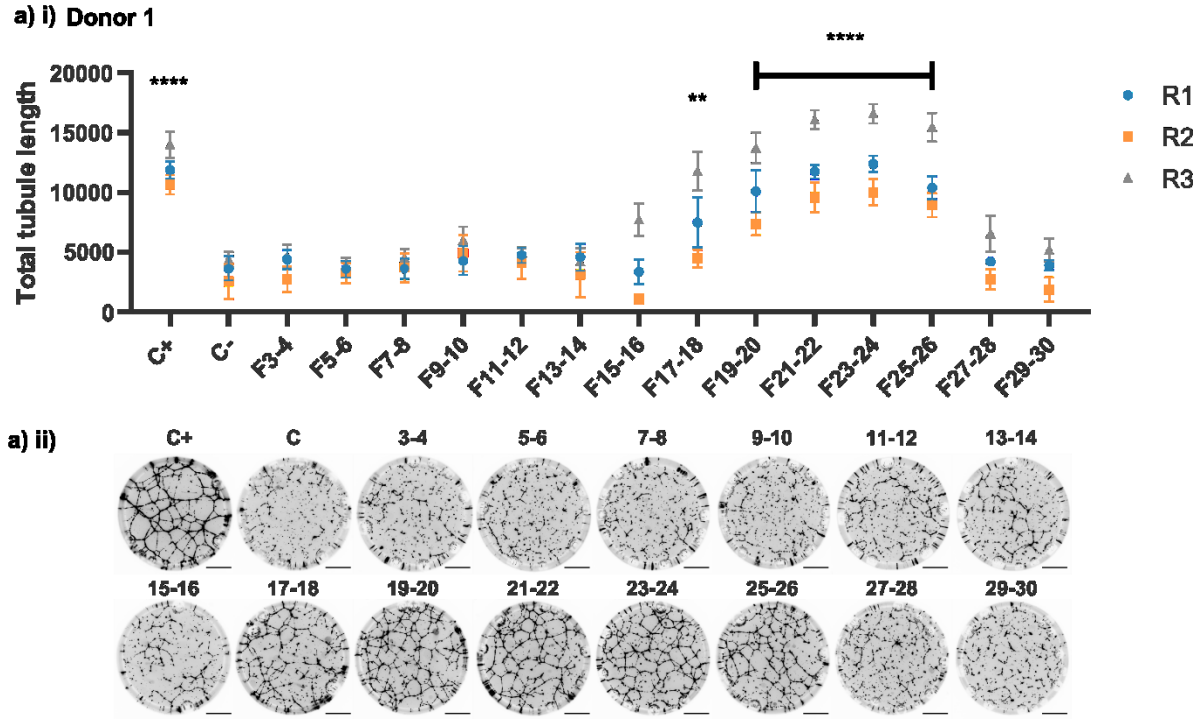


Figure 4.18: Tubule formation assay for analytical SEC fractions. Panel 1 of 2 (see next page).

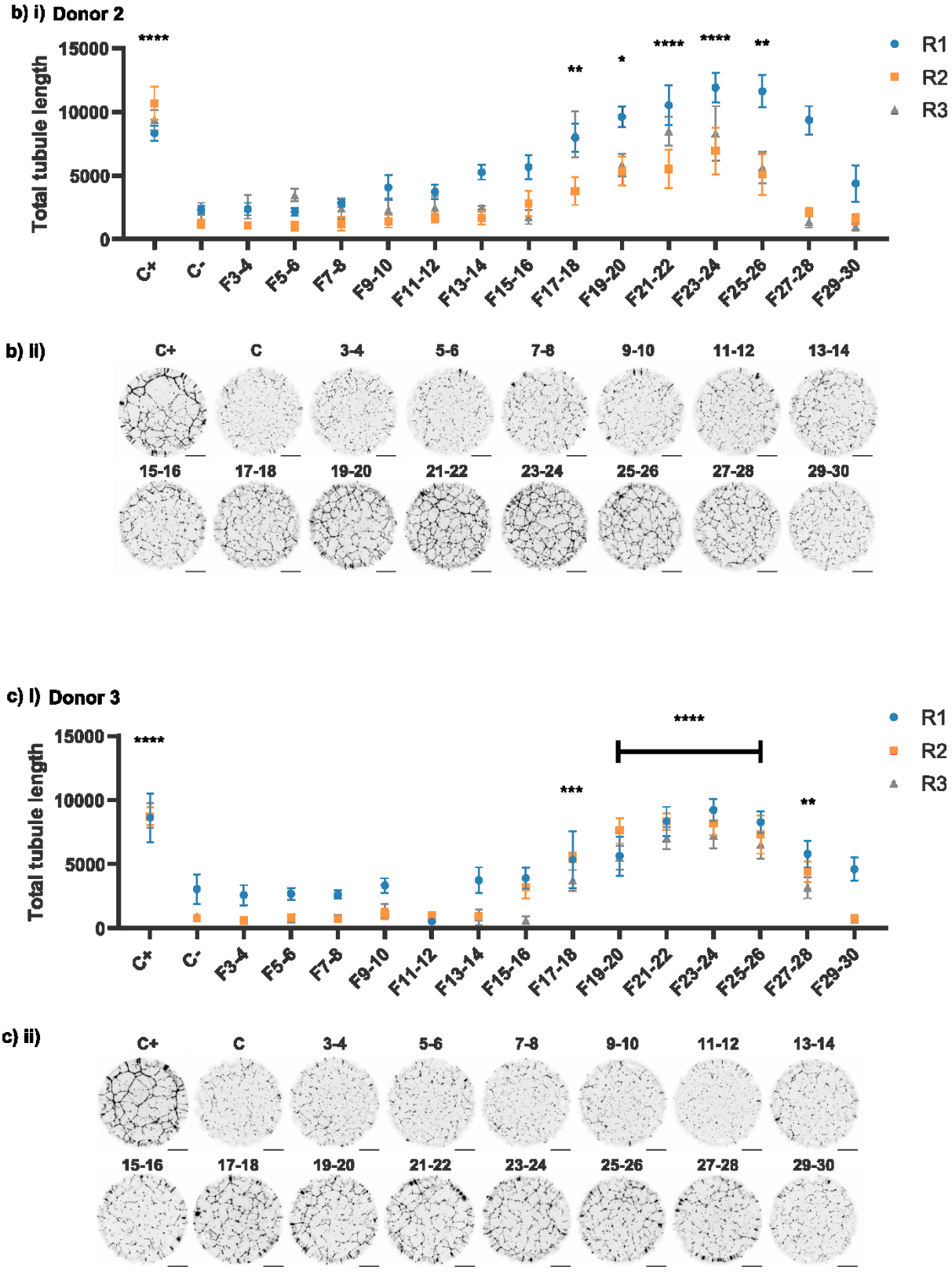


*Figure 4.18-2: Tubule formation assay for analytical SEC fractions. Panel 2 of 2. Results for Donors 1-3 (a-c) are shown. i) Quantification of total tubule length for each sample. (N = 3, n = 6, mean +/- SD shown for individual replicates). * : p <0.05, ** : p < 0.01, *** : p < 0.001, **** : p < 0.0001 (one-way within-subjects ANOVA and post-hoc Dunnett's test against C-). ii) Representative whole-well images of tubule structures formed under each condition. Images inverted for clarity. Scale bar = 1 mm.*

As before, this experiment was performed for each of the three donors, with three replicates each. For all donors, significant proangiogenic activity was detected in fractions 17-26 (Figure 4.18). This coincided with the elution of soluble protein and VEGF. No pro-angiogenic activity was detected associated with the major EV peak at fractions 9-10 in any donor. There was a minor overlap of the activity peak and that of the minor EV peak (F15-18, D1 only) – however the centre of the activity peak was found to be at fractions 23-24, where EVs were not detectable above baseline by NTA or dot blots for EV markers.

The results of this experiment supported the previous data indicating that pro-angiogenic signalling from hMSCs (as measured by *in vitro* tubule formation assays) was entirely mediated by free soluble factors, rather than EVs.

4.3.5.6. Pro-wound healing activity of analytical SEC fractions

As for the tubule formation assay, the scratch wound assay was performed for pooled pairs of adjacent fractions. In a 48-well plate, 16 conditions with three internal replicates each were possible. Again, fractions 1-2 were omitted. Three replicates of the assay were performed for each donor.

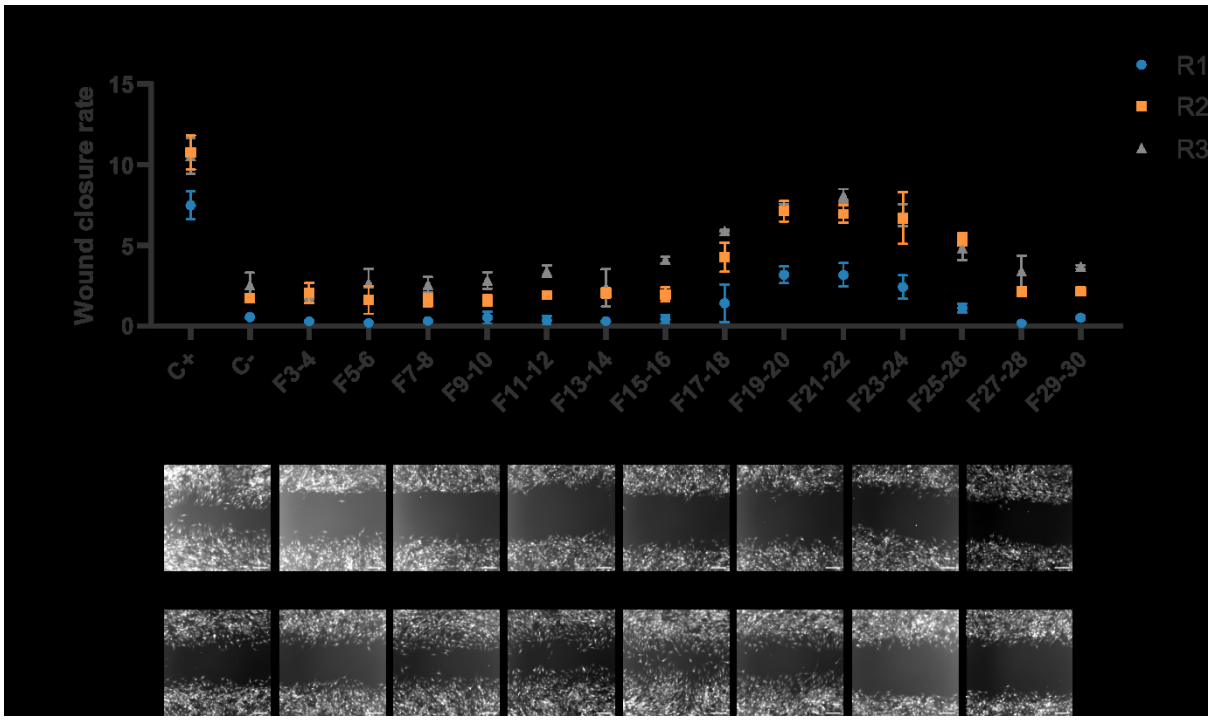


Figure 4.19: Scratch wound assay for analytical SEC fractions. Panel 1 of 2 (see next page).

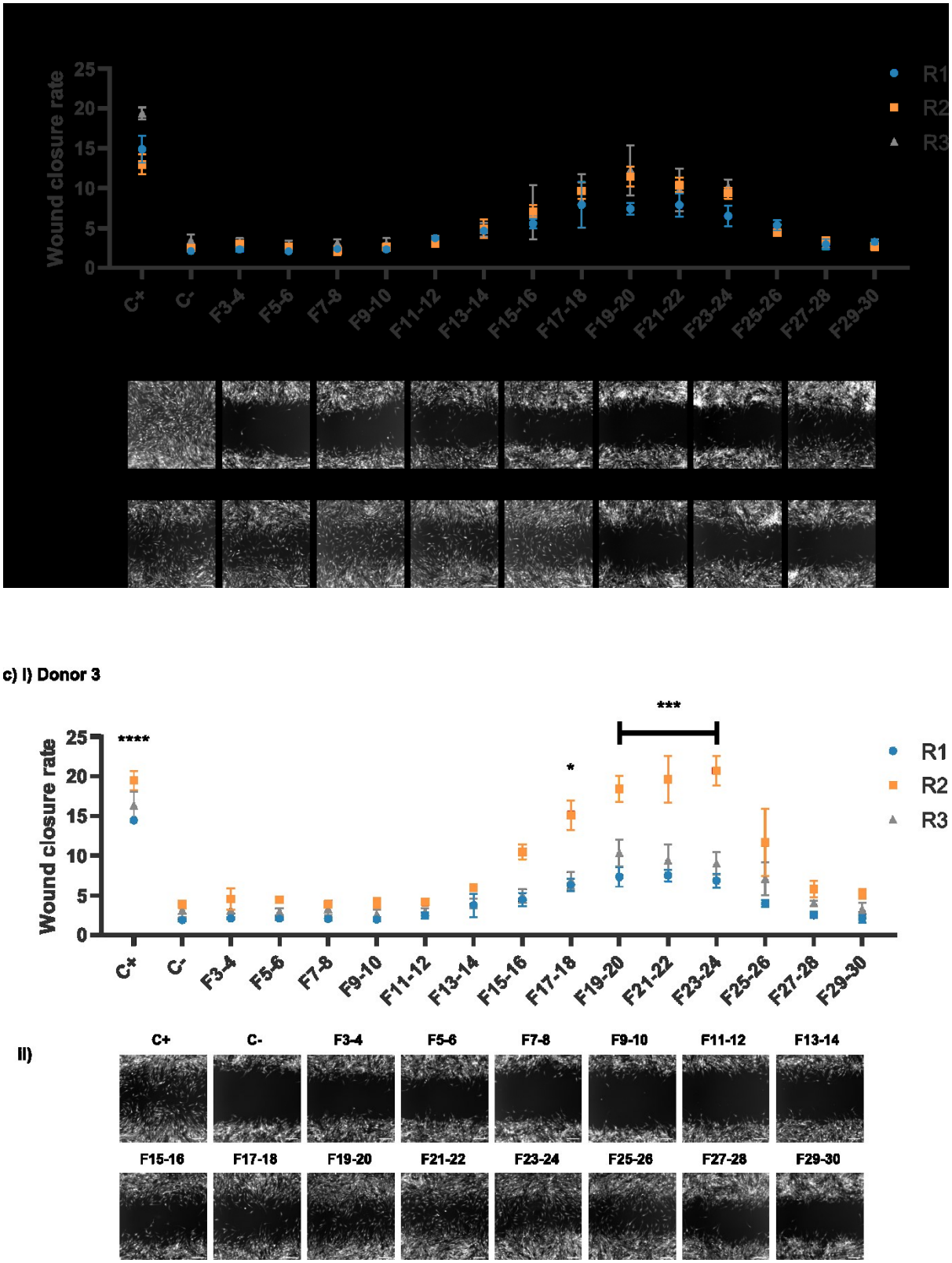


*Figure 4.19-2: Scratch wound assay for analytical SEC fractions. Panel 2 of 2. Results for donors 1-3 (a-c) are shown. i) Quantification of wound closure rate for each condition. Means of individual replicates (N = 3) and standard deviation of internal replicates (n = 3) are shown for each donor. * : p <0.05, ** : p < 0.01, *** : p < 0.001, **** : p < 0.0001 (one-way within-subjects ANOVA and post-hoc Dunnett's test against C-). ii) Representative endpoint images (t = 15 h) for each condition. Scale bar = 100 µm.*

A rate of wound closure significantly above baseline was observed with fractions 17-26 for Donor 1, 15-24 for Donor 2, and 17-24 for Donor 3 (Figure 4.19 a-c). As was the case for the angiogenesis assay, this coincided with elution of soluble protein and VEGF from the column. There was no detectable increase in the rate of wound closure associated with the major EV peak (F9-10) in any of the three donors. As with the angiogenesis assay, there was some overlap between the activity peak and the secondary minor EV peak (F15-18, Donor 1 only). However, as before, the fractions in which the peak wound closure occurs (F19-20 for Donor 2, F21-22 for Donors 1 and 3) did not appear to contain a significant population of EVs.

As was the case for the angiogenesis assay, this result confirmed previous data. EVs did not appear to significantly contribute to hMSC paracrine stimulation of wound healing, as measured by this assay. Instead, the effect appeared to be entirely mediated by free soluble factors.

4.3.6. Biological activity of hMSC-EVs; resolving the discrepancy

All analyses performed so far indicated that EVs did not contribute significantly to hMSC paracrine signalling, as measured by tubule formation and scratch wound healing assays. Yet hMSC-EVs are widely reported to be pro-angiogenic and pro-wound healing, in both these and other assays. It was considered important to identify the source of this discrepancy. Two potential factors were identified. Firstly, effectiveness of purification. Many EV isolation and purification techniques are known to co-isolate non-EV proteins. Despite the research and debate around the matter, many of these techniques remain widely used. Secondly, sample quantity. EV samples are typically quantified by protein and/or particle concentration. Studies rarely if ever relate the quantity of EVs used for stimulation to the quantity of EVs in the conditioned medium itself. It may be possible that, despite contributing little in relative terms compared to soluble factors, pure EVs in very high quantities may have some capacity for stimulation of biological processes.

4.3.7. hMSC-EVs purification by polymer precipitation

To test the hypothesis that ineffective removal of soluble factors at the purification stage could lead to misattribution of biological activity to EVs, EVs were isolated from hMSC-CM using Total Exosome Isolation Reagent (TEI). TEI and similar products such as ExoQuick isolate EVs by binding water molecules, encouraging EVs to aggregate and precipitate out of solution. EVs can then be pelleted with a relatively low-speed centrifugation (10,000 g) before resuspension. Critics of this technique have argued that factors other than EVs also aggregate and are pelleted, and that the polymers themselves are present in the final sample. Despite this, it remains in common use, including for studies using hMSC-EVs.

4.3.7.1. Isolation and characterisation of TEI-isolated hMSC-EV

As for previous analytical SEC experiments, EVs were isolated from 100 mL of hMSC-CM (Figure 18a). Media from Donor 1 was used. The media was concentrated 100 x to 1 mL, 150 µL of which was reserved for quantification and characterisation. The remaining 850 µL was mixed 2:1 with TEI reagent, vortexed, left for 16 hours at 4 °C and then centrifuged at 10,000 x g for 1 hour at 4 °C, resulting in a small off-white pellet. All supernatant was carefully aspirated, and the pellet resuspended in 100 µL of particle-free PBS.

NTA quantification of the resuspended TEI-EVs revealed a high particle concentration of 4.62 +/- 0.41 x 10^{11} particles/mL (Figure 4.20 b-i). However, the total quantity of particles recovered (4.62 +/- 0.41 x 10^{10}) was only 10.2 +/- 4.6 % of that measured in the input CM, with the majority lost at the concentration stage (b-ii), as previously observed. The low percentage recovery yet high actual concentration is accounted for by the 1000-fold decrease in volume.

Dot blots against CD63 confirmed the presence of the EV marker in all samples (Figure 4.20 c). Previous experiments loaded equal volumes onto the blot to compare relative quantity – however, this was not possible for this experiment and so instead known particle concentrations were loaded (as previously measured by NTA). CD63 intensity appeared to correlate with particle concentration (Figure 4.20 c-ii)

The concentration of VEGF in CM, CCM and TEI-EV was also measured (Figure 4.20 d). Carry-through of VEGF from CM to the final TEI-EV isolate was observed. The concentration of VEGF in the isolated EVs was 2516 +/- 669 pg/mL, approximately 12.5 times greater than that of the input conditioned media (203 +/- 100 pg/mL) (d-i). This high concentration was the result of a carry-through of a total of only 251.6 +/- 66.9 pg of VEGF, or approximately 1.4 % of the input.

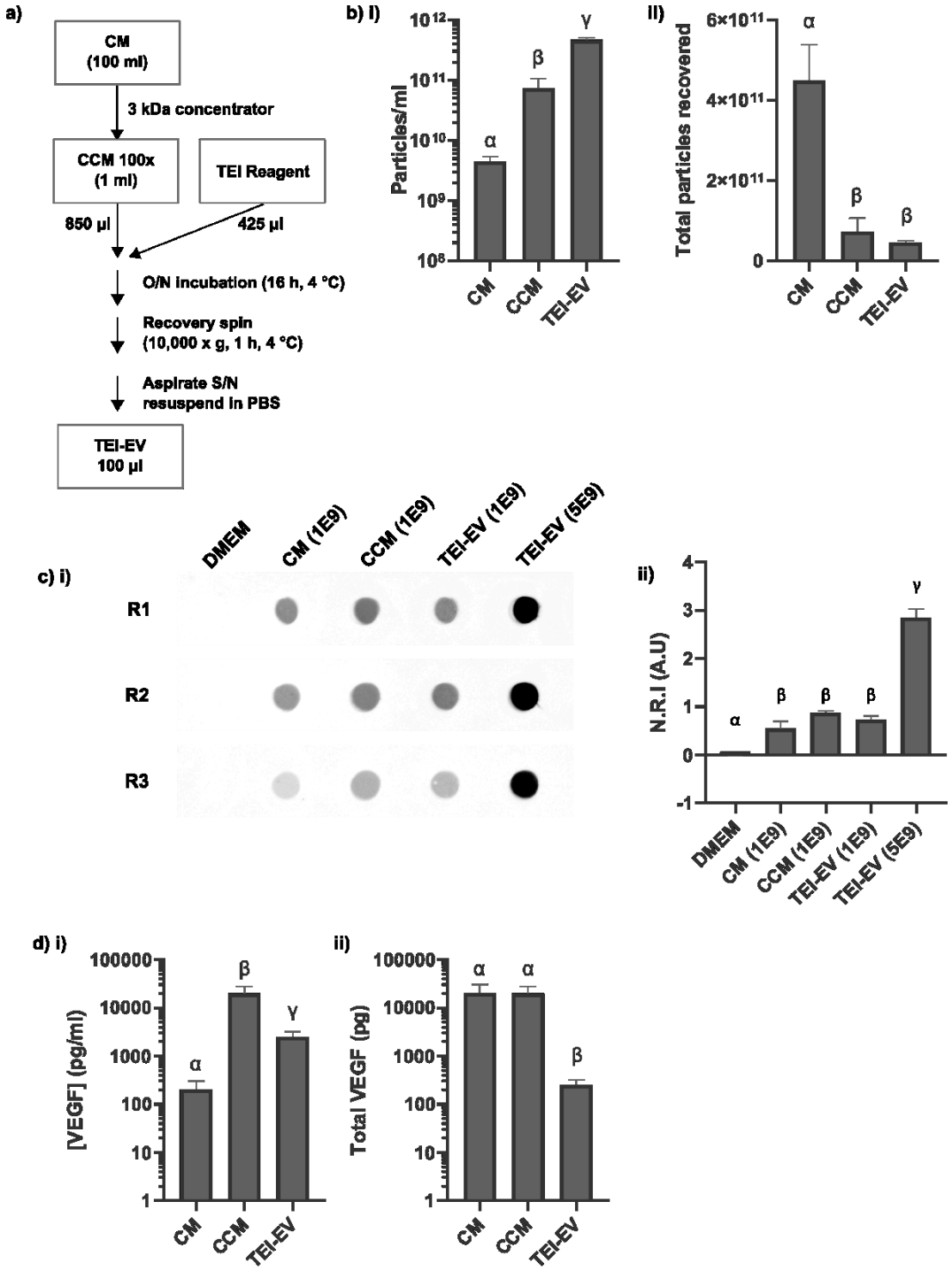


Figure 4.20: Isolation of hMSC-EVs by TEI and characterisation. a) Experimental plan. Media was concentrated as before, before isolation with TEI according to manufacturer instructions. b) NTA quantification of samples, shown as measured concentrations (i) and total particles (ii). (N = 3, n = 3, mean +/- SD shown). c)i) Dot blot against CD63 for each sample. Numbers show particle number loaded in each condition. Independently prepared replicate samples were blotted onto the same membrane and analysed simultaneously. ii) Quantification of dot blots, as described in materials and methods. N.R.I: Normalised Relative Intensity. Mean +/- SD shown (N = 3). Samples are significantly different unless they share a letter ($p < 0.05$, one-way within-subjects ANOVA and post-hoc Tukey's test). d) Quantification of VEGF in each sample by ELISA, shown as measured concentration (i) and total VEGF (ii). (N = 3, n = 2, mean +/- SD shown). Where data is plotted on a logarithmic axis, data was log_{10}-transformed before statistical analysis.

The protein concentration in the isolated TEI-EVs was found to be 589 +/- 21 µg/mL (Table 4.3). There was therefore a particle to protein ratio in the TEI-EV samples of 7.84 +/- 0.46 x 10^8 particles/µg. By the standards proposed by Webber and Clayton [108], this indicates a very low sample purity, with significant contamination from free protein. Similarly, a ratio of particles to VEGF was calculated (1.98 +/- 0.79 x 10^8 particles/pg). These ratios can be used to compare the EVs isolated by TEI with those isolated during analytical SEC. The average particle concentration in the peak fraction (F9) across donors was 1.44 +/- 0.61 x 10^{10} particles/mL (Figure 4.14). If the protein and VEGF co-isolating with the EVs isolated by TEI were genuinely EV-associated, their expected average concentrations in the peak fraction would be 18.3 µg/mL and 72.8 pg/mL respectively. Both of these concentrations are well within the ranges of sensitivity for the assays used. As neither were detected, it was concluded that they were present in TEI-isolated EV samples as contaminants, not as bona fide EV-associated factors.

Table 4.3: Particle, protein, and VEGF concentrations for TEI-EVs. Particle and VEGF concentrations previously shown in figure 18. Individual replicates and averages are shown. Ratios of particles:protein and particles:VEGF are calculated.

Sample	Particles/ml	[Protein] (µg/ml)	[VEGF] (pg/ml)	Particles/µg protein	Particles/pg VEGF
R1	4.22E+11	576.57	2954.81	7.32E+08	1.43E+08
R2	4.61E+11	577.64	2848.64	7.98E+08	1.62E+08
R3	5.04E+11	613.43	1746.51	8.22E+08	2.89E+08
Average	4.62E+11	589.21	2516.65	7.84E+08	1.98E+08
Std. Dev	4.10E+10	20.98	669.07	4.65E+07	7.92E+07

4.3.7.2. Stimulation of angiogenesis by TEI-EVs

The ability of TEI-isolated EVs to stimulate angiogenesis was investigated with a tubule formation assay as before (Figure 4.21). A dilution series of TEI-EVs was prepared, with particle concentrations of 4 x 10^{10}, 1 x 10^{10}, 4 x 10^9 and 1 x 10^9 particles/mL. In-assay dilution halved these concentrations, such that the in-well concentrations experienced by the cells were 2 x 10^{10}, 5 x 10^9, 2 x 10^9 and 5 x 10^8 particles/mL respectively.

TEI-isolated EVs stimulated angiogenesis at all but the lowest concentration used in the assay (Figure 4.21 a). A dose-dependent effect was observed, with the mean total tubule length decreasing with decreasing sample concentration.

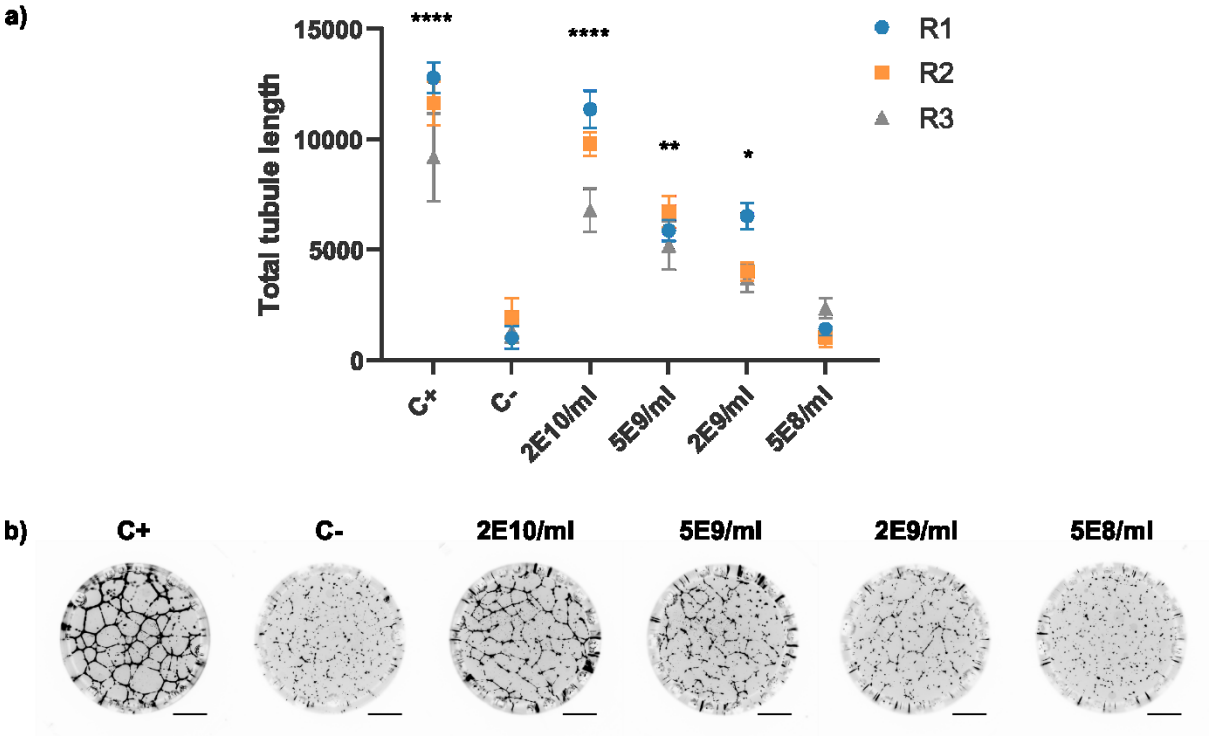


*Figure 4.21: Tubule formation assay for TEI-isolated EVs. a) Quantification of total tubule length for each sample. Means of individual replicates (N = 3) are shown, with std. dev of internal technical replicates (n = 6). * : p <0.05, ** : p < 0.01, *** : p < 0.001, **** : p < 0.0001 (one-way within-subjects ANOVA and post-hoc Dunnett's test against C-). b) Representative whole-well images of tubule structures formed under each condition. Images inverted for clarity. Scale bar = 1 mm.*

The peak concentrations of EVs eluted during analytical SEC ranged between 4.66 x 10^9 and 2.21 x 10^{10} particles/mL, with a mean concentration of 1.44 x 10^{10} particles/mL (Figure 4.14). In-assay concentrations would have been half these values. This would fall within the range of concentrations of TEI-isolated EVs found in this assay to stimulate angiogenesis. If the proangiogenic signalling in Figure 19 was due to EVs, it should have been possible to detect this activity in the earlier analytical SEC experiments. This indicated that the pro-angiogenic effect observed in this assay was likely due to the presence of non-EV contaminants, as also indicated by quantification of particles, protein and VEGF concentrations in Table 4.3.

4.3.7.3. Stimulation of wound healing by TEI-EVs

As for stimulation of angiogenesis, TEI-isolated EVs were diluted to 4 x 10^{10}, 1 x 10^{10}, 4 x 10^{9} and 1 x 10^{9} particles/mL, for in-assay concentrations of 2 x 10^{10}, 5 x 10^{9}, 2 x 10^{9} and 5 x 10^{8} particles/mL respectively. Scratch-wound assays were performed as before. The highest two concentrations were found to stimulate cell migration (Figure 4.22). As for stimulation of angiogenesis, a dose-dependence was observed, with higher concentrations stimulating more rapid gap closure.

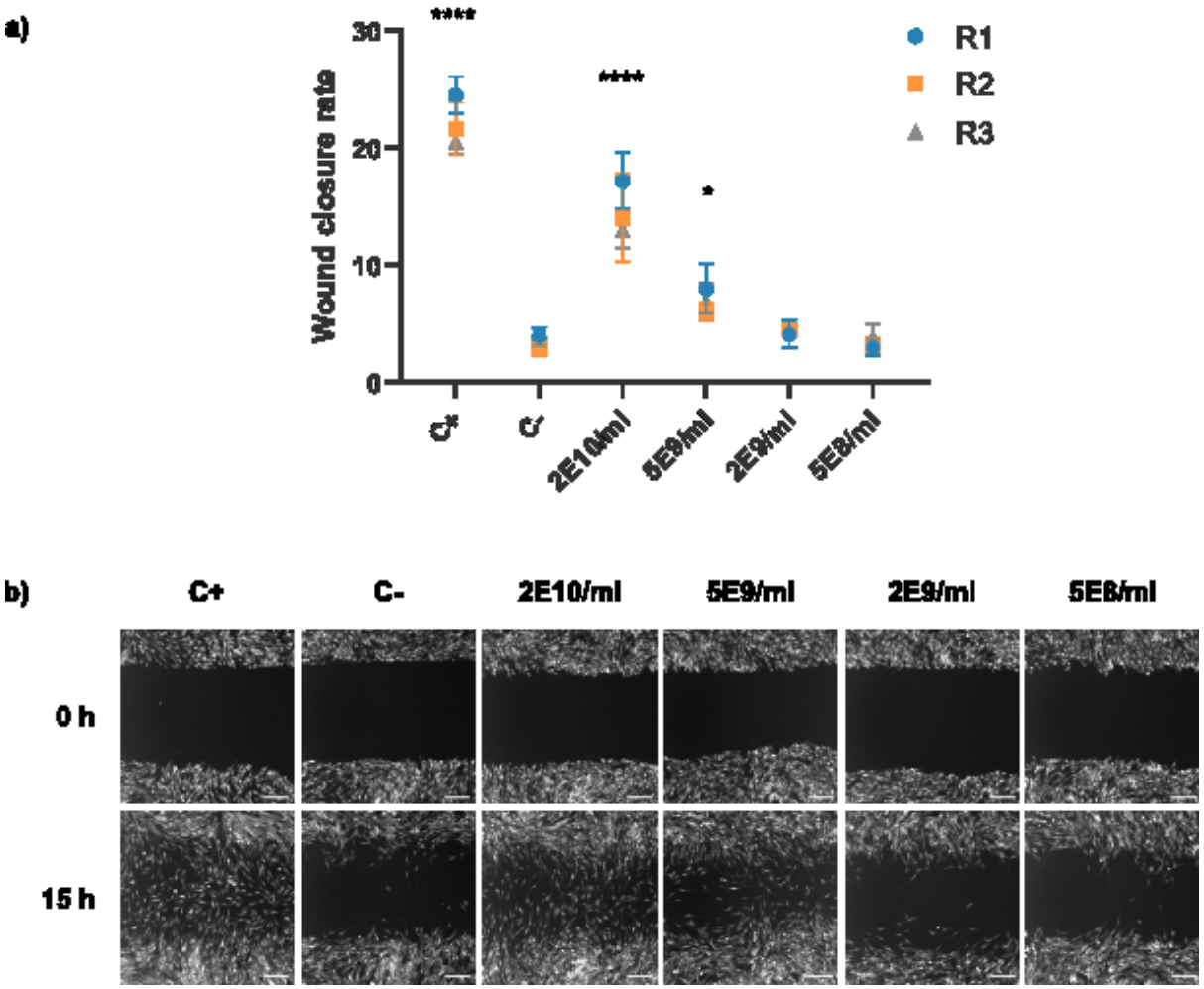


*Figure 4.22: Scratch wound assay for TEI-isolated EVs. a) Quantification of wound closure rate for each condition. Means of individual replicates (N = 3) and standard deviation of internal replicates (n = 3) are shown. * : p <0.05, ** : p < 0.01, *** : p < 0.001, **** : p < 0.0001 (one-way within-subjects ANOVA and post-hoc Dunnett's test against C-). b) Representative images for the assay start and endpoint (t = 15 h) for each condition. Scale bar = 100 µm.*

As previously stated, the peak particle concentrations from analytical SEC ranged between 4.66 x 10^9 and 2.21 x 10^{10} particles/mL, with a mean concentration of 1.44 x 10^{10} particles/mL (Figure 4.14). After in-assay dilution, 6 of 9 replicates across all 3 donors would have had a peak concentration above the lower stimulation threshold of 5 x 10^9 particles/mL found in this assay, with the remaining three at 4.87, 4.72 and 2.33 x 10^9 particles/mL. Therefore, if the pro-wound healing stimulation from TEI-isolated EVs observed in this assay was genuinely due to EVs, this activity should have been detected in the majority of analytical SEC replicates. As was found for angiogenesis, this indicated that the effect seen in this assay is due to non-EV contaminants.

4.3.8. Stimulation of angiogenesis with high quantities of pure hMSC-EV

Contamination with non-EV factors during EV isolation appeared to be a potential explanation for the some of the discrepancy between the results presented here and those in the wider literature. However, another potential explanation might be the use of very high quantities of EVs relative to the quantities in the original conditioned medium.

Here, EVs were purified from hMSC-CM using ultrafiltration and SEC as before; however, the initial starting volume of hMSC-CM was significantly greater. For each replicate, 1.25 L of conditioned medium was concentrated using twelve 100 kDa centrifugal concentrators to a final volume of 1.5 mL. The CCM was loaded in three batches of 500 µl onto the column, collecting three sets of thirty 1 mL fractions. The CCM was split in this way as when concentrated further it became overly viscous, which compromised separation on the column. Previously performed characterisations of fractions were not carried out in order to conserve as much sample as possible for the downstream experiment. Fractions 8-14 from all three batches were pooled and then concentrated to a final volume of approximately 300 µl.

The particle and protein concentrations of this final concentrate were measured (Table 4.4). A fair quantity of EVs appeared to have been lost during the purification process, likely due to the additional concentration step after elution from the column. The particle to protein ratio was approximately an order of magnitude higher than that of TEI-isolated EVs and indicated good purity. Sample quantity was limited. In order to allow use of high EV concentrations, only the stimulation of tubule formation was investigated, which was chosen as previous experiments had indicated it to be the more sensitive of the two assays.

Table 4.4: Particle and protein concentrations for high-quantity hMSC-EV isolation by SEC.

	Particles/mL	Protein (µg/mL)	Particles/µg protein
R1	2.33E+11	41.74	5.59E+09
R2	1.99E+11	39.64	5.02E+09
R3	2.59E+11	50.99	5.08E+09
Av	2.30E+11	44.12	5.23E+09
SD	3.01E+10	6.04	3.14E+08

These pure SEC-EV isolates were diluted to in-assay concentrations of 1 x 10^{11}, 2 x 10^{10} and 4 x 10^{9} particles/mL. A very small but statistically significant increase in tubule formation relative to the negative control was observed for the highest two concentrations (Figure 4.23 a).

It was noted across other experiments that when the sample buffer used was PBS, rather than DMEM, the overall tubule length formed in the controls of the angiogenesis assay was lower. The experiment was repeated, with the alteration of transferring the final EV concentrate to DMEM during the final concentration stage. This was intended to encourage an overall higher level of angiogenesis and potentially magnify the small effect. It also allowed direct comparison of pure EVs in DMEM to concentrated conditioned media. CCM was prepared from 100 mL hMSC-CM against a 3 kDa membrane as before and diluted to matching particle concentrations.

It was found that all particle concentrations of CCM measured significantly stimulated angiogenesis (Figure 4.23 b). By contrast, no stimulatory effect was found for any EV concentration, including those found to be significant in Figure 4.23 a. This may have been due to increased variability between experiments overshadowing the effect, which was small in magnitude.

This experiment again demonstrated that soluble factors appeared to be more important in hMSC paracrine stimulation of *in vitro* angiogenesis than EVs. EVs alone at high concentrations were found to have some pro-stimulatory activity in one assay. However, this effect was very small. Higher quantities of EVs that might be more readily achievable with lower-stringency isolation techniques or different hMSC culture systems might have increased the size of this effect.

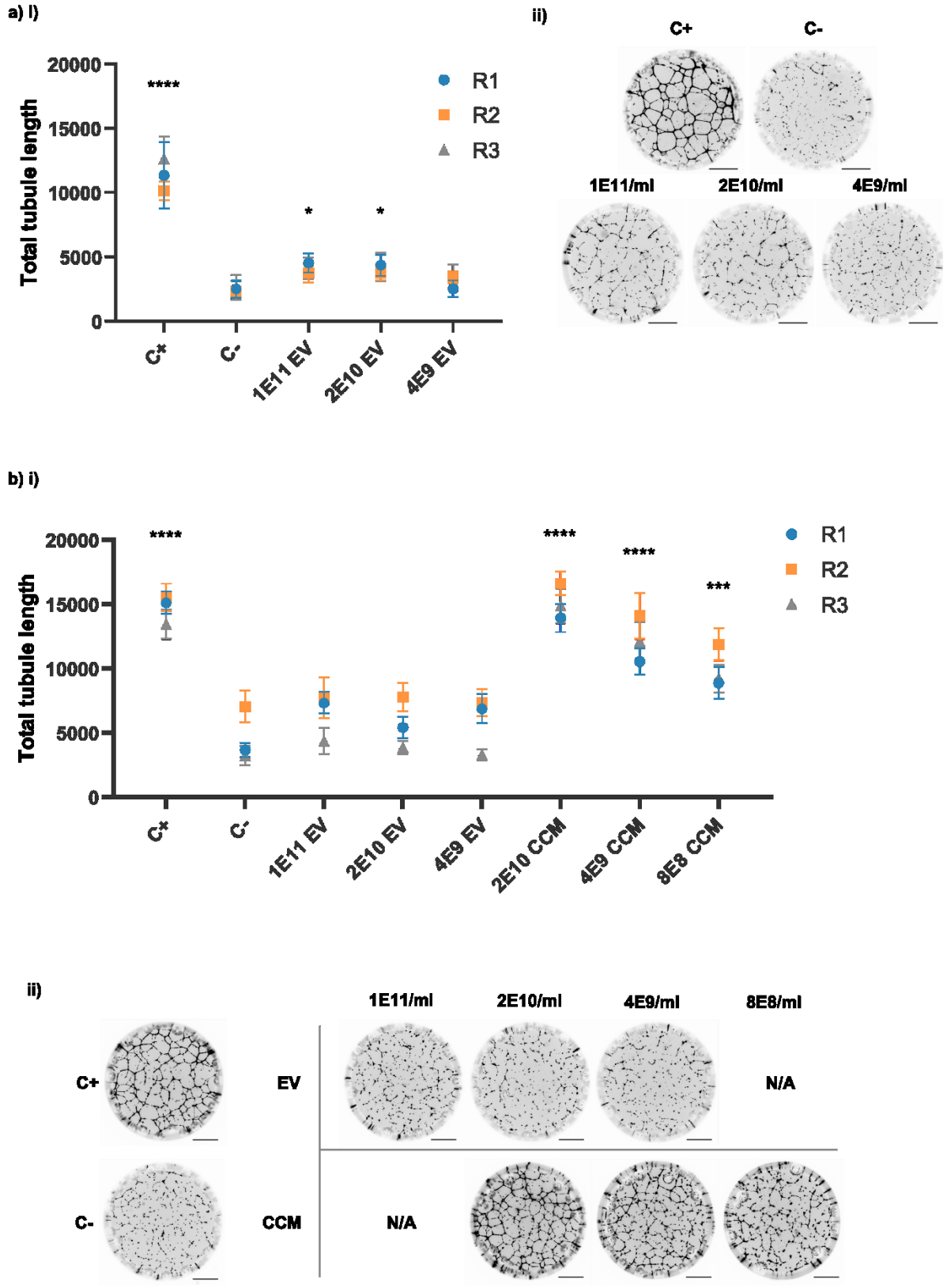


*Figure 4.23: Tubule formation assay with high-purity SEC-isolated EVs. a) Assay with EVs in PBS. I) quantification of total tubule length. (N = 3, n = 8-10, mean +/- SD of individual replicates shown). Ii) Representative images. b) Assay with EVs in DMEM and CCM. I) quantification of total tubule length. (N = 3, n = 10, mean +/- SD of individual replicates shown). Ii) Representative images. * : p <0.05, ** : p < 0.01, *** : p < 0.001, **** : p < 0.0001 (one-way within-subjects ANOVA and post-hoc Dunnett's test against C-). Scale bar = 1 mm.*

4.3.9. EV-Mediated Effect Ratio (EVMER)

It was apparent from these results that the contribution of hMSC-EVs to *in vitro* angiogenesis and wound healing was minimal. A generic metric is proposed to quantify the potency of EVs relative to the conditioned medium from which they were isolated. This metric may be used for studies in which conditioned medium and purified EVs are both used to stimulate a quantifiable biological assay. Where "K" is the effect size caused by conditioned medium;

$$EVMER = \frac{Particle\ concentration\ of\ conditioned\ medium\ required\ for\ effect\ size\ K}{Particle\ concentration\ of\ purified\ EVs\ required\ for\ effect\ size\ K}$$

The identity of K is assay-specific. It may be preferable to define K relative to control values. EVMER may be expressed as a range between two values bounding K, or as an inequality. The closer the ratio is to 1, the greater the contribution of EVs. In the case of hMSC-CM-mediated stimulation of angiogenesis, from Figure 4.3 and Figure 4.4, angiogenesis was stimulated to approximately halfway between the positive and negative control values, and the mean in-assay particle concentration was 1.45 x 10^9 particles/ml (measured concentration of 2.9 x 10^9 particles/ml, diluted two-fold in-assay). K was taken to be a total tubule length halfway between the positive and negative controls. From Figure 4.23, even the highest concentration of 1 x 10^{11} particles/ml did not reach K. Therefore;

$$EVMER_{SEC-EV} < \frac{1.45 \times 10^9}{1 \times 10^{11}}$$

$$EVMER_{SEC-EV} < 0.0145$$

In other words, SEC-purified EVs were less than 1.45 % as potent as hMSC-CM. By contrast, TEI-purified EVs did reach K, between the in-assay concentrations of 2 x 10^{10} and 5 x 10^9 particles/ml (Figure 4.21). Therefore;

$$\frac{1.45 \times 10^9}{2 \times 10^{10}} < EVMER_{TEI-EV} < \frac{1.45 \times 10^9}{5 \times 10^9}$$

$$0.0725 < EVMER_{TEI-EV} < 0.29$$

TEI-EVs were found to be between 7.25 – 29 % as potent as hMSC-CM. This was, however, likely due to contamination of TEI-EVs with other factors, rather than reflecting genuine potency. This metric has caveats and limitations which will be discussed more thoroughly in section 4.4. Nevertheless, it may provide a useful conceptual benchmark currently unavailable to the field.

4.4. Discussion: hMSC-EVs and their role in paracrine signalling

It was found that the presence or absence of EVs in hMSC-conditioned medium did not appear to affect its activity in *in vitro* of angiogenesis and wound healing assays, and that EVs were only able to stimulate these assays when either poorly purified or used in comparatively high quantities. This is in contrast to other reports in the wider literature, which broadly indicate that hMSC-EVs can act as agents of regeneration (see section 4.1). This discrepancy is attributed to experimental and conceptual differences between this study and others, which will be discussed in this section.

4.4.1. Conceptual framework for hMSC paracrine signalling investigation

Prior to discussion of the apparent role of hMSC-EVs in paracrine signalling, it is helpful to reintroduce two fundamental logical concepts often used in molecular biology; *necessity* and *sufficiency*. Expressed generally:

- A is necessary for B if B cannot occur without A; however, B still may not occur even with A.
- A is sufficient for B if A can cause B; however, B may also be caused by factors other than A.

The concepts of necessity and sufficiency are contextual; to take the example of apoptosis, the binding of Fas ligand to Fas receptor is sufficient to initiate apoptosis via "extrinsic" pathways [259]. However, apoptosis can also be initiated by other "intrinsic" pathways such as p53-mediated activation of Bax. Here, Fas ligand binding is sufficient but not necessary for activation of apoptosis. In contrast, the presence of caspase proteins is necessary but not sufficient; apoptosis could not occur without them, but the presence of pro-apoptotic signalling is required to activate them.

4.4.2. Assessing necessity: conditioned medium without EVs.

A logical first step to implicating the involvement of EVs in a process is to exclude them from the medium or fluid in which they are present, and to then investigate whether there is an effect on the process being studied – i.e. to confirm necessity. This was the approach taken by Timmers [238] and later Lai [239] et al in pioneering studies implicating the involvement of EVs in hMSC paracrine signalling. Both observed that passing hMSC-CM through a filter intended to exclude EVs essentially removed its ability to reduce infarct size after reperfusion in porcine and mouse models of myocardial infarction. The filters are described as ultrafiltration membranes manufactured by Sartorius, although the product names and materials of the membranes were not reported, making it difficult to confirm the similarity of the ultrafiltration membranes used between their studies and the study reported here. It was found in this study that similar ultrafiltration membranes led to off-target depletion of non-EV factors, which appeared to be responsible for the loss of activity in the assays used. The concentration of VEGF was used throughout this work as an indicator for the presence of low-

abundance soluble factors in general, and VEGF is not asserted to be wholly responsible for stimulation. Based on reported data, the possibility that a similar off-target depletion may have been responsible for the loss of activity seen in previous studies cannot be excluded. However, it was observed that this depletion was volume dependent, and it was considered likely to also depend on the initial concentration of the medium and the surface area and material of the ultrafiltration membranes. It is therefore not entirely clear to what extent these artefactual effects may have influenced previously published work. Based on the data presented here, there is concluded to be a potential risk in utilising this approach to implicate the contribution of EVs.

It was subsequently found that pre-treating filter membranes with BSA to minimise off-target depletion also prevented the previously observed loss of activity. EVs were not present in the flowthrough, but its proangiogenic activity was equivalent to that of the initial conditioned medium sample. Similarly, equilibrium dialysis showed equilibration of activity in association with equilibration of VEGF but not EVs. To the best of the author's knowledge, these experimental approaches have not previously been used in the context of EVs. These modified experimental approaches, in which off-target depletion is avoided, demonstrated that EVs were not necessary for signalling in the *in vitro* assays used. However, this did not exclude the possibility that EVs by themselves were able to stimulate angiogenesis and wound healing – just that they were not required.

After the pioneering studies by Timmers [238] and Lai [239], there are few reports of similar media-depletion experiments in the context of hMSC-EVs. Rather, most researchers have chosen to purify the EVs directly and then assess their properties, rather than explicitly re-confirm the requirement for EVs in signalling. This approach confirms *sufficiency* without confirming *necessity*. Purified hMSC-EVs have since been investigated for a wide range of therapeutic applications, with some degree of therapeutic benefit reported for many injury types (see sections 4.1.10-4.1.12). Given this evidence, it was considered possible that the EV signalling pathway was simply one arm of a larger paracrine signalling system with redundancy between the different pathways. However, further evidence gathered during this study did not support this conclusion in relation to stimulation of the assays used.

Prior to analysis of the relative contribution of EVs and proteins by analytical SEC, it was considered important to confirm that media concentration prior to SEC did not lead to loss of activity. Had loss of activity been detected, it would have indicated that concentration was destroying the factors responsible for signalling. This would have presented a problem for subsequent comparison of EVs and soluble factors if their losses were not found to be equivalent. Concentration of conditioned medium and subsequent dilution by the same factor did not lead to any loss of signalling activity, indicating that the factors responsible for signalling were not depleted by concentration. Therefore,

the observed loss of EVs but not VEGF was interpreted as a further indication that EVs were not necessary in these assays, and that any bias introduced at this stage could only be in favour of the as yet unidentified necessary signalling factors.

4.4.3. Assessing sufficiency: direct comparison of separated EVs and protein

Prior experiments had indicated that EVs were not necessary for hMSC-mediated stimulation of the assays used. However, it still remained possible that isolated EVs might be sufficient to stimulate angiogenesis and wound healing. Analytical SEC using the techniques developed in section 2.3 allowed separation of EVs and free protein from hMSC-CM. Two additional donors were included in this most detailed analysis, in order to exclude the possibility of donor-specific effects. *In vitro* assays, molecular analysis and nanoparticle quantification techniques had been optimised for sensitivity and low volumes, and so it was possible to perform several analyses simultaneously on each fraction or pair of fractions. EVs and free protein were confirmed to be separated by SEC, with EVs eluting predominantly in F9-10 and free protein (including VEGF) between F17-25. Unexpectedly, a minor EV peak was detected between F15-18. However, it did not substantially overlap with the elution of free protein. It is not clear why this population of EVs eluted later, or how it might differ from those eluting in the major peak, if at all. Much as it had been important to investigate the potential bias introduced by concentrating medium, so the potential bias of the column itself was investigated. The percentage recoveries of VEGF and EVs (as measured by NTA) from the input concentrated hMSC-CM were not significantly different for the column as a whole or the peak fractions. Even if the lack of significant difference was due to lack of statistical power rather than a genuine equivalence between samples, the mean difference at the point of the column was no more than two-fold in favour of VEGF.

The results of analytical SEC were consistent between all three donors. Stimulatory activity in both biological assays was associated exclusively with free protein and not with EVs. The activity appeared dependent on the dose of free protein/VEGF. Therefore, when comparing the stimulatory efficacy of EVs and soluble protein at concentrations that were approximately proportionate relative to their original concentrations in the stimulatory hMSC-CM, free protein appeared sufficient for stimulation of wound healing and angiogenesis, whereas EVs were neither necessary nor sufficient. This result begs the question; why do hMSC-EVs appear to be sufficient for stimulation of wound healing and angiogenesis in other reports from the wider literature but not in this study?

4.4.4. Resolving the discrepancy

One possible explanation for the discrepancy was considered to be the influence of ineffective purification techniques. As discussed in section 2.1, many EV isolation strategies are well-known to co-isolate non-EV material. Despite this, they remain in widespread use, including in studies involving hMSC-EVs. Given the apparently strong contribution of free protein to stimulation of these assays, it was considered possible that use of such a technique might lead to co-isolation of other stimulatory factors, leading to overestimation of the apparent activity of the isolated EVs. By contrast, the UF/SEC method used in this study was shown to effectively separate EVs from free protein, which would avoid misattribution of stimulatory activity from free protein to EV-mediated signalling.

The other potential explanation identified was the possibility that hMSC-EVs are sufficient to stimulate angiogenesis and wound healing, but only when used in much higher quantities than were used in this work. Within the wider literature, studies on extracellular vesicles rarely relate the quantity of EVs used to engender a biological effect back to the quantity of EVs actually released by the cells themselves, or to the quantities of other factors released by the cell. EVs are typically purified in bulk, by themselves, without assessment of their wider signalling context. This risks inadvertently using a quantity of EVs that is disproportionately high, inflating the apparent role of EVs in the process being studied.

Two further experiments were performed to test these hypotheses. To investigate whether a low-purity isolation procedure could influence biological activity, EVs were purified from hMSC-CM using Total Exosome Isolation Reagent (TEI), a commercial product which isolates EVs by polymeric precipitation. Existing work has demonstrated polymeric precipitation to be prone to co-isolating contaminants [117], yet it remains in relatively common use. It was found that EVs isolated using TEI were able to stimulate angiogenesis and wound healing in the *in vitro* assays used. The concentrations at which TEI-isolated EVs were stimulatory were comparable to those at which EVs were present in the peak fractions in the previous analytical SEC experiments. Unlike EVs analysed during analytical SEC, TEI-isolated EV samples also contained a considerable amount of VEGF and protein. If the detected VEGF and protein were genuinely EV-associated, they should also have been detected during analytical SEC. The per-EV concentrations of protein and VEGF when isolated by TEI would have been within the sensitivity of the assays, based on the measured particle concentrations eluting in the EV peak during SEC. Additionally, the protein to particle ratio indicated an impure sample. This indicated that VEGF and other proteins were present as contaminants. Given the previously established role of soluble factors, it appears that they were responsible for the activity of TEI-isolated EVs in the assays tested. It therefore appears that under some circumstances, less effective EV isolation methods can lead to misleading positive results.

The final experiments performed aimed to investigate the stimulatory potential of high quantities of hMSC-EVs. It was found that high concentrations (2-10 x 10^{10} particles/ml) of SEC-purified EVs caused a small but statistically significant increase in tubule length in the angiogenesis assay used. This experiment was repeated with the modification of transferring purified EVs from PBS to DMEM, in order to allow direct comparison with particle concentration-matched hMSC-CM samples and encourage an overall higher level of tubule formation. It was assumed that the proportion of particles that were EVs was the same in both pure EVs and conditioned medium samples. However, stimulation by SEC-purified hMSC-EVs was not observed in this second assay. There was more variation between replicates, which may have obscured the relatively small effect. In contrast to the weak stimulation from high concentrations of SEC-purified EVs, the same number of EVs in the context of the conditioned medium background were strongly pro-angiogenic even at the lowest concentration tested, further confirming the proportionately greater contribution of soluble factors to signalling. It is entirely possible that use of higher concentrations of pure EVs would have led to a stronger proangiogenic effect; however, the concentrations used were towards the limit of what was found to be logistically practical with standard 2D hMSC culture and the purification system used. A less stringent purification strategy would likely have isolated more particles at a lower purity; however, it was considered critically important to maximise the purity of the EV isolate.

4.4.5. Considering quantity

It was found that SEC-purified hMSC-EVs were only weakly stimulatory, and only when used in relatively high quantities. It is worth considering how the quantities used here compare to those reported in the literature, and how these quantities relate to the quantities produced by the cells themselves. As mentioned, EV doses are typically reported as µg of protein. In applications of hMSC-EVs to treatment of models of disease, doses of 1-100 µg are typically used [251], and concentrations of 1-100 µg/ml are reported for *in vitro* assays of wound healing and angiogenesis [253, 260, 261]. Where less stringent purification techniques were used, the reported protein concentration is likely to also reflect the present of contaminants. Some studies have used lower doses – notably the seminal 2010 study by Lai et al [239], which observed an *in vivo* cardioprotective effect of exosomes with 0.4 µg of EV protein. In the study described in this thesis, doses were quantified by particle number. The protein concentration was also measured. For SEC-isolated EVs, the lowest in-assay particle concentration with a measurable effect (2 x 10^{10} particles/ml) would have had an average protein concentration of 3.82 µg/ml (Table 4.4), and for the lowest active concentration of TEI-isolated EVs (2 x 10^{9} particles/ml) the average protein concentration would have been 2.55 µg/ml (Table 4.3). Compared to the literature, these are low quantities. However, if considered in relation to the quantity of conditioned medium required for similar stimulation, they are in fact quite high.

In this study, a near-confluent T225 flask of hMSCs was used to condition 35 ml of medium over a period of 40 hours. Without any further concentration, this medium was capable of stimulating *in vitro* angiogenesis, with a single well requiring only 25 µL. From Figure 4.3, conditioned medium contained 2.9 x 10^9 particles/ml, or 7.25 x 10^7 particles per well in the *in vitro* angiogenesis assay. If the particle to protein ratio measured here for SEC-purified hMSC-EVs was accurate (Table 4.4), the quantity of EV protein in each well would have been just 13.9 ng (277 ng/ml). This is far below the quantities used in the majority of reports, and the quantities of purified EV protein required in this study to stimulate angiogenesis or wound healing. It therefore appears that purified EVs are markedly less potent than the conditioned medium from which they are isolated. In the context of other experiments in this study, this was interpreted to further suggest that EVs do not significantly contribute to hMSC paracrine stimulation of *in vitro* assays when in their full signalling context.

4.4.6. Quantifying relative EV potency with EVMER

As discussed, the majority of studies do not consider the overall signalling context within which EVs are typically present. It appears that the concentrations of EV protein necessary to stimulate a cell response is far higher than their concentration in conditioned medium, and in this context, EVs appear to be less potent than conditioned medium itself. In order to aid more routine consideration of the overall context of EV-mediated signalling within the field, a simple metric is proposed.

Considering a generic experiment in which conditioned medium is used to stimulate a quantifiable biological assay, if the conditioned medium itself causes a biological effect with a quantifiable effect size, one can ask: how many EVs are required to cause the same effect size, and how does that quantity of EVs compare to the quantity present in the conditioned medium? It was suggested in this work that this difference could be expressed generically as a ratio. For an effect size K, the EV-Mediated Effect Ratio (EVMER) can be calculated;

$$EVMER = \frac{Particle\ concentration\ of\ conditioned\ medium\ required\ for\ effect\ size\ K}{Particle\ concentration\ of\ purified\ EVs\ required\ for\ effect\ size\ K}$$

The EVMER for a biological effect might most appropriately be expressed as a range between the highest pure EV concentration causing an effect size < K, and the lowest pure EV concentration causing an effect size > K. If the effect sizes achieved by EVs do not overlap K, it can be expressed as an inequality. Assuming effective removal of non-EV material during purification, an EVMER approaching 1 would suggest equivalent potency of EVs and conditioned medium. As ever, ineffective purification strategies would inflate the apparent potency of EVs, increasing the EVMER. As an example of this, in this study SEC-purified EVs were found to have an EVMER of less than 0.0145, whereas TEI-purified EVs had an EVMER between 0.0725 and 0.29 (see section 4.3.9).

The EVMER, as a metric of relative potency, might be taken to indicate the overall contribution of EVs to signalling in their normal context. However, this makes several assumptions that may not always be valid. It assumes independence of the EV and non-EV-mediated effects. It relies on the effect size K being within a relatively linear dose-dependent response regime, rather than being saturated with an excess of stimulation. It assumes that the same proportion of particles measured by NTA are EVs in both CM and the purified EV sample. It also requires that cells be conditioned in media that does not contain particles or have any significant effect on the assay itself – media containing EV-depleted FBS would likely violate both of these assumptions. And it does not account for any loss of per-particle activity that might reasonably occur during the purification process. However, it is hoped that it may provide a straightforward method to indicate whether the quantities of EVs being used in an experiment are higher than is biologically relevant.

It could be argued that, if it works, the relationship of a treatment to physiological signalling is unimportant. It is of course the case that hMSC-mediated therapy is manifestly unphysiological in and of itself. However, in the case of hMSC-EVs, it may be the case that if their apparent activity may be due to (in at least some reports) contamination with conventional signalling factors, it may be more appropriate to reinvestigate and identify the soluble factors responsible for the observed benefit. Similarly, it is not clear whether use of very high quantities of hMSC-EVs is advantageous over lesser quantities of more conventional factors, which have themselves been shown to be therapeutic (see sections 4.1.7 - 4.1.9) and are considerably more straightforward to produce.

4.4.7. Limitations and caveats

Within the scope of the present work, it appears that for the systems studied EVs do not have a major role in hMSC paracrine signalling. However, it is important to clarify the scope and boundaries of this study. Although this study used two *in vitro* assays commonly used to assess the apparent pro-regeneration properties of hMSC-EVs, it did not involve any *in vivo* investigation. EVs from hMSCs have been tested in preclinical animal models for several disease types [251]. Although *in vitro* assays are typically used to indicate the *in vivo* potential of EVs (and other treatments), it cannot be assumed that the apparent dependence of *in vitro* assays on free protein rather than EVs would also hold true *in vivo*.

It is also important to consider the impact of culture conditions on the behaviour and EV secretion of hMSCs. Some studies have previously chosen to use EV-depleted FBS during the EV collection period [240, 242]. Other studies have utilised growth factors such as FGF2 (Fibroblast Growth Factor 2) and PDGF [238, 262], or commercially available “advanced” media such as OptiMEM [263] when collecting conditioned medium. In order to compare hMSC-secreted EVs and soluble factors, in this study it was

necessary to generate hMSC-conditioned medium using basal media, without addition of any exogenous growth factors or supplements which might themselves contribute to angiogenesis or wound healing. In particular, EV-depleted FBS was not considered a viable option, given that it had been found to be not wholly devoid of bovine EVs and had a high protein concentration. Other studies have stimulated hMSCs with hypoxia during the EV isolation period. It is well-known that hypoxic stimulation of hMSCs has a strong impact on their paracrine signalling [264], and it has been reported that hypoxia also increases the therapeutic effect of hMSC-EVs [240]. High-density culture of hMSCs in hollow-fibre bioreactors or as spheroids might have influenced the properties of their EVs and might also have allowed higher overall yields. Different stimulations experienced by hMSCs during EV collection might have led to packaging of different factors into the EVs themselves, and hence to different therapeutic capabilities. Nevertheless, EVs isolated from basal media conditioned by hMSCs in 2D culture under normoxia (as in this study) have previously been shown to have therapeutic effects in multiple models of disease [252, 253, 260, 265-267], including models of angiogenesis and wound healing very similar to the ones presented here [252, 253, 260].

4.4.8. Recommendations for EV research

The results presented here are interpreted as having both biological and technical implications for EV research. This study indicated that hMSC-EVs may not be necessary for hMSC-mediated paracrine signalling. As previously discussed, the scope of this conclusion is limited due to the lack of *in vivo* testing and due to the possibility of altered EV potency when hMSCs are cultured under different conditions. However, this study identified potential blind spots that do not appear to have been addressed in the literature. If the hMSC paracrine effect is to be exploited therapeutically, it may be unwise to focus on EVs to the exclusion of other more conventional signalling factors.

Assessment of the purity of the final EV isolate is recommended as a litmus test for potential contamination issues. It is important to quantify the resulting EVs beyond measuring protein concentration, as that is highly dependent on sample purity. Many studies report EV yield and doses in terms of protein concentration alone, and so the true quantities of EVs used (and their purity) are not clear. Particle quantification by NTA or other technologies or quantitative assessment of EV-specific markers are appropriate additional measurements. The risk of contamination with bioactive non-EV material is considered to be particularly high when using EVs isolated from conditioned media containing EV-depleted FBS, or other high-concentration supplements. Robust purification is especially critical in these cases. If use of EV-depleted FBS or other enriched media is necessary, it is also recommended that a control isolation be performed in parallel, using non-conditioned media. When performing experiments intended to deplete EVs from a sample, the experiment should be designed such that off-target depletion may be detected and accounted for. A suitable control might

involve use of a membrane made from the same material but with a pore size high enough to allow the passage of EVs.

Irrespective of the generalisability of the conclusions reached by this study on the activity of hMSC-EVs specifically, this study identified potentially serious risks in previously used experimental techniques that had not previously been identified and is believed to be the first to directly compare EV and non-EV signalling from the same cells simultaneously. There are implications for choice of technique and experimental design that are thought to be relevant to EV research more widely. It has previously been demonstrated that less effective isolation techniques lead to contamination. To the best of the author's knowledge, it had not previously been demonstrated that contamination can lead to false attribution of stimulatory potency to EVs. This finding underscores the critical importance of using an effective purification technique that robustly removes as much non-EV material as possible. It is apparent from these results that the use of low-purity isolation techniques poses a serious risk. Yet purification techniques that have been shown here and elsewhere [108, 117] to result in low purity EV samples remain in common use. No purification technique should be assumed to work "out of the box". Extensive validation should be carried out in order to confirm that the final EV sample contains only EVs, to the extent to which that is achievable. As validation of this sort is not always reported, it is unclear to what extent similar contamination issues may have influenced some previous work.

5. Future work and conclusions

This chapter provides suggestions for future investigations and provides a summary of the conclusions of the study, including recommendations for the field.

5.1. Future work

In this study, it was found that hMSC-EVs were not necessary or sufficient to stimulate *in vitro* assays of angiogenesis and wound healing. This result was surprising as EVs have previously been reported to be critical mediators of the hMSC paracrine effect [239] and have been widely investigated for therapeutic properties across a range of injuries [252, 253, 260, 265-267], including using *in vitro* models similar to those used in this study [252, 253, 260]. Upon detailed investigation, potential methodological explanations for this discrepancy were discovered, as discussed in detail in section 4.4. Briefly, this study used a stringent and well-validated purification system to thoroughly separate EVs from all detectable non-EV protein contaminants. Some other studies used techniques known to be less effective at removing contaminants, without similar validation. It is also unclear whether the quantities of purified EVs typically used to stimulate cells *in vitro* or tissues *in vivo* are comparable to the quantities of EVs produced by the cells thought to mediate therapeutic paracrine signalling. An ultrafiltration technique previously used to demonstrate the necessity of EVs for hMSC paracrine signalling was found to give misleading results due to off-target depletion of non-EV factors.

There are three major strands of future investigation that might follow on from this work. Firstly, to what extent do these experiments, in which hMSCs cultured under specific conditions were used to stimulate *in vitro* assays, reflect the signalling from hMSCs under other conditions and *in vivo*? Secondly, to what extent do the technical and conceptual issues identified in this study apply more widely to EV research in general? And thirdly, following on from this research, how can biological therapies be identified in future?

In this study, hMSCs were cultured under commonly used conditions, with EVs isolated from hMSCs cultured temporarily in serum-free media, in 2D culture, under normoxia. HMSCs from three donors of different ages, sexes and ethnic backgrounds were used in order to rule out donor-specific effects. Conditioned medium and EVs were tested in two commonly used *in vitro* assays. However, it would be inappropriate to assert that the conclusions drawn here (that EVs are not necessary for paracrine signalling) necessarily apply to all situations in which hMSCs might stimulate regeneration or prevent injury. HMSC-EVs have also previously been isolated under quite different conditions. Use of EV-depleted FBS or growth factor enriched media is also common, and there is also evidence that hypoxic conditions enhance EV-mediated paracrine signalling (see section 4.1). It is possible that EVs may be more potent when the cells producing them are differently stimulated, or that more EVs are

produced per cell. Future work to assess the impact of culture conditions on EV potency could involve purification of EVs from hMSCs cultured under different conditions (i.e. with EV-depleted FBS, growth factor supplementation, or hypoxia). When adding exogenous growth factors (or bovine EVs from FBS), it would not be possible to directly compare EVs and cell-derived soluble factors. However, one could compare the stimulatory potencies of EVs isolated under different conditions. As SEC isolation of hMSC-EVs results in a pure sample, this might lend itself to reliable proteomic and transcriptomic analysis to determine whether there are major differences in composition. Achieving a similar level of purity might be challenging, especially with supplementation from EV-depleted FBS. If EVs from each source could be purified and validated as pure, then the per-EV potency could be evaluated and compared. The number of EVs produced per cell could also be compared. This might be challenging due to the background present of bovine EVs in EV-depleted FBS. With this information, it might become apparent whether EV-mediated signalling is similarly proportionately important across different conditions, or whether the conditions used in this study were unusually inhibitory to EV-mediated signalling.

An obvious next step for this project would be investigation using an *in vivo* model of disease. Animal models of MI and I/R injury, wound healing of burns and other skin damage, acute kidney injury, stroke and others [251] have all been used to assess the therapeutic capacity of hMSC-EVs. Although *in vitro* models similar to those presented here are typically used to validate hMSC-EVs prior to *in vivo* use, it cannot be assumed that *in vitro* results translate to *in vivo* results. Individual testing of fractions eluting from a SEC column would likely be unnecessarily complicated and costly for *in vivo* testing. EV-containing and EV-depleted conditioned medium prepared by equilibrium dialysis or pre-blocked ultrafiltration (as described in sections 4.3.2 and 4.3.4) could be compared, as could the EV and soluble protein peak fractions from SEC. Testing in even relatively straightforward assays such as cutaneous wound healing could considerably strengthen the link of these results to proposed therapies as used *in vivo*. Testing in a model of MI could be particularly informative. Reduction of the size of the infarct after reperfusion is considered to be one of the more promising applications of hMSC-EVs. If this result can be reproduced without EVs, it could have profound consequences for current understanding of hMSC-mediated signalling, and the development of future therapies.

As discussed in section 4.4, whether or not the results shown here for hMSC-EVs apply across different growth conditions and assays, this study identified technical risks and new concepts that could have implications for EV research in general. In particular, off-target depletion was identified as a risk in experiments where EVs are removed from conditioned medium in order to demonstrate their necessity for signalling. Low-purity isolation techniques were demonstrated to have serious

consequences for downstream assessment of biological activity. Finally, it was suggested that a more quantitative assessment of the amount of EV material needed to stimulate a cell response might reveal that the quantities used are excessive in comparison to the other factors made by the cell.

These observations and concepts may be widely relevant to EV research. Ideally, communication of these potential risks might stimulate future research by other groups into the applicability of these issues to their own experimental systems. It might, however, be beneficial to investigate and directly compare some other *in vitro* experimental systems in which EVs have been found to be important for signalling, such as *in vitro* assays of immune modulation [6, 268] or signalling in cancer [269, 270]. The experimental approach used here might not always be directly applicable, but in general, assessment of potential issues relating to sample purity and how the quantity of EVs used relates to the quantity of EVs made would be informative. This approach might be beneficial in strengthening the quantitative understanding of the roles of EVs in the many processes in which they have been implicated. It might also be informative to investigate additional combinations of purification techniques. Other studies have previously compared the yield and purity of EVs isolated by different methods such as differential ultracentrifugation and density-based purification [108]. It would be informative to conduct a similar study with the addition of assessing the carry-through of biological activity due to contamination from cell-derived or exogenous non-EV growth factors. There is widespread discussion concerning how best to isolate EVs and what standards for reporting their properties should be encouraged [271, 272]. The results of this and similar studies could inform these and further discussions.

Investigation of the paracrine effect of hMSCs is ultimately intended to lead to new therapies for otherwise incompletely treatable diseases and injuries. Large-scale culture of hMSCs would be logistically challenging to implement for widespread use, especially for treatment of relatively common diseases such as myocardial infarction. Ideally, if the factors that are necessary and sufficient for the therapeutic effect of hMSCs could be made synthetically – either by expression in microorganisms or by chemical synthesis – this would significantly increase the feasibility of their adoption as treatments. With this in mind, resolving whether EVs or soluble factors are most appropriate for treatment is of great importance. If EVs held a significant advantage over soluble factors, then they would be worth pursuing as a therapeutic. However, if soluble factors were to be capable of similar therapeutic effects, their practical advantages would greatly simplify the path to therapy. It should also not necessarily be assumed that the factors (or combination of factors) produced by hMSCs during signalling would represent the best possible treatment. Treatment of disease and injury by hMSCs does not appear to have a physiological analogue, and so the EVs or

signalling factors responsible will not have been optimised by evolution. They might instead represent a starting point for further development – for example, changing the concentrations of factors (EV or non-EV) might allow a stronger therapeutic effect.

It is worth mentioning, however, that simple soluble factors such as bFGF and VEGF have already been shown to be therapeutic in animal models of myocardial infarction [224], with some studies taking place over two decades ago [225], and yet there is no such therapy in widespread use. It might be productive to identify why apparently promising therapies fail to reach the clinic, as well as investing effort in generating new therapeutic leads. Possible reasons might include regulatory issues, incompatibility with current procedures for clinical care, difficulties in organising and conducting clinical trials, researchers choosing not to continue their work or assuming that it would be continued elsewhere, additional complications associated with delivery of the therapy, or simply the discovery that the treatment is not as effective as it initially appeared to be. Greater communication between researchers and clinical practitioners is likely to be valuable in realising the potential of the many promising treatments that have been identified through laboratory research.

5.2. Conclusions

An effective EV isolation and purification protocol was developed and validated. Assessment of the contribution of EVs to hMSC paracrine signalling by several different techniques suggested that EVs were neither necessary nor sufficient to mediate stimulation of *in vitro* angiogenesis or wound healing. Several experimental techniques were identified that could lead to misleading results and erroneous identification of EVs as major signalling effectors. Further research could clarify whether these results are limited to signalling under the conditions studied or are more widely relevant to hMSC signalling in general. Insights from the detailed analysis of commonly used techniques have led to the following general suggestions for EV research:

- Use of EV-depleted FBS should be avoided if possible. If unavoidable, a non-conditioned media control should be included for all experiments.
- When depleting EVs from media to confirm their necessity for signalling, off-target depletion should be assessed or otherwise controlled for.
- The purity of the final EV sample should be assessed, and low-purity isolation methods avoided.
- EV signalling should be considered quantitatively within the context of total cell signalling. Calculation of the EVMER, or other assessment of the relative contribution of EVs within total cell signalling, should be considered when asserting the function of EVs.

It is hoped that adoption of these suggestions could assist robust and rigorous assessment of the roles of EVs within their overall signalling contexts. This would aid identification of their true physiological roles and therapeutic potentials, eventually allowing identification and development of effective cell-free therapies.

6. Appendix

Initial investigations that led to the identification of ultrafiltration and size exclusion as a potential method for purification are shown here.

A review of the literature suggested that a purification strategy based on separation by density was likely to be effective. Therefore, a three-stage purification strategy was initially investigated, in which MDA-MB-231-derived conditioned medium underwent ultracentrifugation to form an initial pellet, and the pellet was resuspended in PBS and purified by capture in a sucrose cushion. The sucrose cushion was then recovered, diluted in PBS and then EVs pelleted by ultracentrifugation again (Figure 6.1 a). The conditioned medium had been pre-processed to remove dead cells and debris by low-speed centrifugations (500 x g, 5 minutes, 4500 x g, 15 minutes) and filtration through a 0.45 µm filter, as described in materials and methods. Very few particles were recovered in the final pellet (Figure 6.1 b). No obvious pellets were seen at any stage of purification; however, this is not considered unusual [102, 273]. Comparison of the particle concentrations in the initial resuspended pellet, the sucrose cushion, and the final pellet suggested that the majority of loss occurred at the pelleting stage (Figure 6.1 b). It could not be determined why the recovery from pelleting by ultracentrifugation was lower than anticipated. Increasing g-forces, increasing the time of centrifugation, changing rotors and centrifuge tubes or changing the method of resuspension did not increase recovery (data not shown).

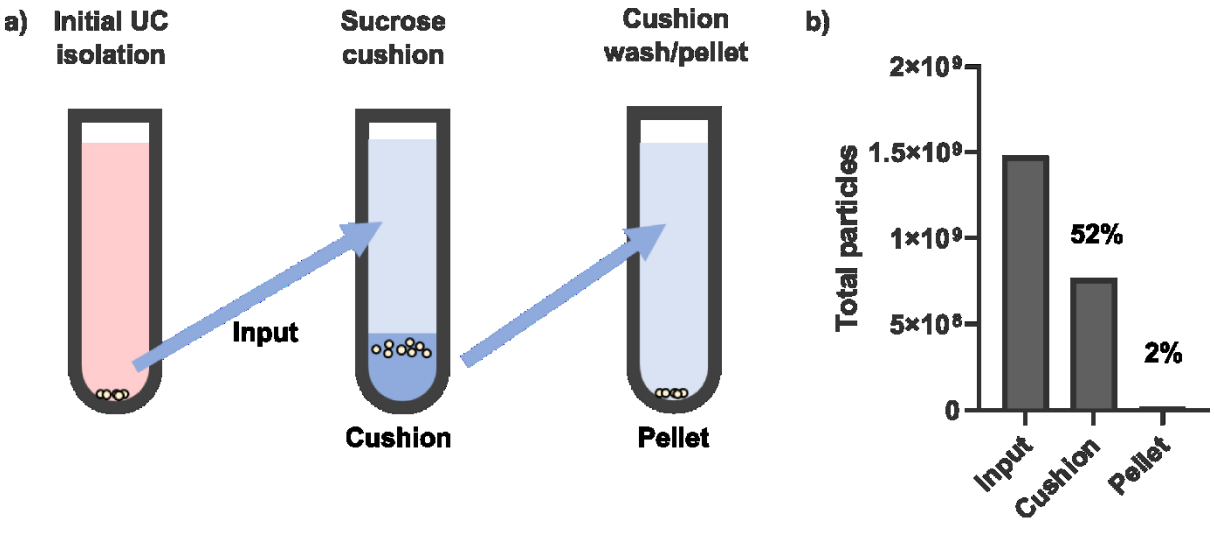


Figure 6.1: Initial sucrose cushion purification. a) Experimental schematic. b) Particle concentrations at various stages of purification. Particles were quantified using a Nanosight LM10 with 642 nm laser. N = 1, n = 1.

Initial data indicated that the main point of EV loss in the purification process was during ultracentrifugation to pellet EVs. Methods to circumvent this stage were therefore investigated. Some studies reported use of a sucrose cushion directly with conditioned medium, without initial ultracentrifugation [274]. It was found that although it was possible to layer the sucrose cushion under the CM successfully, the boundary between the medium and the sucrose cushion was not always maintained (Figure 6.2 a). The effect was not consistent and varied between seemingly identical experiments, and the underlying cause could not be determined. The inconsistency in maintaining a defined boundary suggested that this method was unlikely to consistently retrieve a high-purity isolate. As a concentration method still appeared to be necessary, additional potential methods were investigated. Using MDA-MB-231 EVs previously isolated by a single ultracentrifugation, EVs were captured by passing resuspended EVs through a 100 nm PVDF membrane using a syringe filter as in [138]. The membrane was then vortexed in PBS. (Figure 6.2 b-i). It was found that only approximately 5 % of the input particles (as measured by NTA) were recovered. This was considered too great a loss for further use. However, it was hypothesised that use of small-pore filters in some other format could still be effective. Dialysis membranes in a centrifuge tube format were then investigated – this format allowed fluid to be forced through the membrane under several thousand equivalent gravities. This allowed rapid reduction of volume. It was found that a 50 kDa pore size Amicon Ultra-15 centrifugal concentrator recovered 32 % of input particles (Figure 6.2 b-ii). This was promising, and centrifugal concentrators were selected as a candidate for more in-depth characterisation and assessment.

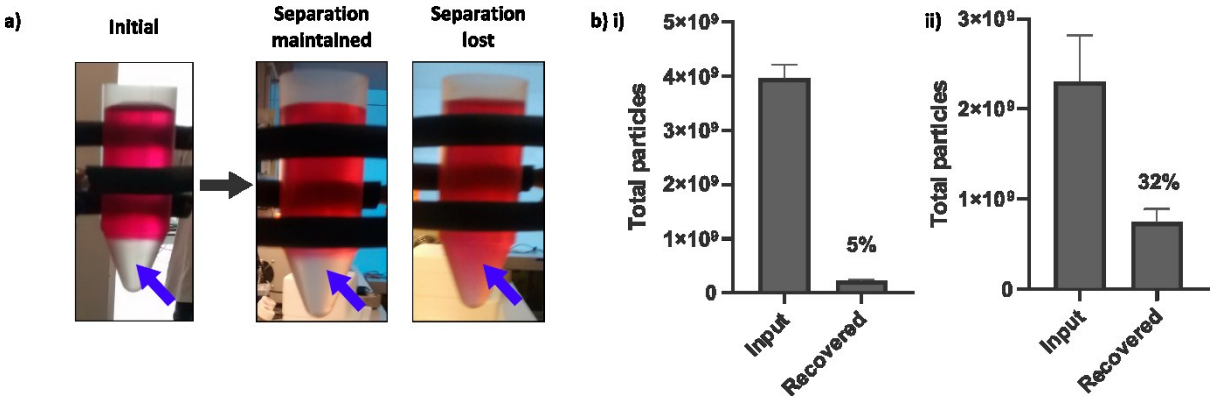


Figure 6.2: Evaluation of methods to circumvent pelleting by ultracentrifugation. a) Direct ultracentrifugation of CM into a sucrose cushion. The boundary between media and cushion was not consistently maintained (see arrows). b) Recovery of particles from i) 100 nm PVDF filter, ii) 50 kDa Amicon Ultra-15 centrifugal concentrator. N = 1, n = 3 x 30 second videos. This experiment used the LM10 model nanosight with 642 nm laser, and videos were analysed with software v2.3.

7. Bibliography

1. Trams, E.G., et al., *Exfoliation of membrane ecto-enzymes in the form of micro-vesicles.* Biochim Biophys Acta, 1981. **645**(1): p. 63-70.
2. Harding, C. and P. Stahl, *Transferrin Recycling in Reticulocytes - Ph and Iron Are Important Determinants of Ligand-Binding and Processing.* Biochem Biophys Res Commun, 1983. **113**(2): p. 650-658.
3. Hanson, P.I. and A. Cashikar, *Multivesicular Body Morphogenesis.* Annual Review of Cell and Developmental Biology, Vol 28, 2012. **28**: p. 337-362.
4. Raposo, G., et al., *B lymphocytes secrete antigen-presenting vesicles.* J Exp Med, 1996. **183**(3): p. 1161-1172.
5. Owens, A.P., 3rd and N. Mackman, *Microparticles in hemostasis and thrombosis.* Circ Res, 2011. **108**(10): p. 1284-1297.
6. Lugini, L., et al., *Immune surveillance properties of human NK cell-derived exosomes.* J Immunol, 2012. **189**(6): p. 2833-2842.
7. Gross, J.C., et al., *Active Wnt proteins are secreted on exosomes.* Nat Cell Biol, 2012. **14**(10): p. 1036-1045.
8. Schwarz, A., et al., *Vesicular transfer of membrane components to bovine epididymal spermatozoa.* Cell Tissue Res, 2013. **353**(3): p. 549-561.
9. Tominaga, N., T. Katsuda, and T. Ochiya, *Micromanaging of tumor metastasis by extracellular vesicles.* Semin Cell Dev Biol, 2015. **40**: p. 52-59.
10. Katsuda, T., et al., *The therapeutic potential of mesenchymal stem cell-derived extracellular vesicles.* Proteomics, 2013. **13**(10-11): p. 1637-1653.
11. Yanez-Mo, M., et al., *Biological properties of extracellular vesicles and their physiological functions.* J Extracell Vesicles, 2015. **4**: p. 27066.
12. Marcilla, A., et al., *Extracellular vesicles from parasitic helminths contain specific excretory/secretory proteins and are internalized in intestinal host cells.* PLoS One, 2012. **7**(9): p. e45974.
13. Silverman, J.M., et al., *An exosome-based secretion pathway is responsible for protein export from Leishmania and communication with macrophages.* Journal of Cell Science, 2010. **123**(Pt 6): p. 842-852.
14. Deatherage, B.L. and B.T. Cookson, *Membrane vesicle release in bacteria, eukaryotes, and archaea: a conserved yet underappreciated aspect of microbial life.* Infect Immun, 2012. **80**(6): p. 1948-1957.
15. Regente, M., et al., *Vesicular fractions of sunflower apoplastic fluids are associated with potential exosome marker proteins.* FEBS Lett, 2009. **583**(20): p. 3363-3366.
16. Chargaff, E. and R. West, *The biological significance of the thromboplastic protein of blood.* J Biol Chem, 1946. **166**(1): p. 189-197.
17. Anderson, H.C., *Vesicles associated with calcification in the matrix of epiphyseal cartilage.* J Cell Biol, 1969. **41**(1): p. 59-72.
18. Gould, S.J. and G. Raposo, *As we wait: coping with an imperfect nomenclature for extracellular vesicles.* J Extracell Vesicles, 2013. **2**.
19. Minciacchi, V.R., M.R. Freeman, and D. Di Vizio, *Extracellular vesicles in cancer: exosomes, microvesicles and the emerging role of large oncosomes.* Semin Cell Dev Biol, 2015. **40**: p. 41-51.
20. Bobrie, A., et al., *Diverse subpopulations of vesicles secreted by different intracellular mechanisms are present in exosome preparations obtained by differential ultracentrifugation.* J Extracell Vesicles, 2012. **1**.
21. Aalberts, M., et al., *Identification of distinct populations of prostasomes that differentially express prostate stem cell antigen, annexin A1, and GLIPR2 in humans.* Biol Reprod, 2012. **86**(3): p. 82.

22. Willms, E., et al., *Cells release subpopulations of exosomes with distinct molecular and biological properties.* Sci Rep, 2016. **6**: p. 22519.
23. Subra, C., et al., *Exosome lipidomics unravels lipid sorting at the level of multivesicular bodies.* Biochimie, 2007. **89**(2): p. 205-212.
24. Colombo, M., G. Raposo, and C. Thery, *Biogenesis, secretion, and intercellular interactions of exosomes and other extracellular vesicles.* Annu Rev Cell Dev Biol, 2014. **30**: p. 255-289.
25. Trajkovic, K., et al., *Ceramide triggers budding of exosome vesicles into multivesicular endosomes.* Science, 2008. **319**(5867): p. 1244-1247.
26. Nazarenko, I., et al., *Cell surface tetraspanin Tspan8 contributes to molecular pathways of exosome-induced endothelial cell activation.* Cancer Res, 2010. **70**(4): p. 1668-1678.
27. Mobius, W., et al., *Recycling compartments and the internal vesicles of multivesicular bodies harbor most of the cholesterol found in the endocytic pathway.* Traffic, 2003. **4**(4): p. 222-231.
28. Fader, C.M., et al., *TI-VAMP/VAMP7 and VAMP3/cellubrevin: two v-SNARE proteins involved in specific steps of the autophagy/multivesicular body pathways.* Biochim Biophys Acta, 2009. **1793**(12): p. 1901-1916.
29. Raposo, G. and W. Stoorvogel, *Extracellular vesicles: exosomes, microvesicles, and friends.* J Cell Biol, 2013. **200**(4): p. 373-383.
30. Cai, H., K. Reinisch, and S. Ferro-Novick, *Coats, tethers, Rabs, and SNAREs work together to mediate the intracellular destination of a transport vesicle.* Developmental Cell, 2007. **12**(5): p. 671-682.
31. Eldh, M., et al., *Importance of RNA isolation methods for analysis of exosomal RNA: evaluation of different methods.* Mol Immunol, 2012. **50**(4): p. 278-286.
32. Lai, R.C., et al., *Proteolytic Potential of the MSC Exosome Proteome: Implications for an Exosome-Mediated Delivery of Therapeutic Proteasome.* Int J Proteomics, 2012. **2012**: p. 971907.
33. Mathivanan, S., et al., *ExoCarta 2012: database of exosomal proteins, RNA and lipids.* Nucleic Acids Res, 2012. **40**(Database issue): p. D1241-1244.
34. Thery, C., et al., *Indirect activation of naive CD4+ T cells by dendritic cell-derived exosomes.* Nat Immunol, 2002. **3**(12): p. 1156-1162.
35. Mallegol, J., et al., *T84-intestinal epithelial exosomes bear MHC class II/peptide complexes potentiating antigen presentation by dendritic cells.* Gastroenterology, 2007. **132**(5): p. 1866-1876.
36. Walker, J.D., C.L. Maier, and J.S. Pober, *Cytomegalovirus-infected human endothelial cells can stimulate allogeneic CD4+ memory T cells by releasing antigenic exosomes.* J Immunol, 2009. **182**(3): p. 1548-1559.
37. Cooper, T.G., *Interactions between epididymal secretions and spermatozoa.* J Reprod Fertil Suppl, 1998. **53**: p. 119-136.
38. Legare, C., et al., *Hamster sperm antigen P26h is a phosphatidylinositol-anchored protein.* Mol Reprod Dev, 1999. **52**(2): p. 225-233.
39. Frenette, G., M. Thabet, and R. Sullivan, *Polyol pathway in human epididymis and semen.* J Androl, 2006. **27**(2): p. 233-239.
40. Aalberts, M., T.A. Stout, and W. Stoorvogel, *Prostasomes: extracellular vesicles from the prostate.* Reproduction, 2014. **147**(1): p. R1-14.
41. Valadi, H., et al., *Exosome-mediated transfer of mRNAs and microRNAs is a novel mechanism of genetic exchange between cells.* Nat Cell Biol, 2007. **9**(6): p. 654-659.
42. Ratajczak, J., et al., *Embryonic stem cell-derived microvesicles reprogram hematopoietic progenitors: evidence for horizontal transfer of mRNA and protein delivery.* Leukemia, 2006. **20**(5): p. 847-856.
43. Chevillet, J.R., et al., *Quantitative and stoichiometric analysis of the microRNA content of exosomes.* Proc Natl Acad Sci U S A, 2014. **111**(41): p. 14888-14893.

44. Mittelbrunn, M., et al., *Unidirectional transfer of microRNA-loaded exosomes from T cells to antigen-presenting cells.* Nat Commun, 2011. **2**: p. 282.
45. Villarroya-Beltri, C., et al., *Sumoylated hnRNPA2B1 controls the sorting of miRNAs into exosomes through binding to specific motifs.* Nat Commun, 2013. **4**: p. 2980.
46. Bolukbasi, M.F., et al., *miR-1289 and "Zipcode"-like Sequence Enrich mRNAs in Microvesicles.* Mol Ther Nucleic Acids, 2012. **1**: p. e10.
47. Alvarez-Erviti, L., et al., *Delivery of siRNA to the mouse brain by systemic injection of targeted exosomes.* Nat Biotechnol, 2011. **29**(4): p. 341-345.
48. Zhang, Y., et al., *Secreted monocytic miR-150 enhances targeted endothelial cell migration.* Mol Cell, 2010. **39**(1): p. 133-144.
49. Thakur, B.K., et al., *Double-stranded DNA in exosomes: a novel biomarker in cancer detection.* Cell Res, 2014. **24**(6): p. 766-769.
50. Bergsmedh, A., et al., *Horizontal transfer of oncogenes by uptake of apoptotic bodies.* Proc Natl Acad Sci U S A, 2001. **98**(11): p. 6407-6411.
51. Kanada, M., et al., *Differential fates of biomolecules delivered to target cells via extracellular vesicles.* Proc Natl Acad Sci U S A, 2015. **112**(12): p. E1433-1442.
52. Record, M., et al., *Exosomes as new vesicular lipid transporters involved in cell-cell communication and various pathophysiologies.* Biochim Biophys Acta, 2014. **1841**(1): p. 108-120.
53. Armengol, X. and J. Estelrich, *Physical stability of different liposome compositions obtained by extrusion method.* J Microencapsul, 1995. **12**(5): p. 525-535.
54. Kim, C.W., et al., *Extracellular membrane vesicles from tumor cells promote angiogenesis via sphingomyelin.* Cancer Res, 2002. **62**(21): p. 6312-6317.
55. Feng, D., et al., *Cellular internalization of exosomes occurs through phagocytosis.* Traffic, 2010. **11**(5): p. 675-687.
56. Montecalvo, A., et al., *Mechanism of transfer of functional microRNAs between mouse dendritic cells via exosomes.* Blood, 2012. **119**(3): p. 756-766.
57. Mulcahy, L.A., R.C. Pink, and D.R. Carter, *Routes and mechanisms of extracellular vesicle uptake.* J Extracell Vesicles, 2014. **3**.
58. Simpson, R.J., et al., *Exosomes: proteomic insights and diagnostic potential.* Expert Rev Proteomics, 2009. **6**(3): p. 267-283.
59. Muller, L., et al., *Isolation of biologically-active exosomes from human plasma.* J Immunol Methods, 2014. **411**: p. 55-65.
60. Pisitkun, T., R.F. Shen, and M.A. Knepper, *Identification and proteomic profiling of exosomes in human urine.* Proc Natl Acad Sci U S A, 2004. **101**(36): p. 13368-13373.
61. Palanisamy, V., et al., *Nanostructural and transcriptomic analyses of human saliva derived exosomes.* PLoS One, 2010. **5**(1): p. e8577.
62. Poliakov, A., et al., *Structural heterogeneity and protein composition of exosome-like vesicles (prostasomes) in human semen.* Prostate, 2009. **69**(2): p. 159-167.
63. Nam, R.K., et al., *Increasing hospital admission rates for urological complications after transrectal ultrasound guided prostate biopsy.* J Urol, 2013. **189**(1 Suppl): p. S12-17; discussion S17-18.
64. Britt-Marie, L., et al., *Diagnostic accuracy of fine-needle aspiration biopsy is determined by physician training in sampling technique.* Cancer Cytopathology, 2001. **93**(4): p. 263-268.
65. M., C.N., et al., *Underestimation of Gleason score at prostate biopsy reflects sampling error in lower volume tumours.* BJU International, 2012. **109**(5): p. 660-664.
66. Nilsson, J., et al., *Prostate cancer-derived urine exosomes: a novel approach to biomarkers for prostate cancer.* Br J Cancer, 2009. **100**(10): p. 1603-1607.
67. Rosell, R., J. Wei, and M. Taron, *Circulating MicroRNA Signatures of Tumor-Derived Exosomes for Early Diagnosis of Non-Small-Cell Lung Cancer.* Clin Lung Cancer, 2009. **10**(1): p. 8-9.

68. Taylor, D.D. and C. Gercel-Taylor, *MicroRNA signatures of tumor-derived exosomes as diagnostic biomarkers of ovarian cancer.* Gynecol Oncol, 2008. **110**(1): p. 13-21.
69. Sheridan, C., *Exosome cancer diagnostic reaches market.* Nat Biotechnol, 2016. **34**(4): p. 359-360.
70. Allen, T.M. and P.R. Cullis, *Liposomal drug delivery systems: from concept to clinical applications.* Adv Drug Deliv Rev, 2013. **65**(1): p. 36-48.
71. Yeo, R.W., et al., *Mesenchymal stem cell: an efficient mass producer of exosomes for drug delivery.* Adv Drug Deliv Rev, 2013. **65**(3): p. 336-341.
72. Quah, B.J. and H.C. O'Neill, *The immunogenicity of dendritic cell-derived exosomes.* Blood Cells Mol Dis, 2005. **35**(2): p. 94-110.
73. Ohno, S., et al., *Systemically injected exosomes targeted to EGFR deliver antitumor microRNA to breast cancer cells.* Mol Ther, 2013. **21**(1): p. 185-191.
74. Sugahara, K.N., et al., *Tissue-penetrating delivery of compounds and nanoparticles into tumors.* Cancer Cell, 2009. **16**(6): p. 510-520.
75. Willekens, F.L., et al., *Liver Kupffer cells rapidly remove red blood cell-derived vesicles from the circulation by scavenger receptors.* Blood, 2005. **105**(5): p. 2141-2145.
76. Peinado, H., et al., *Melanoma exosomes educate bone marrow progenitor cells toward a pro-metastatic phenotype through MET.* Nat Med, 2012. **18**(6): p. 883-891.
77. Gabizon, A., et al., *Clinical studies of liposome-encapsulated doxorubicin.* Acta Oncol, 1994. **33**(7): p. 779-786.
78. Taylor, D.D. and S. Shah, *Methods of isolating extracellular vesicles impact down-stream analyses of their cargoes.* Methods, 2015. **87**: p. 3-10.
79. Ha, D., N. Yang, and V. Nadithe, *Exosomes as therapeutic drug carriers and delivery vehicles across biological membranes: current perspectives and future challenges.* Acta Pharm Sin B, 2016. **6**(4): p. 287-296.
80. Mendt, M., et al., *Generation and testing of clinical-grade exosomes for pancreatic cancer.* JCI Insight, 2018. **3**(8).
81. Pachler, K., et al., *A Good Manufacturing Practice-grade standard protocol for exclusively human mesenchymal stromal cell-derived extracellular vesicles.* Cytotherapy, 2017. **19**(4): p. 458-472.
82. Zitvogel, L., et al., *Eradication of established murine tumors using a novel cell-free vaccine: dendritic cell-derived exosomes.* Nat Med, 1998. **4**(5): p. 594-600.
83. Cheever, M.A. and C.S. Higano, *PROVENGE (Sipuleucel-T) in prostate cancer: the first FDA-approved therapeutic cancer vaccine.* Clin Cancer Res, 2011. **17**(11): p. 3520-3526.
84. Bach, P.B., S.A. Giralt, and L.B. Saltz, *FDA Approval of Tisagenlecleucel: Promise and Complexities of a $475000 Cancer Drug.* JAMA, 2017. **318**(19): p. 1861-1862.
85. S, E.L.A., et al., *Extracellular vesicles: biology and emerging therapeutic opportunities.* Nat Rev Drug Discov, 2013. **12**(5): p. 347-357.
86. Dai, S., et al., *Phase I clinical trial of autologous ascites-derived exosomes combined with GM-CSF for colorectal cancer.* Mol Ther, 2008. **16**(4): p. 782-790.
87. Morse, M.A., et al., *A phase I study of dexosome immunotherapy in patients with advanced non-small cell lung cancer.* J Transl Med, 2005. **3**(1): p. 9.
88. Tan, A., H. De La Pena, and A.M. Seifalian, *The application of exosomes as a nanoscale cancer vaccine.* Int J Nanomedicine, 2010. **5**: p. 889-900.
89. Mummery, C.L., R.P. Davis, and J.E. Krieger, *Challenges in using stem cells for cardiac repair.* Sci Transl Med, 2010. **2**(27): p. 27ps17.
90. Lai, R.C., T.S. Chen, and S.K. Lim, *Mesenchymal stem cell exosome: a novel stem cell-based therapy for cardiovascular disease.* Regen Med, 2011. **6**(4): p. 481-492.
91. Li, P., et al., *Progress in Exosome Isolation Techniques.* Theranostics, 2017. **7**(3): p. 789-804.

92. Kalra, H., et al., *Comparative proteomics evaluation of plasma exosome isolation techniques and assessment of the stability of exosomes in normal human blood plasma.* Proteomics, 2013. **13**(22): p. 3354-3364.
93. Wu, C.X. and Z.F. Liu, *Proteomic Profiling of Sweat Exosome Suggests its Involvement in Skin Immunity.* J Invest Dermatol, 2018. **138**(1): p. 89-97.
94. Admyre, C., et al., *Exosomes with immune modulatory features are present in human breast milk.* J Immunol, 2007. **179**(3): p. 1969-1978.
95. Michael, A., et al., *Exosomes from human saliva as a source of microRNA biomarkers.* Oral Dis, 2010. **16**(1): p. 34-38.
96. Huleihel, L., et al., *Matrix-bound nanovesicles within ECM bioscaffolds.* Sci Adv, 2016. **2**(6): p. e1600502.
97. Baek, R., et al., *The impact of various preanalytical treatments on the phenotype of small extracellular vesicles in blood analyzed by protein microarray.* J Immunol Methods, 2016. **438**: p. 11-20.
98. Shelke, G.V., et al., *Importance of exosome depletion protocols to eliminate functional and RNA-containing extracellular vesicles from fetal bovine serum.* J Extracell Vesicles, 2014. **3**.
99. Aswad, H., A. Jalabert, and S. Rome, *Depleting extracellular vesicles from fetal bovine serum alters proliferation and differentiation of skeletal muscle cells in vitro.* BMC Biotechnol, 2016. **16**: p. 32.
100. Wei, Z., et al., *Fetal Bovine Serum RNA Interferes with the Cell Culture derived Extracellular RNA.* Sci Rep, 2016. **6**: p. 31175.
101. Gardiner, C., et al., *Techniques used for the isolation and characterization of extracellular vesicles: results of a worldwide survey.* J Extracell Vesicles, 2016. **5**: p. 32945.
102. Thery, C., et al., *Isolation and characterization of exosomes from cell culture supernatants and biological fluids.* Curr Protoc Cell Biol, 2006. **Chapter 3**: p. Unit 3 22.
103. Cvjetkovic, A., J. Lotvall, and C. Lasser, *The influence of rotor type and centrifugation time on the yield and purity of extracellular vesicles.* J Extracell Vesicles, 2014. **3**.
104. Witwer, K.W., et al., *Standardization of sample collection, isolation and analysis methods in extracellular vesicle research.* J Extracell Vesicles, 2013. **2**.
105. Momen-Heravi, F., et al., *Impact of biofluid viscosity on size and sedimentation efficiency of the isolated microvesicles.* Front Physiol, 2012. **3**: p. 162.
106. Caradec, J., et al., *Reproducibility and efficiency of serum-derived exosome extraction methods.* Clin Biochem, 2014. **47**(13-14): p. 1286-1292.
107. Sodar, B.W., et al., *Low-density lipoprotein mimics blood plasma-derived exosomes and microvesicles during isolation and detection.* Sci Rep, 2016. **6**: p. 24316.
108. Webber, J. and A. Clayton, *How pure are your vesicles?* J Extracell Vesicles, 2013. **2**.
109. Nordin, J.Z., et al., *Ultrafiltration with size-exclusion liquid chromatography for high yield isolation of extracellular vesicles preserving intact biophysical and functional properties.* Nanomedicine (Lond), 2015. **11**(4): p. 879-883.
110. Vergauwen, G., et al., *Confounding factors of ultrafiltration and protein analysis in extracellular vesicle research.* Sci Rep, 2017. **7**(1): p. 2704.
111. Lobb, R.J., et al., *Optimized exosome isolation protocol for cell culture supernatant and human plasma.* J Extracell Vesicles, 2015. **4**: p. 27031.
112. Benedikter, B.J., et al., *Ultrafiltration combined with size exclusion chromatography efficiently isolates extracellular vesicles from cell culture media for compositional and functional studies.* Sci Rep, 2017. **7**(1): p. 15297.
113. Mol, E.A., et al., *Higher functionality of extracellular vesicles isolated using size-exclusion chromatography compared to ultracentrifugation.* Nanomedicine (Lond), 2017. **13**(6): p. 2061-2065.
114. Albertsson, P.A. and G. Frick, *Partition of virus particles in a liquid two-phase system.* Biochim Biophys Acta, 1960. **37**: p. 230-237.

115. Rider, M.A., S.N. Hurwitz, and D.G. Meckes, Jr., *ExtraPEG: A Polyethylene Glycol-Based Method for Enrichment of Extracellular Vesicles.* Sci Rep, 2016. **6**: p. 23978.
116. Weng, Y., et al., *Effective isolation of exosomes with polyethylene glycol from cell culture supernatant for in-depth proteome profiling.* Analyst, 2016. **141**(15): p. 4640-4646.
117. Van Deun, J., et al., *The impact of disparate isolation methods for extracellular vesicles on downstream RNA profiling.* J Extracell Vesicles, 2014. **3**.
118. Gamez-Valero, A., et al., *Size-Exclusion Chromatography-based isolation minimally alters Extracellular Vesicles' characteristics compared to precipitating agents.* Sci Rep, 2016. **6**: p. 33641.
119. Kowal, J., M. Tkach, and C. Thery, *Biogenesis and secretion of exosomes.* Curr Opin Cell Biol, 2014. **29**: p. 116-125.
120. Peterson, M.F., et al., *Integrated systems for exosome investigation.* Methods, 2015. **87**: p. 31-45.
121. Balaj, L., et al., *Heparin affinity purification of extracellular vesicles.* Sci Rep, 2015. **5**: p. 10266.
122. Kanwar, S.S., et al., *Microfluidic device (ExoChip) for on-chip isolation, quantification and characterization of circulating exosomes.* Lab Chip, 2014. **14**(11): p. 1891-1900.
123. Fischer, H., I. Polikarpov, and A.F. Craievich, *Average protein density is a molecular-weight-dependent function.* Protein Sci, 2004. **13**(10): p. 2825-2828.
124. Meselson, M. and F.W. Stahl, *The Replication of DNA in Escherichia Coli.* Proc Natl Acad Sci U S A, 1958. **44**(7): p. 671-682.
125. Palma, J., et al., *MicroRNAs are exported from malignant cells in customized particles.* Nucleic Acids Res, 2012. **40**(18): p. 9125-9138.
126. Lamparski, H.G., et al., *Production and characterization of clinical grade exosomes derived from dendritic cells.* Journal of Immunological Methods, 2002. **270**(2): p. 211-226.
127. Greening, D.W., et al., *A protocol for exosome isolation and characterization: evaluation of ultracentrifugation, density-gradient separation, and immunoaffinity capture methods.* Methods Mol Biol, 2015. **1295**: p. 179-209.
128. Knox, J.H. and H.P. Scott, *Theoretical-Models for Size-Exclusion Chromatography and Calculation of Pore-Size Distribution from Size-Exclusion Chromatography Data.* Journal of Chromatography, 1984. **316**(Dec): p. 311-332.
129. Boing, A.N., et al., *Single-step isolation of extracellular vesicles by size-exclusion chromatography.* J Extracell Vesicles, 2014. **3**.
130. Benedikter, B.J., et al., *Ultrafiltration combined with size exclusion chromatography efficiently isolates extracellular vesicles from cell culture media for compositional and functional studies.* Sci Rep, 2017. **7**.
131. Mol, E.A., et al., *Higher functionality of extracellular vesicles isolated using size-exclusion chromatography compared to ultracentrifugation.* Nanomedicine-Nanotechnology Biology and Medicine, 2017. **13**(6): p. 2061-2065.
132. Nordin, J.Z., et al., *Ultrafiltration with size-exclusion liquid chromatography for high yield isolation of extracellular vesicles preserving intact biophysical and functional properties.* Nanomedicine-Nanotechnology Biology and Medicine, 2015. **11**(4): p. 879-883.
133. Feingold, K.R. and C. Grunfeld, *Introduction to Lipids and Lipoproteins*, in *Endotext*, L.J. De Groot, et al., Editors. 2000: South Dartmouth (MA).
134. Vickers, K.C., et al., *MicroRNAs are transported in plasma and delivered to recipient cells by high-density lipoproteins.* Nat Cell Biol, 2011. **13**(4): p. 423-433.
135. Lasser, C., M. Eldh, and J. Lotvall, *Isolation and characterization of RNA-containing exosomes.* J Vis Exp, 2012(59): p. e3037.
136. Schindelin, J., et al., *Fiji: an open-source platform for biological-image analysis.* Nat Methods, 2012. **9**(7): p. 676-682.
137. Carpentier, G., *Contribution: Angiogenesis Analyzer.* ImageJ News, 2012.

138. Fuhrmann, G., et al., *Active loading into extracellular vesicles significantly improves the cellular uptake and photodynamic effect of porphyrins.* J Control Release, 2015. **205**: p. 35-44.
139. Engering, A., et al., *Differential post-translational modification of CD63 molecules during maturation of human dendritic cells.* Eur J Biochem, 2003. **270**(11): p. 2412-2420.
140. Kronenberg, H.M., *Developmental regulation of the growth plate.* Nature, 2003. **423**(6937): p. 332-336.
141. Sophia Fox, A.J., A. Bedi, and S.A. Rodeo, *The basic science of articular cartilage: structure, composition, and function.* Sports Health, 2009. **1**(6): p. 461-468.
142. Rees, J.A. and S.Y. Ali, *Ultrastructural localisation of alkaline phosphatase activity in osteoarthritic human articular cartilage.* Ann Rheum Dis, 1988. **47**(9): p. 747-753.
143. Anderson, H.C., *Molecular biology of matrix vesicles.* Clin Orthop Relat Res, 1995(314): p. 266-280.
144. Genge, B.R., L.N. Wu, and R.E. Wuthier, *Mineralization of annexin-5-containing lipid-calcium-phosphate complexes: modulation by varying lipid composition and incubation with cartilage collagens.* J Biol Chem, 2008. **283**(15): p. 9737-9748.
145. Wu, L.N., et al., *Characterization of the nucleational core complex responsible for mineral induction by growth plate cartilage matrix vesicles.* J Biol Chem, 1993. **268**(33): p. 25084-25094.
146. Azoidis, I., S.C. Cox, and O.G. Davies, *The role of extracellular vesicles in biomineralisation: current perspective and application in regenerative medicine.* J Tissue Eng, 2018. **9**: p. 2041731418810130.
147. Anderson, H.C., et al., *Matrix vesicles in osteomalacic hypophosphatasia bone contain apatite-like mineral crystals.* Am J Pathol, 1997. **151**(6): p. 1555-1561.
148. Shapiro, I.M., W.J. Landis, and M.V. Risbud, *Matrix vesicles: Are they anchored exosomes?* Bone, 2015. **79**: p. 29-36.
149. Borg, T.K., R. Runyan, and R.E. Wuthier, *A freeze-fracture study of avian epiphyseal cartilage differentiation.* Anat Rec, 1981. **199**(4): p. 449-457.
150. Akisaka, T. and C.V. Gay, *The plasma membrane and matrix vesicles of mouse growth plate chondrocytes during differentiation as revealed in freeze-fracture replicas.* Am J Anat, 1985. **173**(4): p. 269-286.
151. Thouverey, C., et al., *Matrix vesicles originate from apical membrane microvilli of mineralizing osteoblast-like Saos-2 cells.* J Cell Biochem, 2009. **106**(1): p. 127-138.
152. Yang, L., Y. Zhang, and F.Z. Cui, *Two types of mineral-related matrix vesicles in the bone mineralization of zebrafish.* Biomed Mater, 2007. **2**(1): p. 21-25.
153. Kretlow, J.D. and A.G. Mikos, *Review: mineralization of synthetic polymer scaffolds for bone tissue engineering.* Tissue Eng, 2007. **13**(5): p. 927-938.
154. Kim, H.M., et al., *Composition and structure of apatite formed on organic polymer in simulated body fluid with a high content of carbonate ion.* J Mater Sci Mater Med, 2000. **11**(7): p. 421-426.
155. Kim, H.M., et al., *Composition and structure of the apatite formed on PET substrates in SBF modified with various ionic activity products.* J Biomed Mater Res, 1999. **46**(2): p. 228-235.
156. Tanahashi, M. and T. Matsuda, *Surface functional group dependence on apatite formation on self-assembled monolayers in a simulated body fluid.* J Biomed Mater Res, 1997. **34**(3): p. 305-315.
157. Hunter, G.K. and H.A. Goldberg, *Nucleation of hydroxyapatite by bone sialoprotein.* Proc Natl Acad Sci U S A, 1993. **90**(18): p. 8562-8565.
158. Khanarian, N.T., et al., *A hydrogel-mineral composite scaffold for osteochondral interface tissue engineering.* Tissue Eng Part A, 2012. **18**(5-6): p. 533-545.
159. Ahlers, J., *Kinetics of alkaline phosphatase from pig kidney. Mechanism of activation by magnesium ions.* Biochem J, 1974. **141**(1): p. 257-263.

160. Dorozhkin, S.V., *Calcium orthophosphates (CaPO4): Occurrence and properties.* Morphologie, 2017. **101**(334): p. 125-142.
161. Sauer, G.R., et al., *Fourier transform Raman spectroscopy of synthetic and biological calcium phosphates.* Calcif Tissue Int, 1994. **54**(5): p. 414-420.
162. Salem, H.K. and C. Thiemermann, *Mesenchymal stromal cells: current understanding and clinical status.* Stem Cells, 2010. **28**(3): p. 585-596.
163. Okita, K., T. Ichisaka, and S. Yamanaka, *Generation of germline-competent induced pluripotent stem cells.* Nature, 2007. **448**(7151): p. 313-317.
164. Wollert, K.C. and H. Drexler, *Cell therapy for the treatment of coronary heart disease: a critical appraisal.* Nat Rev Cardiol, 2010. **7**(4): p. 204-215.
165. Iso, Y., et al., *Multipotent human stromal cells improve cardiac function after myocardial infarction in mice without long-term engraftment.* Biochem Biophys Res Commun, 2007. **354**(3): p. 700-706.
166. Thygesen, K., et al., *Fourth universal definition of myocardial infarction (2018).* Eur Heart J, 2018.
167. George, P.M. and G.K. Steinberg, *Novel Stroke Therapeutics: Unraveling Stroke Pathophysiology and Its Impact on Clinical Treatments.* Neuron, 2015. **87**(2): p. 297-309.
168. Boland, M.J., et al., *Adult mice generated from induced pluripotent stem cells.* Nature, 2009. **461**(7260): p. 91-94.
169. Ginis, I., et al., *Differences between human and mouse embryonic stem cells.* Dev Biol, 2004. **269**(2): p. 360-380.
170. Ethics Committee of the American Society for Reproductive, M., *Donating spare embryos for embryonic stem-cell research.* Fertil Steril, 2004. **82 Suppl 1**: p. S224-227.
171. Okita, K., et al., *A more efficient method to generate integration-free human iPS cells.* Nat Methods, 2011. **8**(5): p. 409-412.
172. Yang, X., L. Pabon, and C.E. Murry, *Engineering adolescence: maturation of human pluripotent stem cell-derived cardiomyocytes.* Circ Res, 2014. **114**(3): p. 511-523.
173. Friedenstein, A.J., R.K. Chailakhjan, and K.S. Lalykina, *The development of fibroblast colonies in monolayer cultures of guinea-pig bone marrow and spleen cells.* Cell Tissue Kinet, 1970. **3**(4): p. 393-403.
174. Chamberlain, G., et al., *Concise review: mesenchymal stem cells: their phenotype, differentiation capacity, immunological features, and potential for homing.* Stem Cells, 2007. **25**(11): p. 2739-2749.
175. Nauta, A.J. and W.E. Fibbe, *Immunomodulatory properties of mesenchymal stromal cells.* Blood, 2007. **110**(10): p. 3499-3506.
176. Sordi, V., *Mesenchymal stem cell homing capacity.* Transplantation, 2009. **87**(9 Suppl): p. S42-45.
177. Mushahary, D., et al., *Isolation, cultivation, and characterization of human mesenchymal stem cells.* Cytometry A, 2018. **93**(1): p. 19-31.
178. Zuk, P.A., et al., *Human adipose tissue is a source of multipotent stem cells.* Mol Biol Cell, 2002. **13**(12): p. 4279-4295.
179. Gang, E.J., et al., *In vitro mesengenic potential of human umbilical cord blood-derived mesenchymal stem cells.* Biochem Biophys Res Commun, 2004. **321**(1): p. 102-108.
180. Vishnubalaji, R., et al., *In vitro differentiation of human skin-derived multipotent stromal cells into putative endothelial-like cells.* BMC Dev Biol, 2012. **12**: p. 7.
181. Cervello, I., et al., *Human endometrial side population cells exhibit genotypic, phenotypic and functional features of somatic stem cells.* PLoS One, 2010. **5**(6): p. e10964.
182. Dominici, M., et al., *Minimal criteria for defining multipotent mesenchymal stromal cells. The International Society for Cellular Therapy position statement.* Cytotherapy, 2006. **8**(4): p. 315-317.

183. Delorme, B., et al., *Specific plasma membrane protein phenotype of culture-amplified and native human bone marrow mesenchymal stem cells.* Blood, 2008. **111**(5): p. 2631-2635.
184. Pittenger, M.F., et al., *Multilineage potential of adult human mesenchymal stem cells.* Science, 1999. **284**(5411): p. 143-147.
185. Kern, S., et al., *Comparative analysis of mesenchymal stem cells from bone marrow, umbilical cord blood, or adipose tissue.* Stem Cells, 2006. **24**(5): p. 1294-1301.
186. Bonab, M.M., et al., *Aging of mesenchymal stem cell in vitro.* BMC Cell Biol, 2006. **7**: p. 14.
187. Wagner, W., et al., *Replicative senescence of mesenchymal stem cells: a continuous and organized process.* PLoS One, 2008. **3**(5): p. e2213.
188. Abdallah, B.M., et al., *Maintenance of differentiation potential of human bone marrow mesenchymal stem cells immortalized by human telomerase reverse transcriptase gene despite [corrected] extensive proliferation.* Biochem Biophys Res Commun, 2005. **326**(3): p. 527-538.
189. Caplan, A.I., *Mesenchymal stem cells.* J Orthop Res, 1991. **9**(5): p. 641-650.
190. Bergers, G. and S. Song, *The role of pericytes in blood-vessel formation and maintenance.* Neuro Oncol, 2005. **7**(4): p. 452-464.
191. Guillemin, G.J. and B.J. Brew, *Microglia, macrophages, perivascular macrophages, and pericytes: a review of function and identification.* J Leukoc Biol, 2004. **75**(3): p. 388-397.
192. Orlova, V.V., et al., *Functionality of endothelial cells and pericytes from human pluripotent stem cells demonstrated in cultured vascular plexus and zebrafish xenografts.* Arterioscler Thromb Vasc Biol, 2014. **34**(1): p. 177-186.
193. Ribatti, D., B. Nico, and E. Crivellato, *The role of pericytes in angiogenesis.* Int J Dev Biol, 2011. **55**(3): p. 261-268.
194. Mills, S.J., A.J. Cowin, and P. Kaur, *Pericytes, mesenchymal stem cells and the wound healing process.* Cells, 2013. **2**(3): p. 621-634.
195. Sa da Bandeira, D., J. Casamitjana, and M. Crisan, *Pericytes, integral components of adult hematopoietic stem cell niches.* Pharmacol Ther, 2017. **171**: p. 104-113.
196. Crisan, M., et al., *A perivascular origin for mesenchymal stem cells in multiple human organs.* Cell Stem Cell, 2008. **3**(3): p. 301-313.
197. Jaiswal, N., et al., *Osteogenic differentiation of purified, culture-expanded human mesenchymal stem cells in vitro.* J Cell Biochem, 1997. **64**(2): p. 295-312.
198. Makino, S., et al., *Cardiomyocytes can be generated from marrow stromal cells in vitro.* J Clin Invest, 1999. **103**(5): p. 697-705.
199. Wislet-Gendebien, S., et al., *Plasticity of cultured mesenchymal stem cells: switch from nestin-positive to excitable neuron-like phenotype.* Stem Cells, 2005. **23**(3): p. 392-402.
200. Hong, S.H., et al., *In vitro differentiation of human umbilical cord blood-derived mesenchymal stem cells into hepatocyte-like cells.* Biochem Biophys Res Commun, 2005. **330**(4): p. 1153-1161.
201. Timper, K., et al., *Human adipose tissue-derived mesenchymal stem cells differentiate into insulin, somatostatin, and glucagon expressing cells.* Biochem Biophys Res Commun, 2006. **341**(4): p. 1135-1140.
202. Kordelas, L., et al., *MSC-derived exosomes: a novel tool to treat therapy-refractory graft-versus-host disease.* Leukemia, 2014. **28**(4): p. 970-973.
203. *clinicaltrials.gov (U.S. National Library of Medicine)*. [cited 2018 17th of September]; Available from: clinicaltrials.gov.
204. Morigi, M., *Mesenchymal Stem Cells Are Renotropic, Helping to Repair the Kidney and Improve Function in Acute Renal Failure.* Journal of the American Society of Nephrology, 2004. **15**(7): p. 1794-1804.
205. Choi, Y.H., A. Kurtz, and C. Stamm, *Mesenchymal stem cells for cardiac cell therapy.* Hum Gene Ther, 2011. **22**(1): p. 3-17.

206. De Miguel, M.P., et al., *Immunosuppressive properties of mesenchymal stem cells: advances and applications.* Curr Mol Med, 2012. **12**(5): p. 574-591.
207. Orlic, D., et al., *Bone marrow cells regenerate infarcted myocardium.* Nature, 2001. **410**(6829): p. 701-705.
208. Gnecchi, M., et al., *Evidence supporting paracrine hypothesis for Akt-modified mesenchymal stem cell-mediated cardiac protection and functional improvement.* FASEB J, 2006. **20**(6): p. 661-669.
209. Humphreys, B.D. and J.V. Bonventre, *Mesenchymal stem cells in acute kidney injury.* Annu Rev Med, 2008. **59**: p. 311-325.
210. Nowbar, A.N., et al., *Discrepancies in autologous bone marrow stem cell trials and enhancement of ejection fraction (DAMASCENE): weighted regression and meta-analysis.* BMJ, 2014. **348**: p. g2688.
211. Moye, L., *DAMASCENE and Meta-Ecological Research: A Bridge Too Far.* Circ Res, 2014. **115**(5): p. 484-487.
212. Afzal, M.R., et al., *Adult Bone Marrow Cell Therapy for Ischemic Heart Disease: Evidence and Insights From Randomized Controlled Trials.* Circ Res, 2015. **117**(6): p. 558-575.
213. Donndorf, P., et al., *Intramyocardial bone marrow stem cell transplantation during coronary artery bypass surgery: a meta-analysis.* J Thorac Cardiovasc Surg, 2011. **142**(4): p. 911-920.
214. Go, A.S., et al., *Heart disease and stroke statistics--2014 update: a report from the American Heart Association.* Circulation, 2014. **129**(3): p. e28-e292.
215. Bassand, J.P., et al., *Implementation of reperfusion therapy in acute myocardial infarction. A policy statement from the European Society of Cardiology.* Eur Heart J, 2005. **26**(24): p. 2733-2741.
216. Verma, S., *Fundamentals of Reperfusion Injury for the Clinical Cardiologist.* Circulation, 2002. **105**(20): p. 2332-2336.
217. Hausenloy, D.J. and D.M. Yellon, *Myocardial ischemia-reperfusion injury: a neglected therapeutic target.* J Clin Invest, 2013. **123**(1): p. 92-100.
218. Mewton, N., et al., *Effect of cyclosporine on left ventricular remodeling after reperfused myocardial infarction.* J Am Coll Cardiol, 2010. **55**(12): p. 1200-1205.
219. Yellon, D.M. and D.J. Hausenloy, *Myocardial reperfusion injury.* N Engl J Med, 2007. **357**(11): p. 1121-1135.
220. Gnecchi, M., et al., *Paracrine action accounts for marked protection of ischemic heart by Akt-modified mesenchymal stem cells.* Nat Med, 2005. **11**(4): p. 367-368.
221. Uemura, R., et al., *Bone marrow stem cells prevent left ventricular remodeling of ischemic heart through paracrine signaling.* Circ Res, 2006. **98**(11): p. 1414-1421.
222. Xu, M., et al., *In vitro and in vivo effects of bone marrow stem cells on cardiac structure and function.* J Mol Cell Cardiol, 2007. **42**(2): p. 441-448.
223. Korf-Klingebiel, M., et al., *Bone marrow cells are a rich source of growth factors and cytokines: implications for cell therapy trials after myocardial infarction.* Eur Heart J, 2008. **29**(23): p. 2851-2858.
224. Thiagarajan, H., et al., *Angiogenic growth factors in myocardial infarction: a critical appraisal.* Heart Fail Rev, 2017. **22**(6): p. 665-683.
225. Yanagisawa-Miwa, A., et al., *Salvage of infarcted myocardium by angiogenic action of basic fibroblast growth factor.* Science, 1992. **257**(5075): p. 1401-1403.
226. Herrera, M.B., et al., *Mesenchymal stem cells contribute to the renal repair of acute tubular epithelial injury.* Int J Mol Med, 2004. **14**(6): p. 1035-1041.
227. Lin, F., A. Moran, and P. Igarashi, *Intrarenal cells, not bone marrow-derived cells, are the major source for regeneration in postischemic kidney.* J Clin Invest, 2005. **115**(7): p. 1756-1764.

228. Duffield, J.S., et al., *Restoration of tubular epithelial cells during repair of the postischemic kidney occurs independently of bone marrow-derived stem cells.* J Clin Invest, 2005. **115**(7): p. 1743-1755.
229. Herrera, M.B., et al., *Exogenous mesenchymal stem cells localize to the kidney by means of CD44 following acute tubular injury.* Kidney Int, 2007. **72**(4): p. 430-441.
230. Togel, F., et al., *Vasculotropic, paracrine actions of infused mesenchymal stem cells are important to the recovery from acute kidney injury.* Am J Physiol Renal Physiol, 2007. **292**(5): p. F1626-1635.
231. Yuan, L., et al., *VEGF-modified human embryonic mesenchymal stem cell implantation enhances protection against cisplatin-induced acute kidney injury.* Am J Physiol Renal Physiol, 2011. **300**(1): p. F207-218.
232. Honmou, O., et al., *Mesenchymal stem cells: therapeutic outlook for stroke.* Trends Mol Med, 2012. **18**(5): p. 292-297.
233. Nomura, T., et al., *I.V. infusion of brain-derived neurotrophic factor gene-modified human mesenchymal stem cells protects against injury in a cerebral ischemia model in adult rat.* Neuroscience, 2005. **136**(1): p. 161-169.
234. Chen, Q., et al., *Protective effects of bone marrow stromal cell transplantation in injured rodent brain: synthesis of neurotrophic factors.* J Neurosci Res, 2005. **80**(5): p. 611-619.
235. Onda, T., et al., *Therapeutic benefits by human mesenchymal stem cells (hMSCs) and Ang-1 gene-modified hMSCs after cerebral ischemia.* J Cereb Blood Flow Metab, 2008. **28**(2): p. 329-340.
236. Miki, Y., et al., *Vascular endothelial growth factor gene-transferred bone marrow stromal cells engineered with a herpes simplex virus type 1 vector can improve neurological deficits and reduce infarction volume in rat brain ischemia.* Neurosurgery, 2007. **61**(3): p. 586-594; discussion 594-585.
237. Arslan, F., et al., *Mesenchymal stem cell-derived exosomes increase ATP levels, decrease oxidative stress and activate PI3K/Akt pathway to enhance myocardial viability and prevent adverse remodeling after myocardial ischemia/reperfusion injury.* Stem Cell Res, 2013. **10**(3): p. 301-312.
238. Timmers, L., et al., *Reduction of myocardial infarct size by human mesenchymal stem cell conditioned medium.* Stem Cell Res, 2007. **1**(2): p. 129-137.
239. Lai, R.C., et al., *Exosome secreted by MSC reduces myocardial ischemia/reperfusion injury.* Stem Cell Res, 2010. **4**(3): p. 214-222.
240. Bian, S., et al., *Extracellular vesicles derived from human bone marrow mesenchymal stem cells promote angiogenesis in a rat myocardial infarction model.* J Mol Med (Berl), 2014. **92**(4): p. 387-397.
241. Feng, Y., et al., *Ischemic preconditioning potentiates the protective effect of stem cells through secretion of exosomes by targeting Mecp2 via miR-22.* PLoS One, 2014. **9**(2): p. e88685.
242. Yu, B., et al., *Exosomes secreted from GATA-4 overexpressing mesenchymal stem cells serve as a reservoir of anti-apoptotic microRNAs for cardioprotection.* Int J Cardiol, 2015. **182**: p. 349-360.
243. Zhao, Y., et al., *Exosomes Derived from Human Umbilical Cord Mesenchymal Stem Cells Relieve Acute Myocardial Ischemic Injury.* Stem Cells Int, 2015. **2015**: p. 761643.
244. Iyer, S.S. and M. Rojas, *Anti-inflammatory effects of mesenchymal stem cells: novel concept for future therapies.* Expert Opin Biol Ther, 2008. **8**(5): p. 569-581.
245. Bruno, S., et al., *Mesenchymal stem cell-derived microvesicles protect against acute tubular injury.* J Am Soc Nephrol, 2009. **20**(5): p. 1053-1067.
246. Bruno, S., et al., *Microvesicles derived from mesenchymal stem cells enhance survival in a lethal model of acute kidney injury.* PLoS One, 2012. **7**(3): p. e33115.

247. Gatti, S., et al., *Microvesicles derived from human adult mesenchymal stem cells protect against ischaemia-reperfusion-induced acute and chronic kidney injury.* Nephrol Dial Transplant, 2011. **26**(5): p. 1474-1483.
248. Xin, H., et al., *Exosome-mediated transfer of miR-133b from multipotent mesenchymal stromal cells to neural cells contributes to neurite outgrowth.* Stem Cells, 2012. **30**(7): p. 1556-1564.
249. Xin, H., et al., *Systemic administration of exosomes released from mesenchymal stromal cells promote functional recovery and neurovascular plasticity after stroke in rats.* J Cereb Blood Flow Metab, 2013. **33**(11): p. 1711-1715.
250. Caplan, A.I., *Mesenchymal Stem Cells: Time to Change the Name!* Stem Cells Transl Med, 2017. **6**(6): p. 1445-1451.
251. Phinney, D.G. and M.F. Pittenger, *Concise Review: MSC-Derived Exosomes for Cell-Free Therapy.* Stem Cells, 2017. **35**(4): p. 851-858.
252. Nakamura, Y., et al., *Mesenchymal-stem-cell-derived exosomes accelerate skeletal muscle regeneration.* FEBS Lett, 2015. **589**(11): p. 1257-1265.
253. Hu, L., et al., *Exosomes derived from human adipose mensenchymal stem cells accelerates cutaneous wound healing via optimizing the characteristics of fibroblasts.* Sci Rep, 2016. **6**: p. 32993.
254. Shabbir, A., et al., *Mesenchymal Stem Cell Exosomes Induce Proliferation and Migration of Normal and Chronic Wound Fibroblasts, and Enhance Angiogenesis In Vitro.* Stem Cells Dev, 2015. **24**(14): p. 1635-1647.
255. Tao, S.C., et al., *Chitosan Wound Dressings Incorporating Exosomes Derived from MicroRNA-126-Overexpressing Synovium Mesenchymal Stem Cells Provide Sustained Release of Exosomes and Heal Full-Thickness Skin Defects in a Diabetic Rat Model.* Stem Cells Transl Med, 2017. **6**(3): p. 736-747.
256. Teng, X., et al., *Mesenchymal Stem Cell-Derived Exosomes Improve the Microenvironment of Infarcted Myocardium Contributing to Angiogenesis and Anti-Inflammation.* Cell Physiol Biochem, 2015. **37**(6): p. 2415-2424.
257. Zhang, B., et al., *Human umbilical cord mesenchymal stem cell exosomes enhance angiogenesis through the Wnt4/beta-catenin pathway.* Stem Cells Transl Med, 2015. **4**(5): p. 513-522.
258. Baecker, V., *ImageJ macro tool sets for biological image analysis.* ImageJ User and Developer Conference 2012, 2012.
259. Ouyang, L., et al., *Programmed cell death pathways in cancer: a review of apoptosis, autophagy and programmed necrosis.* Cell Prolif, 2012. **45**(6): p. 487-498.
260. Zhang, B., et al., *HucMSC-Exosome Mediated-Wnt4 Signaling Is Required for Cutaneous Wound Healing.* Stem Cells, 2015. **33**(7): p. 2158-2168.
261. Liang, X., et al., *Exosomes secreted by mesenchymal stem cells promote endothelial cell angiogenesis by transferring miR-125a.* Journal of Cell Science, 2016. **129**(11): p. 2182-2189.
262. Sze, S.K., et al., *Elucidating the secretion proteome of human embryonic stem cell-derived mesenchymal stem cells.* Mol Cell Proteomics, 2007. **6**(10): p. 1680-1689.
263. Anderson, J.D., et al., *Comprehensive Proteomic Analysis of Mesenchymal Stem Cell Exosomes Reveals Modulation of Angiogenesis via Nuclear Factor-KappaB Signaling.* Stem Cells, 2016. **34**(3): p. 601-613.
264. Gnecchi, M., et al., *Evidence supporting paracrine hypothesis for Akt-modified mesenchymal stem cell-mediated cardiac protection and functional improvement.* Faseb Journal, 2006. **20**(6): p. 661-669.
265. Reis, L.A., et al., *Bone marrow-derived mesenchymal stem cells repaired but did not prevent gentamicin-induced acute kidney injury through paracrine effects in rats.* PLoS One, 2012. **7**(9): p. e44092.

266. Zhou, Y., et al., *Exosomes released by human umbilical cord mesenchymal stem cells protect against cisplatin-induced renal oxidative stress and apoptosis in vivo and in vitro.* Stem Cell Res Ther, 2013. **4**(2): p. 34.
267. Rager, T.M., et al., *Exosomes secreted from bone marrow-derived mesenchymal stem cells protect the intestines from experimental necrotizing enterocolitis.* J Pediatr Surg, 2016. **51**(6): p. 942-947.
268. Zhu, L., et al., *Exosomes Derived From Natural Killer Cells Exert Therapeutic Effect in Melanoma.* Theranostics, 2017. **7**(10): p. 2732-2745.
269. Webber, J., et al., *Cancer exosomes trigger fibroblast to myofibroblast differentiation.* Cancer Res, 2010. **70**(23): p. 9621-9630.
270. Maitland, N.J., *Carcinoma-derived exosomes modify microenvironment.* Oncotarget, 2015. **6**(3): p. 1344-1345.
271. Consortium, E.-T., et al., *EV-TRACK: transparent reporting and centralizing knowledge in extracellular vesicle research.* Nat Methods, 2017. **14**(3): p. 228-232.
272. Lotvall, J., et al., *Minimal experimental requirements for definition of extracellular vesicles and their functions: a position statement from the International Society for Extracellular Vesicles.* J Extracell Vesicles, 2014. **3**: p. 26913.
273. Nakai, W., et al., *A novel affinity-based method for the isolation of highly purified extracellular vesicles.* Sci Rep, 2016. **6**: p. 33935.
274. Welton, J.L., et al., *Proteomics analysis of bladder cancer exosomes.* Mol Cell Proteomics, 2010. **9**(6): p. 1324-1338.